Print ISSN: 0975-5861
Online ISSN : 2249-4596

Global Journal of Researches in Engineering: F Electrical and electronics Engineering

Revolutions 12 in Engineering World

February 2012

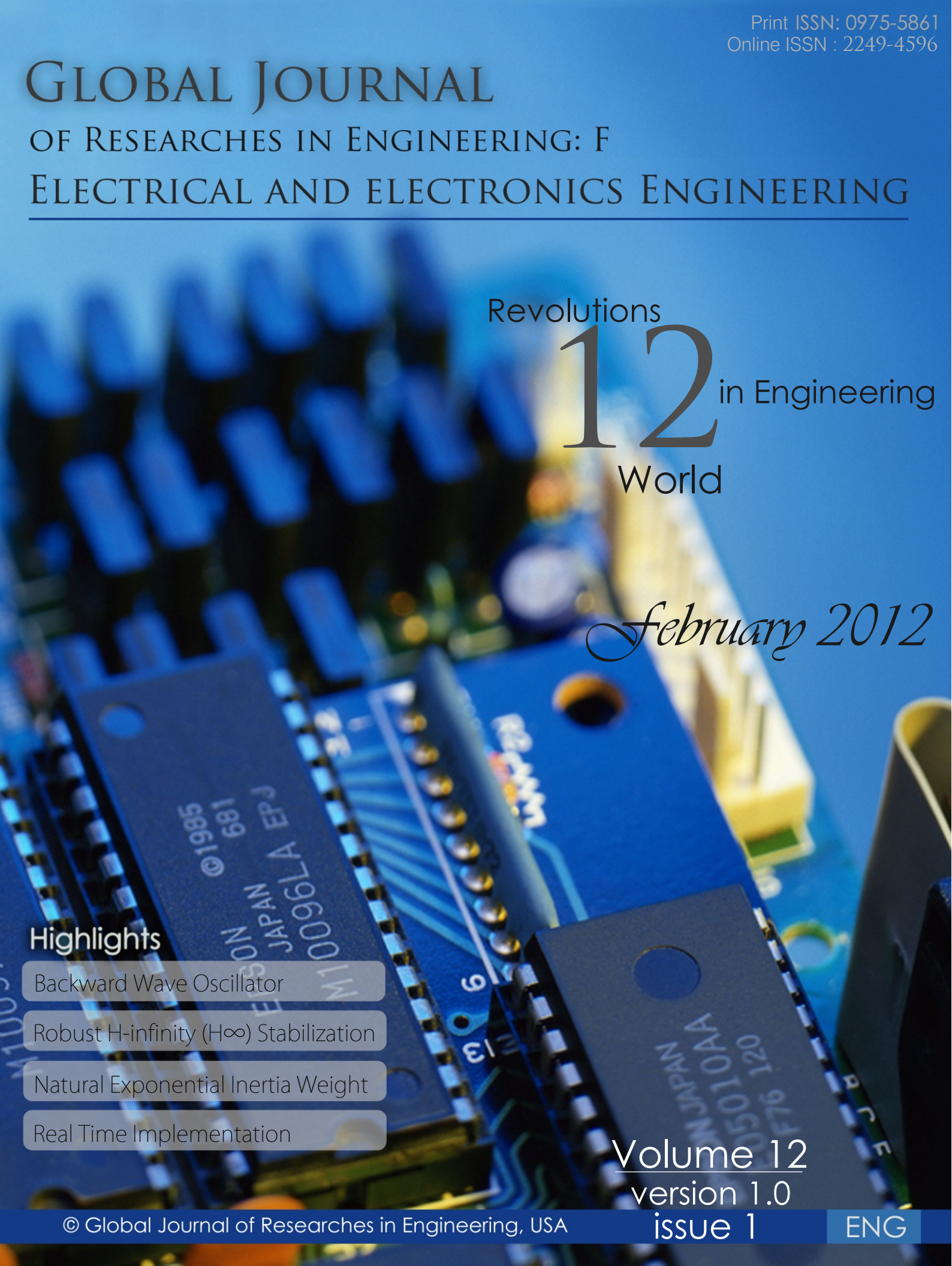

Highlights

- Backward Wave Oscillator
- Robust H-infinity (H∞) Stabilization
- Natural Exponential Inertia Weight
- Real Time Implementation

Volume 12
version 1.0
issue 1
ENG

Global Journal of Research in Engineering :F
Electrical And Electronical Engineering

Global Journal of Research in Engineering : F
Electrical And Electronical Engineering
Volume 12 Issue 1 (Ver. 1.0)

Open Association of Research Society

Incorporation No.: 0423089
License No.: 42125/022010/1186
Registration No.: 430374
Import-Export Code: 1109007027
Employer Identification Number (EIN):
USA Tax ID: 98-0673427

Global Journals Inc.

*(A Delaware USA Incorporation with "Good Standing"; **Reg. Number: 0423089**)*

Sponsors: Open Association of Research Society
Open Scientific Standards

Publisher's Headquarters office

Global Journals Inc., Headquarters Corporate Office, Cambridge Office Center, II Canal Park, Floor No. 5th, ***Cambridge (Massachusetts)***, Pin: MA 02141 United States
USA Toll Free: +001-888-839-7392
USA Toll Free Fax: +001-888-839-7392

Offset Typesetting

Open Association of Research Society, Marsh Road, Rainham, Essex, London RM13 8EU
United Kingdom.

Packaging & Continental Dispatching

Global Journals, India

Find a correspondence nodal officer near you

To find nodal officer of your country, please email us at *local@globaljournals.org*

eContacts

Press Inquiries: *press@globaljournals.org*
Investor Inquiries: *investers@globaljournals.org*
Technical Support: *technology@globaljournals.org*
Media & Releases: *media@globaljournals.org*

Pricing (Including by Air Parcel Charges):

For Authors:
22 USD (B/W) & 50 USD (Color)
Yearly Subscription (Personal & Institutional):
200 USD (B/W) & 250 USD (Color)

Editorial Board Members (HON.)

Dr. Bart Lambrecht
Director of Research in Accounting and FinanceProfessor of Finance
Lancaster University Management School
BA (Antwerp); MPhil, MA, PhD (Cambridge)

Dr. Carlos García Pont
Associate Professor of Marketing
IESE Business School, University of Navarra
Doctor of Philosophy (Management), Massachusetts Institute of Technology (MIT)
Master in Business Administration, IESE, University of Navarra
Degree in Industrial Engineering, Universitat Politècnica de Catalunya

Dr. Fotini Labropulu
Mathematics - Luther College
University of ReginaPh.D., M.Sc. in Mathematics
B.A. (Honors) in Mathematics
University of Windso

Dr. Lynn Lim
Reader in Business and Marketing
Roehampton University, London
BCom, PGDip, MBA (Distinction), PhD, FHEA

Dr. Mihaly Mezei
ASSOCIATE PROFESSOR
Department of Structural and Chemical Biology, Mount Sinai School of Medical Center
Ph.D., Etvs Lornd University
Postdoctoral Training,
New York University

Dr. Söhnke M. Bartram
Department of Accounting and FinanceLancaster University Management SchoolPh.D. (WHU Koblenz)
MBA/BBA (University of Saarbrücken)

Dr. Miguel Angel Ariño
Professor of Decision Sciences
IESE Business School
Barcelona, Spain (Universidad de Navarra)
CEIBS (China Europe International Business School).
Beijing, Shanghai and Shenzhen
Ph.D. in Mathematics
University of Barcelona
BA in Mathematics (Licenciatura)
University of Barcelona

Philip G. Moscoso
Technology and Operations Management
IESE Business School, University of Navarra
Ph.D in Industrial Engineering and Management, ETH Zurich
M.Sc. in Chemical Engineering, ETH Zurich

Dr. Sanjay Dixit, M.D.
Director, EP Laboratories, Philadelphia VA Medical Center
Cardiovascular Medicine - Cardiac Arrhythmia
Univ of Penn School of Medicine

Dr. Han-Xiang Deng
MD., Ph.D
Associate Professor and Research
Department Division of Neuromuscular Medicine
Davee Department of Neurology and Clinical NeuroscienceNorthwestern University
Feinberg School of Medicine

Dr. Pina C. Sanelli
Associate Professor of Public Health
Weill Cornell Medical College
Associate Attending Radiologist
NewYork-Presbyterian Hospital
MRI, MRA, CT, and CTA
Neuroradiology and Diagnostic Radiology
M.D., State University of New York at Buffalo,School of Medicine and Biomedical Sciences

Dr. Roberto Sanchez
Associate Professor
Department of Structural and Chemical Biology
Mount Sinai School of Medicine
Ph.D., The Rockefeller University

Dr. Wen-Yih Sun
Professor of Earth and Atmospheric SciencesPurdue University Director
National Center for Typhoon and Flooding Research, Taiwan
University Chair Professor
Department of Atmospheric Sciences, National Central University, Chung-Li, TaiwanUniversity Chair Professor
Institute of Environmental Engineering, National Chiao Tung University, Hsin-chu, Taiwan.Ph.D., MS The University of Chicago, Geophysical Sciences
BS National Taiwan University, Atmospheric Sciences
Associate Professor of Radiology

Dr. Michael R. Rudnick
M.D., FACP
Associate Professor of Medicine
Chief, Renal Electrolyte and Hypertension Division (PMC)
Penn Medicine, University of Pennsylvania
Presbyterian Medical Center, Philadelphia
Nephrology and Internal Medicine
Certified by the American Board of Internal Medicine

Dr. Bassey Benjamin Esu
B.Sc. Marketing; MBA Marketing; Ph.D Marketing
Lecturer, Department of Marketing, University of Calabar
Tourism Consultant, Cross River State Tourism Development Department
Co-ordinator , Sustainable Tourism Initiative, Calabar, Nigeria

Dr. Aziz M. Barbar, Ph.D.
IEEE Senior Member
Chairperson, Department of Computer Science
AUST - American University of Science & Technology
Alfred Naccash Avenue – Ashrafieh

Contents of the Volume

Global Journal of researches in engineering
Electrical and electronics engineering
Volume 12 Issue 1 Version 1.0 January 2012
Type: Double Blind Peer Reviewed International Research Journal
Publisher: Global Journals Inc. (USA)
Online ISSN: 2249-4596 & Print ISSN: 0975-5861

Turbogenerator-System Controller Design Via H∞- Control Techniques

By Anastasios K. Boglou, Dimosthenis I. Pappas
Technological Education Institution (TEI)

Abstract - In the present work an H∞ -control technique is presented in concise form and applied to the design of discrete optimal multirate-output controllers. The technique used is based on multirate-output controllers having a multirate sampling mechanism with different sampling period in each measured output quantity of the system. It relies mainly, under appropriate conditions, on the reduction of the original H∞ -disturbance attenuation problem to an associated discrete H∞ -control problem for which a fictitious static state feedback controller is to be designed, even though some state variables may not be available (measurable) for feedback purposes. The discrete linear open-loop system model under consideration (which includes a disturbance term) is systematically derived from the associated continuous 3th-order MIMO linearized open-loop model of a practical power system, having an 160**M**V**A** synchronous generator supplying power to an infinite grid through a step-up transformer and an appropriate transmission line. Through the obtained pertinent simulation results the validity and practical usefulness of this design control technique is assessed.

Keywords : *H∞ -control, disturbance attenuation, multirate digital control, power system.*

GJRE-F Classification: *FOR Code: 090607*

Strictly as per the compliance and regulations of:

Turbogenerator-System Controller Design Via H^{∞}- Control Techniques

Anastasios K. Boglou[α], Dimosthenis I. Pappas[σ]

Abstract - In the present work an H^{∞} -control technique is presented in concise form and applied to the design of discrete optimal multirate-output controllers. The technique used is based on multirate-output controllers having a multirate sampling mechanism with different sampling period in each measured output quantity of the system. It relies mainly, under appropriate conditions, on the reduction of the original H^{∞} -disturbance attenuation problem to an associated discrete H^{∞} -control problem for which a fictitious static state feedback controller is to be designed, even though some state variables may not be available (measurable) for feedback purposes. The discrete linear open-loop system model under consideration (which includes a disturbance term) is systematically derived from the associated continuous 3th-order MIMO linearized open-loop model of a practical power system, having an 160MVA synchronous generator supplying power to an infinite grid through a step-up transformer and an appropriate transmission line. Through the obtained pertinent simulation results the validity and practical usefulness of this design control technique is assessed.

Keywords : H^{∞} -control, disturbance attenuation, multirate digital control, power system.

I. Introduction

The H^{∞} - optimization control problem as known has drawn great attention [1-17]. In particular, the H^{∞} -control problem for discrete-time and sampled-data singlerate and multirate systems has been treated successfully before [3-15]. Generally speaking, when the state vector is not available for feedback purposes, the H^{∞} - control problem is usually solved in both the continuous and discrete-time cases using dynamic measurement feedback approach.

Recently, a new technique [5,6,9] has been presented for the solution of the H^{∞} - disturbance attenuation problem. This technique is based on optimal multirate-output controllers (OMOCs) and, in order to solve the sampled-data H^{∞} - disturbance attenuation problem, relies mainly on the reduction, under appropriate conditions, of the original H^{∞} -disturbance attenuation problem to an associated discrete H^{∞} -control problem for which a fictitious static state-feedback controller is to be designed, even though some state variables are not available for feedback use.

In the present work the ultimately investigated discrete linear open-loop power system model was obtained through a systematic procedure using a linearized continuous 3th -order MIMO open-loop model, containing an input disturbance, representing a practical power system having an 160MVA synchronous generator supplying power to an infinite grid through a step-up transformer and transmission line [18]. The digital controller leading to the associated designed discrete closed-loop power system model is displaying enhanced dynamic stability characteristics, and it is accomplished by applying properly the presented OMC technique.

II. Overview of Relevant Mathematical Considerations

The general description of the controllable and observable continuous, linear, time-invariant, multivariable MIMO dynamical open-loop system expressed in state-space form is

$$\begin{aligned}\dot{\mathbf{x}}(t) &= \mathbf{A}\mathbf{x}(t) + \mathbf{B}\mathbf{u}(t)\\ \mathbf{y}(t) &= \mathbf{C}\mathbf{x}(t)\end{aligned} \tag{1}$$

where: $\mathbf{x}(t) \in \mathbf{R}^n$, $\mathbf{u}(t) \in \mathbf{R}^m$, $\mathbf{y}(t) \in \mathbf{R}^p$ are state, input and output vectors respectively; and A, B and C are real constant system matrices with proper dimensions.

The associated general discrete description of the system of eq. (1) is as follows

$$\begin{aligned}\mathbf{x}(k+1) &= \mathbf{A}\mathbf{x}(k) + \mathbf{B}\mathbf{u}(k)\\ \mathbf{y}(k) &= \mathbf{C}\mathbf{x}(k)\end{aligned} \tag{2}$$

Where $\mathbf{x}(k) \in \mathbf{R}^n$, $\mathbf{u}(k) \in \mathbf{R}^m$, $\mathbf{y}(k) \in \mathbf{R}^p$ are state, input and output vectors respectively; and A, B and C are real constant system matrices with proper dimensions.

III. Brief Review of H∞-Control With OMOC

Consider the controllable and observable continuous linear state-space system model in the following general form

$$\dot{\mathbf{x}}(t) = \mathbf{A}\mathbf{x}(t) + \mathbf{B}\mathbf{u}(t) + \mathbf{D}\mathbf{q}(t) \quad \mathbf{x}(0) = \mathbf{0} \tag{3a}$$

$$\begin{aligned}\mathbf{y}_m(t) &= \mathbf{C}\mathbf{x}(t) + \mathbf{J}_1\mathbf{u}(t),\\ \mathbf{y}_c(t) &= \mathbf{E}\mathbf{x}(t) + \mathbf{J}_2\mathbf{u}(t)\end{aligned} \tag{3b}$$

Author α : Professor, Technological Education Institution (TEI) of Kavala Faculty of Applied Technology, St. Loukas, 654 04 Kavala, GREECE, E-mail : akbogl@teikav.edu.gr

Author σ : Technological Education Institution (TEI) of Kavala Faculty of Informations Management Kavala, GREECE,

where: $\mathbf{x}(t) \in \mathbf{R}^n$, $\mathbf{u}(t) \in \mathbf{R}^m$, $\mathbf{q}(t) \in \mathbf{L}_2^d$, $\mathbf{y_m}(t) = \in \mathbf{R}^{p_1}$, $\mathbf{y_c}(t) \in \mathbf{R}^{p_2}$ are the state, input, external disturbance, measured output and controlled output vectors, respectively. In equ. (3) all matrices have real elements and appropriate dimensions. Next follows a useful definition.

Definition For an observable matrix pair $(\mathbf{A}, \mathbf{C})$, with $\mathbf{C}^T = \left[\mathbf{c}_1^T \ \mathbf{c}_2^T \ \cdots \ \mathbf{c}_{p_1}^T\right]$ and $\mathbf{c}_i$ with i=1, …,p_1, the ith row of the matrix $\mathbf{C}$, a collection of p_1 integers $\{n_1, n_2, \cdots, n_{p_1}\}$ is called an *observability index vector* of the pair $(\mathbf{A}, \mathbf{C})$, if the following relationships hold simultaneously

$$\sum_{i=1}^{p_1} n_i = n$$

$$rank\left[\mathbf{c}_1^T \ \ldots \ \left(\mathbf{A}^T\right)^{n_1-1}\mathbf{c}_1^T \ \ldots \ \mathbf{c}_{p_1}^T \ \ldots \ \ldots \mathbf{c}_{p_1}^T\left(\mathbf{A}^T\right)^{n_{p_1}-1}\mathbf{c}_{p_1}^T\right] = n \quad (4)$$

The multirate sampling mechanism shown in Fig. 1. is applied to eq. (3).

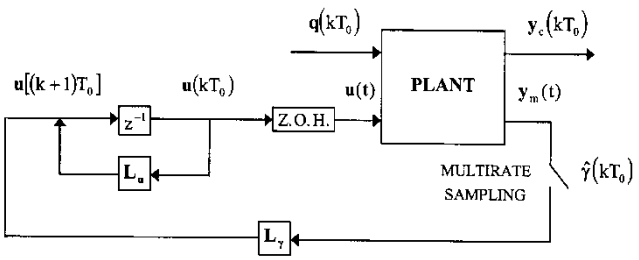

Fig.1 : Simplified block diagram for the control of linear systems using OMC technique

Assuming that all samplers start simultaneously at t = 0, a sampler and a zero-order hold with period T_0 is connected to each plant input $u_i(t)$, i=1,2,…,m, such that

$$\mathbf{u}(t)=\mathbf{u}(kT_0) \ , \ t \in [kT_0, (k+1)T_0) \quad (5)$$

while the ith disturbance $q_i(t)$, i=1,…,d, and the ith controlled output $y_{c,i}(t)$, i=1,…, p_2, are detected at time kT_0, such that for $t \in [kT_0, (k+1)T_0)$

$$\mathbf{q}(t)=\mathbf{q}(kT_0) \ , \ \mathbf{y}_c(kT_0) = \mathbf{E}\mathbf{x}(kT_0)+\mathbf{J}_2(kT_0) \quad (6)$$

where $(\mathbf{J}_2)_i$ is the ith row of the matrix $\mathbf{J}_2$.

The ith measured output $y_{m,i}(t)$, i=1,…, p_1, is detected at every T_i period, such that for $\mu = 0,..., N_i - 1$

$$y_{m,i}(kT_0 + \mu T_i) = \mathbf{c}_i\mathbf{x}(kT_0 + \mu T_i) + (\mathbf{J}_1)_i \mathbf{u}(kT_0)$$

Here $N_i \in \mathbf{Z}^+$ are the output multiplicities of the sampling and $T_i \in \mathbf{R}^+$ are the output sampling periods having rational ratio, i.e. $T_i = T_0 / N_i$ with i=1,…, p_1.

The sampled values of the plant measured outputs obtained over $[kT_0, (k+1)T_0)$ are stored in the N^*-dimensional column vector given by

$$\hat{\gamma}(kT_0) = \left[y_{m,1}(kT_0) \ \cdots \ y_{m,1}(kT_0 + (N_1 - 1)T_1)\ldots \right.$$
$$\left. \ldots y_{m,p_1}(kT_o)\ldots y_{m,p_1}[kT_o + (N_{p_1} - 1)T_{p_1}]\right]^T \quad (7)$$

(where $N^* = \sum_{i=1}^{p_1} N_i$), which is used in the OMC in the form

$$\mathbf{u}[(k+1)T_0] = \mathbf{L}_u\mathbf{u}(kT_0) - \mathbf{L}_\gamma\hat{\gamma}(kT_0) \quad (8)$$

where $\mathbf{L}_u \in \mathbf{R}^{mxm}$, $\mathbf{L}_\gamma \in \mathbf{R}^{mxN^*}$.

Assumptions:

a) The matrix triplets $(\mathbf{A}, \mathbf{B}, \mathbf{C})$ and $(\mathbf{A}, \mathbf{D}, \mathbf{E})$ are stabilizable and detectable.

b) $$\text{rank}\begin{bmatrix} A & D \\ C & 0_{p_1 xd} \end{bmatrix} = n + d,$$

$$\text{rank}\begin{bmatrix} A & B & D \\ C & 0_{p_1 xm} & 0_{p_1 xd} \end{bmatrix} = n + m + d$$

c) $\mathbf{J}_2^T[\mathbf{E} \quad \mathbf{J}_2] = [\mathbf{0}_{m\times n} \quad \mathbf{I}_{m\times m}]$.

d) There is a sampling period T_0, such that the open-loop discrete-time system model in general form becomes

$$\mathbf{x}[(k+1)T_0] = \mathbf{\Phi}\mathbf{x}(kT_0) + \hat{\mathbf{B}}\mathbf{u}(kT_0) + \hat{\mathbf{D}}\mathbf{q}(kT_0)$$
$$\mathbf{y}_c(kT_0) = \mathbf{E}\mathbf{x}(kT_0) + \mathbf{J}_2\mathbf{u}(kT_0) \quad (9)$$

where

$$\mathbf{\Phi} = \exp(\mathbf{A}T_0), \ (\hat{\mathbf{B}}, \hat{\mathbf{D}}) = \int_0^{T_0} \exp(\mathbf{A}\lambda)(\mathbf{B}, \mathbf{D})d\lambda \quad (10)$$

is stabilizable and observable and does not have invariant zeros on the unit circle.

Consequently it follows that the procedure for H^{∞}-disturbance attenuation, using OMC essentially consists in finding for the control law a fictitious state matrix F which equivalently solves the problem, and then either determining the OMC pair $(\mathbf{L}_{\gamma}, \mathbf{L}_{u})$ or choosing a desired $\mathbf{L}_{u}$ and determining the $\mathbf{L}_{\gamma}$. Based in [3] matrix F takes the following form

$$\mathbf{F} = \left(\mathbf{I} + \hat{\mathbf{B}}^{\mathrm{T}}\mathbf{P}\hat{\mathbf{B}}\right)^{-1}\hat{\mathbf{B}}^{\mathrm{T}}\mathbf{P}\boldsymbol{\Phi}$$

where P is an appropriate solution of the following Riccati equation

$$\begin{aligned}\mathbf{P} = \mathbf{E}^{\mathrm{T}}\mathbf{E} + \boldsymbol{\Phi}^{\mathrm{T}}\mathbf{P}\boldsymbol{\Phi} - \boldsymbol{\Phi}^{\mathrm{T}}\mathbf{P}\hat{\mathbf{B}}\left(\mathbf{I} + \hat{\mathbf{B}}^{\mathrm{T}}\mathbf{P}\hat{\mathbf{B}}\right)^{-1}\hat{\mathbf{B}}\mathbf{P}\boldsymbol{\Phi} \\ + \mathbf{P}\hat{\mathbf{D}}_{\gamma}\left(\mathbf{I} + \hat{\mathbf{D}}_{\gamma}^{\mathrm{T}}\mathbf{P}\hat{\mathbf{D}}_{\gamma}\right)\hat{\mathbf{D}}_{\gamma}^{\mathrm{T}}\mathbf{P}, \\ \hat{\mathbf{D}}_{\gamma} = \gamma^{-1}\hat{\mathbf{D}}\end{aligned} \tag{11}$$

It is to be noted that $\gamma \in \mathbf{R}^{+}$, such that $\left\|\mathbf{T}_{\mathbf{qy}_c}(z)\right\| \geq \gamma$ where $\left\|\mathbf{T}_{\mathbf{qy}_c}(z)\right\|_{\infty}$ is the H∞-norm of the proper stable discrete transfer function $\mathbf{T}_{\mathbf{qy}_c}(z)$, from sampled-data external disturbances $\mathbf{q}(kT_o) \in \ell_2^{\mathbf{d}}$ to sampled-data controlled output $\mathbf{y}_c(kT_o)$.

Once matrix F is obtained the OMC matrices $\mathbf{L}_{\gamma}$ and $\mathbf{L}_{u}$ (in the case where $\mathbf{L}_{u}$ is free) can be computed as follows

$$\begin{aligned}\mathbf{L}_{\gamma} &= \left[\mathbf{F} \quad \mathbf{0}_{m\times d}\right]\tilde{\mathbf{H}} + \Lambda\left(\mathbf{I}_{N^{*}\times N^{*}} - \left[\mathbf{H} \quad \Theta_{\mathbf{q}}\right]\tilde{\mathbf{H}}\right) \\ \mathbf{L}_{\mathbf{u}} &= \left\{\left[\mathbf{F} \quad \mathbf{0}_{m\times d}\right]\tilde{\mathbf{H}} + \Lambda\left(\mathbf{I}_{N^{*}\times N^{*}} - \left[\mathbf{H} \quad \Theta_{\mathbf{q}}\right]\tilde{\mathbf{H}}\right)\right\}\Theta_{\mathbf{u}}\end{aligned} \tag{12}$$

where $\tilde{\mathbf{H}}\left[\mathbf{H} \quad \Theta_{\mathbf{q}}\right] = \mathbf{I}$ and $\Lambda \in \mathbf{R}^{\mathbf{mxN}^{*}}$ is an arbitrary specified matrix. In the case where $\mathbf{L}_{u} = \mathbf{L}_{u,sp}$, we have

$$\begin{aligned}\mathrm{L}_{\gamma} &= \left[\mathrm{F} \quad \mathrm{L}_{\mathbf{u},sp} \quad 0_{m\times d}\right]\hat{\mathrm{H}} + \ldots \\ &+ \Sigma\left(\mathrm{I}_{N^{*}\times N^{*}} - \left[\mathrm{H} \quad \Theta_{\mathbf{u}} \quad \Theta_{\mathbf{q}}\right]\hat{\mathrm{H}}\right)\end{aligned} \tag{13}$$

where $\hat{\mathbf{H}}\left[\mathbf{H} \quad \Theta_{\mathbf{u}} \quad \Theta_{\mathbf{q}}\right] = \mathbf{I}$ and $\Sigma \in \mathbf{R}^{\mathbf{mxN}^{*}}$ is arbitrary.

The explicit expressions for $\mathbf{H}$, $\tilde{\mathbf{H}}$, $\hat{\mathbf{H}}$, Λ, Θ_{u} and Θ_{q} are given in [5,8].

The resulting discrete closed-loop system matrix $(\mathbf{A}_{\mathbf{cl/d}})$ takes the following general form

$$\mathbf{A}_{\mathbf{cl/d}} = \mathbf{A}_{\mathbf{ol/d}} - \mathbf{B}_{\mathbf{ol/d}}\mathbf{F} \tag{14}$$

where cl = closed-loop, ol = open-loop and d = discrete.

IV. OMOC Design and Simulations of Resulting Discrete Closed-Loop Power System Model

The power system under study is taken from [18] and is shown here in Fig. 2 (it consists of an 160MVA synchronous generator with conventional exciter supplying power through a transformer and a transmission line to an infinite grid).

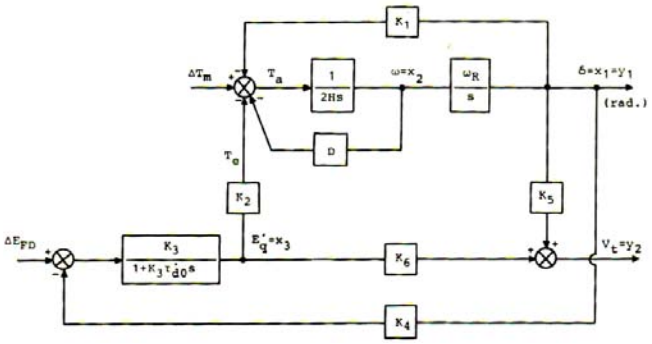

Fig. 2 : Simplified representation of investigated practical power system.

The continuous open-loop model describing this power system (taken from [18]) in the form of eq. (1) (with p_1=4 and p_2=8) is as follows

$$\begin{bmatrix}\dot{x}_1\\ \dot{x}_2\\ \dot{x}_3\end{bmatrix} = \begin{bmatrix}0 & 377 & 0\\ -0.1030 & -0.1818 & -0.1209\\ -0.3091 & 0 & -5.5517\end{bmatrix}\begin{bmatrix}x_1\\ x_2\\ x_3\end{bmatrix} + \begin{bmatrix}0 & 0\\ 0.0909 & 0\\ 0 & 0.1695\end{bmatrix}\begin{bmatrix}\Delta T_m\\ \Delta E_{FD}\end{bmatrix}$$

$$\begin{bmatrix}y_1\\ y_2\end{bmatrix} = \begin{bmatrix}1 & 0 & 0\\ -0.0433 & 0 & 0.4777\end{bmatrix}\begin{bmatrix}x_1\\ x_2\\ x_3\end{bmatrix}$$

Based on the transformed continuous open-loop power system model, the associated discrete one, in relation to equs. (3a), (3b), is given in Appendix B.

Where:

$$x = \left[\delta \;\; \omega \;\; \mathrm{E}_q^{'}\right],\quad u = \left[\Delta T_m \;\; \Delta \mathrm{E}_{FD}\right]^{T},\quad q = u,$$

$$y_m = [\delta \;\; V_t]^T, \quad y_c = x, \quad E = I_{3x3},$$
$$J_1 = 0_{2x2}, \quad J_2 = 0_{3x2}$$

The associated computed discrete linear open-loop power system model, based on the above linearized continuous open-loop system model, is given in Appendix B with a properly selected sampling period, i.e. $T_0 = 0.25$sec

Based on Fig. 1 and using the H^{∞} -control with OMCOs and the computed discrete linear open-loop model of the power system under study, the discrete closed-loop power system model is designed, considering the case with γ=5.68 and the computed values of **K**, $\mathbf{L_u}$ and **F** feedback gain matrices which are:

$$\mathbf{K} = \begin{bmatrix} 0.1790 & -0.4971 & -24.1404 & 52.3042 & -30.1999 \\ -0.0233 & 0.0655 & -0.6778 & 0.6982 & 0.6985 \end{bmatrix}$$

$$\mathrm{L_u} = 10^{-14} \times \begin{bmatrix} -0.0444 & 0.1082 \\ 0.0022 & -0.0329 \end{bmatrix}$$

$$\mathrm{F} = \begin{bmatrix} -0.2299 & 30.1281 & -0.9726 \\ 0.0110 & -0.2976 & 0.3434 \end{bmatrix}$$

The magnitude of the eigenvalues of the discrete original open-loop and of the designed closed-loop power system model are shown in Table 1.

Table 1 : Magnitude of eigenvalues of discrete original open-loop and designed closed-loop power system models.

Original open-loop power system model	$\lvert\lambda\rvert$	0.9342 0.9342 0.9539
Designed closed-loop power system model	$\lvert\hat{\lambda}\rvert$	0.5524 0.5524 0.8817

The simulated responses of the output variables (δ, ω, v_t) of the discrete original open-loop and designed closed-loop power system models, for zero initial conditions and unit step input disturbance, are shown in Fig. 3 and Fig. 4.

By comparing the computed eigenvalues of the simulated responses of the discrete original open-loop power system model and the associated designed discrete closed-loop models, it is clear that the resulting enhancement in the dynamic system stability of the closed-loop system model is remarkable.

It is to be noted that the solution results of the discrete system models (i.e. eigenvalues, eigenvectors, responses of system variables etc.) for zero initial conditions were obtained using a special software program (which is based on the theory of § 2 and runs on MATLAB program environment).

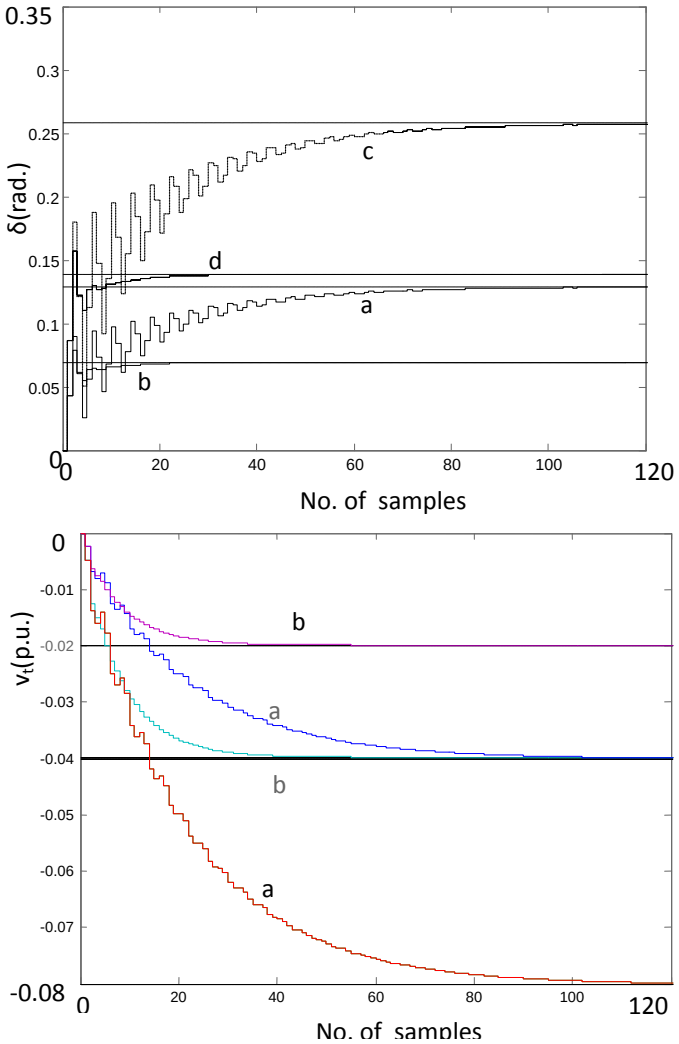

Fig. 3 : Responses of δ and v_t outputs subject to unit step input change and external disturbance where: (a) and (b) refer to discrete open-loop and closed-loop to step input change ΔT_m=0.05 and ΔE_{FD}=0.0p.u., (c) and (d) refer to discrete open-loop and closed-loop to step input change ΔT_m=0.10 and ΔE_{FD}=0.0p.u.)

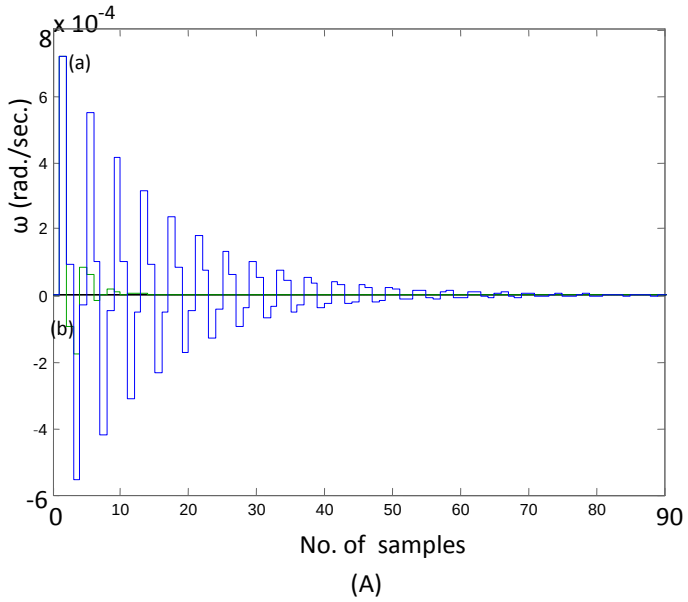

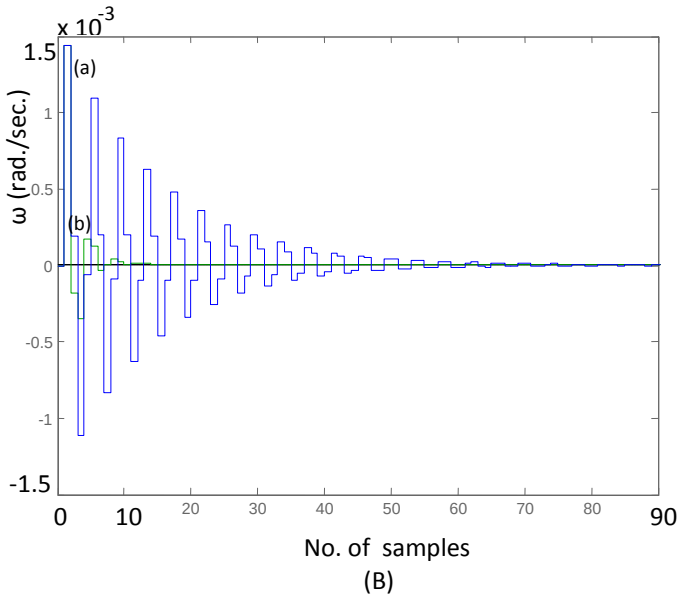

Fig. 4 : Response of ω output subject to unit step input change and external disturbance where: (a) and (b) refer to discrete open-loop and closed-loop to step input change: (A): ΔT_m=0.05 and ΔE_{FD}=0.0p.u., and (B): ΔT_m=0.10 and ΔE_{FD}=0.0p.u.

In Fig. 5, the maximum singular value of $T_{qy^c}(z)$ is depicted, as a function of the frequency ω.

Clearly, the design requirement $\left\|T_{qy_c}(z)\right\|_\infty \le 5.68$, is satisfied. Moreover, as it can be easily checked the poles of the closed loop system , lie inside the unit circle. Therefore, the requirement for the stability of the closed-loop system is also satisfied.

Not that, in the case of unsaturated machine the H^∞ -norm of the open-loop system transfer function between disturbances and controlled outputs has the value $\left\|C(j\omega I - A)^{-1}D\right\|_\infty = 71.9845$ while the minimum achievable disturbance attenuation level is γ_{inf} =0.325.

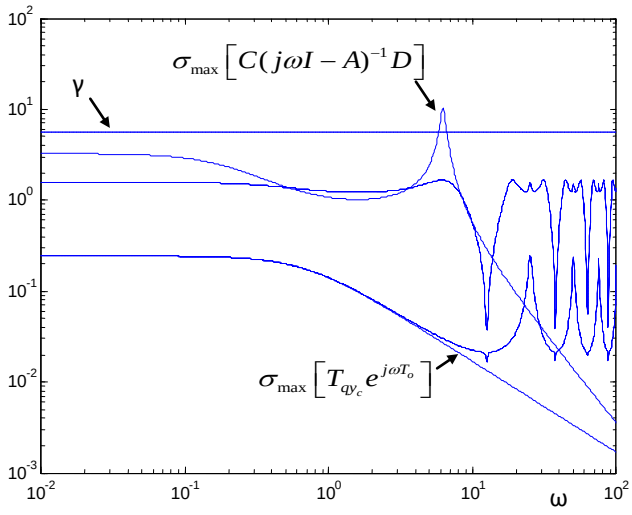

Fig. 5 : The maximum singular value of $Tqy_c(z)$ over ω, for the unsaturated machine and for γ=5.68.

V. Conclusions

An H^∞ -control technique based on optimal multirate-output controllers (OMOCs) has been presented in concise form for the purpose of attenuating in an effective manner system disturbances which otherwise degrade the performance of the synchronous machine. The application of the OMOC technique on the obtained discrete open-loop power system model yielded the associated (or designed) discrete closed-loop power system model. The respective simulation results of the open- and closed-loop models demonstrated clearly that the dynamic stability characteristics of the closed-loop model is far more superior than the associated one of the open-loop model. Therefore the presented H^∞ -control technique proved to be a reliable tool for the design of implementable OMCOs.

References Références Referencias

1. A.S. Rao V.S.R. Rao and M. Chidambaram, "*Direct synthesis-based controller design for integrating processes with time delay*", L. Franklin Inst., vol. 346, pp. 38-56, 2009.
2. R. Padma Sree, M.N. Srinivas and M. Chidambaram, *"A simple method of tuning PID controllers for stable and unstable FOPDT processes"*, Comp. Chemical Engg., vol. 28, pp. 2201-2218, 2004.
3. R.M Palhares and P. L. D Peres *"Robust H∞ - filtering design with pole placement constraint via linear matrix inequalities"* Journal of the Franklin Intitute 337, pp. 713-723, 2000.
4. J. Wang and H. Shao *"Delay-dependent robust and reliable H∞ control for uncertain time-delay systems with actuator failures"* Journal of the Franklin Institute, Volume 337, Issue 6, pp. 781-791, 2000.
5. K.G.Arvanitis, P.N.Paraskevopoulos, "*Sampled-data minimum H∞-norm regulation of linear continuous-*

time systems using multirate-output controllers". J. Optim.Theory Appls., vol. 87, 1995, pp. 235-267.

6. K.G.Arvanitis and G.Kalogeropoulos, *"Stability Robustness of LQ Optimal Regulators Designed on the Basis of the Multirate Sampling of the Plant Output"*, Journal of Optimization Theory and Applications (JOTA), vol. 97, pp. 299-337, 1998.
7. T. Chen and L. Qiu, *"H^{∞} design of general multirate sampled-data control systems"*, Automatica, vol. 30, pp. 1139-1152, 1994.
8. A.A. Stoorvogel, *"The discrete time H^{∞} -control problem with measurement feedback"*, SIAM J. Control Optim., vol. 30, pp. 180-202, 1992.
9. H.T. Toivonen, *"Sampled-data control of continuous-time systems with an H^{∞} -optimality criterion"*, Automatica, vol. 28, pp. 45-54, 1992.
10. I. Yaesh and U. Shaked, *"Minimum H^{∞} -norm regulation of linear discrete-time systems and its relation to linear quadratic discrete games"*, IEEE Trans. Autom. Control, vol. AC-35, pp. 1061-1064, 1990.
11. STOORVOGEL, A. A. *The H^{∞} -Control Problem.* Prentice Hall, Englewood Cliffs, New Jersey, 1992.
12. YAESH, I., SHAKED U. *Minimum H^{∞} -norm regulation of linear discrete-time systems and its relation to linear quadratic discrete games.* IEEE Trans. Autom. Control, vol. AC-35, 1990, pp. 1061-1064.
13. CHEN, QIU, L. *H^{∞} design of general multirate sampled-data control systems*. Automatica, vol. 30, 1994, pp. 1139-1152.
14. AHMED, S. S., CHEN, L., PETROIANU, *A. Design of Suboptimal H∞ Excitation Controllers*, IEEE Transactions on Power Systems, Vol. 11, No. 1, February 1996, pp. 312-318.
15. KIM, J. H., PARK, H. B. *H∞ State Feedback Control for Generalized Continuous/Discrete time-delay System*, Aytomatica 35, 1999, pp. 1443-1451.
16. LEE, S. S., PARK, J. K., LEE, J. J. *Extending standard H∞ controller to H∞ /sliding mode controller with an application to power system stabilisation*, IEE Proc.-Control Theory Appl. Vol. 146, No. 5, 1999, pp. 367-372.
17. GRIMBLE, M. J. Multi-Step H∞ Generalized *Predictive Control, Dynamic and Control*, 8, pp. 303-339, 1998.
18. D.P. Papadopoulos and A.K. Boglou, "Turbo generator system controller design via exact model - following techniques", Int. J. Systems Sci., vol. 18, No 12, 2239-2247, 1987.

APPENDIX A

Numerical values of the system parameters and the operating point (p.u. values on generator ratings)

Turbogenerator:

160 MVA, 2-pole, pf= 0.894, x_q=1.7, x_q=1.6, x'_d=0.245p.u.

τ'_{d0} =5.9, H=5.5s; ω_R=377rad/s D=2,0p.u.

External system:

R_e=0.02, X_e=0.40p.u. (on a 160 MVA base).

Operating point:

P_0=1.0, Q_0=0.5, E_{FDo}=2.5128, E_{qo}=0.9986, V_{t0}=1.0, T_{mo}=1.0p.u.; δ_0=1,1966rad; K_1=1,1330, K_2=1.3295, K_3=0.3072, K_4=1.8235, K_5=-0,0433, K_6=0.4777.

APPENDIX B

Constant matrices of discrete open-loop power system model based on Figs. 1 and 2 with sampling period T_0=0.25sec.

$$\mathbf{A}_{ol/d} = \begin{bmatrix} 0.0543 & 59.8421 & -1.0910 \\ -0.0155 & 0.0255 & -0.0176 \\ -0.0463 & -2.7891 & 0.9011 \end{bmatrix}$$

$$\mathbf{B}_{ol/d} = \begin{bmatrix} 0.8620 & -0.0170 \\ 0.0144 & -0.0005 \\ -0.0234 & 0.0399 \end{bmatrix}$$

$$\mathbf{C}_{ol/d} = \begin{bmatrix} 1 & 0 & 0 \\ -0.0433 & 0 & 0.4777 \end{bmatrix}$$

$$\mathbf{D}_{ol/d} = \begin{bmatrix} 0.08620 & -0.0170 \\ 0.0144 & -0.0005 \\ -0.0234 & 0.0399 \end{bmatrix}$$

Global Journal of researches in engineering
Electrical and electronics engineering
Volume 12 Issue 1 Version 1.0 January 2012
Type: Double Blind Peer Reviewed International Research Journal
Publisher: Global Journals Inc. (USA)
Online ISSN: 2249-4596 & Print ISSN: 0975-5861

Linear Kalman Filter Algorithm with Clarke Transformation for Power System Frequency Estimation

By Soliman Abdel-Handy, A.M. Al-Kandari, R.A.Alammari
Misr University for Science and Technology

Abstract - This paper presents a new application for linear Kalman filter algorithm for power system frequency estimation. The filter uses the digitized samples of the three-phase voltages or current waveform signals. These three phases are transformed into two **αβγ** -phases, using the well-known **αβγ** -transformation matrix. Having obtained the signal of the two new phases, a complex phasor is constructed using the new two-phase voltages. Kalman filter is then applied to extract the frequency and phase angle of the fundamental component of the complex and actual recorded phasor. The proposed algorithm is tested on simulated data at different conditions for the three phase signals; noise free and balanced three phase signals, unbalanced three-phase system and harmonics contaminated three phase signals. It has been shown that the proposed filters with the proposed transformation are succeeded to estimate the signal frequency at off nominal, near nominal and at nominal frequency.

Keywords : *Linear Kalman filter, frequency estimation, **αβ**-transformation.*

GJRE-F Classification: *FOR Code: 090601*

Strictly as per the compliance and regulations of:

Linear Kalman Filter Algorithm with Clarke Transformation for Power System Frequency Estimation

Soliman Abdel-Handy [α], A.M. Al-Kandari [σ], R.A.Alammari [ρ]

Abstract - This paper presents a new application for linear Kalman filter algorithm for power system frequency estimation. The filter uses the digitized samples of the three-phase voltages or current waveform signals. These three phases are transformed into two $\alpha\beta\gamma$ -phases, using the well-known $\alpha\beta\gamma$ -transformation matrix. Having obtained the signal of the two new phases, a complex phasor is constructed using the new two-phase voltages. Kalman filter is then applied to extract the frequency and phase angle of the fundamental component of the complex and actual recorded phasor. The proposed algorithm is tested on simulated data at different conditions for the three phase signals; noise free and balanced three phase signals, unbalanced three-phase system and harmonics contaminated three phase signals. It has been shown that the proposed filters with the proposed transformation are succeeded to estimate the signal frequency at off nominal, near nominal and at nominal frequency.

Keywords : *Linear Kalman filter, frequency estimation, $\alpha\beta$-transformation.*

I. Introduction

An accurate measurement for power system frequency as well as the voltage amplitude is essential in power system digital control and protection. The deviation of the system frequency from nominal frequency is an indication for the system unbalance. If the system frequency is below the nominal frequency, the load-shedding relay must shed the unimportant loads on the system to retain the system frequency to its nominal value. If the system frequency is above nominal frequency the generator governors must decrease the generator-input power to retain the frequency to its nominal value. As such, the power system frequency can be considered as a measure to the power balance in the system.

Many techniques have been proposed over the last twenty-five years for measuring digitally the power system frequency. Recently Ref. [1] presents an approach for measuring the system frequency using the complex extended Kalman filter and the well-known $\alpha\beta$-transformation, by this transformation a nonlinear state space formulation is obtained for extended Kalman filter.

The orthogonal FIR digital filter with least error squares algorithm are applied in Ref.[2] for measuring the operating frequency of a power system. The proposed algorithm in this reference was able to produce a correct and noise free estimate for near nominal, nominal and off-nominal frequency in about 25 ms.

The same algorithm with some modifications to reduce the computing time and improve the resolution is implemented in Ref. [3]. This algorithm has beneficial features including fixed sampling rate, fixed data window size and easy implementation.

Refs.. [4-6] present two orthogonal filters for power system frequency estimation. The essential property of the algorithms proposed in these references is that their outstanding immunity to both signal orthogonal component magnitudes and FIR filter gains variations. All the algorithms use the per-phase digitized voltage samples.

Prony's estimation is applied in Ref. [7] for measuring the system frequency together with the discrete Fourier transform (DFT) with a variable data widow to filter out the noise and harmonics associated with the signal. The static state estimation algorithms have been used in power systems measurements. The static least error squares algorithm is implemented in Refs.{15] and [16], while the dynamic estimation algorithms have been implemented in Ref.[17], these including linear and nonlinear Kalman filtering algorithms. Most but all of these algorithms use the per-phase digitized samples to estimate the system frequency. Each algorithm implemented up till now has its own figure of merit, and is only suitable for the system it works with. Also, all the available algorithms are either tested off-line or on-line, and they produce, in most cases, good estimates for the purposes they are designed for.

The design of an extended complex Kalman filter for the measurement of power system frequency has been presented in Ref. [1]. A complex model has been developed to track a distorted signal that belongs to a power system. The model inherently takes care of the frequency measurement along with the amplitude and phase of the signals. The proposed algorithm is

Author α : Misr University for Science and Technology, Electrical Power and Machines Department, 6th of October City, Giza, EGYPT. E-mail : sasoliman@must.edu.eg
Author σ : College of Technological Studies, Electrical Engineering Department, Shewiekh, Kuwait, Kuwait. E-mail : kandari1@yahoo.com
Author ρ : Qatar University, Electrical Engineering Dept., Doha, Qatar.

suitable for real-time applications where the measurement noise and other disturbances are high. Ref. [2] proposes a precise digital algorithm based on Discrete Fourier Transforms (DFT) to estimate the frequency of a sinusoid with harmonics in real-time. This algorithm is called the Smart Discrete Fourier Transforms (SDFT) smartly avoids the errors that arise when frequency deviates from the nominal frequency, and keeps all the advantages of the DFT e.g., immune to harmonics and the recursive computing can be used in SDFT.

Ref. [3] presents an analysis of methods for tracking the fundamental power frequency to see if they have the performance necessary to cope with the requirements of future protection and control equipment and are robust enough to cope with the more demanding nature of modern power system conditions.

An approach based on extended Kalman filter (EKF) for the measurement of power system frequency has been presented in Ref. [4]. The design principles and the validity of the model have been outlined in this reference. The performance of the proposed filter has been compared with some of the existing methods for estimating the frequency of a signal under noisy conditions. The feasibility of the proposed filter has been tested in the laboratory under worst-case measurement and network conditions, which might occur in a typical power system. Also, the proof of the stability for the proposed filter has been discussed for a single sinusoid. It has been found that the proposed algorithm is suitable for real-time applications especially when the frequency changes are abrupt and the signal is corrupted with noise and other disturbances due to harmonics.

Ref. [5] presents a unified power signal processor (PSP) for use in various applications in power systems. The introduced PSP is capable of providing a large number of signals and pieces of information which are frequently required for control, protection, status evaluation, and power quality monitoring of power systems. The PSP receives a set of locally measured three phase voltage and current signals and provides their fundamental components, amplitudes, phase angles, frequency, harmonics, instantaneous and stationary symmetrical components, active and reactive currents and powers, power factor, and the total harmonic distortion. Simplicity and integrity of its structure as well as its robustness with respect to internal parameters and external disturbances and noise render the proposed scheme very attractive for practical implementations.

An improved recursive Newton-type algorithm suitable for various measurement applications in electric power systems is presented in Ref. [6]. It is used for the power system frequency and spectra estimation. The recursive algorithm form is improved with a strategy of sequential tuning of the forgetting factor. By this, the proposed algorithm convergence and accuracy are significantly improved. A method for estimation of power frequency and its rate of change is presented in Ref.[7]. Unlike conventional methods which are based on the concept of linearization, the proposed scheme accommodates the inherent nonlinearity of the frequency estimation problem. This makes the method capable of providing a fast and accurate estimate of the frequency when its deviation from the nominal value is incremental or large. The estimator is based on a newly developed quadrature phase-locked loop concept. The method is highly immune to noise and distortions. The estimator performance is robust with respect to the parameters of its structure. Structural simplicity and performance robustness are other salient features of the method.

Ref. [8] introduces a phase-locked loop (PLL) system. The proposed system provides the dominant frequency component of the input signal and estimates its frequency. The mechanism of the proposed PLL is based on estimating in-phase and quadrature-phase amplitudes of the desired signal. The PLL provides a superior performance for power system applications. Advantages of the proposed PLL over the conventional PLLs are its capability of providing the fundamental component of the input signal which is not only locked in phase but also in amplitude to the actual signal while providing an estimate of its frequency. An approach to the design of a digital algorithm for local system frequency estimation is presented in Ref. [9]. The algorithm is derived using the maximum likelihood method. One sinusoidal voltage model was assumed. FIR digital filters are used to minimize the noise effect and to eliminate the presence of the harmonics effect. This technique provides accurate estimates with error in the range of 0.005 Hz in about 25 ms and requires modest computations.

A numerical differentiation-based algorithm for high-accuracy, wide-range frequency estimation of power systems is proposed in Ref. [10]. The signal includes up to 31st-order harmonic components. Using the central numerical differentiation of multi-points on the basis of Lagrange interpolation, the estimated frequency of nonsinusoidal signals of power systems can be measured at an accuracy of 99.999% over a wide range of from 10 to 100 Hz with fundamental amplitude varying from 100 to 300 V and with a fundamental phase angle varying from 0 to 360. The proposed algorithm needs at most two cycles or 40 ms for estimation of frequency over 40 to 60 Hz and needs at most three cycles or 60 ms over 10 to 40 Hz or 60 to 100 Hz.

The design of an extended complex Kalman filter for the measurement of power system frequency has been presented in Ref. [17]. A complex model has been developed to track a distorted signal that belongs to a power system. The model inherently takes care of the frequency measurement along with the amplitude and phase of the signals. The proposed algorithm is

suitable for real-time applications where the measurement noise and other disturbances are high. Ref. [18] proposes a precise digital algorithm based on Discrete Fourier Transforms (DFT) to estimate the frequency of a sinusoid with harmonics in real-time. This algorithm is called the Smart Discrete Fourier Transforms (SDFT) smartly avoids the errors that arise when frequency deviates from the nominal frequency, and keeps all the advantages of the DFT e.g., immune to harmonics and the recursive computing can be used in SDFT.

Ref. [19] presents an analysis of methods for tracking the fundamental power frequency to see if they have the performance necessary to cope with the requirements of future protection and control equipment and are robust enough to cope with the more demanding nature of modern power system conditions.

An approach based on extended Kalman filter (EKF) for the measurement of power system frequency has been presented in Ref. [20]. The design principles and the validity of the model have been outlined in this reference. The performance of the proposed filter has been compared with some of the existing methods for estimating the frequency of a signal under noisy conditions. The feasibility of the proposed filter has been tested in the laboratory under worst-case measurement and network conditions, which might occur in a typical power system. Also, the proof of the stability for the proposed filter has been discussed for a single sinusoid. It has been found that the proposed algorithm is suitable for real-time applications especially when the frequency changes are abrupt and the signal is corrupted with noise and other disturbances due to harmonics.

Ref. [21] presents a unified power signal processor (PSP) for use in various applications in power systems. The introduced PSP is capable of providing a large number of signals and pieces of information which are frequently required for control, protection, status evaluation, and power quality monitoring of power systems. The PSP receives a set of locally measured three phase voltage and current signals and provides their fundamental components, amplitudes, phase angles, frequency, harmonics, instantaneous and stationary symmetrical components, active and reactive currents and powers, power factor, and the total harmonic distortion. Simplicity and integrity of its structure as well as its robustness with respect to internal parameters and external disturbances and noise render the proposed scheme very attractive for practical implementations.

An improved recursive Newton-type algorithm suitable for various measurement applications in electric power systems is presented in Ref. [22]. It is used for the power system frequency and spectra estimation. The recursive algorithm form is improved with a strategy of sequential tuning of the forgetting factor. By this, the proposed algorithm convergence and accuracy are significantly improved. A method for estimation of power frequency and its rate of change is presented in Ref.[23]. Unlike conventional methods which are based on the concept of linearization, the proposed scheme accommodates the inherent nonlinearity of the frequency estimation problem. This makes the method capable of providing a fast and accurate estimate of the frequency when its deviation from the nominal value is incremental or large. The estimator is based on a newly developed quadrature phase-locked loop concept. The method is highly immune to noise and distortions. The estimator performance is robust with respect to the parameters of its structure. Structural simplicity and performance robustness are other salient features of the method.

Ref. [24] introduces a phase-locked loop (PLL) system. The proposed system provides the dominant frequency component of the input signal and estimates its frequency. The mechanism of the proposed PLL is based on estimating in-phase and quadrature-phase amplitudes of the desired signal. The PLL provides a superior performance for power system applications. Advantages of the proposed PLL over the conventional PLLs are its capability of providing the fundamental component of the input signal which is not only locked in phase but also in amplitude to the actual signal while providing an estimate of its frequency. An approach to the design of a digital algorithm for local system frequency estimation is presented in Ref. [25]. The algorithm is derived using the maximum likelihood method. One sinusoidal voltage model was assumed. FIR digital filters are used to minimize the noise effect and to eliminate the presence of the harmonics effect. This technique provides accurate estimates with error in the range of 0.005 Hz in about 25 ms and requires modest computations.

A numerical differentiation-based algorithm for high-accuracy, wide-range frequency estimation of power systems is proposed in Ref. [26]. The signal includes up to 31st-order harmonic components. Using the central numerical differentiation of multi-points on the basis of Lagrange interpolation, the estimated frequency of non-sinusoidal signals of power systems can be measured at an accuracy of 99.999% over a wide range of from 10 to 100 Hz with fundamental amplitude varying from 100 to 300 V and with a fundamental phase angle varying from 0 to 360. The proposed algorithm needs at most two cycles or 40 ms for estimation of frequency over 40 to 60 Hz and needs at most three cycles or 60 ms over 10 to 40 Hz or 60 to 100 Hz.

This paper presents a new application for linear Kalman filter algorithm for power system frequency estimation. The filter uses the digitized samples of the three-phase voltages or current waveform signals. These three phases are transformed into two $\alpha\beta\gamma$ -phases, using the well-known $\alpha\beta\gamma$ -transformation matrix. Having obtained the signal of the two new phases, a complex phasor is constructed using the new

two-phase voltages. Kalman filter is then applied to extract the frequency and phase angle of the fundamental component of the complex phasor. The proposed algorithm is tested on simulated data at different conditions for the three phase signals; noise free and balanced three phase signals, unbalanced three-phase system and harmonics contaminated three phase signals. It has been shown that the proposed filters with the proposed transformation are succeeded to estimate the signal frequency at off-nominal, near nominal and at nominal frequency. Also, the proposed algorithm is tested on actual recorded data generated from EMTP.

II. Modeling the Voltage Signals [1]

The three phase voltages of the power systems can be written at any sample k, k=1,..,..,m, m is the total number of samples available, as:

$$\begin{aligned} v_a(k) &= V_{ma}\sin(\omega k\Delta T+\phi_a) + \zeta_a(k)\\ v_b(k) &= V_{mb}\sin(\omega k\Delta T+\phi_b-120) + \zeta_b(k)\\ v_c(k) &= V_{mc}\sin(\omega k\Delta T+\phi_c+120) + \zeta_c(k) \end{aligned} \quad (1)$$

V_m	is the signal amplitude
ω	is the signal nominal frequency
ΔT	is the sampling time= $\frac{1}{F_s}$, F_s is the sampling frequency
k	is the sampling step; $k=1,..,m$
ϕ	is the signal phase angle
$\zeta_a(k),\zeta_b(k),\zeta_c(k)$	are the noise terms which may contain harmonics

The well-known $\alpha\beta$ - transformation (Clarke Transformation) for the three-phase signal is given as:

$$\begin{bmatrix} v_\alpha(k)\\ v_\beta(k)\end{bmatrix} = \sqrt{\frac{2}{3}}\begin{bmatrix}1 & -0.5 & -0.5\\ 0 & \frac{\sqrt{3}}{2} & \frac{-\sqrt{3}}{2}\end{bmatrix}\begin{bmatrix} v_a(k)\\ v_b(k)\\ v_c(k)\end{bmatrix} \quad (2)$$

The above equation can be rewritten as:

$$v_\alpha(k) = \sqrt{\frac{2}{3}}\left[v_a(k) - 0.5v_b(k) - 0.5v_c(k)\right] \quad (3)$$

$$v_\beta(k) = \sqrt{\frac{2}{3}}\left[\frac{\sqrt{3}}{2}v_b(k) - \frac{\sqrt{3}}{2}v_c(k)\right] \quad (4)$$

For m samples of the three-phase signal, then m samples for $v_\alpha(k), v_\beta(k)$ are obtained. By using this transformation, the harmonics of order three and their multiple are suppressed. Equation (3) and (4) give the transformed voltage $v_\alpha(k)$ and $v_\beta(k)$ at any sample k. The complex voltage formed from these two voltages which having the same frequency ω and phase angle Φ as the original three phases is:

$$\begin{aligned} v(k) &= v_\alpha(k) + jv_\beta(k)\\ &= V(k)e^{j(\omega k\Delta T+\phi)} \end{aligned} \quad (5)$$

Where the amplitude $V(k)$ of the complex signal is calculated at any sample k as:

$$V(k) = \left[v_\alpha^2(k) + v_\beta^2(k)\right]^{\frac{1}{2}} \quad (6)$$

and its rms value is

$$V^2K = \frac{1}{m}\sum_{k=1}^{m}\left[v_\alpha^2(k) + v_\beta^2(k)\right] \quad (7)$$

Equation (6) gives the value of complex voltage at any instant k, while e1uation (7) can be used to calculate the rms value of the complex voltage signal, while.

The phase angle of this transformed voltage is

$$\theta(k) = \tan^{-1}\frac{v_\beta(k)}{v_\alpha(k)} \quad (8)$$

Comparing equation (8) with equation (5), we can calculate the frequency of the voltage signals as;

$$\theta(k) = 2\pi kTf(k) + \phi(k) \quad (9)$$

Now, m samples are available for the phase angle of the transformed voltage $\theta(k)$. Define

$$\begin{aligned} &X_1(k) = f(k);\\ &X_2(k) = \varphi(k)\\ &and\\ &h_1(k) = 2\pi k\Delta T\\ &h_2(k) = 1 \end{aligned} \quad (10)$$

Then

$$\theta(k) = \begin{bmatrix}h_1(k) & h_2(k)\end{bmatrix}\begin{bmatrix}X_1(k)\\ X_2(k)\end{bmatrix} \quad (11)$$

For m samples available for $\theta(k)$, equation (11) can be written as:

$$\underline{Z}(k) = H(k)\underline{X}(k) + \underline{\zeta}(k) \quad (12)$$

Where $\underline{Z}(k)$ is $mx1$ vector of phase angle $\theta(k)$ at any instant k, $H(k)$ is $mx2$ measurement matrix whose elements depend on the sampling frequency and can be calculated off-line for a pre-specified sampling frequency. $\underline{X}(k)$ is $2x1$ state vector to be estimated and $\underline{\zeta}(k)$ is $mx1$ noise vector to be minimized.

The state space equation for the two-state model can be written as:

$$\underline{X}(k+1) = \phi(k)\,\underline{X}(k) + \underline{\nu}(k) \quad (13)$$

Where $\phi(k)$ is a $2x2$-identity matrix, and is called the state transition matrix, $\underline{\nu}(k)$ a is $2x1$-noise vector associated with the states when they are moving from k to k+1 sample. Now, equation (12) and (13) are suitable for Kalman filter implementation. Before going further let us interpret equations (6) and (8). Equation 6 gives the amplitude of the complex phasor formed from the two orthogonal voltages V_{α} and V_{β}. If the three phase voltages are balanced and are noise and harmonics free signals, this amplitude will be constant amplitude. Also, equation 8 gives the phase angle of this complex phasor. For the same balanced conditions, the rate of change of this phase angle, which is the speed of rotation of the complex phasor, will be constant and equals to the nominal angular velocity of the original three-phase signals. As such, the frequency of the will be constant during the data window size, and the locus of the complex phasor is a circle as shown in Figure1, by the dashed curve. However, if the three phases are unbalanced, then the locus of the complex Phasor will be just a closed curve as shown in Figure1. By plotting the complex Phasor the following advantages could be obtained

- It provides information about the system balance.
- It provides information about noise and harmonics contamination to the three-phase system.
- It provides information about the system frequency.
- Also, due to the nature of the $\alpha\beta$ -transformation, harmonics of order three and its multiple are suppressed

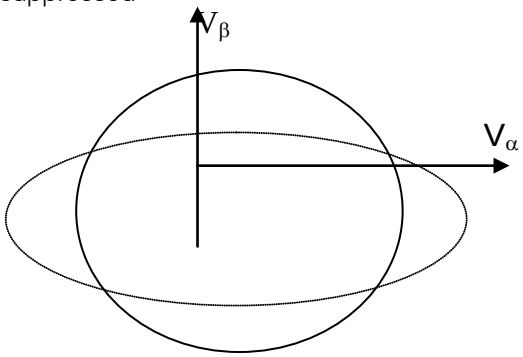

Figure 1 : The locus of the complex phasor

III. Testing the Algorithm Using Simulated Data

a) A balanced and noise free system

The proposed algorithm is tested using samples of a balanced and noise free three-phase system. The voltage amplitude is 1.0 p.u and the phase angle is -2.1 radian. The signal frequency is varied from 45-51 Hz. The three phase voltage signal are sampled at 3000 Hz (60 sample per cycle) and a data window size of 48 sample (0.8 cycle) is used in the estimation process. Figures 2 - 4 give the estimated frequency, phase angle and the amplitude of the complex phasor. Examining these figures reveals the following remarks.

- The proposed technique produces accurate estimates for the system frequency ranging from 45 to 51 Hz, i.e. accurate estimates are obtained for off-nominal, near nominal and at nominal frequency.
- The estimated phase angle is accurate and constant independent of the signal frequency.
- The amplitude of the complex phasor is also accurate and equals to the actual value at all the assumed frequency range.

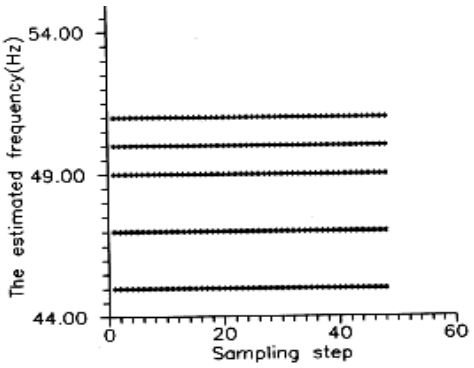

Figure 2 : Estimated frequencies

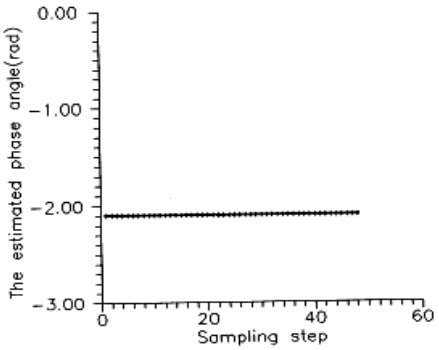

Figure 3 : The estimated phase angle

b) Unbalanced Three-phase Voltage Signal

The proposed algorithm is tested when there is unbalance between phases. Here, we use V_a = 1.0 p.u, V_b= 1.1 p.u and V_c=0.9 p.u, while the phase angle is -2.1 radian. The same sampling frequency, 3000 Hz, and

number of samples 48 samples are used. Figures 5-7 give the results obtained. Examining these figure reveals the following remarks, solid lines are the actual values,

- Good estimates are obtained when the signal frequency is 45, 48, 50, 51 Hz. Although there is about 0.5 Hz errors for the signal frequency of 51 Hz, but it is acceptable error for such unbalanced system.

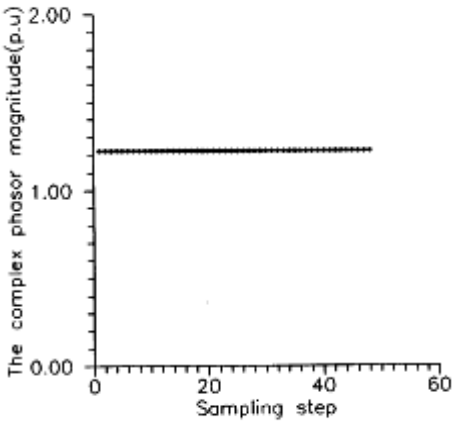

Figure 4 : Amplitude of the complex phasor

- The phase angle estimate is a good quality estimate at all the four frequencies of the signal, and there is a maximum error of about 0.1 radian (4.76 %), which is acceptable error in this unbalanced case.
- Figure 7 gives the amplitude of the complex phasor when the signal frequency is 50 Hz. It can be noticed that the amplitude is a time varying (figure 1 solid curve), but the rms. value over the estimation period gives almost the actual value of the amplitude.

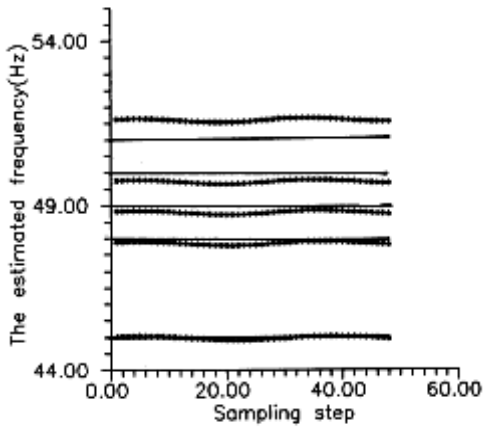

Figure 5 : Estimated frequencies

As such, we can conclude that the system unbalance and the degree of this unbalance have a great effect on the system estimates. Actually, that is true, if one examines Figure 1 carefully, he can notice that the amplitude as well as the argument of the complex phasor will be changed from instant to instant, if the phasor rotates on the solid curve.

IV. Harmonics Pollution

In this test, the proposed algorithm is tested with three-phase voltage signals contaminated with harmonics. The signals contain 1 p.u fundamental, 0.12 p.u second harmonic, 0.3 p.u third harmonic and 0.05 p.u fifth harmonic, all are balanced in the three phases. Figure 8 gives the locus of the complex phasor, which is not a circle; this means that this phasor has different amplitudes and arguments from instant to instant. Figure 9-11 give the estimated frequency, phase angle, and voltage amplitude. The sampling frequency used in this test is 3000 Hz and the data window size is 48 samples. Examining these figures reveals the following:

- ♣ The estimated frequency of the fundamental component is affected by the presence of harmonics in the voltage signal.

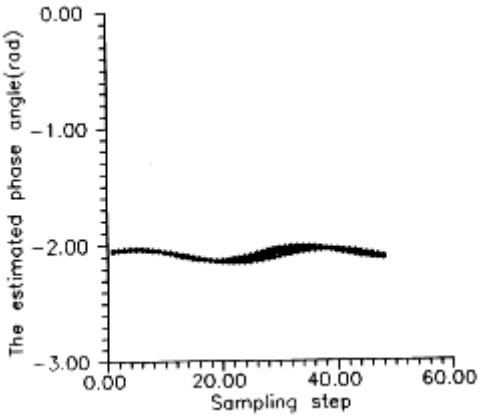

Figure 6 : Estimated phase angle

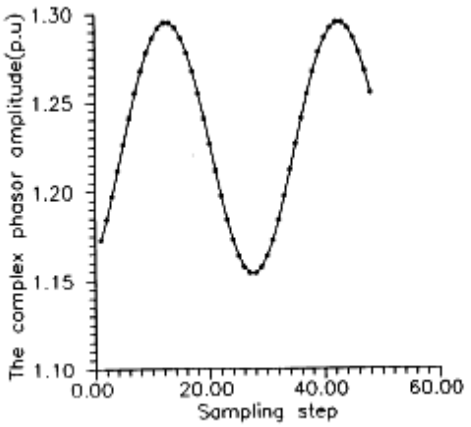

Figure 7 : Estimated complex phasor amplitude

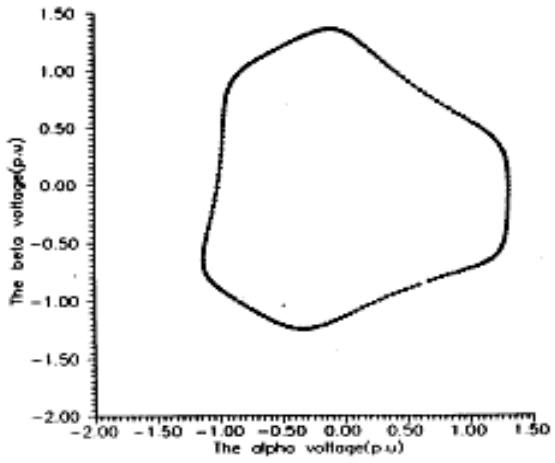

Figure 8 : Locus of complex phasor

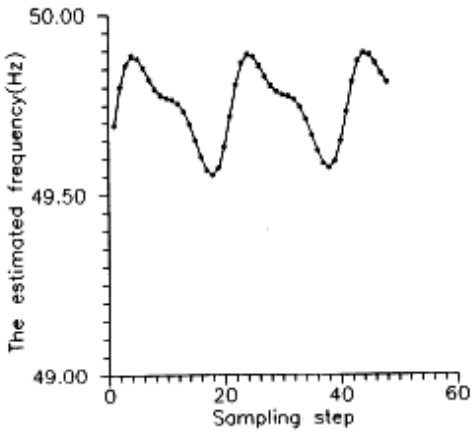

Figure 9 : The estimated frequency

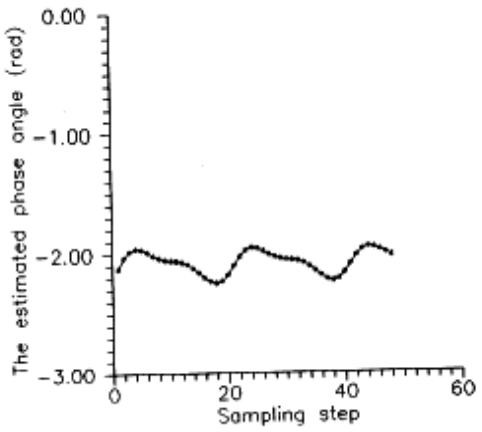

Figure 10 : Estimated phase angle

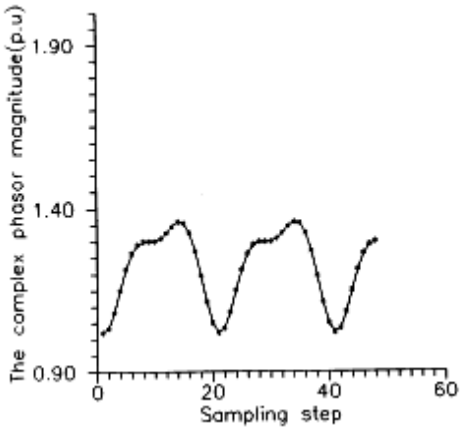

Figure 11 : Estimated complex phasor amplitude

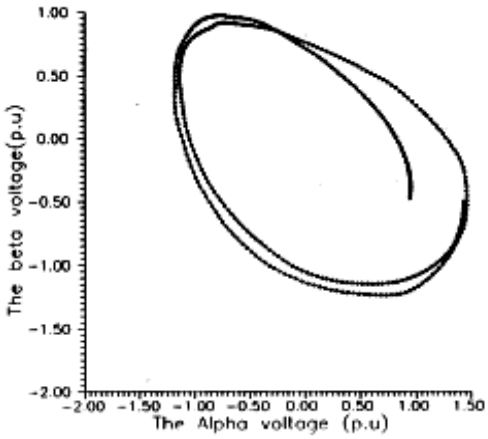

Figure 12 : Locus of the complex phasor

- The minimum frequency estimate for the fundamental component is about 49.6 Hz (error = -0.4 Hz, or -0.8 %), while the maximum frequency estimate is 49.9 (error=-0.1 Hz, or -0.2 %), which are considered good estimates for such polluted signals. However, due to the nature of $\alpha\beta$-transformation, the third harmonic has nothing to do with the estimates
- The average frequency estimate over the data window size used in this test is about 49.75 Hz, which is still a good estimate (error = -0.25 Hz, or -0.5 %)
- The phase angle estimate can be considered as good as the signals are contaminated with harmonics, and the average value is about -2.05 radian (error = -0.05 radian, or -2.3 %)
- As we said earlier, the complex phasor amplitude could be considered as a time varying amplitude, with rms value almost equals to the actual value.

V. Testing the Algorithm Using Actual Recorded data

The algorithm has also been tested using actual recorded data for a practical system in operation. The EMTP program is used to compute the three phase voltages at a certain bus on a system during the switching on of 500 kV transmission systems. Figure 12 gives the locus of the complex phasor formed by using the three phase signals and the proposed transformation. It can be noticed that, such a system is unbalanced and highly contaminated with harmonics system. These harmonics are not periodical waveforms. The sampling frequency used in this study is 10 kHz (ΔT = 0.1 ms) and a number of samples of 55 samples is used. Figures 13-15 give the estimated frequency, phase angle and the amplitude of the complex phasor. Examining these figures reveals the following remarks.

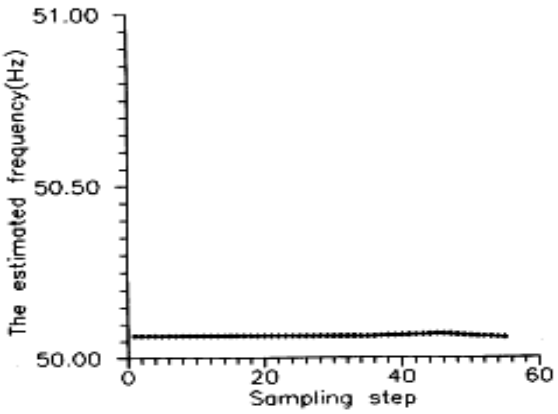

Figure 13 : Estimated frequencies

- The estimated frequency of the fundamental component is about 50.06 Hz, which could be considered as an accurate estimate (error=0.06 Hz, or 0.12%).
- The phase angle estimate can be considered as a good, and is a constant during the data window size used in this analysis.
- Although the amplitude of the complex phasor voltage is constant up to 79 % of the data window size, but its value is about 0.95 p.u. As we said, this value varies from instant to instant and does give induction to the effect of distortion of the three-phase signals amplitude.

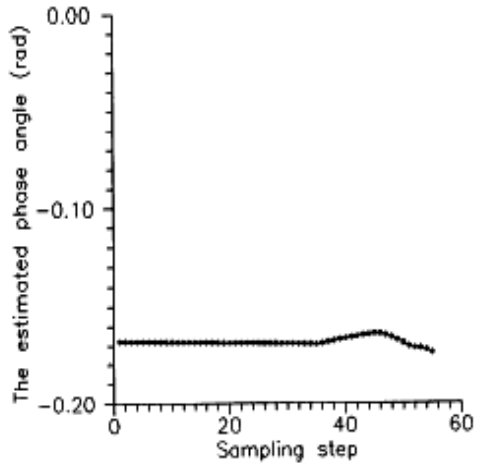

Figure 14 : Estimated phase angle

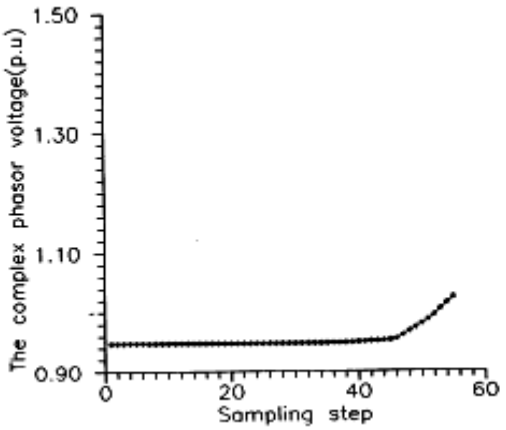

Figure 15 : Estimated complex phasor amplitude

VI. Conclusions

The main contributions of this paper are:

1. A complex phasor is developed which can be used to provide information about the system balance and harmonics contamination.
2. The linear Kalman filter is used to extract the frequency and phase angle of the fundamental component, using the argument of the complex voltage phasor.
3. The three phase voltage signals are used to estimate the system parameters, frequency, phase angle and voltage amplitude, using the well-known $\alpha\beta$-transformation. Unlike the available techniques, which use the per-phase voltage samples to estimate the system parameters?
4. The estimate using this technique is slightly affected by the noise and harmonics contamination.
5. Direct estimates are obtained for the system parameters, without modeling the three phase voltage signals.

References References Referencias

1. P. K. Dash, A. K. Pradhan, and G.Panda, "Frequency Estimation of Distorted Power System Signal Using Extended Complex Kalman Filter" IEEE Trans. on Power Delivery, Vol. 14, No.3, pp.761-766, July 1999.
2. T. S. Sidhu, "accurate Measurement of Power System Frequency Using a Digital Signal Processing" IEEE Trans. On Power Delivery, Vol. 14, No.1, pp.75-81, 1999.
3. T.S. Sidhu, and M. S. Sachdev, "An Accurate Technique for Fast and Accurate Measurement of Power System Frequency", IEEE Trans. on Power Delivery, Vol. 13, No.1, pp.109-115, 1998.
4. Jose A.dela O, H.J.Altave, and I.Diaz, " A New Digital Filter for Phasor Computation, Part I: Theory", IEEE Trans. on Power Systems, Vol.13, No.3, pp.1026-1031, 1998.
5. Jose a. dela O, H. J. Altave, and I. Diaze"A New Digital Filter for Phasor Computation, Part II: Evaluation", IEEE Trans. on Power Systems, Vol.13, No.3, pp.1032-1037, 1998.
6. J. Szafran, and W. Rebizant, "Power System Frequency Estimation", IEE Proc. Gener. Trans. Disturb., Vol.145, No.5, pp.578-582, 1998.
7. T. Lobos and J. Rezmer, "Real-time Determination of Power System Frequency", IEEE Trans. on Inst. and Measurement, Vol.46, No.4, pp.877-881, 1997.
8. P.J.Moore, R.D.Carranza and A.T.Johns, "Model System Test on a New Numeric Method of Power System Frequency Measurement", IEEE Trans. on Power Delivery, Vol.11, No.2, pp.696-701, 1996.
9. P.J.Moore, J.H.Allmeling and A.T.Johns, "Frequency Relaying Based on Instantaneous Frequency Measurement", IEEE Trans. on Power Delivery, Vol.11, No.4, pp.1737-1742, 1996.
10. V.Terzija, M.Djuric and B.Kovacevic, " A New Self-Tuning Algorithm for the Frequency Estimation of Distorted Signals" IEEE Trans. on Power Delivery, Vol.10, No.4 pp.1779-1785, 1995.
11. V.Terzija, M.Djuric and B.Kovacevic, " Voltage Phasor and Local System Frequency Estimation Using Newton-Type Algorithms"" IEEE Trans. on Power Delivery, Vol.14, No.3 pp.1368-1374, 1994.
12. M.M.Begovic, et-al, " Frequency Tracking in Power Network in the Presence of Harmonics", " IEEE Trans. on Power Delivery, Vol.8, No.2 pp.480-486, 1993.
13. M.Kezunovic, et-al, " New Digital Signal Processing Algorithm for Frequency Measurement"," IEEE Trans. on Power Delivery, Vol.7, No.3 pp.1563-1572, 1992.
14. S.A.Soliman, et-al, "Dynamic Tracking of the Steady State Power System Voltage Magnitude and Frequency Using Linear Kalman Filter: A Variable Frequency Model", Electric Machines and Power Systems, Vol. 20, pp.593-611, 1992.
15. S. A. Soliman, et-al ,"Estimating of Steady State Voltage and Frequency of Power Systems from Digitized Bus Voltage Samples", Electric Machines and Power Systems, Vol. 19, pp.555-567, 1991.
16. M. E. El-Hawary, et-al, "A Study of Estimation Techniques for Frequency-Relaying Applications", Can. J. Elect. & Comp. Eng., Vol.21, No.1, pp.9-20, 1996
17. P. K. Dash, R. K. Jena, G. Panda, and A. Routray," An Extended Complex Kalman Filter for Frequency Measurement of Distorted Signals", IEEE TRANSACTIONS ON INSTRUMENTATION AND MEASUREMENT, VOL. 49, NO. 4, AUGUST 2000
18. Jun-Zhe Yang and Chih-Wen Liu," A Precise Calculation of Power System Frequency", IEEE TRANSACTIONS ON POWER DELIVERY, VOL. 16, NO. 3, JULY 2001.
19. D W. P. Thomas, and M. S. Woolfson," Evaluation of Frequency Tracking Methods", IEEE TRANSACTIONS ON POWER DELIVERY, VOL. 16, NO. 3, JULY 2001
20. A. Routray, A. K. Pradhan, and K. P. Rao," A Novel Kalman Filter for Frequency Estimation of Distorted Signals in Power Systems" IEEE TRANSACTIONS ON INSTRUMENTATION AND MEASUREMENT, VOL. 51, NO. 3, JUNE 2002.
21. M. Karimi-Ghartemani and M. R. Iravani," A Signal Processing Module for Power System Applications", IEEE TRANSACTIONS ON POWER DELIVERY, VOL. 18, NO. 4, OCTOBER 2003.
22. Vladimir. V. Terzija," Improved Recursive Newton-Type Algorithm for Frequency and Spectra Estimation in Power Systems" IEEE TRANSACTIONS ON INSTRUMENTATION AND MEASUREMENT, VOL. 52, NO. 5, OCTOBER 2003
23. H. Karimi, M. Karimi-Ghartemani, and M. R. Iravani," Estimation of Frequency and its Rate of Change for Applications in Power Systems" IEEE TRANSACTIONS ON POWER DELIVERY, VOL. 19, NO. 2, APRIL 2004.
24. H. Karimi, M. Karimi-Ghartemani, and M. R. Iravani, " Magnitude/Phase-Locked Loop System Based on Estimation of Frequency and In-Phase/Quadrature-Phase Amplitudes" IEEE TRANSACTIONS ON INDUSTRIAL ELECTRONICS, VOL. 51, NO. 2, APRIL 2004.
25. M. D. Kuˇsljevic," A Simple Recursive Algorithm for Frequency Estimation", IEEE TRANSACTIONS ON INSTRUMENTATION AND MEASUREMENT, VOL. 53, NO. 2, APRIL 2004.
26. Wu Jiekang, Long Jun, and Wang Jixiang," High-Accuracy, Wide-Range Frequency Estimation Methods for Power System Signals under Nonsinusoidal Conditions", IEEE TRANSACTIONS ON POWER DELIVERY, VOL. 20, NO. 1, JANUARY 2005.

Appendix

III. Linear Kalman Filter Algorithm [14]

In the implementation of Kalman filter, the mathematical model for the system under consideration should be in the state form as:

$$\boldsymbol{x}(k+1) = \phi(k)\,\boldsymbol{x}(k) + \boldsymbol{\omega}(k)$$

and the observation(measurement) of the process is assumed to occur at discrete points of time in accordance with the relation

$$\boldsymbol{z}(k) = H(k)\,\boldsymbol{x}(k) + \boldsymbol{v}(k)$$

Assume that we have a prior estimate $\mathbf{x}^{-}(k)$, and its error covariance matrix $P^{-}(k)$; then the general recursive filter equations are as follows

a) Compute the Kalman gain filter, $\boldsymbol{K}(k)$, as

$$K(k) = P^{-}(k)H^{T}(k)[H(k)P^{-}(k)H^{T}(k) + R(k)]^{-1}$$

b) Compute the error covariance for the update

$$P(k) = [\,I - K(k)H(k)]\,P^{-}(k)$$

c) Update the estimate with the measurement $\boldsymbol{z}(k)$ as

$$x(k) = x^{-}(k) + K(k)[z(k) - H(k)x^{-}(k)]$$

d) Project ahead, the error covariance and the estimate

$$P^{-}(k+1) = \phi(k)\,P(k)\,\phi^{T}(k) + Q(k)\;x^{-}(k+1) = \phi(k)\,x^{-}(k)$$

a) Initialization of the Kalman Filter

For off-line application, it is necessary to initialize the recursive process of the Kalman filter, with an initial vector $\mathbf{x}_o^{-}$ and its initial covariance matrix $\mathbf{P}_O$. Also, the system and measurement noise variances are needed.

A simple deterministic procedure is implemented to calculate the initial process vector, as well as its covariance matrix, using the static least error squares estimate of the previous measurements. Thus, in general the initial process vector may be computed as

$$x_o^{-} = [H^{T}H]^{-1}\,H^{T}\,z$$

and the corresponding covariance error matrix is

$$P_o = [H^{T}H]^{-1}H^{T}$$

Global Journal of researches in engineering
Electrical and electronics engineering
Volume 12 Issue 1 Version 1.0 January 2012
Type: Double Blind Peer Reviewed International Research Journal
Publisher: Global Journals Inc. (USA)
Online ISSN: 2249-4596 & Print ISSN: 0975-5861

Analytical Study of a Solid Beam Driven Plasma- Loaded Backward Wave Oscillator

By Dilip Kumar Sarker, Md. Mortuza Ali, Diponkar Kundu, Md. Galib Hasan, Pallab Kanti Podder

Pabna Science & Technology University

Abstract - In this paper, an analytical expression comprising linear instability phenomena leading to microwave generation in a solid beam driven plasma-loaded backward wave oscillator has been developed. This analytical treatment is a process of three-wave interaction and is based on the approximate linear theory of instability established for annular beam driven vacuum backward wave oscillator. The dispersion relation derived here is an approximate one and it can be successfully employed to study a backward wave oscillator system consisting of a sinusoidal corrugated structure having very smaller corrugation depth.

Keywords : *BWO, SWS, instability, plasma-loaded, dispersion, corrugated structure.*

GJRE-F Classification: *FOR Code: 090609, 090699*

Strictly as per the compliance and regulations of:

Analytical Study of a Solid Beam Driven Plasma-Loaded Backward Wave Oscillator

Dilip Kumar Sarker[α], Md. Mortuza Ali[σ], Diponkar Kundu[ρ], Md. Galib Hasan[ω], Pallab Kanti Podder[¥]

Abstract- **In this paper, an analytical expression comprising linear instability phenomena leading to microwave generation in a solid beam driven plasma-loaded backward wave oscillator has been developed. This analytical treatment is a process of three-wave interaction and is based on the approximate linear theory of instability established for annular beam driven vacuum backward wave oscillator. The dispersion relation derived here is an approximate one and it can be successfully employed to study a backward wave oscillator system consisting of a sinusoidal corrugated structure having very smaller corrugation depth.**

Keywords : BWO, SWS, instability, plasma-loaded, dispersion, corrugated structure.

I. Introduction

Backward wave oscillator (BWO) is a well-known device which transforms the kinetic energy of electron beam into microwave radiation [15]. In this device an electron beam is injected into a slow wave structure (SWS) with the guidance of a strong axial magnetic field. During the propagation of beam through the SWS it interacts with the normal electromagnetic modes of the structure. This leads to a transfer of electron kinetic energy to the radiation field. The BWO operates at the vicinity on the dispersion curve, where the group velocity of the structure wave is negative. This causes a propagation of the wave energy against the flow of beam electrons. That is why the device is so named. The phenomenon of interaction among the beam electrons and the normal modes of the BWO structure can be expressed by a linear dispersion relation.

This dispersion relation predicts the existence of an instability that leads to the generation of microwaves. It was found by some researchers that resonance enhancement of microwave radiation can be achieved when a BWO operates in presence of background gas and plasma [2,9]. With this achievement, it was also found theoretically as well as experimentally that plasma injection into the BWO structure enhances the power output, interaction efficiency and spatial growth rates much more than that of vacuum cases [1-8,11,16,17]. Effect of geometrical parameters of BWO structure on the dispersion characteristics and instability phenomena were presented by some researchers [12,14]. In some dissertation, the resonance interaction in the BWO with thin as well as thick annular electron beam has been studied [4, 10]. In this paper, plasma-loaded BWO structure having very smaller corrugation depth with solid electron beam is selected. Thus, it becomes possible to develop a simple analytical form of dispersion relation. To do this work, the cubic dispersion equation describing the frequency and wave number perturbations of the three-waves involved in the resonance interaction as developed earlier [13], is taken as the base. With the realization of the merits of plasma injection into the device, this theory for vacuum case with an annular electron beam is modified and extended for plasma-loaded BWO with a solid electron beam.

Section-2 of this paper contains model description, formulation and pre-requisite comparative studies about the accuracy and concreteness of the SWS model and necessary assumptions. In section-3, the derivation of the analytical dispersion relation has been presented. Section-4 presents discussions and conclusions.

II. Model Description and Formulation

In order to derive the analytical dispersion relation, a BWO system model as shown in Fig. 1 is considered. It consists of a sinusoidally corrugated wall structure, having very smaller corrugation depth, h (i.e., $h<<R_0$) according to the relation:

$$R(z) = R_0\,[1 + a\cos(k_0 z)] \qquad (1)$$

where, R(z)=the inner surface radius of the structure; $a=h/R_0$; $k_0=2\pi/z_0$; z_0=period of corrugation. of the structure inner wall.

Author[α]: Department of Electrical and Electronic Engineering, Pabna Science & Technology University,Pabna-6600, Bangladesh.
Email : dks_ms@yahoo.com
Author[σ]: Department of Electrical and Electronic Engineering, Rajshahi University of Engineering & Technology,Rajshahi, Bangladesh.
Email : mmali.ruet@gmail.com
Author[ρ]: Department of Electrical and Electronic Engineering, Pabna Science & Technology University,Pabna-6600, Bangladesh.
Email : d.kundu.eee@gmail.com
Author[ω]: Department of Electrical and Electronic Engineering, Pabna Science & Technology University, Pabna-6600, Bangladesh.
Email : eeemgh@yahoo.com
Author[¥]: Department of Information and Communication Engineering, Pabna Science & Technology University,Pabna-6600, Bangladesh.
Email : pallab_ice@yahoo.com

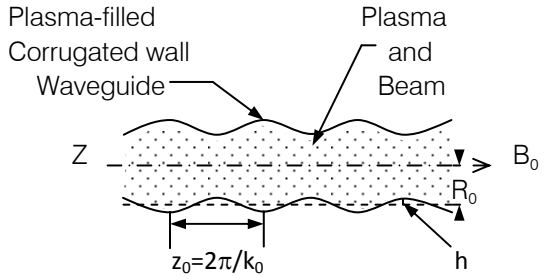

Figure 1. Plasma loaded sinusoidal corrugated slow wave structure and electron beam model.

The structure filled completely and uniformly with cold, collisionless and neutralized plasma of density N_p and a monoenergatic relativistic electron beam of density N_b. The beam is moving along the waveguide axis with a velocity v_b relative to the background plasma with the guidance of a strong and infinite magnetic field B_0. The numerical dispersion relation of this system, D(k, ω) = 0[14], where D is the value of the determinant of a square matrix with elements D_{mn} and k and ω are respectively the wave number and frequency.

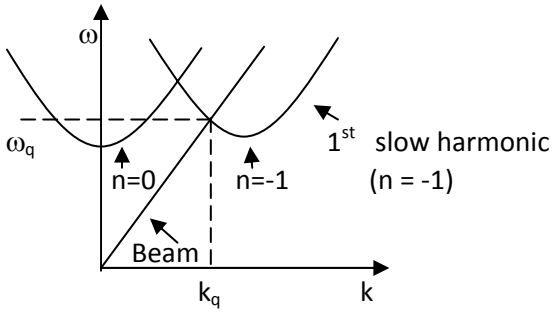

Figure 2: Resonance of the zeroth beam and electromagnetic first slow harmonic.

To derive the analytical expression for growth rates at the saddle point of this system, the resonance interaction of the zeroth beam harmonic with the electromagnetic first slow harmonic (n=-1) as shown in Fig.2 is considered. The approximate dispersion relation for this case is given below:

$$\begin{bmatrix} D_{-1-1} & D_{-10} \\ D_{0-1} & D_{00} \end{bmatrix} = 0 \qquad (2)$$

The matrix elements of the above relation are:

$$\left.\begin{aligned} D_{-1-1} &= J_0(X_{-1}) \\ D_{00} &= J_0(X_0) \\ D_{-10} &= \left(1+\frac{k_0 k}{\frac{\omega^2}{c^2}-k^2}\right)\frac{a}{2}X_0 J_0'(X_0) \\ D_{0-1} &= \left(1-\frac{k_0 k_{-1}}{\frac{\omega^2}{c^2}-k_{-1}^2}\right)\frac{a}{2}X_{-1}J_0'(X_{-1}) \end{aligned}\right\} \qquad (3)$$

Here,

$$\frac{X_n^2}{R_0^2} = \left(\frac{\omega^2}{c^2}-k_n^2\right)\left(1-\frac{\omega_p^2}{\omega^2}\right) - \left[\left(\frac{\omega^2}{c^2}-k^2\right)\frac{\omega_b^2}{\gamma^3(\omega-k_n v_b)^2}\right]\delta_{n,0} \qquad (4)$$

where, c, ω_p, ω_b and v_b are light velocity, plasma frequency, beam frequency and light velocity respectively, and $\delta_{n,0} = 0$ unless n = -1; $k_n = (k + nk_0)$.

The oscillation frequency ω_q and hence the wave number k_q can be obtained by solving eq.(2) with $\omega_b = 0$. However, for the zeroth approximation of the corrugation depth, the approximate value of ω_q and k_q can be obtained by solving simultaneously the following two equations.

$$R_0^2\left(\frac{\omega_q^2}{c^2}-(k_q-k_0)^2\right)\left(1-\frac{\omega_p^2}{\omega_q^2}\right) = (\mu_{0s})^2 \qquad (5)$$

$$\omega_q = k_q v_b \qquad (6)$$

Here $\mu_{0s} = 2.405$, is the first zero of $J_0(X_n)$ in absence of beam i.e., $X_b = 0$

Before approaching the derivation of the analytical dispersion equation, the following two comparative studies have been done, in order to verify it's degree of accuracy. For a full period of wave number of the corrugated structure, the dispersion characteristics of the corrugated as well as cylindrical waveguide have been drawn on the same graph in Fig.3, assuming the same average radius of the two structures. The dispersion curve of the corrugated structure is drawn with a corrugation period 0.02 cm, using the numerical dispersion relation D(k, ω) = 0, and that of the cylindrical one is drawn using eq.(5) with $(k_q - k_0)$ replaced by k.

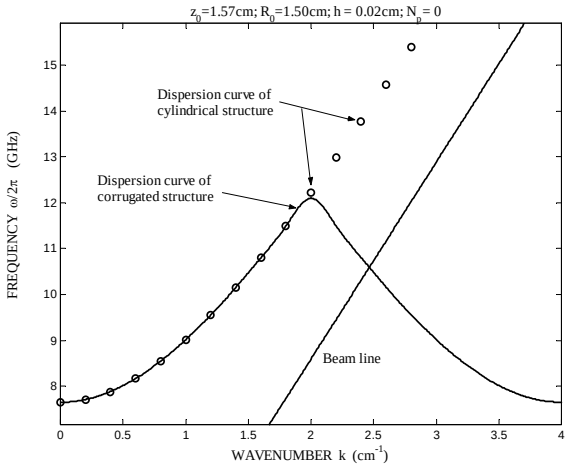

Figure3 : Dispersion characteristics of corrugated and cylindrical waveguides for TM_{01} mode.

The curves of solid line and open circles indicate the dispersion characteristics of corrugated and cylindrical waveguides respectively. Here, it has been carefully observed that, for very smaller corrugation depth, the dispersion curve of the corrugated structure within the range of wave number ($0 \le k \le k_0/2$), coincide completely with that of the cylindrical waveguide.

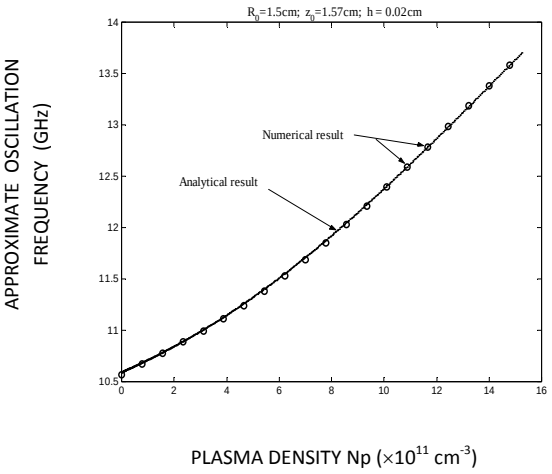

Figure4 : Approximate oscillation frequency versus plasma density characteristics.

This indicates the validity of the proposed analytical expression for resonance interaction as indicated in Fig.2. For the corrugated structure used in this paper having very smaller corrugation depth (h = 0.02cm), approximate oscillation frequency $\omega_q/2\pi$ versus plasma density N_p curves shown in Fig.4 have been drawn analytically as well as numerically in absence of electron beam. Here analytical curve is drawn using the equation that involves with the proposed expression and the numerical curve is obtained from the full dispersion relation [14].The curves of solid line and open circles indicate the analytical and numerical results respectively. In this observation, it is found that the analytical results are in excellent agreement with the numerical ones.

From the above two observations it is decided hopefully that, analytical dispersion expression of three-wave interaction (structure wave with n = 0, structure wave with n = -1 and the beam space charge wave) can be established successfully for the BWO structure used in this paper.

III. Derivation of the Dispersion Relation

At modest beam densities, $D_{mn}(\omega_q,k_q,X_b)$'s arround the root of $D_{mn}(\omega_q,k_q,X_b=0)$ is given by Tailor's series as,

$$D_{mn}(\omega_q,k_q,X_b) = D_{mn}(\omega_q,k_q,X_b=0) + \delta\omega\frac{\partial}{\partial\omega}D_{mn}(\omega_q,k_q,X_b=0) + \delta k\frac{\partial}{\partial k}D_{mn}(\omega_q,k_q,X_b=0) + X_b\frac{\partial}{\partial X_b}D_{mn}(\omega_q,k_q,X_b)\Big|_{\substack{\omega=\omega_q\\k=k_q\\X_b=0}} \quad (7)$$

Here, $X_b = -\left(\frac{\gamma^{-3}\omega_b^2}{(\omega-k_n v_b)^2}\right)$ and $\delta\omega = \omega-\omega_q,\ \delta k = k-k_q$

Therefore in presence of electron beam

$$D_{-1-1} = \left[J_0(X_{-1}) + J_0'(X_{-1})\left(\delta\omega\frac{\partial X_{-1}}{\partial\omega} + \delta k\frac{\partial X_{-1}}{\partial k}\right)\right]\Big|_{\substack{\omega=\omega_q\\k=k_q}}$$

$$D_{00} = \left[J_0(X_0) + J_0'(X_0)\left(\delta\omega\frac{\partial X_0}{\partial\omega} + \delta k\frac{\partial X_0}{\partial k}\right)\right]\Big|_{\substack{\omega=\omega_q\\k=k_q}}$$

$$D_{-10} = \left[1+\frac{k_q k_0}{\frac{\omega_q^2}{c^2}-k_q^2}\right]\frac{a}{2} \times\left\{\left[X_0 J_0'(X_0)\right]_{\substack{\omega=\omega_q\\k=k_q}} + \left[X_b J_0'(X_0)\frac{\partial X_0}{\partial X_b} + X_b X_0 J_0''(X_0)\frac{\partial X_0}{\partial X_b}\right]\Big|_{\substack{\omega=\omega_q\\k=k_q\\X_b=0}}\right\}$$

$$D_{0-1} = \left(1+\frac{k_0(k_q-k_0)}{\frac{\omega_q^2}{c^2}-(k_q-k_0)^2}\right)\frac{a}{2}X_{-1}J_0'(X_{-1})\Big|_{\substack{\omega=\omega_q\\k=k_q}}$$

The terms $\delta\omega\frac{a}{2}$ and $\delta k\frac{a}{2}$ have been neglected.

Therefore, the solution of the determinant of eq.(2) is given by:

$$\left[J_0(\lambda_{-1}) + J_0'(\lambda_{-1})\left(\delta\omega\frac{\partial\lambda_{-1}}{\partial\omega} + \delta k\frac{\partial\lambda_{-1}}{\partial k}\right)\right]$$

$$\times\left[J_0(\lambda_0)+J_0'(\lambda_0)\left(\delta\omega\frac{\partial\lambda_0}{\partial\omega}+\delta k\frac{\partial\lambda_0}{\partial k}\right)\right]=\frac{a^2}{4}\lambda_{-1}J_0'(\lambda_{-1})$$

$$\times\left[1+\frac{k_0k_q}{\frac{\omega_q^2}{c^2}-k_q^2}\right]\left[1-\frac{k_0(k_q-k_0)}{\frac{\omega_q^2}{c^2}-(k_q-k_0)^2}\right]$$

$$\left[\lambda_0J_0'(\lambda_0)+\{J_0'(\lambda_0)+\lambda_0J_0''(\lambda_0)\}X_b\frac{\partial X_0}{\partial X_b}\right] \quad (8)$$

Here, $\lambda_n = X_n(\omega_q, k_q, X_b = 0)$

Defining $\left[1+\frac{k_0k_q}{\frac{\omega_q^2}{c^2}-k_q^2}\right]\left[1-\frac{k_0(k_q-k_0)}{\frac{\omega_q^2}{c^2}-(k_q-k_0)^2}\right]=\beta_1$,

Equation (8) becomes,

$$\left[J_0(\lambda_{-1})+J_0'(\lambda_{-1})\left(\delta\omega\frac{\partial\lambda_{-1}}{\partial\omega}+\delta k\frac{\partial\lambda_{-1}}{\partial k}\right)\right]$$

$$\times\left[J_0(\lambda_0)+J_0'(\lambda_0)\left(\delta\omega\frac{\partial\lambda_0}{\partial\omega}+\delta k\frac{\partial\lambda_0}{\partial k}\right)\right]$$

$$=\beta_1\frac{a^2}{4}\lambda_{-1}J_0'(\lambda_{-1})\left[\lambda_0J_0'(\lambda_0)+\{J_0'(\lambda_0)+\lambda_0J_0''(\lambda_0)\}X_b\frac{\partial X_0}{\partial X_b}\right] \quad (9)$$

After simplification, neglecting the terms containing $\delta^2\omega$, δ^2k, $\delta\omega\,\delta k$ and equating $J_0(\lambda_0)J_0(\lambda_{-1})-\beta_1\frac{a^2}{4}\lambda_0\lambda_{-1}J_0'(\lambda_0)J_0'(\lambda_{-1})$ to zero (as it is the original dispersion relation) yields,

$$J_0(\lambda_0)J_0'(\lambda_{-1})\left(\delta\omega\frac{\partial\lambda_{-1}}{\partial\omega}+\delta k\frac{\partial\lambda_{-1}}{\partial k}\right)=\beta_1\frac{a^2}{4}\lambda_{-1}J_0'(\lambda_{-1}) \quad (10)$$
$$\{J_0'(\lambda_0)+\lambda_0J_0''(\lambda_0)\}X_b\frac{\partial X_0}{\partial X_b}$$

Finally, the following form of analytical dispersion relation of a plasma loaded BWO is obtained:

$$(\delta\omega-v_b\delta k)^2(\delta\omega-v_g\delta k)=\Delta \quad (11)$$

Where, $\Delta=-\frac{\omega_b^2\gamma^{-3}\beta_1a^2\lambda_{-1}^2\left(\frac{\omega_q^2}{c^2}-k_q^2\right)}{8\lambda_0\left[\frac{\omega_q}{c^2}-\frac{\omega_p^2(k_q-k_0)^2}{\omega_q^3}\right]}\times\frac{J_0'(\lambda_{-1})}{J_0(\lambda_0)}\left[1+\lambda_0\frac{J_0''(\lambda_0)}{J_0'(\lambda_0)}\right]$;

$$v_g=\frac{\partial\omega}{\partial k} \text{ and } \frac{J_0'(\lambda_{-1})}{J_0(\lambda_0)}\left[1+\lambda_0\frac{J_0''(\lambda_0)}{J_0'(\lambda_0)}\right]=\begin{cases}1 \text{ for } \lambda_0 \text{ is imaginary}\\ -1 \text{ for } \lambda_0 \text{ is real}\end{cases}$$

Eq. (11) is a cubic equation describing the frequency and wave number perturbations of the three waves involved in the resonance interaction.

The properties of the dispersion relation can be conveniently investigated by converting eq.(11) into dimensionless form in the following way [13]:

$$\left\{\frac{|\alpha\Delta|^{\frac{1}{3}}\frac{\delta\omega}{|\alpha\Delta|^{\frac{1}{3}}}-|\alpha\Delta|^{\frac{1}{3}}\delta k\left|v_b^2v_g/\Delta\right|^{\frac{1}{3}}}{}\right\}^2$$

$$\times\left\{\frac{|\alpha\Delta|^{\frac{1}{3}}\frac{\delta\omega}{|\alpha\Delta|^{\frac{1}{3}}}-|\alpha\Delta|^{\frac{1}{3}}v_g\delta k\left|\frac{v_g/v_b}{\Delta}\right|^{\frac{1}{3}}}{}\right\}=\Delta$$

$$|\alpha\Delta|^{\frac{2}{3}}(x-y)^2\left(x-\frac{y}{\alpha}\right)|\alpha\Delta|^{\frac{1}{3}}=\Delta$$

$$(x-y)^2(y-\alpha x)=-\frac{\alpha\Delta}{|\alpha\Delta|}$$

$$(x-y)^2(y-\alpha x)=-u$$

Where, $\alpha=\frac{v_b}{v_g}$; $x=\frac{\delta\omega}{|\alpha\Delta|^{\frac{1}{3}}}$; $y=\delta k\left|\frac{v_b^2v_g}{\Delta}\right|^{\frac{1}{3}}$; $u=\frac{\alpha\Delta}{|\alpha\Delta|}=\pm1$

Thus, the dimensionless dispersion relation is obtained as,

$$D(x,y)=(y-x)^2(y-\alpha x)+u=0 \quad (12)$$

Equation (12) is quite simillar to that derived for vacum BWO driven by annular electron beam [13].

In the BWO, the instability is absolute and this occurs when the two roots of y in eq.(12) merge with one another for some value of x with positive imaginary part. This value of x can be found from the simultaneous solutions to eq. (12) and eq. (13).

$$\frac{\partial D}{\partial y}=(y-x)[3y-(1+2\alpha)x]=0 \quad (13)$$

The values of x at which the roots of y of the dispersion relation merge are:

$$\left.\begin{aligned}x_b&=\left[\frac{3}{2^{\frac{2}{3}}(\alpha-1)}\right](-u)^{\frac{1}{3}}\\&=\frac{3}{2^{\frac{2}{3}}(\alpha-1)}\left[\exp\left(\frac{i\pi}{3}\right),\ -1,\ \exp\left(\frac{i5\pi}{3}\right)\right],\ u=1\\&=\frac{3}{2^{\frac{2}{3}}(\alpha-1)}\left[1,\ \exp\left(\frac{i2\pi}{3}\right),\ \exp\left(\frac{i4\pi}{3}\right)\right],\ u=-1\end{aligned}\right\} \quad (14)$$

And the three roots of y are:

$$\left.\begin{aligned} y_1 &= s_1 + s_2 + \frac{x}{3}(2+\alpha), \\ y_2 &= \exp\left(\frac{i2\pi}{3}\right)s_1 + \exp\left(\frac{i4\pi}{3}\right)s_2 + \frac{x}{3}(2+\alpha), \\ y_3 &= \exp\left(\frac{i4\pi}{3}\right)s_1 + \exp\left(\frac{i2\pi}{3}\right)s_2 + \frac{x}{3}(2+\alpha) \end{aligned}\right\} \quad (15)$$

Then the equation (12) can be rearranged as,

$$y^3 - x_{bo}(2+\alpha)y^2 + x_{bo}^2(1+2\alpha)y - \alpha x_{bo}^3 + u = 0 \quad (16)$$

where, x_{bo} is the x_b in eq.(14) lying in the upper half plane.

Using the values of x_{bo} and y_1 (which merges with y_2 or y_3) the values of $\delta\omega$ and δk and thus the values of complex angular frequency ω_s and complex wavenumber k_s at the saddle point can be obtained as:

$$\delta\omega = x_{bo}|\alpha\Delta|^{\frac{1}{3}}; \quad \delta k = \frac{y_1}{\left|\frac{v_b^2 v_g}{\Delta}\right|^{\frac{1}{3}}}; \quad \omega_s = \omega_q + \delta\omega$$

and $\quad k_s = k_q + \delta k$

The expression of group velocity, v_g is:

$$v_g = -\frac{\partial\omega}{\partial k} = \frac{\left[\left(1 - \frac{\omega_p^2}{\omega_q^2}\right)(k_q - k_0)\right]}{\left[\frac{\omega_q}{c^2} - \frac{\omega_p^2}{\omega_q^3}(k_q - k_0)^2\right]} \quad (17)$$

One can also express the arbitrary signal strength as,

$$f \propto e^{-j\left(j\omega_i \frac{L}{v_g} - jk_i L\right)} \quad (18)$$

where, L is the distance traversed by the wave in time t = L/ v_g, and is equal to the axial length of the structure and, ω_i and k_i are the imaginary part of angular frequency and wave number respectively.

IV. Conclusion

This paper contains a derivation of an analytical dispersion relation leading to microwave generation in a plasma-loaded BWO. The analytical equation obtained here, is limited in validity to the SWSs having very smaller corrugation depth in comparison to the structure average radius (i.e., $h << R_0$). This dispersion relation is an approximate one and is applicable only in the vicinity of the three-wave resonance point on the dispersion curves. The resulting approximate dispersion relation is cubic in both ω and k, which verifies the three-wave nature of the interaction process involving two normal modes of the SWS (which near resonance are merged into a complex conjugate pair of solutions to the dispersion relation) and a beam space charge wave. From this cubic dispersion relation, temporal as well as spatial growth rates of a solid beam driven plasma-loaded backward wave oscillator can be computed and analyzed with the variation of structure parameters and plasma density.

References Références Referencias

1. Abu-Elfadl, T. M., G. S. Nusinovich, T. M. Antonsen, Jr., and V. L. Granatstein. (September, 2003). Temporal Study of a Plasma Loaded Helix Backward Wave Oscillator. Phys. Plasmas vol.10, no.9.
2. Ali, M. M., K. Minami, K. Ogura, T. Hosokawa, H. Kazama, T. Ozawa, T. Watanabe, Y. Carmel, V. L. Granatstein, W. W. Destler, R. A. Kehs, W. R. Lou, and D. K. Abe.(1990).Absolute Instability for Enhanced Radiation from a High-Power Plasma-Filled Backward-Wave Oscillator. Phys. Rev. Lett. 65 855.
3. Ali, M. M., K. Ogura, K. Minami, T. Watanabe, W. W. Destler and V. L. Granatstein(April, 1992) .Linear Analysis of a Finite Length Plasma-Filled Backward Wave Oscillator.Phys. Fluids B4 (4).
4. Ali, M. M., K. Minami, S. Amano, K. Ogura, and T. Watanabe.(August, 1991).Linear Analysis of a Localized Plasma-Loaded Backward Wave Oscillator Driven by an Annular Intense Relativistic Electron Beam.Journal of Phys. Sci. of Japan, vol.60, no.8, pp. 2655-2664.
5. Bogdankevich, L. S., M. V. Kuzelev, and A. A. Rukhadze. (1980). Theory of excitation of plasma-filled rippled-boundary resonators by relativistic electron beams. Sov. Phys. Tech. Phys. 25 ,143.(2)
6. Carmel, Y., K. Minami, R. A. Kehs, W. W. Destler, V. L. Granatstein, D. Abe, and W. R. Lou.(1989). Demonstration of efficiency enhancement in a high power backward wave oscillator by plasma injection. Phys. Rev. Lett. 62, 2389.
7. Hong-Quan, Xie and Lin Pu-Kun. March, 2007.Theoritical analysis of a relativistic traveling wave tube filled with plasma. Chinese Phys. 16 766.
8. Kurilko, V. I., V. I. Kucherov, and A. O. Ostrovskii.(1981) .Effect of a Plasma on the Amplification of Regular Waves by a Relativistic Beam in a Corrugated Waveguide. Sov. Phys. Tech. Phys. 26, 812.
9. Minami, K., W. R. Lou, W. W. Destler, R. A. Kehs, V. L. Granatstein and Y. Carmel. (1988). Observation of resonance enhancement of microwave radiation from a gas-filled backward wave oscillator. Appl. Phys. Lett. 53, 559.
10. Otubo, Kosuke, Kazuo Ogura, Mitsuhisa Yamakawa and YusukeTakashima.(2010). Numerical Analysis of Slow-wave Instabilities in an Oversized Sinusoidally Corrugated Waveguide Driven by a Finitely Thick Annular Electron Beam. Jpn Soc. of Plasma Sci. & Nuclear Fusion Research, Vol. 5, S1047.

11. Sawhney, R. (1993).Effect of Plasma on Efficiency Enhancement in a High Power Relativistic Backward Wave Oscillator. IEEE Trans. on Plasma Science,vol.21, pp. 609-613.
12. Sharma, B. S. and N. K. Jaiman.(July, 2008).Numerical investigations on the effect of geometrical parameters on free electron laser instability. Journal of Plasma Phys. 74: 741-747, Cambridge University Press.
13. Swegle, John A. (December 1985). Approximate treatment near resonance of backward and traveling wave tubes in the Comton regime. Phys. Fluids 28 (12), pp. 3696-3702.
14. Sarker, D. K., M. M. Ali, and M. R. Amin. (December 2006). Effect of structure size-parameters on the dispersion characteristics of a plasma-loaded backward wave oscillator. Journal of EE, IEB, Vol. EE 33, No. I & II.(17)
15. Tkach, Yu. V., N. P. Gadetskii, Yu. P. Bliokh, E. A. Lemberg, M. G. Lyubarskii, V. V. Ermolenko, V. V. Dyatlova, S. I. Naisteter, I. I. Magda, S. S. Pushkarev, and G. V. Skachek. (1979). Emission by a Relativistic Beam at a Magneto-Cerenkov Resonance in a Periodic Waveguide. Sov. J. Plasma Phys. 5,566.
16. Tkach, Yu. V., Ya. B. Fainberg, I. I. Magda, N. I. Gaponenko, G. V. Skachek, S. S. Pushkarev, N. P. Gadetskii, and A. A. Belukha. (1975). Microwave Emission in the Interaction of a High-Current Relativistic Beam with a Plasma-Filled Slow-Wave Structure. Sov. J. Plasma Phys. 1,43.
17. Yong, Douglas, Osmu Ishihara, C. Grabowski, J. Gahl, and E. Schamiloglu. (June, 1998).Study of Power Enhancement and Frequency Shifting of Microwave Emission in a Plasma Filled Non-Uniform Backward Wave Oscillator. IEEE Conference Record-Abstracts, 1998 IEEE ICOPS.

Global Journal of researches in engineering
Electrical and electronics engineering
Volume 12 Issue 1 Version 1.0 January 2012
Type: Double Blind Peer Reviewed International Research Journal
Publisher: Global Journals Inc. (USA)
Online ISSN: 2249-4596 & Print ISSN: 0975-5861

Robust H-infinity (H∞) Stabilization of Uncertain Wheeled Mobile Robots

By A.Dolly Mary, Abraham T. Mathew, Jeevamma Jacob
National Institute of Technology

Abstract - This paper proposes a robust H-infinity control design of a single unit differential type Wheeled Mobile Robot. Mobile robots are non holonomic systems as their constraint equations are not integrable. Considering the constraints and combining the kinematics and dynamics of the system, a linearized model is obtained. Taking into account the exogenous inputs in the form of model uncertainties and output disturbances, the augmented plant is formulated. The H-infinity controller is designed such that the sensitivity of the closed loop system is minimised. The proposed design renders a robust controller such that the closed loop system is internally stable and the effect of disturbances and model uncertainties on some of the outputs is attenuated. Simulation results showing asymptotic stability plot, disturbance response and Robust Stability and Performance margins are found to be satisfactory.

Keywords : *H∞ control, robust control, wheeled mobile robots, uncertain systems, Disturbance rejection.*

GJRE-F Classification: *FOR Code: 090602p*

Strictly as per the compliance and regulations of:

Robust H-infinity (H_∞) Stabilization of Uncertain Wheeled Mobile Robots

A.Dolly Mary [α], Abraham T. Mathew [σ], Jeevamma Jacob [ρ]

Abstract - This paper proposes a robust H-infinity control design of a single unit differential type Wheeled Mobile Robot. Mobile robots are non holonomic systems as their constraint equations are not integrable. Considering the constraints and combining the kinematics and dynamics of the system, a linearized model is obtained. Taking into account the exogenous inputs in the form of model uncertainties and output disturbances, the augmented plant is formulated. The H-infinity controller is designed such that the sensitivity of the closed loop system is minimised. The proposed design renders a robust controller such that the closed loop system is internally stable and the effect of disturbances and model uncertainties on some of the outputs is attenuated. Simulation results showing asymptotic stability plot, disturbance response and Robust Stability and Performance margins are found to be satisfactory.

Keywords : H_∞ *control, robust control, wheeled mobile robots, uncertain systems, Disturbance rejection.*

I. Introduction

Wheeled Mobile Robots (WMR) can be considered as an isolated system or as a basic unit or a building block of a multi linked articulated vehicle. Alternatively, WMR can be considered an autonomous vehicle in disguise. The development of control strategies for long haul articulated vehicles shall begin by benchmarking the control methods for a single unit of WMR. Non holonomic constraints for control arise out of the kinematics and the uncertainty is consequent to the nonlinearities and parameter variations. Imperfections in the measurements, lead to inaccuracies or noise in the measurement output. So, even if we consider a single unit of WMR, the control issues evolve as a sophisticated problem that needs elaborate treatment. These could be the reasons for active research in the control, stabilization and tracking of WMR for the last several decades.

Non holonomic property of WMR can be attributed to systems using velocity inputs. Such systems cannot autonomously produce a velocity which is transversal to the axle of their wheels. This limitation appears as the non holonomic constraint on the velocity of the system. In order to pursue the modeling, stabilization and tracking of these systems, it is assumed that a wheel has only two degrees of freedom with no sideway slip. This assumption which imposes non holonomic constraint on the motion of the vehicle is called the ideal rolling condition. Unlike robot manipulators, their constraint equations are not integrable. Thus the coordinates cannot be eliminated making the system description with a larger number of coordinates than their degrees of freedom. So our attempt shall be to design a robust controller for such non holonomic WMR systems.

Various control schemes and analysis had been proposed for the WMR system based on the research with the model kinematics. In this kinematic framework there exists no continuous state feedback for WMR as proven by Brockett (1983). Hence research had been focused on other control methods like Lyapunov stability and Feedback linearization. In (Godhavn &.Egeland 1997; Deng &Brady 1993; Sik Shim & Gyeoung Sung 2003; Saso Blazic 2011) investigations were made on the WMR system to design a control that yields asymptotic stabilization of the closed loop for these kinematic models, in the Lyapunov stability analysis framework. The control law achieved global asymptotic stability based on the usual requirement for reference velocity. A drawback of this method was that the stabilizing controllers do not guarantee performance. One of the common methods in the design of controllers for the WMR, employs the dynamic feedback linearization (Giuseppa Oriolo, Alessandra De Luca & Marilena Vendittelli 2002). The control of non linear WMR systems via feedback linearization was achieved, provided the feedback is able to cancel out the nonlinearities. If so, trajectory tracking and setpoint regulation problems can be solved in the case of motion control of WMR. But since it is designed in the kinematic framework, the controller does not take care of uncertainties and input saturations. Uncertainties in the parameters of the system model can invariably affect the stability and performance of the closed loop system and hence have to be addressed. Uncertainty modeling, either structured or unstructured, form an integral part of the robust control design. In the research work as in (Wenjie Dong 2000; Jinbo WU, Guohua XU 2009; Mohammad Ali Sadrnia, and Atiyeh Haji Jafari 2007; Doyle 1985) the need of uncertainty modelling was stressed and the robust controllers were designed for the uncertain systems by adaptive or H-infinity (H_∞) control. Robust approaches for control design renders a fixed controller .

H_∞ has played an important role in the study and analysis of control theory, since its original formulation in an input output setting (Doyle 1989). It is well known that , though conservative , they provide better response in the presence of disturbance than H_2

optimal techniques. The control requirement is that the response of error to the disturbances with the stabilization controller should be brought to less than γ, where γ is the suboptimal H_∞ limits with $0 < \gamma \leq 1$. For the standard H_∞ problem, a controller exists if and only if unique positive definite solutions to the two Riccati equations exists (John C. Doyle 1989). State space formulas can be derived for all controllers such that the H_∞ norm of the closed loop transfer function is less than γ. Based on the above control criteria, investigations on the WMR were carried out as in (Hong Chen et al 2009; Carlos De Souza, Minyue Fu & Lihua Xie 1993; Zhijian Ji 2006; Wenan Sun and Jun Zhao 2005) for different preset conditions aiming at robust stabilization, performance and tracking. In Hong Chen et al (2009) a moving horizon H_∞ control algorithm for WMR was computed in presence of external disturbances and control constraints. The results showed that the H_∞ controller can reduce tracking errors with desired performances. A H_∞ control as applied to a discrete time systems with time-varying uncertainties was synthesised in Carlos De Souza, Minyue Fu & Lihua Xie (1993).The H_∞ problem was converted to a scaled form for quadratic stability analysis. In Wenan Sun and Jun Zhao (2005) a sufficient condition for hybrid output feedback H_∞ control was derived for uncertainties in the state and input matrices. The controller satisfied guaranteed cost with H_∞ disturbance attenuation γ. Thus the above works highlights the possibility that robust stability and performance measure could be achieved by H_∞ control.

In this paper, a robust H_∞ design is addressed for the uncertain, linear WMR system, accounting for disturbances and model uncertainties. Remaining part of the paper is organised as follows. Section II deals about the H_∞ problem and its necessary robustness criteria for WMR implementation. The robust H_∞ control objective and its design procedure are stated. The procedure aims at a controller such that the closed loop system is internally stable and the effect of disturbance inputs on some of the outputs is attenuated. The norm of system sensitivity which is the effect of the disturbance on the output of the system is to be less than unity. In Section III the nominal modelling of WMR is carried out by incorporating the kinematics and the dynamics of the system. The disturbances along with the control input are assumed to act on the system. In Section IV, the uncertain WMR plant is modelled assuming low frequency disturbance inputs to act on the system and outputs. In Section V the H_∞ controller obtained is evaluated to verify its effectiveness. The closed loop response, asymptotic stability plots and stability and performance margins are plotted.

II. H_∞ Problem Statement

The output feedback structure for the proposed H_∞ control scheme is shown in Fig. 1. The system consists of a linear time invariant augmented system P which belongs to the class P of uncertain system. P comprises the nominal model and weighting functions corresponding to model uncertainties and disturbances. The inputs of the system are w and u which represent exogenous and control inputs respectively; z and y would represent the controlled and measured outputs. Considering the input-output relations that are depicted by P, the relation between $[z, y]$ and $[w, u]$ could be written as given in (1)

$$\begin{bmatrix} z \\ y \end{bmatrix} = \begin{bmatrix} P_{11} & P_{12} \\ P_{21} & P_{22} \end{bmatrix} \begin{bmatrix} w \\ u \end{bmatrix} \quad (1)$$

Considering the invariance of the plant P and the separability of the variables for the linear setting, the system has been partitioned into the state space for as given in (2)

$$\dot{x}(t) = A\,x(t) + B_1 w(t) + B_2 u(t) \quad (2a)$$

$$z(t) = C_1 x(t) + D_{11} w(t) + D_{12} u(t) \quad (2b)$$

$$y(t) = C_2 x(t) + D_{21} w(t) + D_{22} u(t) \quad , \quad (2c)$$

where $x \in R^n$ is the state, $u \in R^r$ is the control input, $y \in R^m$ is the observed output, $z \in R^q$ is the controlled output and $w \in R^p$ is the disturbance.

- (A, B_1) is stabilizable and (A, C_1) is detectable.
- (A, B_2) is controllable and (A, C_2) is observable,

The control problem is: with a feedback $u = K(s)y$, find an admissible internally stabilizing control K which would be attenuating disturbances such that the norm of the stable closed loop system from the disturbances to the controlled outputs is less than γ (γ is equal to 1 for optimal and slightly greater than 1 for suboptimal control). The control objective is stated in the mathematical form in (3)

$$\| F_l(P,K) \|_\infty = sup_{\omega \epsilon R} / F_l(P,K)(j\omega) / \; < \gamma \quad (3)$$

The H_∞ solution involves two Hamiltonian matrices (Doyle 1989),

$$H_\infty := \begin{bmatrix} A & \gamma^{-2} B_1 B_1' - B_1 B_1' \\ -C_1' C_1 & -A' \end{bmatrix}$$

$$J_\infty := \begin{bmatrix} A' & \gamma^{-2} C_1' C_1 - C_2' C_2 \\ -B_1 B_1' & -A \end{bmatrix}$$

Theorem (Doyle 1989): There exists an admissible controller such that $\|T_{zw}\|_\infty < \gamma$ iff the following three conditions hold.

i. $H_\infty \in dom(Ric)$ and $X_\infty := Ric(H_\infty) \geq 0$.
ii. $J_\infty \in dom(Ric)$ and $Y_\infty := Ric(J_\infty) \geq 0$.
iii. $\rho(X_\infty Y_\infty) < \gamma^2$

The proof of this theorem is seen in (Doyle 1989). For these conditions being satisfied the suboptimal controller is

$$K_{sub}(s) = \left[\begin{array}{c|c} \hat{A}_\infty & -Z_\infty L_\infty \\ \hline F_\infty & 0 \end{array}\right] \quad (4)$$

where $\hat{A}_\infty := A + \gamma^{-2} B_1 B_1' X_\infty + B_2 F_\infty + Z_\infty L_\infty C_2$

$F_\infty := -B_2' X_\infty$, $L_\infty := -Y_\infty C_2'$, $Z_\infty := (I - \gamma^{-2} Y_\infty X_\infty)^{-1}$

The resulting closed loop system with a feedback $u = K(s)\, y$ obtained by Linear Fractional Transformation is brought to the form

$$\dot{x}_c(t) = A_C x_c(t) + B_1 w(t) \quad (5)$$
$$z(t) = C_1 x_c(t)$$

where x_c indicates the states of the closed loop system.

Definition: Given a scalar $\gamma > 0$, system (5) is said to be stable with disturbance attenuation γ if it satisfies the following conditions

1. A_C is a stable matrix
2. The transfer function from disturbance w to the controlled output z satisfies,

$$\| C_1 (sI - A_C)^{-1} B_1 \|_\infty < \gamma \quad (6)$$

Lemma: Let $\gamma > 0$ be given. The system (5) is stable with disturbance attenuation γ if and only if there exists a symmetric matrix $X_\infty > 0$ such that

$$A_C' X_\infty + X_\infty A_C + \gamma^{-2} X_\infty B_1 B_1' X_\infty + C_1' C_1 < 0 \quad (7)$$

Proof:

Let the Lyapunov function for the system be $V(x_c(t)) = x_c(t)' X_\infty x_c(t)$.Making substitutions from (5) ,

$$\dot{V}(x_c(t)) = x_c'(t)[A_C' X_\infty + X_\infty A_C] x_c(t) + x_c'(t) X_\infty B_1 w(t) + w(t)' B_1' X_\infty x_c(t)$$

Let the performance measure corresponding to disturbance attenuation be

$$J = \int_0^\infty [z(t)' z(t) - \gamma^2 w(t)' w(t)]\, dt$$

$$J \le \int_0^\infty [z(t)' z(t) - \gamma^2 w(t)' w(t) + \dot{V}(x_c(t))]\, dt$$

$$J \le \int_0^\infty \{x_c'(t) C_1' C_1 x_c(t) - \gamma^2 w(t)' w(t) + x_c'(t)[A_C' X_\infty + X_\infty A_C] x_c(t) + x_c'(t) X_\infty B_1 w(t) + w(t)' B_1' X_\infty x_c(t)\}\, dt$$

With

$$w(t)'(B_1' X_\infty x_c(t)) + (B_1' X_\infty x_c(t))' w(t) \le \gamma^2 w(t)' w(t) + \frac{x_c'(t) X_\infty B_1 B_1' X_\infty x_c(t)}{\gamma^2}$$

Since $J \le 0$ to be satisfied,

$$A_C' X_\infty + X_\infty A_C + \gamma^{-2} X_\infty B_1 B_1' X_\infty + C_1' C_1 < 0$$

III. Modeling of WMR

A schematic of the WMR in the {X-O-Y} coordinate axis is shown in Fig. 2. The mobile robotic system consists of two rear wheels (A1-A2) which are driving wheels. The driving wheels are driven by two independent DC motors which are the actuators of the left and right wheels. Along with the driving wheels, there is pasive wheel (C). The movement of the WMR is brought about by the differential control of velocity of the wheels A1 and A2. The linear and rotational motions of WMR are facilitated by the control of A1 and A2. F is the projection of mass centre of the robot and P the centre of two front wheels of the robot. l_f is the distance between point P and point F. θ_p is the heading angle of the robot. v_p is the speed at P. ω is the angular speed of WMR.

Let (x_P, y_P) be the coordinates at P and (x_F, y_F) coordinates at F. The x and y axis speed at P which represent the kinematics of the system can be derived as in (8).

$$\dot{x}_P = v_p cos\theta_p \quad (8a)$$

$$\dot{y}_P = v_p sin\theta_p \quad (8b)$$

also P and F can be related as given in (9).

$$x_F = x_p - l_f cos\theta_p \quad (9a)$$

$$y_F = y_p - l_f sin\theta_p \quad (9b)$$

The non holonomic constraint is written in the form of (10). This equation is not integrable, so the fesible trajectory is limited.

$$\dot{x}_F sin\theta_P - \dot{y}_F cos\theta_P - l_f \dot{\theta}_P = 0 \quad (10)$$

Differentiating (9) twice results in (11).

$$\ddot{x}_F = \ddot{x}_P + l_f \dot{\omega}\, sin\theta_p + l_f \omega^2 cos\theta_p \quad (11a)$$

$$\ddot{y}_F = \ddot{y}_P - l_f \dot{\omega}\, cos\theta_p + l_f \omega^2 sin\theta_p \quad (11b)$$

where $\omega = \frac{d\theta_P}{dt}$ and $\dot{\omega} = \frac{d\omega}{dt} = \frac{d^2\theta_P}{dt^2}$

Let T_1 and T_2 be the driving torques on left and right front wheels of the differential WMR. Then $u_1 = T_1 + T_2$; $u_2 = T_1 - T_2$. The dynamics of the WMR are represented in (12).The accelerations of the system depend not only on the inputs but are acted upon by disturbances. Let $u(t) = [u_1\ u_2]'$ be the control input vectors, $w_0(t) = [w_1\ w_2]'$ the input disturbances representing external forces and torques in the direction of v_p and ω.

$$\dot{v}_p = \beta_1 u_1 + \beta_3 w_1 \quad (12a)$$

$$\dot{\omega} = \beta_2 u_2 + \beta_4 w_2 \quad (12b)$$

Here $\beta_1 = \frac{1}{rM}$, $\beta_2 = \frac{b}{rI}$, $\beta_3 = \frac{1}{M}$, $\beta_4 = \frac{1}{I}$ with r representing the radius of the wheel, M the mass of

the WMR, *I* the moment of inertia with respect to the centre of mass F of the WMR and 2*b* the length of wheel axis.

The state space equations of the dynamical systems can be derived as in Wenping Jaing (2008) by the substitution of (12) and derivative of (8) in (11). The state variables of the system are taken as $x = [\theta_p \ \dot{x}_F \ \dot{y}_F \ \dot{\theta}_P]^T$ angular displacement, x axis speed at F, y axis speed at F and angular speed. Table 1. shows the nominal values of the WMR parameters.

Table 1 : Parameters of the WMR system

Parameter	Nominal value
r (m)	0.105
M (kg)	25
I (kg m^2)	0.5512
2b (m)	0.41
l_f(m)	0.09

Thus the state space representation of the nominal open loop system is in the form of (13)

$$\dot{x} = A\,x + B_1 w_o + B_2 u \tag{13a}$$

$$y = C_2 x \tag{13b}$$

where

$$A = \begin{bmatrix} 0 & 0 & 0 & 1 \\ 0 & 0 & -0.0175 & -0.01 \\ 0 & 0.0175 & 0 & 0 \\ 0 & 0 & 0 & 0 \end{bmatrix}$$

$$B_1 = \begin{bmatrix} 0 & 0 \\ 0.04 & 0 \\ 0 & -0.163 \\ 0 & 1.814 \end{bmatrix}, \quad B_2 = \begin{bmatrix} 0 & 0 \\ 0.381 & 0 \\ 0 & -0.319 \\ 0 & 3.542 \end{bmatrix},$$

$$C_2 = \begin{bmatrix} 1 & 0 & 0 & 0 \\ 0 & 1 & 0 & 0 \end{bmatrix}$$

The nominal open loop system is unstable with all the poles on the imaginary axis

IV. WMR H∞ Control Scheme

The nominal model in (13) do not provide an exact representation of the WMR system. Modelling errors, parameter uncertainties and nonlinearities of the system which were not taken into account do not guarantee a robust controller. For the WMR system, the robot's parameters particularly the mass and inertia are subjected to variations and hence uncertainties arise in system modeling. Also the outputs of the system are subjected to disturbances. Hence uncertainties should be taken into account when designing a robust controller, so that we get satisfactory control over a wider range of the operating variables. It is noted that the input disturbance w_0 was modeled along with the control inputs of the system. To accommodate the parameter variations and nonlinearities w_0 is acted on by unstructured uncertainty weighting W_W. The H_∞ control to the WMR as in Fig. 3 shows the feedback structure of the uncertain plant. Disturbances inputs can act on the model and the output. Let it be $w_i(t)$ and $w_y(t)$ respectively. These disturbances act on the plant in the low frequency range. Let W_W and W_P be the low frequency disturbances weightings for the above inputs.

Then

$$w_o(t) = W_W w_i(t) \tag{14}$$

With uncertainty model weighting being selected as

$$W_W = \frac{6(s+60)}{(s+0.3)} = C_W(sI - A_W)^{-1}B_W + D_W \tag{15}$$

$[A_W, B_W, C_W, D_W]$ which are the state space matrices of the transfer function (15) can be obtained.

The output disturbance weighting W_P is selected based on the maximum steady state error, bandwidth etc of (16). Fig. 4. shows the inverse of performance weighting that is acting on the system.

$$W_P = \frac{s/M + \omega_B}{s + \omega_B A} \tag{16}$$

ω_B is the bandwidth frequency, A is the maximum steady state tracking error and M the maximum peak magnitude of sensitivity. For the WMR design performance weighting W_P is selected as in (17).

$$W_P = \frac{(s+77)}{(s+24)} = C_P(sI - A_P)^{-1}B_P \tag{17}$$

$[A_P, B_P, C_P, D_P]$ are the state space matrices of the transfer function (17).

Next we consider the regulated or controlled output as shown by z_1 and z_2. Stabilization and regulation of the state variables corresponds to z_1 and error on u corresponds to z_2.

$$z_1 = \varphi x \tag{18}$$

φ is a 3 by 3 diagonal matrix corresponding to first 3 state variables to be regulated.

$$z_2 = \rho u \tag{19}$$

ρ is a 2 by 2 diagonal weighting matrix on u.

Let x_w and x_p be the states of the low frequency disturbances W_W and W_P.

Then $w_o = C_W x_W + D_W w_i$ (20a)

and $\dot{x}_W = A_W x_W + B_W w_i$ (20b)

$$\dot{x}_P = A_P x_P + B_P w_y \tag{20c}$$

Combining the nominal model (13) and the above uncertain states, the augmented model is brought to the form of (2).The state space representation is shown in (21), the states of the uncertain plant are $[x^T \ x_w{}^T \ x_p{}^T]$, w $= [w_i{}^T \ w_y{}^T]$ and z $= [z_1{}^T \ z_2{}^T]$.

$$\begin{bmatrix} \dot{x} \\ \dot{x}_W \\ \dot{x}_P \end{bmatrix} = \begin{bmatrix} A & B_1 C_W & 0 \\ 0 & A_W & 0 \\ 0 & 0 & A_P \end{bmatrix} \begin{bmatrix} x \\ x_W \\ x_P \end{bmatrix} + \begin{bmatrix} B_1 D_W & 0 & B_2 \\ B_W & 0 & 0 \\ 0 & B_P & 0 \end{bmatrix} \begin{bmatrix} w_i \\ w_y \\ u \end{bmatrix} \tag{21}$$

$$\begin{bmatrix} z_1 \\ z_2 \\ y \end{bmatrix} = \begin{bmatrix} \varphi & 0 & 0 \\ 0 & 0 & 0 \\ -C_2 & 0 & -C_P \end{bmatrix} \begin{bmatrix} x \\ x_W \\ x_P \end{bmatrix} + \begin{bmatrix} 0 & 0 & 0 \\ 0 & 0 & \rho \\ 0 & -D_P & 0 \end{bmatrix} \begin{bmatrix} w_i \\ w_y \\ u \end{bmatrix}$$

The regulated matrix corresponding to the states and input are selected as

$$\varphi = \begin{bmatrix} .1e^{-3} & 0 & 0 \\ 0 & .4e^{-3} & 0 \\ 0 & 0 & 1e^{-4} \end{bmatrix} \quad , \quad \rho = \begin{bmatrix} 2e^{-2} & 0 \\ 0 & .5e^{-2} \end{bmatrix}.$$

It is noted that (A,B_1) , (A,B_2) are controllable and (A,C_2) observable. Hence the uncertain plant that represents the WMR also satisfies the requirement for the existence of the controller.

V. Controller Evaluation

With the uncertain plant in the general form of (2) and the controllability and observability conditions being satisfied, the controller was simulated in MATLAB ® as per the theorem in Section II. The suboptimal H_∞ controller was obtained in the form of (4) with a γ value of 1.09. The Linear Fractional Transformation of the augmented system and the controller yields a closed loop system in the form of (5). This system with inputs as disturbances w and outputs z represent the robust closed loop system. Fig. 5. shows the magnitude of the uncertain closed loop plant for varying frequencies. The maximum bound of the closed loop system which indicates the sensitivity of the system guarantees robustness for values less than unity. The maximum value of the WMR system was around 0.7.

Fig. 6. shows the impulse response of the uncertain plant from output disturbances w_y to z_1 . The variation in the output z_1 because of the disturbance was negligible ascertaining that the control design is robust. To verify the internal stability with the H_∞ controller, the asymptotic stability of the output of the closed loop system was plotted as in Fig. 7. Both the outputs tend to zero in minimum time thus proving that the controller stabilizes the WMR system. To further evaluate the robustness of the above control design, the stability and performance margins for the closed loop system were calculated subject to variation in the parameters of the robotic system. The mass M of the system was varied between [20 : 30] and moment of inertia I between [0.6 : 0.7]. The stability analysis showed that the uncertain system is robustly stable to modeled uncertainty. It can tolerate up to 500% of the modeled uncertainty. The sensitivity with respect to uncertain element I is 67% and M 129% for robust stability. The robust performance margin for the WMR was calculated subject to the above variations. The uncertain system achieves a robust performance margin of 1.32. A model uncertainty exists of size 131% resulting in a performance margin of 0.761 at 0.0169 rad/sec. For robust performance, the sensitivity with respect to uncertain element I is 17% and M 14% . The above results clearly indicated that the controller design is robust.

VI. Conclusion

In this paper the robust control design of a single unit Wheeled Mobile Robot was presented. Modeling of the WMR system was done taking into account the kinematics and dynamics to achieve a linearized model for these systems. The exogenous inputs in the form of model uncertainties and output disturbances were assumed to act on the system and the augmented plant was formulated. The robust internally stabilizing H_∞ controller was obtained. The above design rendered a controller such that the closed loop system was internally stable and the effect of disturbances and model uncertainties on some of the outputs was attenuated. The asymptotic stability plot, disturbance response and Robust Stability and Performance margins were found to be satisfactory.

References Referencias

1. Brockett R., 1983. Asymptotic stability and feedback stabilization. In: *Differential Geometry Control Theory*, Boston ,MA ,Birkhauser, pp. 181-208,
2. Carlos E. De Souza, Minyue Fu & Lihua Xie, 1993. H_∞ Analysis and Synthesis of Discrete –Time Systems with Time –Varying Uncertainty, *IEEE Transaction of Automatic Control*, 38(3), March ,pp. 459-462.
3. Deng Z.. & Brady J.M., 1993. Dynamic tracking of a wheeled mobile robot. In: *Proceedings of the IEEE/RJS International Conference on Intelligent Robots and Systems*, Yokohama, Japan, July, pp. 1295-1298.
4. Doyle J.C., 1985. Structured Uncertainties in Control System Design. In: *Proceedings of 24th Conference on Decision and Control,* pp. 260-265.
5. Doyle J.C., Keith Glover, Pramod Khargonekar &

Bruce Francis 1989. State–Space Solutions to Standard H_2 and H_∞ Control Problems. *IEEE Transitions on Automatic Control*, 34(8), August.

6. Giuseppa Oriolo, Alessandra De Luca & Marilena Vendittelli, 2002. WMR Control Via Dynamic Feedback Linearization: Design, Implementation, and Experimental Validation. *IEEE Transactions on Control Systems Technology*, 10(6), Nov.
7. Godhavn J.M. & Egeland O., 1997. A Lyapunov approach to exponential stabilization of nonholonomic systems in power form. *IEEE Transcations on Automatic Control* . 42(7), pp. 1028-1032.
8. Hong Chen, Miao-Maio Ma, Hu Wang & Zi-Xing, 2009. Moving Horizon H-infinity Tracking Control of Wheeled Mobile Robots with Actuator Saturation. *IEEE Transactions on Control Systems Technology*, 17(2), March.
9. Hyun –Sik Shim & Yoon-Gyeoung Sung, 2003. Asymptotic control for wheeled mobile robots with driftless constraints. *Robotics and Autonomous Systems*, 43 ,pp. 29-37.
10. Jinbo Wu, Guohua Xu, 2009. Robust adaptive control for a nonholonomic mobile robot with unknown parameters. *J. Control Theory Appl,* 7(2),pp. 212-218.
11. Mohammad Ali Sadrnia & Atiyeh Haji Jafari, 2007. Robust Control Design for Maglev Train with Parametric Uncertainties Using μ – Synthesis, *World Academy of Science, Engineering and Technology*, 31.
12. Saso Blazic, 2011. A novel trajectory- tracking control law for wheeled mobile robots. *Robotics and Autonomous Systems*, 59, pp. 1001-1007.
13. Wenan Sun & Jun Zhao, 2005. Hybrid Output-feedback Guaranteed Cost H_∞ Robust Control for Linear Systems. In: 2005 *American Control Conference* , June 8-10, 2005. Portland, OR, USA.
14. Wenjie Dong, Wei HuoS. K. Tso, & Xu W. L., 2000. Tracking Control of Uncertain Dynamic Nonholonomic System and Its Application to Wheeled Mobile Robots. *IEEE Transactions on Robotics and Automation*, 16(6), Dec.
15. Wenping Jaing, 2008. Robust H∞ Controller Design for Wheeled Mobile Robot with Time-delay. In: 2008 *International Conference on Intelligent Computation Technology and Automation,* pp. 450-454.
16. Zhijian Ji , Xiaoxia Guo , Long Wang & Guangming Xie, 2006. Robust H_∞ Control and Stabilization of Uncertain Switched Linear Systems: A Multiple Lyapunov Functions Approach. *Journal of Dynamic Systems, Measurement, and Control,* 128, Sept.

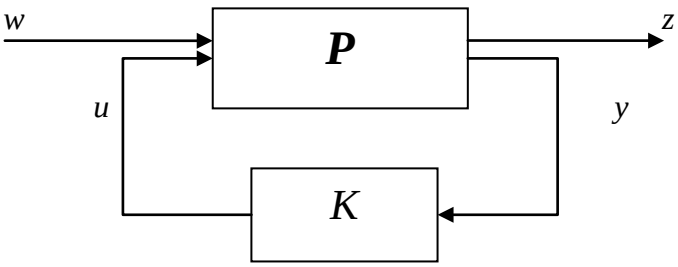

Fig. 1 : H_∞ Feedback control

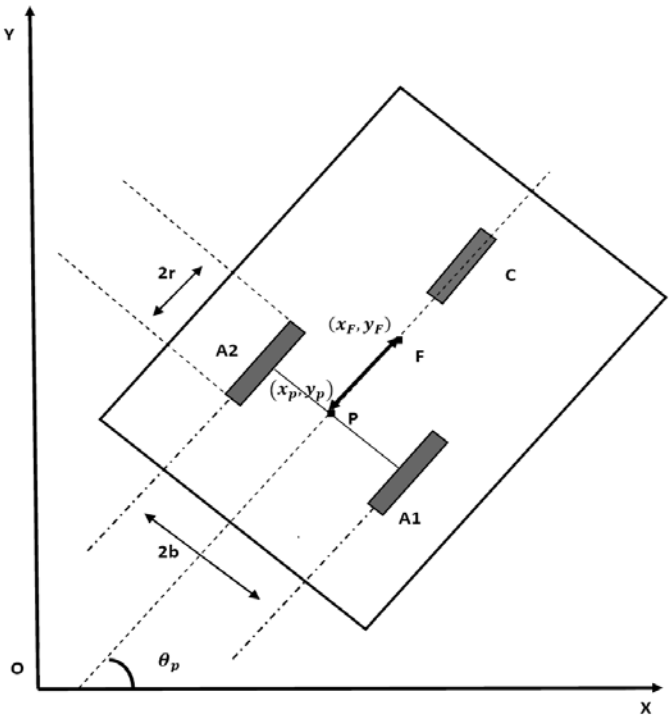

Fig. 2 : Model of a Wheeled Mobile Robot

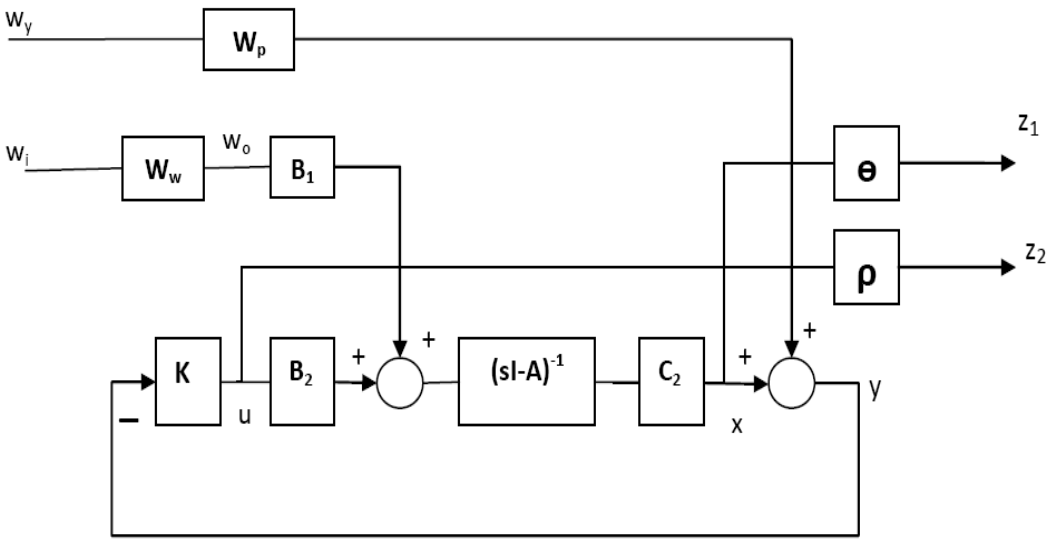

Fig. 3 : Augmented structure of uncertain plant

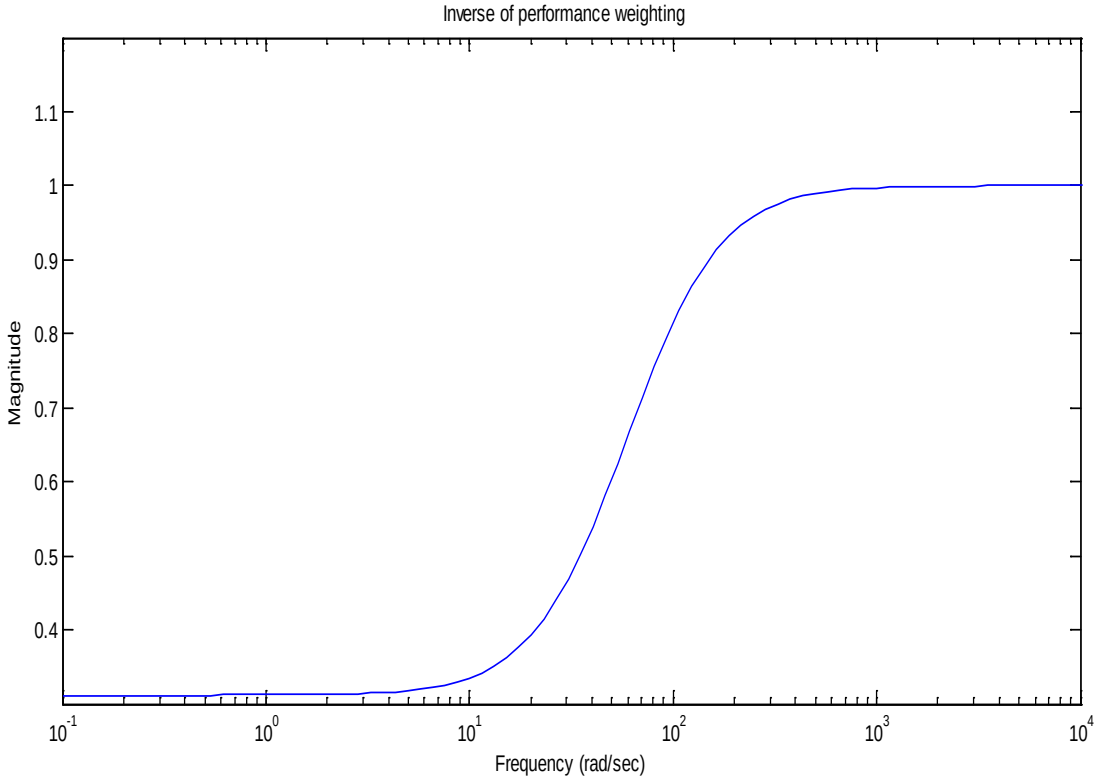

Fig. 4 : Inverse of performance weighting W_P

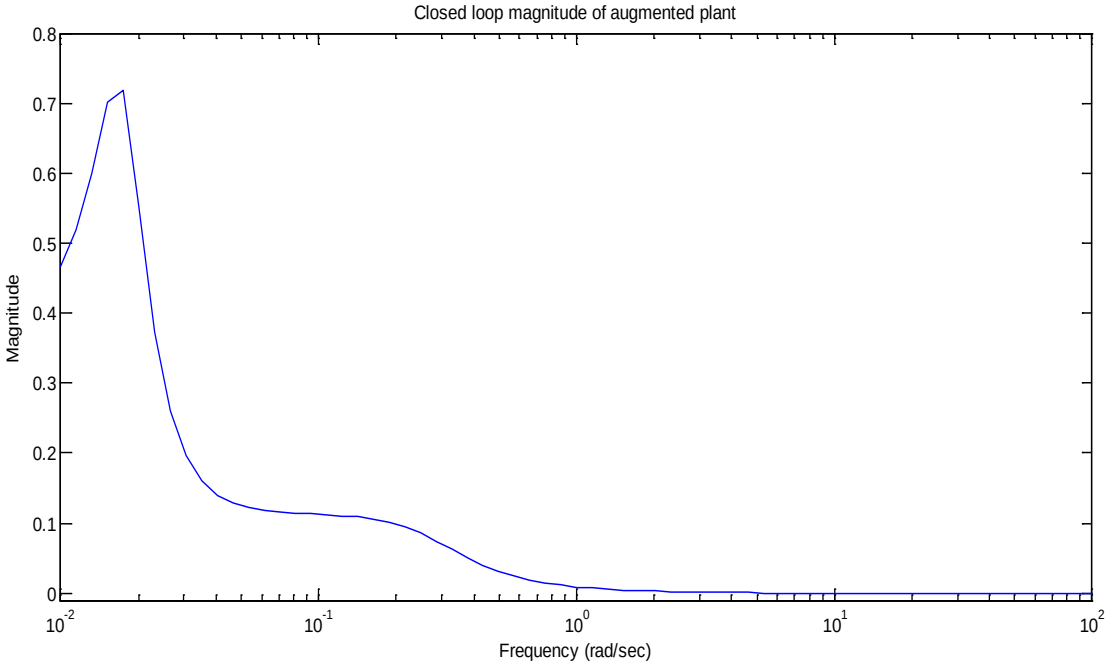

Fig. 5 : Closed loop magnitude of the uncertain plant

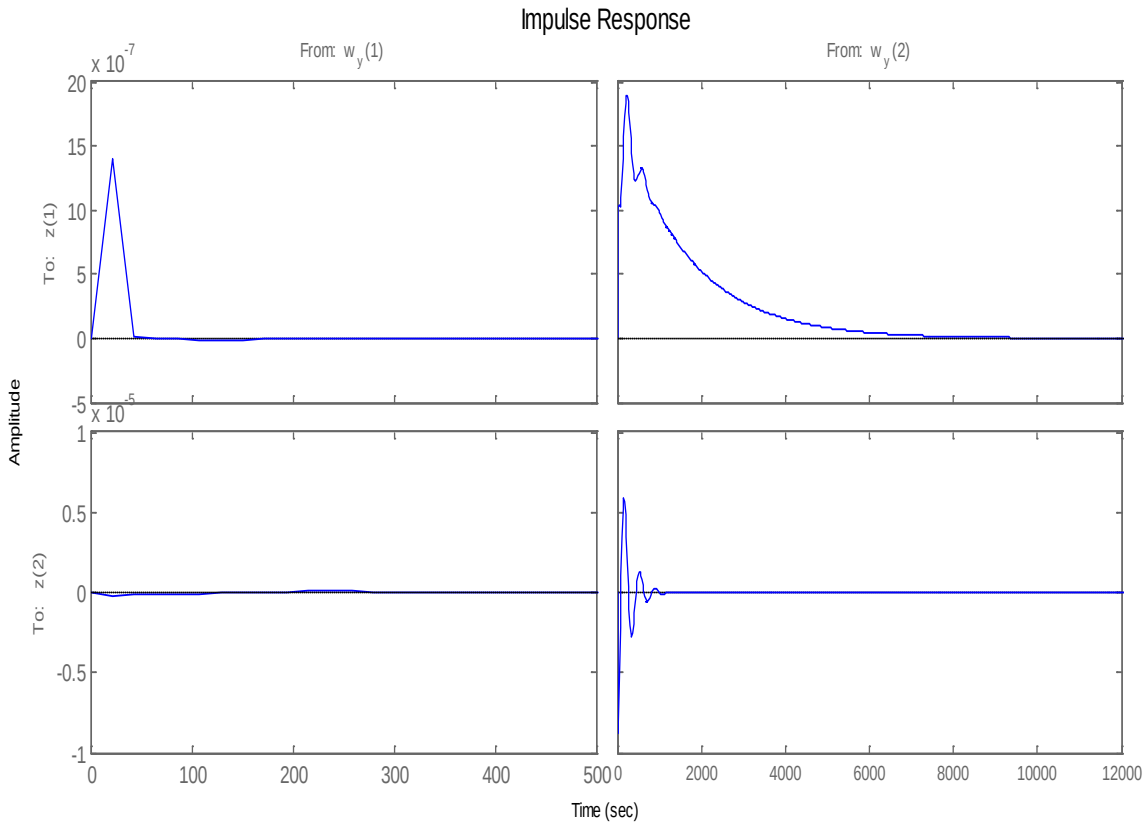

Fig. 6 : Impulse response of the uncertain plant

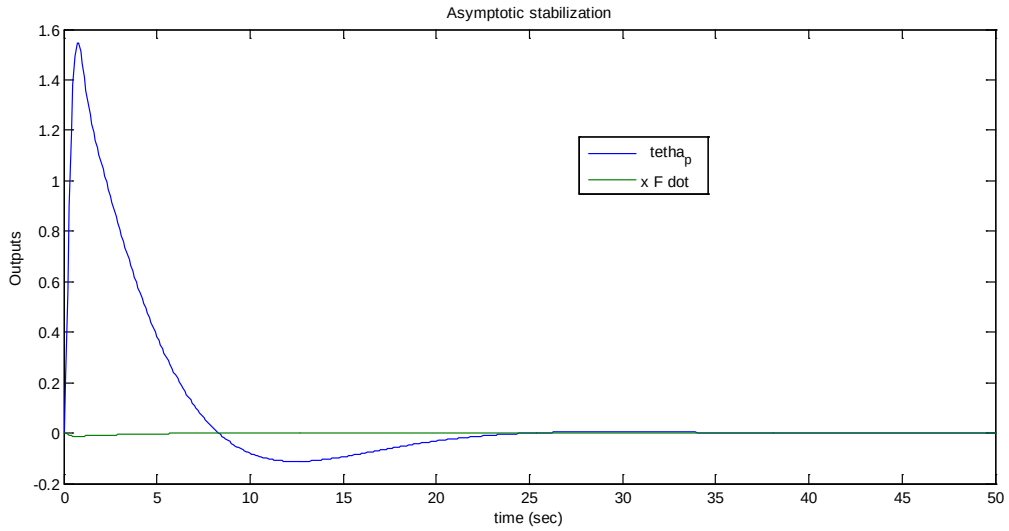

Fig. 7 : Asymptotic stabilization of the closed loop system

This page is intentionally left blank

Global Journal of researches in engineering
Electrical and electronics engineering
Volume 12 Issue 1 Version 1.0 January 2012
Type: Double Blind Peer Reviewed International Research Journal
Publisher: Global Journals Inc. (USA)
Online ISSN: 2249-4596 & Print ISSN: 0975-5861

Calculate Average of an Attribute Including Null Without Aggregate Function

By Mridul Kanti Das, Md. Shakil khan, Md. Mostafa Kamal , Md. Saiful Islam
Dhaka University of Engineering & Technology (DUET), Gazipur, Bangladesh

Abstract - An evaluation of aggregate functions in relational database system considerable impact on performance in many application areas like geographic information systems and statistical and scientific databases. The problem with existing systems is inefficient execution of aggregate functions with large data volumes and lack of flexibility. It is not possible to extend the systems with new aggregate (average) functions. In this paper we extend the concept of aggregate functions from relational databases. This paper introduces the concept of average functions which could enhance flexibility and performance considerably. We show how this could be implemented into a database. Our implemented technique easily detects any changing in replicated data and original data with considering Null values.

Keywords : *Aggregate Function, NULL, SQL, Boolean Algebra, Sub Queries.*

GJRE-F Classification: *FOR Code: 010303*

Strictly as per the compliance and regulations of:

Calculate Average of an Attribute Including Null Without Aggregate Function

Mridul Kanti Das[α], Md. Shakil khan[σ], Md. Mostafa Kamal [ρ], Md. Saiful Islam [ω]

Abstract - An evaluation of aggregate functions in relational database system considerable impact on performance in many application areas like geographic information systems and statistical and scientific databases. The problem with existing systems is inefficient execution of aggregate functions with large data volumes and lack of flexibility. It is not possible to extend the systems with new aggregate (average) functions. In this paper we extend the concept of aggregate functions from relational databases. This paper introduces the concept of average functions which could enhance flexibility and performance considerably. We show how this could be implemented into a database. Our implemented technique easily detects any changing in replicated data and original data with considering Null values.

Keywords : Aggregate Function, NULL, SQL, Boolean Algebra, Sub Queries.

I. Introduction

Aggregate functions perform a calculation on a set of values and return a single value. Aggregate function avg( ) only calculate average without null values. It provides average result, eliminating null values. Null does not have a value (and is not a member of any data domain) but it is a placeholder or "mark" for missing information. Comparisons with Null can never result in either True or False but always in the third logical result is Unknown. So comparing two null is difficult. We discus about (1) review of the research for handling null values in database system using aggregate function (2) problem structure with null value with respect to database (3) describes existing solution and proposed solution and its algorithm as well as how it works (4) details the experimental work that has been carried out. The experimental evaluation has been performed using a large amount of datasets.

Application:

Database System & its related Application software.

Author[α] : Bachelor of Science in Engineering degree from Department of Computer Science and Engineering (CSE), Dhaka University of Engineering & Technology (DUET), Gazipur, Bangladesh. PH:+8801715543754. Email : mridul.duet@yahoo.com

Author[σ] : Bachelor of Science in Engineering degree from Department of Electrical & Electronic Engineering (EEE), Dhaka University of Engineering & Technology (DUET), Gazipur, Bangladesh. PH:+8801719452365. E-mail: shakil.khan027@gmail.com

Author[ρ] : Bachelor of Science in Engineering degree from Department of Computer Science and Engineering (CSE), Dhaka University of Engineering & Technology (DUET), Gazipur, Bangladesh. PH:+8801917317521. Email: mostofa49@yahoo.com

Author[ω]: Bachelor of Science in Engineering degree from Department of Electrical & Electronic Engineering (EEE), Dhaka University of Engineering & Technology (DUET), Gazipur, Bangladesh. PH:+8801718871213. E-mail: saifful69@gmail.com

II. Related Woks

Baekgraard and Mark [1] on this work, developing a nested algebra for describing sub-queries, but without considering aggregates, duplicates, or null values.

Jeff Smith [2] is software developer, he compare all columns in database, and also handles comparing NULL values to other NULLs, Using UNION operator.

- Aggregate function avg (X) returns the average value of all non-NULL X within a group ignoring null values.

Aggregate avg ( ) function with Null value problem solution:

- ***SQL>select avg (Amount) from bank;***

Table bank

name	*Address*	*account_no*	*amount*
Mridul	*Sylhet*	*701*	*700*
Sakil	*Kushtia*	*702*	*NULL*
Shuva	*Rangpur*	*703*	*600*
Shahid	*Jessore*	*704*	*1000*
Ujjal	*Sylhet*	*705*	*800*
Babul	*Sylhet*	*706*	*600*
Nupur	*Netrakuna*	*707*	*1100*
Mian	*Comilla*	*708*	*NULL*

Normal Avg Query Result is
Avg=(4800)/6

III. Existing Solution

- Aggregate avg ( ) function with Null value problem solution:

SQL>**select sum (amount)/count(*) from bank;**

Table bank

name	*Address*	*account_no*	*amount*
Mridul	*Sylhet*	*701*	*700*
Sakil	*Kushtia*	*702*	*NULL*
Shuva	*Rangpur*	*703*	*600*
Shahid	*Jessore*	*704*	*1000*
Ujjal	*Sylhet*	*705*	*800*
Babul	*Sylhet*	*706*	*600*
Nupur	*Netrakuna*	*707*	*1100*
Mian	*Comilla*	*708*	*NULL*

Normal Avg Query Result is
Avg=(4200)/7=600

a) Performance Measure Table

Table bank

Amount of Data	*Amount of NULL*	*Existing solution Execution Time (ms)*
10000	1930	0.01250
20000	4411	0.06125
30000	6094	0.10937
40000	7367	0.13120
50000	8262	0.18750
55000	13268	0.18750
70000	14725	0.25000

b) Flowchart

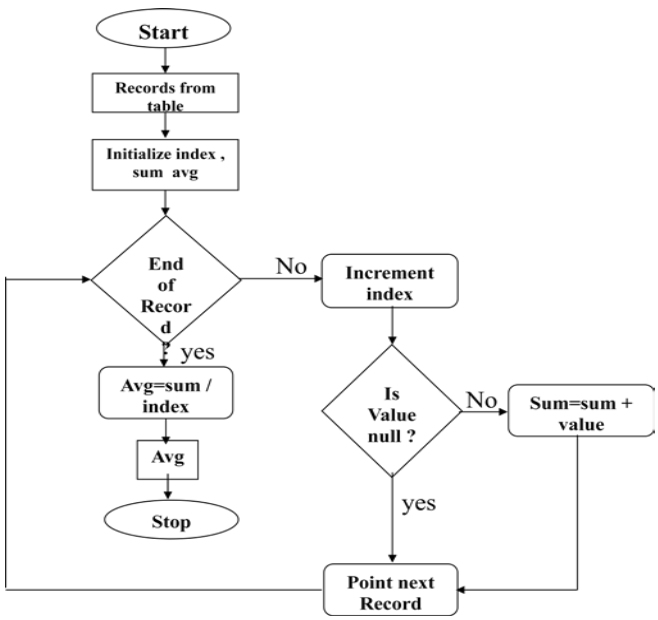

c) Proposed Algorithm

1. Begin
2. Algorithm_average_with_null ()
3. Initialize index, average, sum as double
4. While until end of the table
5. Increment index
6. If field is null then
7. point next record
8. Go to step 3
9. Otherwise
10. sum=sum + field_value
11. point next record
12. end if
13. end while
14. average=sum/index
15. end

d) Performance measure table of Proposed Solution

Table bank

Amount of Data	*Amount of NULL*	*Proposed Solution Execution Time (ms)*
10000	1930	0.03126
20000	4411	0.07125
30000	6094	0.09370
40000	7367	0.12530
50000	8262	0.17181
55000	13268	0.18543
70000	14725	0.21870

In this solution we see that if the number of data in database gradually increased then the execution time is increased. Built-in function sum() and count() scan record individually from top to bottom in a table. Therefore Existing query are not efficient to calculating average value in large amount of data with Null values.

e) Comparison Table between Existing and Proposed Solution

Table bank		
Amount of Data	*Existing solution Execution Time (ms)*	*Proposed Solution Execution Time (ms)*
10000	0.01250	0.03126
20000	0.06125	0.07125
30000	0.10937	0.09370
40000	0.13120	0.12530
50000	0.18750	0.17181
55000	0.18750	0.18543
70000	0.25000	0.21870

From comparison table we see that our propose system takes less times than existing system. By proposed system can reduce time and reduce the problem of existing system. To understand easily a graph chart is given below.

f) Graph of Existing Solution vs. Proposed Solution

Our propose solution is efficient to calculate average value with Null values from large amount of data.

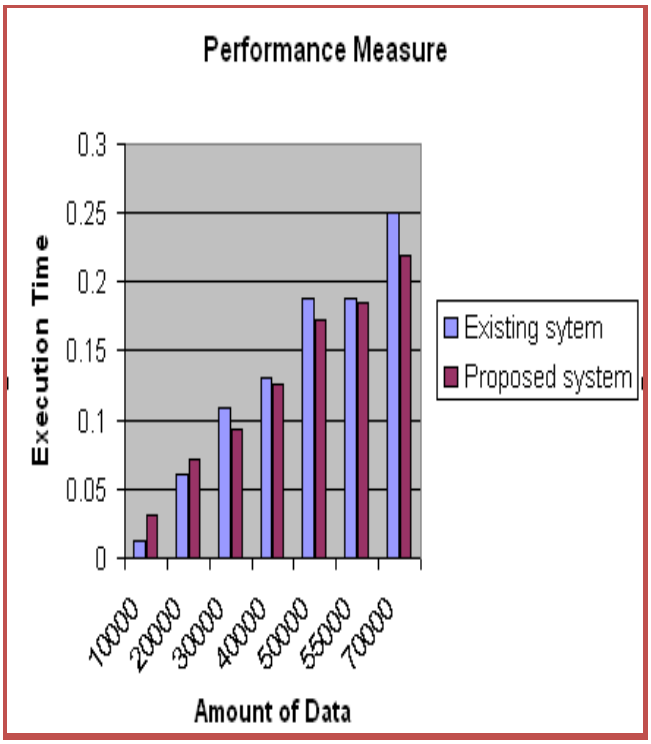

From the above graph Green bar indicates Existing solution time and Red Bar indicates proposed solution time. We see that in proposed system needs execution time less than existing system.

IV. Conclusion

At the age of globalization most of all bank already has been computerized. They store their customer information, balance, transaction etc. in database. And they need to calculate average number of transaction after a certain period of time. Even stock exchange Ltd. Hospital, Airlines etc. need to calculate average number of transaction frequently. So our proposed system will be best for them which can save their times.

References References Referencias

1. L. Baekgraard and L. Mark. Incremental computation of nested relational query expression. ACM TODS, 20(2):111-148, June 1995.
2. Jeff Smith is software developer, he using UNION operator comparing NULL values to other NULLs. www.weblogs.sqlteam.com.
3. Comparing Tables By Bill Graziano on 07 January 2002.
4. Domain (Data Type) and null. .http://dbtips. wordpress.com/2009/05/31/some-notes-about-null/
5. SQL Functions from Oracle Database Globalization Support Guide
6. Analytic Functions from Oracle® Database SQL Reference 10g Release 1 (10.1) Part Number B10759-01
7. Improving the performance of SQL Data Compare from Red Gate® Software Ltd web site.
8. "Structured Query Language (SQL)". International Business Machines. October 27, 2006. Retrieved 2007-06-10.
9. "A Relational Model of Data for Large Shared Data Banks" E. F. Codd, Communications of the ACM, Vol. 13, No. 6, June 1970, pp. 377–387.

This page is intentionally left blank

Global Journal of researches in engineering
Electrical and electronics engineering
Volume 12 Issue 1 Version 1.0 January 2012
Type: Double Blind Peer Reviewed International Research Journal
Publisher: Global Journals Inc. (USA)
Online ISSN: 2249-4596 & Print ISSN: 0975-5861

A New Approach for Modeling the System Dynamics

By T.S.Sirish, Sujalakshmy .V, Dr.K.S.Sivanandan
National Institute of Technology, Calicut

Abstract - This paper addresses the development of an average value based model for the processing system. The continuous observation of that process variable, fixation of its average value on real time basis, mathematical model development of above average value as base factor are the basic steps of this method, which subsequently leads to time based dynamics. The validation of the models developed by this method is done through experiments. The method is tested by taking two types of systems: one a biological system and second an electrical distribution system. The process variables selected are the angular displacement for biological system and rms value of current for electrical systems. The simulated results of the model agree with that of experimental reading in both cases within tolerable limits.

Keywords : *Average value based model, base average value, electrical distribution system, biological system.*

GJRE-F Classification: *FOR Code: 090699*

Strictly as per the compliance and regulations of:

A New Approach for Modeling the System Dynamics

T.S.Sirish[α], Sujalakshmy .V[σ], Dr.K.S.Sivanandan[ρ]

Abstract - This paper addresses the development of an average value based model for the processing system. The continuous observation of that process variable, fixation of its average value on real time basis, mathematical model development of above average value as base factor are the basic steps of this method, which subsequently leads to time based dynamics. The validation of the models developed by this method is done through experiments. The method is tested by taking two types of systems: one a biological system and second an electrical distribution system. The process variables selected are the angular displacement for biological system and rms value of current for electrical systems. The simulated results of the model agree with that of experimental reading in both cases within tolerable limits.

Keywords : Average value based model, base average value, electrical distribution system, biological system.

I. Introduction

Modern process systems are continuously undergoing modifications and improvements so is the case of their characteristics – static as well as dynamic. Complexity of their analysis follows subsequently. Dynamic correction, characteristic determination, balance establishment, equilibrium maintenance etc are all the important tasks associated with them. Spatially distributed and geographically dependent consumer electric distribution system and its process variables is a typical example and biological human locomotion system and its dynamics variables is another one.

The associated control systems should be modified accordingly with the attachment of suitable central console to supervise the process variable dimensions so as to establish appropriate dynamic stability and balance. Continuous real time monitoring of the process variables will be a routine process of such systems. Real time analysis is of paramount importance. An easy and efficient analytical technique takes an important role in the operations. Sufficient attempts are already being made for making the analytical methods more and more efficient and attempts are still continuing for more efficient ones.

The aim of the present paper is towards these directions. Here an analytical technique based upon the average values of the process variables, its use in developing dynamic models of systems etc are considered in detail. The so developed model is validated experimentally.

E Ortojann et.al presented an approach for power distribution in hybrid power systems using an RMS (root mean squared) model for the electrical part of the system in combination with the set of differential equations to describe the dynamic behavior of the mechanical part of the system [1]. A three phase power system dynamic modeling based on the information about boundary components is presented in [2].Here the power system is divided in to a study system which can be a regional system and several external systems. The external system is a MIMO (Multiple Input Multiple Output) system and it is represented by Auto regressive model (ARX) and the analysis is made. An improved model for representing the voltage sensitive dynamic loads ,distribution system equivalents with load tap changers etc has been presented with specific selected operational study scenario of AEP Central AP company area[3].Dynamic equivalents of distribution systems including dynamics of electric loads and on load tap changer with reference to a radial distribution system and thereby developing an equivalent model is depicted in [4].Power system composite load dynamics is well represented in[5] whereas determination of dynamic load model parameters on the basis of secondary side measurements of 110/10KV transformer is the content of [6].The characterization of the distribution system load as a function of the substation voltages is done by Micheal .J.Gorman, Sehyan Civanlar in [7].The dynamic variation of the composite system load on distribution feeders is captured and the most effective substation voltage level is obtained. Model validation principle using hybrid dynamic simulation and an algorithm for obtaining optimal feeder configuration of a power system distribution network are represented in [8, 9] respectively.

The approach described in the paper can also be applied to the biological systems. The mathematical model of the human locomotion for knee joint can be obtained with the above approach. The general processing problems occurring in such systems are cited by many researches mentioned below.

Gait analysis is gaining prominence for evaluation of disability of handicapped people on

Author α : Research scholar, Department of Electrical Engineering, National Institute of Technology, Calicut. Telephone: 9037260927
E-mail : srinivassirish@nitc.ac.in
Author σ : Research scholar, Department of Electrical Engineering, National Institute of Technology, Calicut.
Email : suja_lakshmy@yahoo.com
Author ρ : Professor, Department of Electrical Engineering, National Institute of Technology, Calicut. Email : kss@nitc.ac.in

comparison of such analysis of healthy people with the disabled. This is motivated by study conducted by Tommy Oberg and et.al [11] on 233 healthy subjects ((116men and 117 women) up to 79 years of age. Berbyuk and et.al [12] has made a mathematical modeling of the dynamics of human gait in a saggital plane as an optimal control problem for a nonlinear multidimensional mechanical system with phase constraints given by experimental data. Nishchenko and et.al [13] proposed a new formulation of the problem of designing a femoral prosthesis.. Jerry E.Pratt and et.al [14] developed a one degree of freedom exoskeleton called RoboKnee. User intent is determined through the knee joint angle and ground reaction forces.. Hayashi and et.al [15] developed Hybrid Assistive Limb, a robot suit as an assistive device for lower limbs. This method uses biological and motion interaction. Yamamoto and et.al [16] proposes a stand alone wearable power assisting suit which gives nurses the extra muscle they need to lift their patients and avoid back injuries. D Jin and et.al [17] investigated the advantages of the mechanism as used in the prosthetic knee from the kinematic and dynamic points of view. Takahiko Nakamura and et.al [18] propose a wearable antigravity muscles support system to support activities of physically weak persons. Satio and et.al [19] proposed wearable walking support system In this paper to validate the usefulness of proposed system, the Standing up motion, one of the hardest activities of daily life is analyzed and the usefulness of proposed method is discussed. Sunil K Agarwal and et.al [20] proposes a gravity balancing lower extremity exoskeleton a simple mechanical device composed of rigid links, joints and springs, which is adjustable to the geometry and inertia of the leg of a human subject wearing it.

Even though sufficient quantities of work in the broad area for different dynamic model of systems are done a serious study on dynamic model aiming towards their self balancing concept was not commonly seen or rather properly observed. This paper addresses the development of an advanced model using average value for predicting the dynamics of the process variables of a continuous time varying systems. The average values of the parameters of the system are utilized for the development of the model. As usual here also the entire system is divided into number of subsystems and the dynamic model of the subsystem is derived. The same approach can be extended hierarchically and the dynamic model of the entire system is obtained. The continuous observation of the parameters of the system for a sample period is carried out and an average value is fixed on a real time basis, mathematical model development with the above average value as the base factor is the ideology behind the paper.

II. Process System -a General Approach

The general process system suitable for this analytical approach shall be represented by block diagrams shown in Fig 1(a), 1(b), 1(c) or similar of any of the types shown in Fig 1(a), 1(b), 1(c) .The system can be divided into either subsystem shown in Fig 1(a) and 1(c) or it can be applied to system shown in Fig 1(b) also. The control system considered as in fig 1(a) and 1(c) is divided into a number of subsystems such that the input of the entire system is the input to the subsystem1.The output of the subsystem1is fed to the subsystem2 and the output of the subsystem2 is fed to the subsystem3 etc.. The output of the subsystem N will be the output of the entire system. There are possibilities such that each of the subsystems mentioned above is further divided in to sub subsystems shown in Fig 1(c). Such that the input to the subsystem will be the sum of the inputs to each of the sub subsystems and the output of the subsystem will either be the sum of the outputs of the sub systems or direct outputs from the sub subsystems i.e. Subsystems considered can either be a MIMO (multiple input and multiple output) system or an SISO (single input and single output) system.

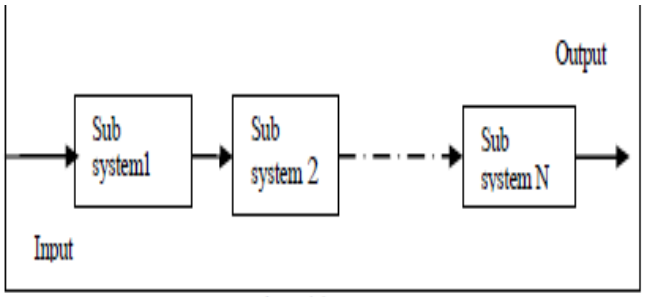

Fig.1 (a)

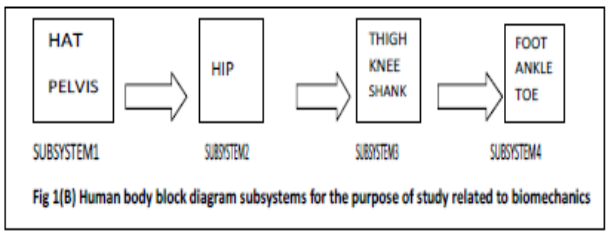

Fig 1(B) Human body block diagram subsystems for the purpose of study related to biomechanics

Fig.1 (b)

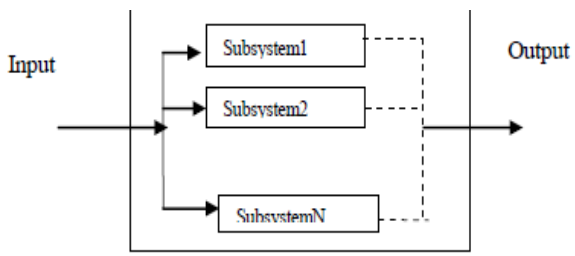

Fig.1(c)

Fig.1 : General Representation

The block diagram shown in Fig 1(b) is a general representation of a biological system specifically the human biological system whose physiological description is given as follows. Human body comprises of various bones, muscles and joints. These bones, muscles and joints are very important for proper functioning of our body. According to fig 1(b) subsystem 1 called HAT consists of head, arms and trunk. The subsystem 2 consists of HIP, the hip joint scientifically refereed as the joint between the femur and pelvis and its primary function is to support the weight of the body in both static i.e. standing and dynamic i.e. walking and running. The details of subsystem 2 and 3 are not much elaborated. The subsystem 3 consists of knee joint, joins the thigh with the leg. It is the largest joint in the human body and is very complicated. The dynamics and mathematical modeling of subsystem 3 i.e. knee is considered thoroughly throughout the paper in the following sections. Finally subsystem 4 consists of Ankle, one of the important body parts. The study of the dynamics of subsystem 2 and 4 i.e. HIP and Ankle are considered latter and the experimental study of the knee is considered in the following sections of the paper.

According to medical literature the subsystem3, the knee is considered as a complex, compound, condyloid variety of a synovial joint [14]. The shape of the condyloid joint permits movement in two planes allowing flexion and extension in one plane and adduction and abduction in another. Typically biological movement is explained by a popular biological terms Flexion and Extension as explained under. Flexion is an anatomical term that refers to a movement produced at a joint by a muscle or muscles that causes the angle of the joint to decrease relative to its anatomical position as shown in fig 2. For example, when a person is standing normally, the hip joint is considered to be in a neutral or 180-degree position. Flexion at the hip occurs when that person raises her knee into the air, thus bending the hip and decreasing the joint angle at the hip from 180 degrees to 90, if the knee is brought to hip height. A large number of joints in the human body are capable of flexion and its opposite movement, extension as shown in fig 2.

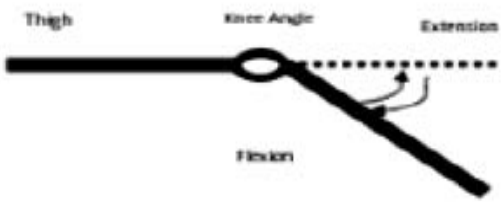

Fig 2 Flexion and Extension Movements of Knee Joint

Having given a detailed explanation of the characteristics of systems categorized through fig 1(a)-1(c), description of these systems with special aim for analytical development is shown in the subsequent sections. Systems under the category shown in fig 1(a) and 1(c) is considered first and that of fig 1(b) is considered latter. As mentioned above a detailed description of the operational characteristics is considered in the previous section. Now what is required is description specially aiming towards the analytical part of systems.

III. System Modeling

The type of systems such as that in fig 1(a) and 1(c) having process variables say voltage, current, power factor, speed, frequency etc which determines the system behavior may be observed for a time period say from T1 to Tn and the readings are recorded as shown in Table1. The variations in the values of these variables show the actual dynamics of the output variables of the system

Time	System parameter input	System Parameter Output
T1	X1	Y1
T2	X2	Y2
T3	X3	Y3
Tn	Xn	Yn

Table 1

The types of systems such as that shown in fig 1(b) having process variable knee joint angle which determines the system behavior may be observed for a time period say from T1 to Tn. The variations in the values of this variable (knee joint angle) show the actual dynamics of the output variables of the system. The objective of the work is to develop a linear mathematical model for the dynamics of above types of system. The model is formulated on the assumption that the dynamic variable is a linear combination of a base average value and infinitely number of hierarchically considered variational terms. These variational terms are called variational part in the base average value, second variational part in the base average value and so on. The procedure for deriving these factors is explained in detail as follows:

- **Identical average value sectors**

From the observed values of the output in Table 1, Find out certain sectors (eg: time period from T1 to T4 or Time period from T2 to T3 etc) such that the average values of these sectors are the same. These sectors are called the identical average value sectors or primary sectors and the average value corresponding to these sectors are called primary averages.

- **Secondary sectors**

For further experimentation with the observed values inside the primary sectors, inner secondary

sectors exists which yields the average value which are slightly and independently different from the average value of the primary sectors. These are named as secondary averages.

- Tertiary sectors

Similarly some tertiary sectors are identified inside each of the above secondary sectors which further yields slightly different average values from the respective average values of the secondary sectors. They are termed as tertiary averages.

- Special sectors

In reality, possibilities cannot be ruled out for some small time sectors called special sectors which exhibit widely different average value from the uniform average value of the primary sector.

IV. Derivation of Input Output Equation

The variation of the system parameters in the output is due to the structural changes occurring in the system. The so changed structure is the main reason for the so reflected dynamics. In such cases, it is always possible to have a relationship between the input and output dynamics or rather an equality relationship incorporating the input and out put values and structural variational parts exist. Assuming the system as linear, the following empirical relationship is guessed.

As indicated above, It will be quiet conforming to think that the output dynamics is a linear combination of components involving abase average value, A, a variational part over the above average value, ΔA, a factor containing the variational term in $\Delta A, \Delta^2 A$, and so on. Here ΔA is first change in base average value, A and $\Delta^2 A$ is variational term in ΔA .It can be stated in another way that the output is a combination of a base average value and infinite number of hierarchically considered variational terms. To make it more clear, these variational terms must be multiplied by the factors M1, M2, M3…….. to take care of the effect of variable structure or the input-output relationship can be represented empirically as

$$BQ=M1\ A+M2\ \Delta A+M3\ \Delta^2 A+ \ldots\ldots\ldots\ldots\ldots$$

To accommodate the dynamics contributed by special sectors, a constant (K) is also considered. Strictly speaking, the input part also has to be considered as a summation of infinite number of terms involving a base value and subsequent variational terms. But to avoid practical complexity, only one term i.e. base term alone (Q along with the factor B) is considered for the input dynamics. This approach is somewhat similar to the dynamic models described in [10].The main difference that occur with that described in [10] is that the present argument is based upon an average value whereas the one in [10] is treated mainly taking time as the base.

In the light of above explanations, the input-output dynamics of the sub subsystem can be represented as

$$BQ=M1\ A+M2\ \Delta A+M3\ \Delta^2 A+K \ldots\ldots\ldots\ldots \quad (1)$$

(A) Procedure for findings the variational terms

The steps to be followed to obtain the variational terms are as under:

1. To find ΔA:

Obtain the average value of the primary sector.

Divide the primary sector into secondary sectors and find the secondary averages.

Obtain the differences between the primary averages and the secondary averages.

The average of these differences are ΔA.

2. To find $\Delta^2 A$:

Divide the secondary sectors in to tertiary sectors

Determine the tertiary averages.

Obtain the differences between the secondary averages and tertiary averages.

The average of these differences is $\Delta^2 A$

V. Algorithm/Steps

Step1: Obtain the primary sectors P1,P2,P3,…… ……and the primary averages PA1, PA2……..

Step2: Obtain the variational terms as explained in section IV (A).

Step3: Frame the equations corresponding to each of the primary averages as

$$B\ QA1=M1\ PA1+M2\ \Delta PA1+\ M3\ \Delta^2 P\,A1+K+\ldots\ldots\ldots\ldots \quad (1.a)$$

$$B\ QA2=M1\ PA2+M2\ \Delta PA2+\ M3\ \Delta^2 P\,A2+K+\ldots\ldots\ldots\ldots \quad (1.b)$$

$$B\ QA3=M1\ PA3+M2\ \Delta PA3+\ M3\ \Delta^2 P\,A3+K+\ldots\ldots\ldots\ldots \quad (1.c)$$

$$\vdots$$

$$B\ Q\ An=M1\ PAn+M2\ \Delta P\ An+\ M3\ \Delta^2 P\,An\ +K+\ldots\ldots\ldots\ldots \quad (1.n)$$

Step 4: Solving these equations results in the values of constants M1/B, M2/B,…….

Step 5: Representation of the equations (1.a),(1.b),(1.c)…….(1.n) in terms of general variable corresponding to A, ΔA, $\Delta^2 A$ …… i.e. the equality statement as per (1) is obtained.

- Identification of best model

Different combinations of primary, secondary and tertiary sectors are chosen for the same output variable so as to enable us to choose best equality statement.

VI. Sample System Modeling

a) Case study 1(Distribution power system)

To demonstrate and test the proposed method, a system with the above characteristics mentioned in earlier section, power system network can be considered as a universal system and the average based model has been developed for the three output phases of a distribution transformer, considering it as a sub subsystem of the distribution subsystem. The subsystem is characterized by sets of output variables which in reality exhibits different values both in phase and magnitude resulting in distinct levels. The sets of variables described above will be classified in to different subsets and the elements of which will be three phase outputs of each distribution transformer. Each three phase outputs are normally identified by R,Y,B. The dynamic analysis of these R, Y, B variables is done using the above proposed method. The observed value of the output currents (Ro, Yo, Bo) of a distribution transformer is indicated as shown in Table 2.

	100KVA Transformer				
	Input current	Output current			
Time	Ri =Yi =Bi	R phase (Ro)	y phase (Y0)	B phase (Bo	Neutral (No)
9.00 AM	2.5	70.3	70.3	70.3	0
10.00 AM	2.5	65	55	92.2	32
11.00 AM	2.2	60	43	83	29
12.00 AM	2.2	63	35	82	27
1.00PM	2.3	66	48	75	16
2.00 PM	2.1	62	46	69	13
3.00 PM	2.0	60	45	65	11
4.00 PM	2.2	56	45	80	29
5.00 PM	2.2	64.5	52	63	4
6.00 PM	1.9	58	36	66	15
7.00 PM	2.3	68	25	102	42
8.00 PM	2.8	94	30	110	27
9.00 PM	3.0	92	58	102	21
10.00 PM	2.4	60	55	83	25
11.00 PM	2.3	65	43	82	25
12.00 PM	2.3	70	48	75	13
1.00 AM	2.1	60	45	69	15
2.00AM	2.2	65	52	70	10
3.00 AM	2.4	88	36	80	3
4.00 AM	1.9	62	30	66	12
5.00 AM	1.9	56	32	71	22
6.00 AM	2.5	64.5	35	110	54
7.00 AM	2.2	56	25	105	56
8.00 AM	2.3	58	32	104	54
9.00 AM	2.3	94	30	66	17
10.00 AM	2.1	65	35	75	19
11.00 AM	2.1	60	48	69	14
12.00 AM	2.0	56	45	65	14
1.00 PM	2.2	64.5	35	80	24
2.00 PM	2.2	68	48	71	10
3.00PM	2.3	56	45	87	36
4.00PM	2.1	58	52	65	10
5.00PM	2.3	68	46	80	20
6.00PM	2.3	62	55	71	12
7.00PM	2.3	66	43	82	24
8.00PM	2.2	63	35	83	28

Table 2

Table2 : Observed Values Of The Output Currents

The actual dynamics of the four distinct outputs is shown in Fig (3) to (6) and that of the input is shown in Fig (7).

On developing the model, it is assumed that the variational terms at the output is restricted up to two terms and that constant term is assumed as zero even though the same will reflect as an error.

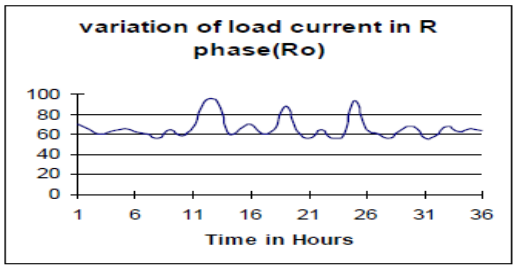

Fig 3

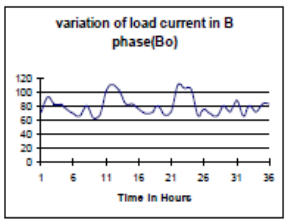

Fig .4

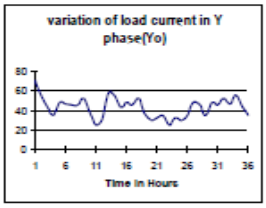

Fig .5

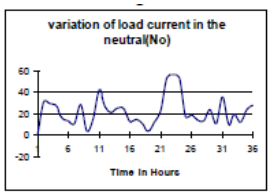

Fig.6

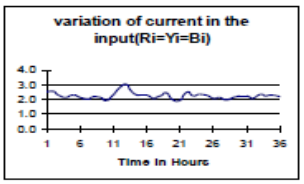

Fig 7.

i. *Experimental Steps*

The experimental analysis for the development of average value based model for R phase of the distribution transformer is explained below:

a. Determination of Primary sectors and primary averages

70.3
65
60
63
66
62
60
56
64.5
58
68

Table 3

60
65
70
60
65
88
62
56

Table 4

88
62
56
64.5
56
58
94
65
60
56
64.5

Table 5

PRIMARY SECTORS

b. Determination of secondary sectors and secondary averages:

-	Average value of the output (Ro) (Primary averages)	Average value of the input
Sector1	65.566	2.2746
Sector2	65.75	2.1945
Sector 3	65.818	2.179

Table 6

PRIMARY SECTOR AVERAGES

The secondary sectors chosen from the primary sectors are represented in Table 7 and the secondary averages are shown in Table 8.

Secondary sectors					
from primary1		from primary2		from primary3	
70.3	56	60	88	88	94
65	64.5	65	62	62	65
60	58	70	56	56	60
63	68	60		64.5	56
66	94	65		56	64.5
62				58	
60					

Table 7

	Secondary sectors	Secondary averages of the output (Ro)
Primary sector1	Sector1	63.757
	Sector2	68.1
Primary sector 2	Sector 3	64
	Sector4	68.66
Primary sector 3	Sector 5	64.08
	Sector 6	67.9

Table 8

SECONDARY SECTOR AVERAGES

c. Determination of Tertiary sectors and Tertiary averages: The tertiary sectors chosen from the secondary sectors are represented in Table 9 and the tertiary averages are shown in Table 10.

from primary2			
from secondary3		from secondary4	
60	60	88	56
65	65	62	
70			

from primary3			
from secondary5		from secondary6	
88	56	94	56
62	58	65	64.5
56		60	
64.5			

Table 9

TERTIARY SECTORS

		Tertiary sectors	Tertiary averages of the output
Primary sector1	secondary sector1	Sector1	64.575
		Sector2	62.66
	secondary sector2	Sector3	59.5
		Sector4	81
Primary sector2	secondary sector3	Sector 5	65
		Sector6	62.5
	secondary sector4	Sector7	75
		Sector8	56
Primary sector3	secondary sector5	Sector 9	67.625
		Sector10	57
	secondary sector6	Sector11	73
		Sector12	60.25

Table 10

TERTIARY SECTOR AVERAGES

d. Special sectors: The special sectors are shown in Table 11

68	92
56	
58	
68	
62	
66	
63	

Table 11

SPECIAL SECTORS

ii. *Determination of variational terms ΔA, $\Delta^2 A$: The variational terms obtained for the above combination of primary sectors, secondary sectors and tertiary sectors are shown in Table 12.*

combination	A	ΔA	Δ^2 A
1	65.56	-0.3685	-1.005
	65.75	-0.58	1.705
	65.818	-0.19	1.521

Table 12

VARIATIONAL TERM

iii. *The equations corresponding to the above combination are as follows:*

A. $B\ 2.2746 = M_1 65.56 - M_2 0.3685 - M_3 1.005$ (2)

B. $B\ 2.195 = {}_{M1}65.75 - {}_{M2}0.58 + {}_{M3}1.705$ (3)

C. $B\ 2.179 = M_1 65.818 - M_2 0.19 + M_3 1.521$ (4)

Where $_{M1}$, $_{M2}$, $_{M3}$ represents variation in structure at the output. B represents variation of structure in the input.

On solving the equations (2), (3), (4), the values of M1/B, M2/B and M3/B are obtained as in Table 13.

Combination	M1/B	M2/B	M3/B
1	0.034	-0.06	-0.0367

Table 13

iv. *The equality statement for R phase of the distribution transformer for the above combination of primary sectors is obtained as :*

$$Q = 0.035\ A - 0.06\ \Delta A - 0.0367\ \Delta^2 A \qquad (5)$$

v. Derivation of time based plot

The above developed average based mathematical model can be utilized to obtain a time based plot from the observations of the output. By choosing any time period of desired choice from Table 2, the base value A, the variational factors Δ A and Δ^2 A for this time period is calculated. The result of the average based equalities can be converted in to a time based plot whose procedure is as given below.

a. Identify a particular time as reference.
b. Choose ideal time duration on both sides of the above reference value as the primary sector.
c. Derive corresponding secondary sectors and tertiary sectors within this time duration and derive the base average value of the primary sector and the variational factors ΔA and Δ^2A from secondary sectors and tertiary sectors respectively.
d. Substitute the obtained values of A, Δ A and Δ^2A in the equation (5).
e. Calculate the value of the equation.
f. The so determined value is plotted against time described in step a.
g. Increment the identified time in step a.
h. Repeat step b to step f to get the time based plot.

The above step give a time based plot for the above combination of primary sectors and is shown in Fig .8.

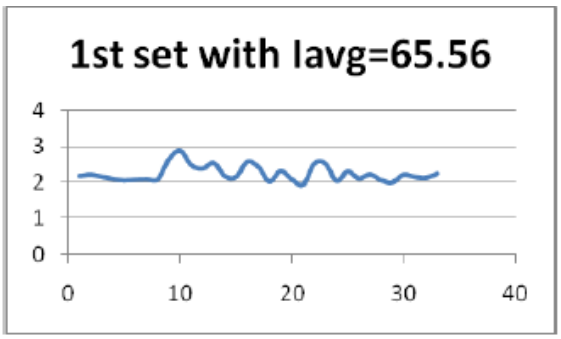

Fig 8

vi. Identification of best model

The above steps are repeated for different combinations of primary sectors and time based plots are obtained for each and every combination. This is compared with the corresponding experimentally detected input variables shown in Table 2 and the best possible one is selected on the basis of minimum error they produced with the experimental one. The values of error obtained for different combinations are shown in Table 14.

Combination	Error	A	M1/B	M2/B	M3/B
1	8.0175	65.5	0.034	-0.06	-0.0367
2	4.6509	70	0.035	-0.021	0.039
3	3.2916	63	0.035	0.0256	0.00094
4	4.1808	64	0.035	0.049	-0.01
5	4.104	67	0.033	0.0095	-0.01
6	9.9934	68	0.03	-0.05	0.018

Table 14.

ERROR OBTAINED FOR DIFFERENT COMBINATIONS

The so selected equation is considered as the best dynamic counterpart corresponding to the average based model of equation (5) represented by the combination 3 as shown.

$$Q = 0.035\ A + 0.0256\ \Delta A + 0.00094\ \Delta^2 A \qquad (6)$$

The so identified average based equation (6) is adopted as the best mathematical model for the variable(R).

Similarly the best models are identified for the other two variables(Y phase and B phase) of the distribution transformer and are obtained as follows.

$$Q\ (Y) = 0.05A(Y) - 0.0065\Delta A(Y) - 0.01\Delta^2 A(Y) \qquad (7)$$

$$Q\ (B) = 0.028A\ (B) - 0.0009\Delta A\ (B) + 0.01\Delta^2 A\ (B) \qquad (8)$$

vii. Model validation

The above developed mathematical model is validated by comparing the calculated dynamics represented by equation (6) with the experimentally detected values from the real system. For this three sets of samples at different time periods of the real working system (Table 15, 16, 17) is considered and the error is calculated as shown in Table 18. The error is found to be in reasonable limits so as to establish the validity of the model.

Time	Observed Input current	Output current R phase (Ro
12:00	2.47	70
1:00	2.53	75
2:00	2.51	73
3:00	2.47	72
4:00	2.31	60
12:00	2.77	70

Table 15:Sample1

Time	Observed input current	Output current
8:00	3.13	80
9:00	2.93	75
10:00	2.77	70

Table 16:sample2

Time	Input current	Output current
10:00	2.33	65
11:00	2.51	68
12:00	2.64	70
1:00	2.87	75
2:00	2.91	75

Table 17: Sample3.

A	ΔA	Δ^2A	Calculated input	observed input	Error
71.38	-0.682	0.231	2.481	2.64	0.159
70	-0.67	0.045	2.432	2.458	0.026
70.6	0.73	0.295	2.489	2.652	0.163

Table 18

ERROR ANALYSIS

b) Case Study 2(Biological Human Locomotion)

The proposed algorithm is applied to the normal walking case and the mathematical model of the variation of knee joint angle is developed as below. The normal walking video is captured for a finite time i.e. 20 seconds. The knee joint angle of human locomotion is observed and tabulated as shown in Table B1

Time in sec	Angular position (degrees)	Time in sec	Angular position (degrees)	Time in sec	Angular position (degrees)	Time in sec	Angular position (degrees)
0.0	180	5.0	165	10	135	15	160
0.1	175	5.1	170	10.1	120	15.1	160
0.2	170	5.2	165	10.2	120	15.2	160
0.3	165	5.3	165	10.3	130	15.3	160
0.4	140	5.4	160	10.4	150	15.4	160
0.5	135	5.5	160	10.5	170	15.5	150
0.6	155	5.6	155	10.6	160	15.6	140
0.7	170	5.7	140	10.7	165	15.7	120
0.8	165	5.8	120	10.8	160	15.8	120
0.9	160	5.9	120	10.9	165	15.9	130
1.0	170	6.0	130	11	165	16	150
1.1	170	6.1	150	11.1	160	16.1	170
1.2	170	6.2	170	11.2	160	16.2	170
1.3	160	6.3	165	11.3	155	16.3	160
1.4	155	6.4	160	11.4	140	16.4	165
1.5	145	6.5	165	11.5	135	16.5	160
1.6	140	6.6	165	11.6	120	16.6	160
1.7	120	6.7	160	11.7	125	16.7	160
1.8	120	6.8	160	11.8	140	16.8	155
1.9	130	6.9	160	11.9	170	16.9	150
2.0	165	7.0	150	12	165	17	140
2.1	170	7.1	140	12.1	160	17.1	140
2.2	165	7.2	120	12.2	160	17.2	120
2.3	160	7.3	120	12.3	160	17.3	120
2.4	160	7.4	130	12.4	160	17.4	140
2.5	165	7.5	140	12.5	160	17.5	165
2.6	160	7.6	165	12.6	160	17.6	170
2.7	150	7.7	165	12.7	150	17.7	165
2.8	140	7.8	160	12.8	130	17.8	160
2.9	130	7.9	160	12.9	125	17.9	160
3.0	130	8.0	160	13	120	18	160
3.1	120	8.1	160	13.1	130	18.1	160
3.2	135	8.2	160	13.2	150	18.2	160
3.3	155	8.3	155	13.3	165	18.3	160
3.4	170	8.4	160	13.4	165	18.4	140
3.5	170	8.5	150	13.5	160	18.5	130
3.6	160	8.6	150	13.6	160	18.6	120
3.7	160	8.7	120	13.7	160	18.7	120
3.8	165	8.8	120	13.8	160	18.8	140
3.9	165	8.9	130	13.9	160	18.9	165
4.0	160	9.0	160	14	160	19	170
4.1	150	9.1	170	14.1	145	19.1	160
4.2	150	9.2	165	14.2	120	19.2	160
4.3	135	9.3	165	14.3	120	19.3	160
4.4	120	9.4	160	14.4	120	19.4	160
4.5	120	9.5	165	14.5	130	19.5	160
4.6	130	9.6	160	14.6	160	19.6	160
4.7	150	9.7	160	14.7	170	19.7	160
4.8	170	9.8	160	14.8	160	19.8	150
4.9	170	9.9	155	14.9	160	19.9	130

TableB 1

KNEE JOINT ANGLE OF HUMAN LOCOMOTION

i. *Experimental Steps*

The experimental analysis for the development of average value based model for knee joint angle of the human locomotion is explained below:

a. The primary sectors chosen from the observed readings shown in TableB1 for knee joint angle are represented in Table B2, B3 and B4 and the primary averages are shown in Table B5.

180	170	165	130	160
175	170	170	120	150
170	170	165	135	150
165	160	160	155	135
140	155	160	170	120
135	145	165	170	120
155	140	160	160	130
170	120	150	160	150
165	120	140	165	170
160	130	130	165	170

Table B2 : Primary Sector 1

180	170	165	130	160
175	170	170	120	150
170	170	165	135	150
165	160	160	155	135
140	155	160	170	120
135	145	165	170	120
155	140	160	160	130
170	120	150	160	150
165	120	140	165	170
160	130	130	165	170

Table B3 : Primary Sector 2

180	170	165	130	160
175	170	170	120	150
170	170	165	135	150
165	160	160	155	135
140	155	160	170	120
135	145	165	170	120
155	140	160	160	130
170	120	150	160	150
165	120	140	165	170
160	130	130	165	170

Table B4 : Primary Sector 3

	Average value of the output knee joint angle
Primary sector 1	154
Primary sector 2	153
Primary sector 3	150

Table B5 : Primary Sector Averages

b. Determination of secondary sectors and secondary averages: The secondary sectors chosen from the primary sectors are represented in Table B2, B3, B4 i.e. each column in the corresponding table2, 3, 4 corresponds to secondary sectors and the secondary averages are shown in TableB6.

Primary sector1		Primary sector2		Primary sector3	
Secondary sectors	Secondary averages of the output	Secondary sectors	Secondary averages of the output	Secondary sectors	Secondary averages of the output
1	**162**	1	**152**	1	**148**
2	**148**	2	**159**	2	**147**
3	**157**	3	**145**	3	**153**
4	**153**	4	**147**	4	**153**
5	**146**	5	**162**	5	**145**

Table B6

SECONDARY SECTORS AND SECONDARY SECTOR AVERAGES

c. Determination of Tertiary sectors and Tertiary averages: The tertiary sectors chosen from the secondary sectors are shown in table B2, B3, B4 i.e. each element of row corresponds to tertiary sector and the tertiary averages are value of the element itself.

ii. *Determination of variational terms ΔA, Δ^2A: The variational terms obtained for the above combination of primary sectors, secondary sectors and tertiary sectors are shown in Table B7.*

A	ΔA	Δ^2A
154	5.2	15.3
153	6.4	10.88
150	3.2	14.4

Table B7

VARIATIONAL TERMS

iii. *The equations corresponding to the above combination are as follows*

The entire distance covered in 20 seconds is 14.4 M and for each set of data of duration 5 seconds the distance covered is 3.6M.

$$154*B1 + 5.2* B2 + 15.3 *B3= 3.6 \text{ --------} \quad (1)$$

$$153*B1 + 6.4* B2 + 10.88 *B3= 3.6 \text{ ------} \quad (2)$$

$$150*B1 + 3.2* B2 + 14.4 *B3= 3.6 \text{ -------} \quad (3)$$

Where B_1, B_2, B_3 represents variation in structure at the output.

iv. Here the relation between a dependent variable and independent variable is not accurately available from theory. So statistical model buildng technique called Multiple regression is used for finding the optimum form of relation and the 'best ' set of numerical coefficients, given a set of measured data. The three unknown coefficients B1,B2 and B3 are 0.0267, -0.0452 and -0.0183 respectively.

B1	B2	B3
0.0267	-0.0452	-0.0183

Table B8

$$0.0267*A+(-0.0452)*\Delta A+(-0.0183)*\Delta^2 A = \text{distance covered} \ldots\ldots\ldots \quad (4)$$

v. *Derivation of time based plot*

The above developed average based mathematical model can be utilized to obtain time based plot from the observations of the output. By choosing primary sector time period from table1, the base value , the variational factors for this period is calculated. The time based plot of the knee joint angle for different sectors are ploted as shown in figB-1.

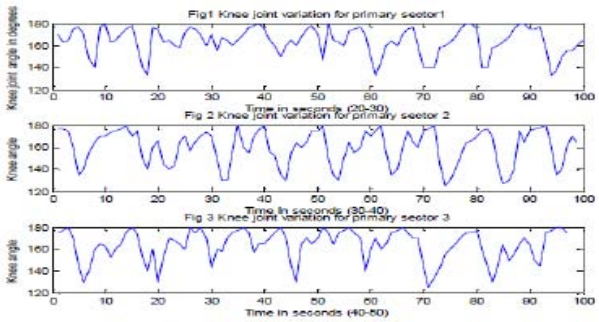

Fig B-1 : knee joint angle of different sectors

vi. *Model validation*

The above developed mathematical model is validated by comparing the calculated dynamics through equations 1 and 4 with the experimentally detected values from the real system. The details of the validation procedure is shown as under

Now the correctness of the developed equation using the proposed method is checked using the fourth set of data. For the fourth set of data Base Avg is 152 First change in Base Avg is 5.8 and Second change in Base Avg is 11.62. for the above values equation 1 and 4 becomes

$$0.0267*(152)+(-0.0452)*(5.8)+(-0.0183)*(11.62) = 3.6 \quad \text{.....(5)}$$

The detailed error[table B9] is found to be in reasonable limits so as to establish the validity of the model.The performance evaluation can be summarised for both the cases in the following table with respect to the error in the distance covered.

Type of Gait	Practicle(from Video)	Proposed method	%Error
Normal Walking	3.6	3.58	0.55

TableB9 Error Analysis

VII. Conclusion

An average value based model has been developed in this paper. The requirements of this approach are a set of readings from the real time system to calculate the base average value and the variational terms. The derived model is an input-output relationship. The above model developed is experimented on a spatially distributed distribution system and a biological system and the dynamics of the process variables are derived. This model is extended to a time based plot for convenience in analysis and subsequent applications. The limitations of the proposed method are no definite strict mathematical method for identifying the sectors; this division is done through intelligent guess. The length of the sectors or number of readings considered in each sector is fixed arbitrarily and Weather the system selected for modeling is linear or nonlinear the method considered everything in a linear approximation. This approximation will introduce its own merits and demerits in the analytical results/conclusions.

References Références Referencias

1. E.Ortjohann, W.Sinsukthavorn etal, Modeling/Simulation of Power Distribution in Hybrid Power systems Using Dynamic-RMS Technique, International Conference on Power Engineering, Energy and Electrical Drives, POWER ENG 2007,April 12-14,2007,Setubai,Portugal,pp779-784.
2. JunQiu, HengChen, Adly.A.Girgis, Dynamic Modeling and Parameter Estimation of a radial and Loop type Distribution system network. IEEE Transactions on Power systems , Vol 8 No:2,May 1993,pp 483-490.
3. Robert.J.O.Keefe, Richard.P.Schaulz, Navin B.Bhatt, Improved Representation of generator and Load dynamics in the study of voltage limited power system operations. IEEE Transactions on Power systems, Vol 12, No: 1, February 1997,pp 304-314.
4. P.Jhu and X.Y.Zhou, Dynamic Equivalents of distribution systems for voltage stability studies ,IEE Proceedings -Generation, Transmission, Distribution, vol 148,No:1, January 2001 pp 49-53
5. F.John Mayor,Kwang.Y.Lee, improved dynamic load model for power system stability studies ,IEEE Transactions on power apparatus and systems, Vol PAS 101,No:9,September 1982 ,pp3303-3309.
6. Dobrivoje.P.Stojanovie, Lidija.M.Koronovie etal, Dynamic load modeling on measurements in medium voltage distribution network, Electric power systems Research (2008) 228-238
7. Michael J.Gorman, Seyhan Civanlar, Load/voltage modeling of distribution systems: A system Identification approach ,IEEE Proceedings-1989 South east con.
8. Zhenyu Huang,Tony Nguyen, Model Validation of power system components using Hybrid dynamic simulation ,Transmission and Distribution Conference and Exhibition 2005/2006,IEEE PES 21-24 May 2006,pp153-160
9. Mournir.A.Yehia, Ehie.E.matar, A Heuristic Algorithm for electric distribution networks optimal feeder configuration using Geographic Information system ,IEEE Xplore 2002.H. Poor, *An Introduction to Signal Detection and Estimation*. New York: Springer-Verlag, 1985, ch. 4.
10. Ernest.O.Doeblin, System Dynamics: Modeling, Analysis, Simulation and Design, CRC Press,1998B. Smith, "An approach to graphs of linear forms (Unpublished work style)," unpublished.
11. Tommy Oberg, Alek Karsznia, Kurt Oberg "Joint Angle Parameters in Gait: Reference data for normal subjects,10-79 years of age" Journal of Rehabilitation Research and Development Vol 31 No 3 , August 1994 Pages 199-213
12. V.E.Berbyuk,G.V.Grasyuk and N.I.Nishchenko " Mathematical Modeling of the Dynamics of the Human Gait in the saggital plane" Journal of Mathematical Sciences, Vol 96,No2,1999
13. V.E.Berbyuk and N.I.Nishchenko "Mathematical Design of Energy-Optimal Femoral Prostheses" Journal of Mathematical Sciences, Vol 107, No1, 2001.
14. Jerry E.Pratt, Benjamin T Krupp, Christopher J Morse and Steven H Collins "The RoboKnee: An

Exoskeleton for Enhancing Strength and Endurance During Walking" Proceedings of the 2004 IEEE International Conference on Robotics & Automation.
15. T Hayashi,H Kawamoto and Y Sankai " Control Method of Robot Suit HAL working as operator's Muscle using Biological and Dynamical Information" IEEE /RSJ International conference on Intelligent Robots and Systems 2005.
16. K Yamamoto, Mineo Ishii, H Noborisaka and K Hyodo "Stand Alone Wearable Power Assisting Suit-Sensing and Control Systems" Proceeding of the 2004 IEEE International Workshop on Robot and Human Interactive Communication Japan September 20-22, 2004.
17. D Jin, R Zhang, HO Dimo, Rencheng Wang and Jincuan Zhang "Kinematic and dynamic performance of prosthetic knee joint using six-bar mechanism" Journal of Rehabilitation Research and Development Vol 49,No1 2003.
18. Takahiko Nakamura, Kazunari Saito, ZhiDong Wang and Kazuhiro Kosuge, "Realizing a Posture-based Wearable Antigravity Muscles Support System for Lower Extremities" Proceedings of the 2005 IEEE 9th International Conference on Rehabilitation Robotics June 28 - July 1, 2005, Chicago, IL, USA.
19. T Nakamura,K Satio,Z Wang and K Kosuge " Control of Model-based wearable Anti-Gravity Muscles Support System for Standing up Motion" proceeding of the 2005 IEEE/ASM International conference on Advanced Intelligent Mechatronics July 2005.
20. Sunil K Agarwal, Sai K .Banala, Abbas Fattah,John P Scholz and Vijaya Krishnamoorthy "A Gravity Balancing Passive Exoskeleton for the Human Leg" Robotic Proceedings pg 24
21. http://www.technovelgy.com/ct/Science-Fiction-News.AKROD, Active Knee Rehabilitation Device Human Trials.

This page is intentionally left blank

Global Journal of researches in engineering
Electrical and electronics engineering
Volume 12 Issue 1 Version 1.0 January 2012
Type: Double Blind Peer Reviewed International Research Journal
Publisher: Global Journals Inc. (USA)
Online ISSN: 2249-4596 & Print ISSN: 0975-5861

Genetic Algorithm based Dispatch Strategy of Voltage Stability Limited Power Transfer using a Unique Model of UPFC

By Neena Ramesh, B.V Sanker Ram, Vedam Subrahmanyam
SRM Easwari Engineering College ,Chennai

Abstract - This paper proposes a method of dispatch strategy using a unique power injection model of UPFC demonstrating the capability of voltage stability limited power transfer and minimum transmission loss based on Modified Real Coded Genetic Algorithm Optimization . This paper also discusses the compatibility of this model for matrix converter based UPFC. To maximize the voltage stability limited power transfer, bus voltage regulation alone is not sufficient. Hence a dispatch strategy is evolved using GA so as to control the power circulation between the shunt and series end of the transmission line for the specified real and reactive power transfer at target voltage magnitude. The UPFC is operated in automatic power flow control mode at its rated capacity. The UPFC controllable parameter values are obtained from the modified GA solution.GA also offers the best location for the UPFC to be placed along with the optimum operating conditions so as to minimize the transmission losses. Voltage stability evaluation and analysis is carried out using PV analysis on the standard IEEE 14 Test Bus and the test results with and without GA are compared. It was found that GA algorithm offers the best solution to minimize the transmission losses.

Keywords : *GA, Voltage Stability, UPFC, Dispatch strategy, Unique Power Injection Model, Transmission Losses.*

GJRE-F Classification: *FOR Code: 090607*

Strictly as per the compliance and regulations of:

Genetic Algorithm based Dispatch Strategy of Voltage Stability Limited Power Transfer using a Unique Model of UPFC

Neena Ramesh[α], B.V Sanker Ram[σ], Vedam Subrahmanyam[ρ]

Abstract - This paper proposes a method of dispatch strategy using a unique power injection model of UPFC demonstrating the capability of voltage stability limited power transfer and minimum transmission loss based on Modified Real Coded Genetic Algorithm Optimization . This paper also discusses the compatibility of this model for matrix converter based UPFC. To maximize the voltage stability limited power transfer, bus voltage regulation alone is not sufficient. Hence a dispatch strategy is evolved using GA so as to control the power circulation between the shunt and series end of the transmission line for the specified real and reactive power transfer at target voltage magnitude. The UPFC is operated in automatic power flow control mode at its rated capacity. The UPFC controllable parameter values are obtained from the modified GA solution.GA also offers the best location for the UPFC to be placed along with the optimum operating conditions so as to minimize the transmission losses. Voltage stability evaluation and analysis is carried out using PV analysis on the standard IEEE 14 Test Bus and the test results with and without GA are compared. It was found that GA algorithm offers the best solution to minimize the transmission losses.

Keywords : GA, Voltage Stability, UPFC, Dispatch strategy, Unique Power Injection Model, Transmission Losses.

I. Introduction

Deregulation and restructuring of electricity market, has made it necessary to utilize the existing utilities and resources to the fullest capacity. UPFC is a powerful FACTS device for real time control and dynamic compensation of transmission systems capable of operating in four quadrants of complex P + j Q plane. Thus the UPFC, based on its VA rating can be regarded as an ideal active and reactive power generator which is capable of providing beyond voltage regulation and phase angle control [6].

A lot of investigation has been done on various models of UPFC for the implementation of the device in NR load flow algorithm. This paper proposes a unique model of UPFC which bypasses the representation of both voltage sources and produces a symmetric admittance matrix [2]. Hence a compatibility study is also done on Z Source Matrix Converter type UPFC using this novel model [10][11]. A dispatch strategy is adopted in this proposal with the objective of maximizing voltage stability limited power transfer at target bus voltage magnitude with minimum transmission losses through automatic adjustment of UPFC parameters. The UPFC is operated in automatic power flow control mode at its rated capacity. The loadability real power margin and reactive power margin is obtained from the voltage stability analysis. For these specified powers and target bus voltage magnitude the UPFC state variables, the voltage magnitude, V_{VR} and the phase angle θ_{VR} at the shunt end and V_{CR} and phase angle θ_{CR} at the series end are adjusted. The voltage magnitude ranges from maximum to minimum limits and is a function of the DC capacitor rating and the phase angle ranges from 0 to 2π radians. Thus it is a highly nonlinear, multimodal, discontinuous and non differentiable, mixed integer, combinatorial optimization problem. Classic optimization methods based on gradient search and non linear programming methods are suitable for differential and convex objective functions and can handle only continuous variables [15]. In addition to these limitations these algorithms lead to local and suboptimal solutions often. Hence evolutionary optimization technique, such as genetic algorithm GA, has been developed for the global optimization problems.[16][17] .Hence this paper proposes a modified real coded genetic algorithm. The UPFC controllable parameter values are obtained from the modified GA solution. GA also offers the best location for the UPFC to be placed along with the optimum operating conditions so as to minimize the transmission losses.

The power system loses its voltage stability when the voltage decreases drastically. The voltage stability is mostly load driven, when the power system is unable to meet the load increment or meet the excess reactive power demand. The voltage instability ultimately may lead to voltage collapse a catastrophic disaster.

Voltage stability though a dynamic phenomenon, use of steady state analysis is acceptable. In long term voltage stability, the dynamics is assumed to have died out and the compensation has

Author α : Asst Professor in the Department of Electrical and Electronics Engineering at SRM Easwari Engineering College ,Chennai. 09840357995, rneena1504@yahoo.co.in
Author σ : Professor in the Department of Electrical Engineering College at JNTU Hyderabad .
Author ρ : Professor in the Department of Electrical and Electronics Engineering College at RMK College of Engineering ,Chennai.

been implemented .In steady state voltage stability studies, the state matrix is approximated by the Jacobean matrix at the equilibrium operating point. Voltage stability being a non linear phenomenon, bifurcation theory, technique is used to study voltage collapse. Bifurcation occurs at the collapse point indicating transition from stable zone to unstable zone and the Jacobean matrix becomes singular. Many methods are available to estimate the proximity of voltage collapse point [5]. Most reliable method is PV curve analysis for which the bifurcation parameter is the active loading .The loading at the voltage collapse point is called as the loadability margin.

The organization of this paper is as following. Section 2 details the novel model of UPFC suitable for a dispatch strategy and also the compatibility of this model for a matrix converter based UPFC is discussed. Overview of modified real coded GA is described in section 3. Section 4 discusses the GA based load flow results with UPFC and finally the conclusion is given.

II. Power Injection Model (PIM)

The objective is to maximize the total active power transfer in the transmission system while simultaneously maintaining the desired voltage profile at all buses .A novel power injection model (PIM) of UPFC in unified power flow algorithm is described in this section. In the conventional model illustrated by Gyugi[6] the UPFC is represented by two voltage sources shunt and series along with their impedances and coupling transformers. To acquire a square UPFC admittance matrix, two fictitious nodes are introduced .These problems are overcome using a power injection model [2][3].The power injections at the shunt and series transformers are interpreted as real and reactive node injections. At these two controlled nodes the nodal voltage magnitude, the nodal active and reactive powers are specified while the voltage magnitude and phase angle of the voltage source converters are handled as state variables.

[2]In this work, the UPFC modeling includes a detailed power injection model with internal UPFC state and control variables, series and shunt impedances, incorporated in the OPF formulation. $V_{VR} = V_{VR}\angle\theta_{VR}$ and $V_{CR} = V_{CR}\angle\theta_{CR}$ are the variable output voltages of each converter. The output voltage at the series converter end $V_{CR}\angle\theta_{CR}$ is added to the bus voltage V_K thus increasing the bus voltage V_M at bus m..The phase angle θ_{CR} decides the operation and mode of power control. The DC link source connecting both the VSC provides the path for transfer of real power. Thus the real power exchange is established between the SSSC and the transmission line. Also at the shunt end the STATCOM can supply or absorb reactive power independently to regulate the bus voltage at the point of coupling to the line.

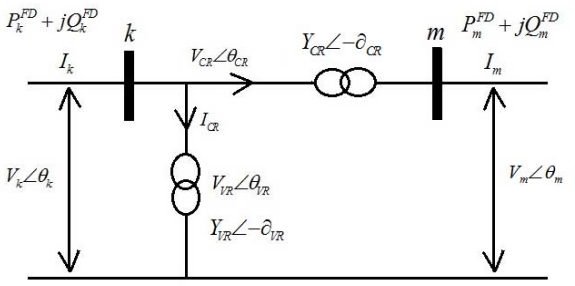

Fig.1 : UPFC Power Injection Model

The input information includes the voltage magnitude and phase angle at both sides of the UPFC at bus k and bus m. The real and reactive power in the transmission line is calculated to detect the deviations from their pre-set values.

Using standard notation

$$V_K=V_K \angle \theta_K \quad , V_M=V_M \angle \theta_M,$$
$$V_{VR}=V_{VR} \angle \theta_{VR} \quad V_{CR} = V_{CR} \angle \theta_{CR}$$
$$Y_{VR}= Y_{VR} \angle \delta_{VR}, \quad Y_{CR} = YCR \angle \delta_{CR},$$

The transfer admittance equations of UPFC are as shown below.

$$Y = \begin{pmatrix} Y_{VR} + Y_{CR} & -Y_{CR} \\ -Y_{CR} & Y_{CR} \end{pmatrix}$$

The power injection at nodes, bus k and bus m is

$$S_k = V_k I_k^* = V_k^2(Y_{VR} + Y_{CR}) - V_k V_m Y_{CR} + V_k(V_{CR} Y_{CR} - V_{VR} Y_{VR})$$
$$S_m = V_m I_m^* = V_m^2(Y_{CR}) - V_m V_k Y_{CR} + V_m(-V_{CR} Y_{CR})$$

$P_k = V_k^2(Y_{VR}\cos\delta_{VR} + Y_{CR}\cos\delta CR) - V_K V_{VR} Y_{VR} \cos(\theta_K - \theta_{VR} + \delta_{VR}) - V_K V_M Y_{CR} \cos(\theta_K - \theta_M + \delta_{CR}) - V_K V_{CR} Y_{CR} \cos(\theta_K - \theta_{CR} + \delta_{CR})$

$Q_k = V_k^2(Y_{VR}\sin\delta_{VR} + Y_{CR} \sin\delta_{CR}) - V_K V_{VR} Y_{VR} \sin(\theta_K - \theta_{VR} + \delta_{VR}) - V_K V_M Y_{CR} \sin(\theta_K - \theta_M + \delta_{CR}) - V_K V_{CR} Y_{CR} \sin(\theta_K - \theta_{CR} + \delta_{CR})$

$P_M = V_M^2 Y_{CR}\cos\delta_{CR} + V_M V_{CR} Y_{CR}\cos(\theta_K - \theta_{CR} + \delta_{CR}) - V_M V_K Y_{CR} \cos(\theta_M - \theta_K + \delta_{CR})$

$Q_M = V_M^2 Y_{CR}\sin\delta_{CR} + V_M V_{CR} Y_{CR}\sin(\theta_M - \theta_{CR} + \delta_{CR}) - V_M V_K Y_{CR} \cos(\theta_M - \theta_K + \delta_{CR})$

The Power Injection Model of UPFC in load flow equations identifies additional injections as function of UPFC internal variables, V_{VR}, V_{CR} and parameters Y_{VR} and Y_{CR}, The mathematical expressions are

$$S_k^{INJ} \quad V_k(Y_{CR}V_{CR} \quad Y_{VR}V_{VR}) \quad P_k^{INJ} \quad jQ_k^{INJ}$$

$$S_m^{INJ} = -V_m Y_{CR} V_{CR} = P_m^{INJ} + jQ_m^{INJ}$$

Where

$$P_k^{INJ} = P_m^{INJ}$$

$P_K = V_K(Y_{VR} \cos \delta_{VR} + Y_{CR} \cos \delta_{VR}) - V_K V_M Y_{CR}$ $\cos(\theta_K - \theta_M + \delta_{CR}) - P_K^{INJ}$

$P_K^{INJ} = V_K V_{CR} Y_{CR} \cos(\theta_K - \theta_{CR} + \delta_{CR}) + V_K V_{VR} Y_{VR}$ $\cos(\theta_K - \theta_{VR} + \delta_{VR})$

$Q_K^{INJ} = V_K V_{CR} Y_{CR} \sin(\theta_K - \theta_{CR} + \delta_{CR}) + V_K V_{VR} Y_{VR}$ $\sin(\theta_K - \theta_{VR} + \delta_{VR})$

$P_M^{INJ} = -V_M V_{CR} Y_{CR} \cos(\theta_M - \theta_{CR} + \delta_{CR})$

$Q_M^{INJ} = -V_M V_{CR} Y_{CR} \sin(\theta_M - \theta_{CR} + \delta_{CR})$

$\delta_{CR} = \delta_{VR} = \pi/2$ The impedences of the UPFC transformers are reactive.

$P_K^{INJ} + P_M^{INJ} = 0$; UPFC equality constraint.

Where P_K^{INJ} and Q_K^{INJ} represents the active power and reactive power injection of the UPFC source at node k and respectively P_M^{INJ},Q_M^{INJ} at node m.

Thus with this PIM the voltage sources have been omitted and instead the UPFC power injections is adopted. The state variables V_{CR} , V_{VR} θ_{CR}, θ_{VR} and the system variables are adjusted automatically for a unified load flow solution. When the UPFC is stated to control the total real and reactive power injections at node m in the branch k-m where k and m are PQ nodes, the load flow equations for branch k-m are as follows

$$P_{Kspec} - P_K - P_K^{INJ} = 0$$
$$P_{Mspec} - P_M - P_M^{INJ} = 0$$
$$Q_{Kspec} - Q_K - Q_K^{INJ} = 0$$
$$Q_{Kspec} - Q_K - Q_K^{INJ} = 0$$
$$P_{MK(spec)} - P_{MK} - P_{MK}^{INJ} = 0$$
$$Q_{MK(spec)} - Q_{MK} - Q_{MK}^{INJ} = 0$$
$$-(P_K^{INJ} + P_M^{INJ}) = 0$$

The UPFC can be made to control the real and reactive powers, the target voltage magnitude by varying the UPFC variables V_{CR} , θ_{CR} and θ_{VR} and V_{VR} .

The UPFC has a local coordination of both converters in order to produce the desired control action on the network, voltage control, reactive compensation and active power transmission control simultaneously. For optimised values of the line power, to obtain minimum losses in the system, the Genetic Algorithm tool is used. The UPFC incorporated program is embedded into the genetic algorithm program. GA in a more global level defines the control mode and optimal placement of the UPFC with the objective of minimum transmission losses.

III. PIM for Matrix Converter Based UPFC

This paper also has carried out an investigation on the compatibility of the PIM using matrix converter based UPFC. Boon [8] deals with voltage source matrix converters for UPFC topology. Replacing the two voltage source converters by one matrix converter the DC link capacitors are eliminated, reducing costs, size, maintenance, increasing reliability and lifetime thus offering more improved reliability than other conventional AC-AC converters [9]. Matrix converters have several advantages such as bidirectional power flow less number of switches, controllable input displacement factor, etc.

However in all these topologies, the AC output voltage cannot exceed the AC input voltage since no energy storage components are present between the input and output side. Therefore in UPFC topology the small real power losses associated with the converters switching losses is drawn from the power system.

These limitations can be overcome by using Z-source topology [7]. This arrangement has the advantage of independent control of the current in both directions..The symmetrical Z source network is a combination of two inductors and two capacitors serving as energy storage elements for a single phase Z source buck boost matrix converter. Since the switching frequency is much higher than the line frequency the size of inductors and capacitors is very small.

Z-source Single-Phase Matrix Converter uses four bi-directional switches i.e. a combination of two diodes and two IGBTs connected in anti parallel (common emitter back to back) as shown in Fig 3. This arrangement has the advantage of independent control of the current in both directions. Fig 4 shows the simulated diagram of the Single Phase Matrix Converter. The AC input voltage is boosted by the Z-source converter. The frequency of the input voltage is then modulated in Single Phase Matrix Converter. Thus, the output voltage is obtained with a step-changed frequency and variable amplitude. The LC input filter is required to reduce the switching ripple in an input current .This control produces output voltage in buck-boost mode with a step-changed frequency. The matrix converter in UPFC topology is a variable amplitude and frequency changer. Frequency changers are also phase-shifters, with the phase shift ranging up to 360 degrees which can operate as an asynchronous link connecting power systems at the 60 Hz and 50 Hz frequency standards. The amplitude of the output voltage is controlled by duty ratio whereas the frequency depends on the switching strategy.

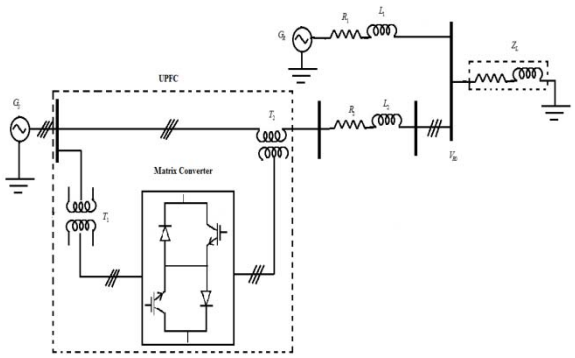

Fig 2 : Matrix Converter UPFC connected to transmission Line

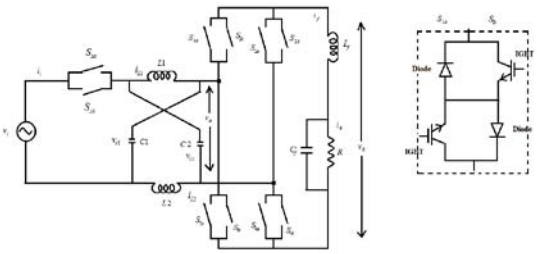

Fig 3 : Z Source Matrix Converter

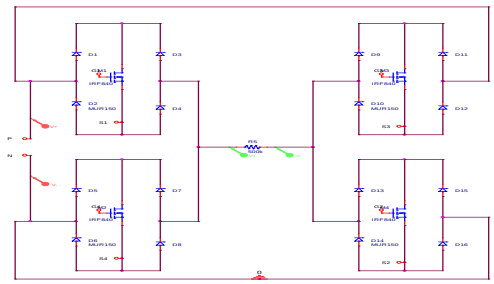

Fig 4 : Matrix Converter Simulated

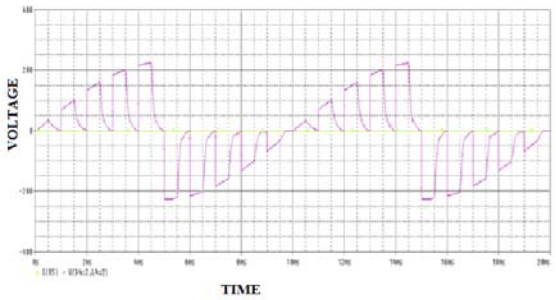

Fig.5 : Matrix Converter Output Voltage Simulated

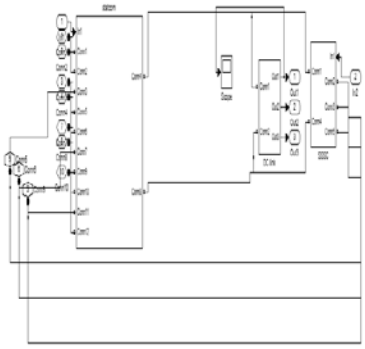

Fig .6 : UPFC Simulink Block Diagram

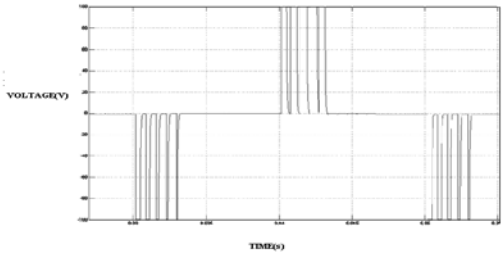

Fig .7 : Simulation Ouput at SSSt

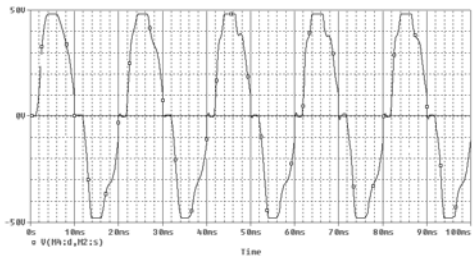

Fig .8 : Simulation output of UPFC

It has been illustrated earlier that the PIM has the capability of bypassing the two voltage source converters and the DC link. Hence the basic model of UPFC with two voltage source converters and DC link capacitor and the Z source matrix converter block diagram was constructed in Matlab/Simulink for comparison of performance. The simulation results Fig 4,5,6,7,8 show the matrix converters output voltages is the same as obtained at SSSC .. The shunt and series transformer are connected at the two ends of this matrix converter and linked to the transmission line as shown in Fig 2. Thus PIM model is found highly suitable for matrix converter based UPFC with respect to performance.

IV. GA Optimisation

Optimization is defined as a search for feasible solutions which correspond to extreme values (maximum or minimum) of one or more objectives

Classical optimization is point-by-point algorithm using deterministic rules.

Natural evolutionary laws are mimicked in recent evolutionary algorithms like GA, ES, EP, and GP. Other nature inspired EA algorithms are ANT Colony Optimization, , PSO, Bacterial Foraging etc. One of the striking differences with classic type is that evolutionary algorithms use a population of solutions in each iteration instead of a single solution. EA is based on stochastic sampling methods[15].

GA algorithm first founded by Holland in 1975 is one of meta-heuristic optimization algorithms which are based on natural evolution and population .It has widespread applications since it is not bounded by limitations like continuity, derivatives, unimodality etc. GA is basically grouped as binary GA and real coded GA. This paper has proposed modified real coded GA for the optimal power flow. [16]The application of GA starts with initial random population and probabilistic transition rules, measuring the fitness value of the population, operation of genetic operators like reproduction, crossover and mutation to the strings of OPF until the termination tolerance is reached. [17]Though the operators are simple they are highly nonlinear, multifaceted stochastic and complex. The control parameters of GA are the population size, the selection operator, the crossover rate, the mutation rate and the number of generations to evolve a new solution. More than one string is processed simultaneously and used to update every string in the population.

a) Real Coded Genetic Algorithms

In a real parameter GA the action of a selection operator causes the above average solutions to survive in the population [18]. In each decision variable these sub regions of above average solutions constitute virtual characters of a virtual alphabet. Thus after a few generations a real parameter GA treats a continuous search space as a discrete search space problem. In real parameter GA implementation crossover and mutation operators are applied directly to real parameter values. Unlike in the binary coded GA, decision variables can be directly used to compute the fitness values. The difficulty arises with the search operators. Since real parameter crossovers directly manipulate real numbers to create the offspring, the need of mutation operator is questionable. They do the same task. The main distinction between a crossover and a mutation operator lies mainly in the number of parent solutions used for changes. The range of perturbations has to be predefined. The fitness for feasible solutions is the objective value and for infeasible solutions the penalty is added in proportion to constraint violation.

b) GA applied to the Load Flow Solution

A real coded Genetic Algorithm modified and implemented in MATLAB is used for optimization. For optimized values of the line power, to obtain minimum losses in the system, the Genetic Algorithm tool is used. The UPFC incorporated program is embedded into the genetic algorithm program.

The load flow was conducted on IEEE 14 bus for the base, distributed peak load, and single line outages. .The ranking of buses was done as listed in Table 1 based on the voltage magnitude under peak load and contingency load factors. Bus 4 and Bus 5 is connected to generator 2. Hence PV and QV curve was drawn for the other critical buses 7, 9, and 10 to determine the loadability P and Q margin and are given as in Table 2. The reference values for specified powers Psp and Qsp are fixed taking into account the corresponding loadabilty margins. The range for parameters like line location of UPFC, Psp, Qsp, V_{VR}, V_{CR} etc whose optimum values are required to obtain minimum losses are declared in the m-file titled 'test'. To run the GA using this test function a function is called from the Matlab. This function call will use all of the default parameters and functions of GA required .The evaluation function in the 'test' m-file is the inverse of the total losses in the system. For the specified power and lines corresponding to weak buses, the best of GA solution regarding the bus placement, and the UPFC rating is determined. The technique of penalization is used so that the solutions which do not converge and the solutions which violate the limits of voltage stability are eliminated for the succeeding generation. Evaluation Function is called from the GA to determine the fitness of each solution string or program generated during the search.

Function[x, val] = test(x, parameters)

Value = 1/PQ Loss

These values generated by GA are incorporated in the power flow equations and UPFC data and the load flow solution is run again. The minimized losses are compared for different specified powers and repeated till optimum. The search is quickened since the critical buses are only considered for reactive compensation by UPFC.

V. SIMULATION RESULTS

Table I : V_{min} with Loadability Margin for Weak Buses

Bus No	V_{min} p.u	P Index w/o UPFC p.u	V_{min} p.u	P Index with UPFC p.u
7	0.65	0.77	0.82	1.35
9	0.60	0.70	0.99	1.4
10	0.60	0.75	0.85	1.25
14	0.65	0.78	0.90	1.3

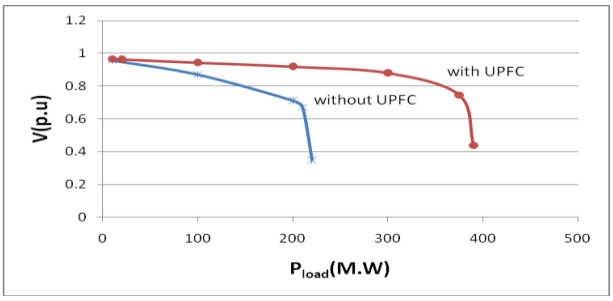

Fig.9 : P-V Curve at bus 7 P_{SP}=0.4, Q_{SP}=0.02, V_{CR}=0.04, V_{VR}=1.0,X_{CR}=0.1,X_{VR}=0.1)

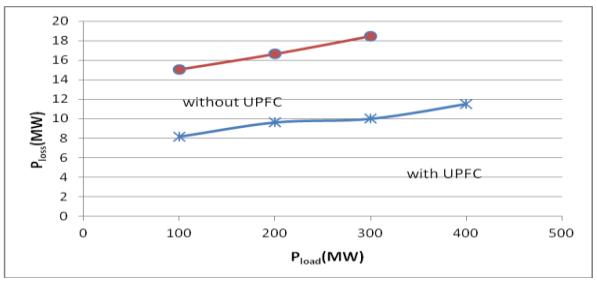

Fig. 10 : Pload vs Ploss at bus 7 (P_{SP} = 0.4, Q_{SP} =0.02, V_{CR}=0.04, V_{VR}=1.0, X_{CR}=0.1,X_{VR}=0.1)

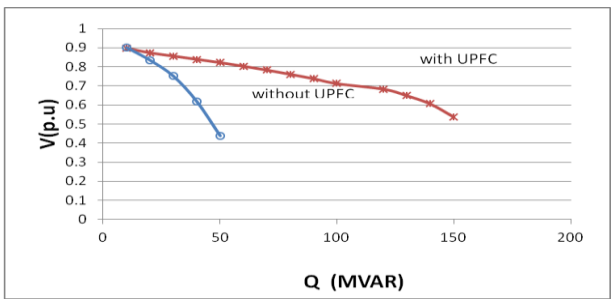

Fig.8 : Q-V Curve at bus 4 (P_{SP} = 0.4, Q_{SP} =0.02, V_{CR}=0.04, V_{VR}=1.0,X_{CR}=0.1,X_{VR}=0.1)

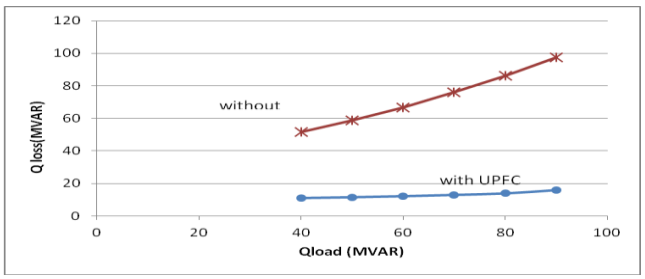

Fig.9 : Qload vs Qloss at bus 4 (P_{SP} = 0.4, Q_{SP} =0.02, V_{CR}=0.04, V_{VR}=1.0,X_{CR}=0.1,X_{VR}=0.1)

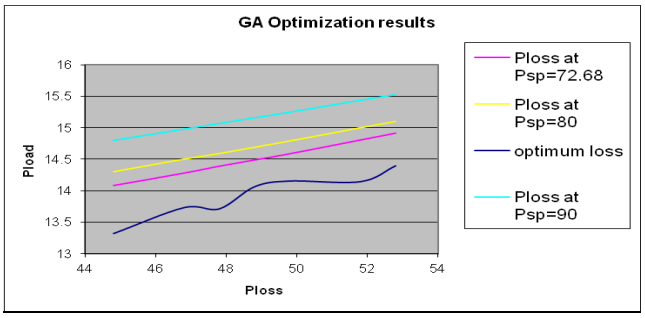

Fig 10 : Pload vs Ploss for different Specified Powers

VI. GA Results and Discussion

The load buses 7, 9, 10, and 14 have been identified as critical from the peak load and contingency load flow results clearly illustrating deficiency of reactive power in the Table 1 and Fig1, 2, 3. The voltage stability analysis using PV curve and the QV curve at these critical buses has provided the loadability margin P index and Q index .Now the placement and the rating of UPFC plays an important role in the maximization of voltage stability limited power transfer. The range for parameters like line location of UPFC, Psp, Qsp, V_{VR}, V_{CR} etc whose optimum values are required to obtain minimum losses are declared in the m-file titled 'test' For the placement of UPFC the transmission line data range is considered for the critical buses only. For different values of specified power Psp and Qsp , the Ploss is obtained and compared for optimum location of the UPFC.

VII. Conclusion

The unique PIM of UPFC is thus capable of maximizing voltage stability limited power transfer to increase economic operation of power system with transmission losses minimized. Simulation results have also demonstrated the PIM suitable for Matrix Converter based UPFC. The placement and the rating of UPFC plays an important role in the maximization of voltage stability limited power transfer .The GA optimization results has clearly illustrated the minimum transmission power loss on IEEE 14 bus system for a specified power and target voltage magnitude with the UPFC optimally placed.

References References Referencias

1. Xuan Wei, Member, IEEE, Joe H. Chow, Fellow, B. Fardanesh Member, and Abdel-Aty Edris,"Dispatch Strategy for UPFC to Maximize Voltage-Stability-Limited Power Transfer" IEEE Trans. Power Del Volume 20 No.3,July 2005.
2. Xuan Wei,Joe H. Chow, B. Fardanesh, Abdel-Aty Edris "Advanced steady state models of UPFC for power system studies", ,IEEE Trans Vol 22 2009.
3. M. Z. EL-S'adek, A. Ahmed, H. E. Zidan "Comparison of UPFC model for power flow studies" IEEE Power Dly Vol 16 ,2007

4. Enrique Acha, Claudio R. Fuerte-Esquivel, Hugo Ambriz-Perez and Cesar Angeles-Camacho FACTS: "Modelling and Simulation in Power Networks" Wiley & Sons Publications2004.
5. C. W. Taylor, "Power System Voltage Stability", Tata McGraw-Hill, 1994
6. G. Hingorani and L. Gyugyi, "Understanding FACTS". Piscataway, NJ: IEEE Press, 2000.
7. Abhijit Chakraborthy and Sunita Halder "Power System Analysis: Operation and Control" Prentice Hall India ,2010.
8. Boon-Teck Ooi Mehrdad Kazerani Unified Power Flow Controller Based on Matrix Converter. IEEE proc 2006
9. P. C. Loh, R. Rong, F. Blaabjerg, and P.Wang, "Digital carrier modulation and sampling issues of matrix converters," IEEE Trans. Power Electron, vol. 24, no. 7, pp. 1690–1700, Jul. 2009.
10. Z. Idris, M. K. Hamzah, and M. F. Saidon, Implementation of single phase matrix converter as a direct ac-ac converter with commutation strategies," in Conf. Rec. IEEE PESC 2006, pp. 2240–2246
11. Y. Tang, S. Xie, and C. Zhang, "Z-source AC-AC converters solving commutation problem," IEEE Transactions on Power Electronics, vol.22, pp. 2146-2154, 2007.
12. F. Dong, B. H. Chowdhury, M. Crow, L. Acar, "Cause and Effects of Voltage Collapse-Case Studies with Dynamic Simulations", IEEE Power Engineering Society General Meeting, 2004, pp. 1806-1812.
13. G. K. Morison, B. Gao and P. Kundur, "Voltage stability analysis using static and dynamic approaches", IEEE Transactions on Power Systems, Vol. 8, No. 3, August 1993, pp. 1159–1171.
14. Thukaram. D, Yesuratnam. G, Vyjayanthi. C.V, Optimal Reactive Power Dispatch based on Voltage Stability Criteria in a Large Power System with AC/DC and FACTS Devices International Conference on Power Electronics Drives and Energy Systems, 2006. PEDES '06. 2006,
15. Yin, X., Germay, N., 1991, Investigations on solving the load flow problem by genetic algorithms. Electric PowerSystem Research Journal, 22(3):151-163.
16. Lee, K.Y., Bai, X.M., Park, Y.M., 1995. Optimization method for reactive power planning by using a modified genetic algorithm. IEEE Trans. on Power Systems, 10(4):1843-1850.
17. Wu, Q.H., Cao, Y.J., Wen, J.Y., 1998. Optimal reactive power dispatch using an adaptive genetic algorithm. Int. J. Elect. Power Energy Syst., 20(8):563-569.
18. Gold Berg "Genetic Algorithm, PHI, 1991.

This page is intentionally left blank

Global Journal of researches in engineering
Electrical and electronics engineering
Volume 12 Issue 1 Version 1.0 January 2012
Type: Double Blind Peer Reviewed International Research Journal
Publisher: Global Journals Inc. (USA)
Online ISSN: 2249-4596 & Print ISSN: 0975-5861

Impact of Temperature, Wind Flow, Solar Radiation, Skin Effect and Proximity Effect on Overhead Conductor

By Md. Saiful Islam, Foredul Islam
Dhaka University of Engineering & Technology (DUET), Bangladesh

Abstract - When a conductor is using in an over head line it has to face the weather surrounding of it .In any aluminium conductor like ACSR or for other conductors the whole conductor is not uniform and that why its current carrying capacity is not only dependent upon ambient temperature but also depends upon wind flow, solar radiation, skin effect, proximity effect etc. Resistance depends upon temperature of conductor and the temperature is affected by those effects. If one of those effects is changed than that impact upon total current carrying capacity of the conductor.

Keywords : Temperature effect, Wind flow effect, Solar radiation effect, Skin effect, Proximity effect, Current rating.

GJRE-F Classification: FOR Code: 090608

Strictly as per the compliance and regulations of:

Impact of Temperature, Wind Flow, Solar Radiation, Skin Effect and Proximity Effect on Overhead Conductor

Md. Saiful Islam[α], Foredul Islam[σ]

Abstract - When a conductor is using in an over head line it has to face the weather surrounding of it .In any aluminium conductor like ACSR or for other conductors the whole conductor is not uniform and that why its current carrying capacity is not only dependent upon ambient temperature but also depends upon wind flow, solar radiation, skin effect, proximity effect etc. Resistance depends upon temperature of conductor and the temperature is affected by those effects. If one of those effects is changed than that impact upon total current carrying capacity of the conductor.

Index terms : *Temperature effect, Wind flow effect, Solar radiation effect, Skin effect, Proximity effect, Current rating.*

I. Introduction

Resistance is simply depended on temperature and it shows a linear relationship. For different material is exhibits different slop but relationship is same .here it is assumed for even layered conductor the AC resistance and DC resistance are in linear relationship.

The temperature might be generated within conductor or due to surrounding higher temperature or due to solar heat incident.

On the other hand the heats are reduced due to wind flow or if the surrounding temperature is lower than the conductor temperature. Radiation of heat from On the other hand the heats are reduced due to wind flow or if the surrounding temperature is lower than the conductor temperature. Radiation of heat from conductor to air is also depends upon material and the outer surface condition like dust jacket and inter spacing among the conductor wires. The skin effects and proximity effects are also contribute on current of the conductor.

From the catalog of cable industries and from different equations it is tried to show the individual and overall variations among the factors and overall effect on current carrying capacity of the conductor.

Author α : Graduated from Department of Electrical & Electronic Engineering at Dhaka University of Engineering & Technology (DUET), Bangladesh.St. Id :062119. PH-8801718871213.
E-mail : saifful69@gmail.com
Author σ : Graduated from Department of Electrical & Electronic Engineering at Dhaka University of Engineering & Technology (DUET), Bangladesh. . St. Id.: 062119. PH:+8801718871213
E-mail: saifful69@gmail.com

II. Resistance Dependence on the Temperature

Since the stranding of the conductor has a negligible effect on the ratio of effective to dc resistance [9] and the conductor operates in the temperature range far from the melting point, temperature dependence can be determined as:

$$R_{Tc} = R_{To}[1 + \alpha(T_c - T_0)] \quad (2.1)$$

Where $\alpha = 0.0039$ [C−1] is the temperature coefficient for aluminium, R_{Tc} and R_{To} are the resistances at temperatures T_c and T_0 correspondingly.

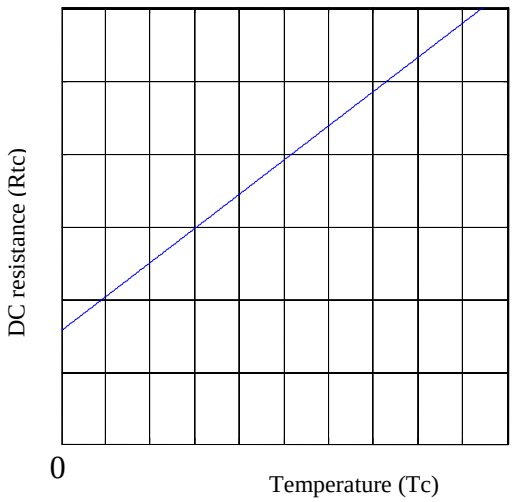

Figure-2.1 : DC resistance Vs Temperature.

AC resistance increases due to the skin effect. For even number layered ACSR conductors it can be determined with a good accuracy either by the analytical expressions or through recomputed Rac/Rdc curves [9]. For the conductors with odd number of layers, the additional influence of the eddy currents and hysteresis losses in the steel core cannot be neglected and the AC resistance depends on both temperature and the current. In the following computations, we assume even layered conductors and linear dependence of AC resistance only on the conductor temperature, although nonlinear dependence could be accounted for in the similar manner.

III. Heat loss Due to Wind Flow

Due to wind velocity the heat dissipates from the conductor to air. That reduces the temperature of conductor. So it has an effect on conductor current carrying capacity.

The formula of heat dissipated due to wind velocity (h_w) is given by TENAGA CABLE INDUSTRIES SDN.BHD

$$h_w = \frac{0.00572}{(273+T+0.5\theta)^{0.123}}\sqrt{\frac{u}{D}} \quad w/^0c\ cm^2 \qquad (3.1)$$

Where: Wind velocity u in m/s , Conductor diameter(D) in cm, Ambient temperature T in °C, Permissible temperature increase θ in °C.

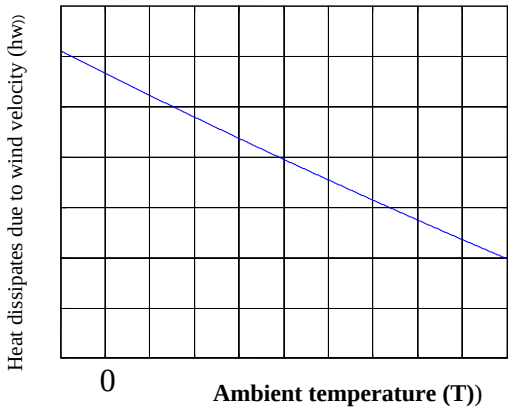

Figure-3.1 : Heat dissipated due to wind velocity Vs Ambient temperature.

Another statement [14] forced convection heat loss at low wind speed is:

$$q_c = K_\emptyset K_f (T_c - T_a)[1.01 + 0.371\left(\frac{D_{pf}\, qV_w}{\mu_f}\right)^{0.52}] \qquad (3.2)$$

where$K_\varnothing$=1.194−cos(ϕ)+0.194cos(2ϕ)+0.368 s in(2ϕ) is a term that accounts for the angle ϕ , K_f is air thermal conductivity coefficient in W/ft, pf is air density in lb/ft3 & μf is absolute viscosity of air in lb/(ft-h).

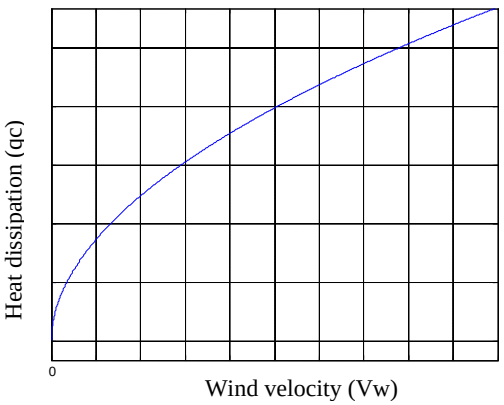

Figure-3.2 : Heat dissipation Vs Wind velocity.

IV. Heat Dissipated Due to Radiation

The formula of heat dissipated due to radiation is (hr) is given by TENAGA CABLE INDUSTRIES SDN.BHD

$$hr = 0.0567\frac{(273+T+\theta)^4-(273+T)^4}{10\times10^5\theta} \quad w/^0c\ cm^2 \qquad (4.1)$$

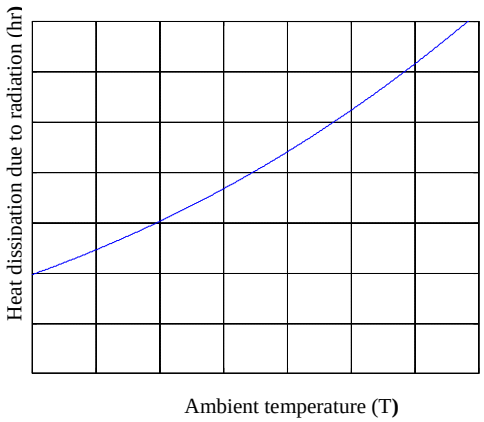

Figure-4.1 : Heat dissipation Vs Ambient temperature.

And also can be expressed as

$$hr = 0.138D€\frac{(273+T_c)^4-(273+T_a)^4}{100^4} \qquad (4.2)$$

€=0.5 is the approximate value to be used. The solar heat gain also can be computed as

$$q_s = \alpha Q_s A' sin\theta \qquad (4.3)$$

Where $\theta = cos^{-1}[\cos(H_c)\cos(Z_c - Z_l)]$ and H_c ,Z_c ,Z_l are altitude of the sun in degree azimuth1of sun in degree azimuth of line in degree respectively. Solar absorptivity α increases with the conductor age depending on the atmospheric pollution and line operating voltage α= 0.7 can be used, if the exact value is unknown.

V. Skin Effect Factor (y_s)

If the conductor is composed of one or more concentric circular elements, then the centre portion of the conductor will be enveloped by a greater magnetic flux than those on the outside. Consequently the self induced back-emf will be greater towards the centre of the conductor, thus causing the current density to be less at the centre than the conductor surface. This extra concentration at the surface is known as skin effect, and results in an increase in the effective resistance of the conductor.

$y_s = \frac{{x_s}^4}{192+{x_s}^4}$ Where ${x_s}^2 = 8.\pi.f.10^{-7}.k_s/R_{dct}$

and f = Frequency (Hz), Ks=Factor determined by conductor construction 1 for circular, stranded, compacted and sectored .Rdct=DC resistance at operating temperature t.

VI. Proximity Effect Factor (y_p)

The proximity effect also increases the effective resistance and is associated with the magnetic fields of two conductors which are close together. If each carries a current in the same direction, the halves of the conductors in close proximity are cut by more magnetic flux than the remote halves. Consequently the current distribution is not even throughout the cross-section, a greater proportion being carried by the remote halves. If the currents are in opposite directions, the halves in close proximity will carry the greater density of current.

$$y_P = x_P{}^4/(192 + 0.8x_P{}^4) \cdot (d_c/S)^2 \cdot [0.312.(d_c/S)^2 + 1.18/\{x_p{}^4/(192 + 0.8x_p{}^4) + 0.27\}]$$

Where $x_p{}^2 = 8.\pi.f.10^{-7}.k_p/R_{dct}$

kp = Factor determined by conductor construction 1 for circular, stranded, compacted and sectored 0.8 if above conductors are dried and impregnated dc = Diameter of conductor (mm)

Since the spacing S(mm) between two conductors is very large as compared with diameter the proximity effect can be neglected for overhead lines.

VII. Current-Temperature Relationship

The current-temperature relationship of a bare overhead conductor is addressed by IEEE standard [10], The overhead line temperature depends on the following conditions:

- Conductor material properties
- Conductor electrical current
- Conductor diameter and surface conditions
- Ambient weather conditions: wind, sun, air.

The contribution of the mentioned above factors in steady state can be summarized by the Heat Balance equation [11], as follows:

$$I^2 R_{Tc} + q_s = q_c + q_r \qquad (7.1)$$

Where, I is the conductor current carrying capacity.

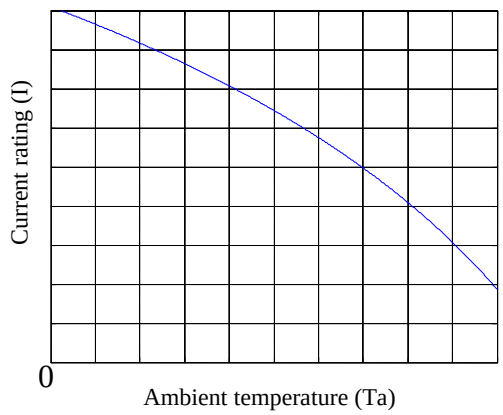

Figure-7.1 : Current rating Vs Ambient temperature.

The formula [8] of current also can be expressed as

$$I = \sqrt{\frac{hw + \{hr - (ws/\pi\theta)\eta\}\pi D\theta}{Rac}} \qquad (7.2)$$

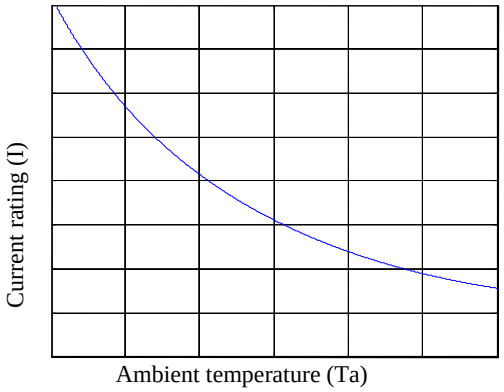

Figure-7.2 : Current rating Vs Ambient temperature.

VIII. Current Rating-Wind Flow Relationship

Heat is generated in conductor due to various circumstances and air acts as a cooling agent. So wind flow is a very active parameter to dissipate and minimize heat from conductor. It has a contribution on current rating expressed by equation (7.1) and (7.2).

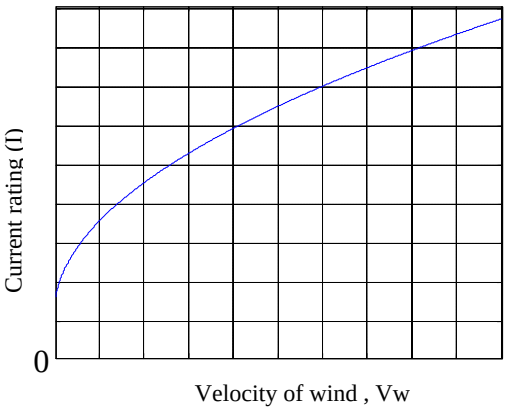

Figure-8.1 : Current rating Vs Wind velocity.

IX. Conclusion

Equation 2.1 and Figure-2.1 shows that the resistance is directly proportional to temperature. Heat dissipated due to wind velocity is inversely proportional to ambient temperature. But heat dissipation increases with the increase of wind velocity and heat dissipation due to radiation including solar radiation with ambient temperature. Considering all the circumstances, it can be said that overall current carrying capacity of a conductor increases with decrease of ambient temperature but wind flow in reasonable range assist to increase the current carrying capacity of an ACSR conductor.

References Refferences Refferencias

1. Plane and Solid Geometry by J.M. Aarts
2. Fractional area calculation of a circle URL: http://www.math10.com/en/geometry/circles.html
3. The Pythagorean Theorem: A 4,000-Year History by Eli Maor & URL: http://www.themathpage.com/atrig/theorems-of- geometry.htm ,Theorem -10
4. AutoCAD: professional tips and techniques By Lynn Allen, Scott Onstott
5. Getting started with MATLAB 7 by RUDRA PRATAP. Chapter6,Graphics.
6. Topics in elementary geometry By Oene Bottema, Robin Hartshorne URL: http://www.themathpage.com/atrig/theorems-of-geometry.htm , Theorem-11.
7. "Alternating current (AC) resistance of helically strande conductors "published in the April 2008 issue of Electra, the members' journal of Cigré, energize - June 2008 - Page 31-34;
8. "OVERHED ALUMINIUM CONDUCTORS" Catalog of TENAGA CABLE INDUSTRIES SDN.BHD page 70-73;
9. W.A.Lewis, P. D. Tuttle, "The Resistance and Reactance of Aluminium Conductors, Steel Reinforced", IEEE Transactions on Power Apparatus and Systems, pp. 1189-1215, Feb. 1958.
10. IEEE standard for Calculation the Current-Temperature Relationship of Bare Overhead Conductors, IEEE Std 738-1993, 8 Nov 1993;
11. H. E. House, P. D. Tuttle, "Current carrying capacity of ACSR", IEEE Transactions on Power Apparatus and Systems, pp. 1169-1178, Feb. 1958.
12. Reichman, J., 'Bundled conductor Voltage Gradient Calculations," AIEE Tarns.1959,Pt III,78;598
13. The Aluminium Association, Aluminium Electrical Conductor handbook, New York ,1971.
14. Marija Bockarjova ,G¨oran Andersson," Transmission Line Conductor Temperature Impact on State Estimation Accuracy"

Global Journal of researches in engineering
Electrical and electronics engineering
Volume 12 Issue 1 Version 1.0 January 2012
Type: Double Blind Peer Reviewed International Research Journal
Publisher: Global Journals Inc. (USA)
Online ISSN: 2249-4596 & Print ISSN: 0975-5861

Optimal Generation Scheduling of Cascaded Hydroelectric System using Natural Exponential Inertia Weight PSO

By Nand Kishore, Amita Mahor
Department of Electrical & Electronics Engineering, NIIST Bhopal

Abstract - Generation scheduling is a most important task in the operation and planning of power system. It can be on real term, short term, medium term, and long term basis as per the scheduled horizon. Scheduling of purely hydroelectric system differ from the thermal scheduling and hydrothermal scheduling problems in two aspects firstly fuel cost for the thermal part of the system can no longer be used in the objective function. Secondly water availability in seasonal reservoirs is the necessary part of such system. Many researchers suggested different solution algorithms of optimization for each type of problem and claimed better solution. This paper presents a Natural Exponential Inertia Weight Particle Swarm Optimization (NEIW_PSO) approach to determine the optimal generation schedule of hydro power plants of cascaded hydroelectric test system.

Keywords : Particle Swarm Optimization, Natural Exponential Inertia Weight PSO, short term generation scheduling.

GJRE-F Classification: FOR Code: 090608

Strictly as per the compliance and regulations of:

Optimal Generation Scheduling of Cascaded Hydroelectric System using Natural Exponential Inertia Weight PSO

Nand Kishore [α], Amita Mahor [σ]

Abstract - Generation scheduling is a most important task in the operation and planning of power system. It can be on real term, short term, medium term, and long term basis as per the scheduled horizon. Scheduling of purely hydroelectric system differ from the thermal scheduling and hydrothermal scheduling problems in two aspects firstly fuel cost for the thermal part of the system can no longer be used in the objective function. Secondly water availability in seasonal reservoirs is the necessary part of such system. Many researchers suggested different solution algorithms of optimization for each type of problem and claimed better solution. This paper presents a Natural Exponential Inertia Weight Particle Swarm Optimization (NEIW_PSO) approach to determine the optimal generation schedule of hydro power plants of cascaded hydroelectric test system.

Index Terms : Particle Swarm Optimization, Natural Exponential Inertia Weight PSO, short term generation scheduling.

I. Introduction

The biggest share of electricity in all countries is produced by power plants driven by water, fossil fuels and nuclear resources. Worldwide there is a shortage of power and to fulfill the demand it is required that the existing generation installed capacity should enhance. To fulfill this gap of power generation and demand, generation utilities are facing issues like depletion of available power generation resources fossil fuels, continuous increase in its prices and environmental aspects. Considering above it become must that utilization of available hydro resources should be optimum. Connection of Hydro power plants in cascaded fashion is a step in this direction, where the water discharge from upstream hydro power plants increase the water level of reservoir at downstream. Various conventional [1] [2] and non-conventional methods [3], [4], [5], [6] are suggested in literature to solve such problems. Amongst all Particle swarm optimization technique [7] is the most popular algorithm due to its fast dynamic convergence and quality solution. Here NEIW_PSO has been used to determine the hourly optimal generation schedule of hydro power plants of cascaded hydro electric test system [8] for the time horizon of 24 hours.

Author α : M.Tech. Power Electronics Student, Department of Electrical & Electronics Engineering, NIIST Bhopal, E-mail : nkmeena83@gmail.com
Author σ : Professor & Head, Department of Electrical & Electronics Engineering, NIIST Bhopal, E-mail : amitamahor@yahoo.co.in

II. Problem Formulation

Short term hydroelectric power generation scheduling problem of cascaded hydro electric system can be stated to find out the water discharges through each hydro power plants of cascaded system satisfying all physical and operational constraints. These are in form of demand supply balance, flow balance or continuity equation, bounds on reservoir storage, bound on water release or discharge, limits on spillage, and coupling constraints that put a boundary condition on the initial and final reservoir level.

Hydro scheduling problems requires an optimization problem formulation. During formulation, water travelling time from upstream power plant to immediate downstream plant is considered of constant value in spite of varying discharges. In present work hydro plant problem has been formulated without considering natural inflows, irrigation requirement and evaporation losses.

a) Objective function

An objective function expresses the main aim of the model which is either to be minimized or maximized. It is expressed in terms of design variables and other problem parameters. In present hydroelectric scheduling problem, the goal is to minimize the deviation between load demand including transmission losses and generation through hydroelectric power plants as given below:

$$E = \text{Min} \sum_{t=1}^{T} E^{t} \quad (1)$$

Where E^t is the deviation between load demand and generated power at time t and calculated as below:

$$E^{t} = \text{Min}\ (1/2) \times [(P_D{}^{t} - \sum_{j=1}^{n} P^{t}{}_{j})^2] \quad (2)$$

Where P^t_D and P^t_j represented load demand, power generated through jth hydro power plants of hydroelectric system at time t respectively.

b) Constraints

The optimal value of the objective function as given in eq. (1) is computed subjected to constraints of two kinds of equality constraints and inequality constraints or simple variable bounds as given below. The decision is discretized into 1 h period.

i. *Equality constraints*

a. Water balance equation

Naturally occurring reservoirs are not standard geometric shapes. Generation associated discharge varies with time and there are environmental and weather factors which also contribute directly to change in water level. A reservoir thus has a number of independent inflows and outflows. This water continuity equation relates the previous interval water storage in reservoirs with current storage including delay in water transportation between successive reservoirs water continuity has been expressed as:

$$X_j^{t+1} = X_j^t + Yjt + Uup^{t-\delta} + S_{up}^{t-\delta} - U_j^t - S_j^t - IR_j^t - EL_j^t \quad (3)$$

For these cases average hourly evaporation loss, irrigation requirement & natural inflows in reservoirs of each plant of cascaded system is assumed zero. Hence the above eq. (3) can be rewrite as given below.

$$X_j^{t+1} = X_j^t + Uup^{t-\delta} + S_{up}^{t-\delta} - U_j^t - S_j^t \quad (4)$$

As hydro power plants are connected in cascaded mode hence the water release from upstream hydro power plants will reach to its immediate downstream plant with appropriate time delay. The delay time between the successive reservoirs of the Cascaded Hydro-electric System have been mentioned in Table 1.

Table 1 : Water travel time between consecutive hydro electric power plant of test system

Name of plant	Travel time	Name of plant	Travel time	Name of plant	Travel time
P1	62 hrs	P2	4 hrs	P3	3 hrs
P4	17 hrs	P5	0 hrs	-	-

ii. *Inequality Constraints*

Reservoir storage, turbine discharges rates, spillages and power generation limit should be in minimum and maximum bound due to the physical limitation of the dam and turbine. Reservoir storage before scheduled horizon and at the end of the horizon should be taken from midterm planning.

a. Reservoir storage bounds

Hydro electric plants are the multipurpose projects. Hence the min and max reservoir volume should be as per the Indian standard guidelines IS 7323:1994 of reservoir operation. In hydro power plants volume of water stored in reservoir up-to Full Reservoir Level (FRL) is called the gross storage and is considered as maximum bound on reservoir storage. Generally in hydro power plants the volume of water available between the Minimum Draw down Level (MDDL) and Full Reservoir Level (FRL) which is also called the live storage capacity has been used for power generation. Hence in present work the minimum bound of reservoir storage are the difference of gross storage and live storage of the concerned power plants.

$$X_j^{min} \le X_j^t \le X_j^{max} \quad (5)$$

b. Water Discharge Bounds

This is a minimum and maximum bound on the release of the hydro power plant through turbine.

$$U_j^{min} \le U_j^t \le U_j^{max} \quad (6)$$

c. Power Generation Bounds

Power generated through hydro power plants should be minimum and maximum bounds.

$$P_j^{min} \le P_j^t \le P_j^{max} \quad (7)$$

d. Spillage

Spillage from the reservoir is allowed only when to be released from reservoir exceeds the maximum discharge limits. Water spilled from reservoir j during time t can be calculated as follows:

$$S_j^t = Q_j^t - U_j^{max} \text{ if } Q_j^t > U_j^{max} \quad (8)$$

$$= 0 \qquad \text{otherwise}$$

e. Initial & end reservoir storage volumes

Terminal reservoir volumes are generally set through midterm scheduling process. This constraints implies the total quantity of utilized water for short term scheduling should be within limit so that the user of the reservoir should not be penalized. In present research work it has been assumed that all five reservoirs are filled up-to FRL hence gross storage has been considered as beginning or initial storage in reservoir at the starting of scheduled horizon. Live storage capacity at that time considered as available water for generation for scheduled horizon i.e. the water storage at the end of scheduled horizon of 24 hrs has been calculated as given below:

$$X_j^0 = X_j^{begin} \qquad X_j^t = X_j^{end} \quad (9)$$

$$X_j^0 = X_j^{begin} = X_j^{max} \quad (10)$$

$$X_j^{oneday} = (X_j^{max} - X_j^{min})/365 \quad (11)$$

$$X_j^{end} = X_j^0 - X_j^{oneday} \quad (12)$$

III. Overview of Particle Swarm Optimization

Particle swarm optimization is a population based stochastic search algorithm which is the most

recent developments in the category combinatorial meta-heuristic optimization. It was first introduced by Kennedy and eberhart in 1995 [9] as new heuristic method. The original objective of their research was to graphically model to the social behavior of bird flocks and fish schools. But this original version can only handle the non-linear continuous optimization problems. Further; the advancement in this PSO algorithm can explore the global optimal solution of complex problems of engineering and sciences. Amongst various version of PSO, most familiar version was proposed by Shi and Eberhart [10].the key attractive feature of PSO is its simplicity as it involves only two model eq.(1) and eq.(2).In PSO, the co-ordinates of each particle represent a possible solution called particle associated with position and velocity vector. At each iteration particle moves towards an optimum solution through its present velocity and their individual best solution obtained by themselves and global best solution obtained by all particles. In a physical dimensional search space, the position and velocity of the particle I are represented as the vector of

$Xi = [x_{i1}, x_{i2}, \ldots\ldots\ldots x_{id}]$ and $v_i = [V_{i1}, v_{i2}, \ldots\ldots\ldots\ldots V_{id}]$in the PSO algorithm.

Let $P\_best(i) = [X_{i1pbest}, x_{i2pbest} \ldots\ldots\ldots X_{idpbest}]$ and

$G\_best = [X_{1gbest}, X_{2gbest} \ldots\ldots\ldots\ldots X_{ngbest}]$ be the best position of particle I and global best position respectively. The modified velocity and position of each particle can be calculated using the current velocity and distance from P-best (i) and G_best as shown fig 1.

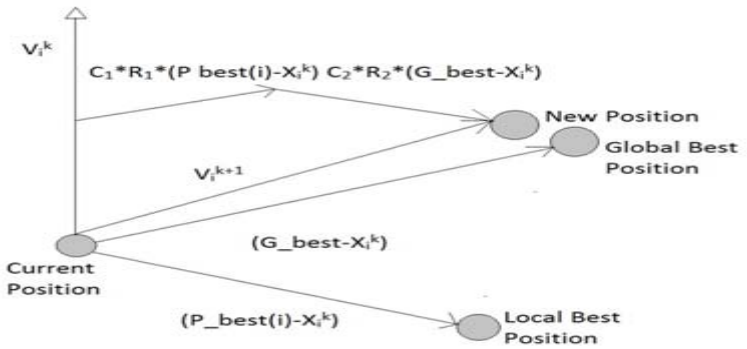

Fig.1 : Ilustration of PSO

Mathematically velocity and position of the particle have been updated as given below:

$$V_i^{k+1} = K\ \{V_i^k \times \omega + C_1 \times R_1 \times (P\_best(i) - X_i^k) + C_2 \times R_2 \times (G\text{-}best - X_i^k)\} \quad (13)$$

$$X_i^{k+1} = X_i^k + V_i^{k+1} \quad (14)$$

$$K = 2/abs\ \{2\text{-}C\text{-}\sqrt{(C^2 - 4 * C)}\} \quad (15)$$

Where $C = C_1 + C_2$

In this velocity updating process, the value of the parameter such as inertia weight ω, cognitive rate C1, social rate C2, random function between 0 to 1 {R1 and R2},constriction factor K should be determined in advance. The inertia weight ω is linearly decreasing as the inertia proceeds and obtained as:

$$\omega = \omega_{max} - \{(\omega_{max} - \omega_{min})\ iter\}\ /iter\_max \quad (16)$$

The key attractive feature of PSO is its simplicity as it is involves only tow eq.(13) and eq.(14)the first part of eq. (13) represent the previous velocity, which provides the necessary momentum for particle to roam across the search space. The second part knows as "cognitive "component represent the personal thinking of each particle. Cognitive component encourages the particle moves toward their own best positions found so far .The third part is known as the "social" component, which represent the collaborative effect of the particle, in finding the global optimal solution. The social component always pulls the particle towards global best t particle so far.

IV. Description of Cascaded Hydroelectric Test System

In order to verify the feasibility and effectiveness of the proposed method, a test system taken from ref. [11] is used. The system consists of a multi-chain cascade of five hydro power plants. The scheduling period is one day of 24 hrs with one hour time intervals. The test hydro system configuration is shown in fig. (2).This hydraulic test system having huge hydraulic coupling amongst plant 2, 3 & 4 as the maximum tail race level of plant 2 will act as full reservoir level of plant 3 and so on.

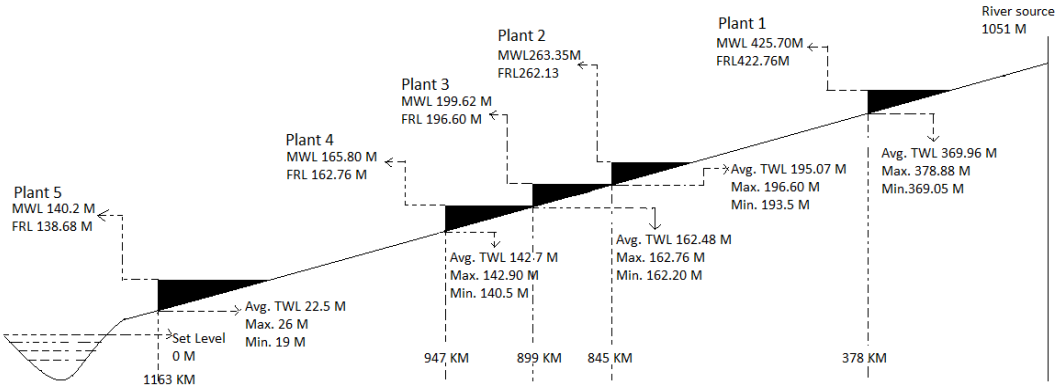

Fig.2 : Hydraulic coupling of hydro power plants of test system

V. Generation Scheduling Using of Natural Exponential Inertia Weight PSO

In PSO particles movement is governed by its previous own velocity and two acceleration components i.e. cognitive component & social component. Usually implementation of PSO needs predefine parameters inertia weight ω, cognitive rate C1, social rate C2, constriction factor K, maximum velocity V_{max}, swarm size, topology and random number generation techniques. Proper selection and control of these parameters is necessary to get the good quality solution from PSO. Many researchers has proposed modification in PSO to improve its performance by adopt change in any of above parameters. Natural Exponential Inertia Weight PSO NEIW_PSO method is one of the variants proposed by [12] where Inertia weight exponentially decreases as given in eq. (17).In present work NEIW_PSO has been used to determine the hourly optimal generation schedule of power plants of cascaded test system for the time horizon of 24 hrs. Details steps of implementation are given below:

$$\omega = \omega \max - \{(\omega \max - \omega \min).e^{-[t/(MAXITER)/4]2} \quad (17)$$

Step 1: Initialize position of discharge particle between U_j^{min} & U_j^{max} for population size PS.
Step 2: Initialize velocity of discharge particle between $-V_j^{max}$ to $+V_j^{max}$, where V_j^{max} calculated is given

$$V_j^{max} = (U_j^{max} - U_j^{min})/10 \quad (18)$$

Step 3: Initialize dependent discharge matrix.
Step 4: Inialize the p_best (i) and G_best.
Step 5: Set iteration count = 0.
Step 6: Calculate the dependent reservoir storage X_j^t.
Step 7:Check whether X_j^t is within limit X_j^{min} ,X_j^{max}.

- If $X_j^t < X_j^{min}$ then set $X_j^t = X_j^{min}$
- If $X_j^t > X_j^{max}$ then set $X_j^t = X_j^{max}$
- If $X_j^{min} \le X_j^t \le X_j^{max}$ then set $X_j^t = X_j^t$

Step 8: Evaluate the fitness function as given below:

$$F(X_j^t, U_j^t) = 1/[1+\min(1/2)\times P_l^t - \sum_{j=1}^{5} P_j^t)^2] \quad (19)$$

Step 9: Is fitness value is greater than G_best(i)?

- If yes,set it as new P_best(i) then go to next step.
- Else go to next step.

Step 10: Is fitness value is greater than G_best?

- If yes,set it as new G_best than go to next step.
- Else go to next step.

Step 11: check whether stopping criteria max iteration (iter_max) reached?

- If yes than go to step 19.
- Else go to next step.

Step 12: Update inertia weight using eq. (17)
Step 13: Update velocity of discharge particle using eq.(13).
Step 14: Check whether V_j^t is within limit V_j^{min},V_j^{max}

- If $V_j^t < V_j^{min}$ then set $V_j^t = V_j^{min}$
- If $V_j^t > V_j^{max}$ then set $V_j^t = V_j^{max}$
- If $V_j^{min} \le V_j^t \le V_j^{max}$ then set $V_j^t = V_j^t$

Step 15: Update position of discharge particles using eq.(14).
Step 16: Check whether U_j^t is with in limit U_j^{min},U_j^{max}.

- If $U_j^t < U_j^{min}$ then set $U_j^t = U_j^{min}$
- If $U_j^t > U_j^{max}$ then set $U_j^t = U_j^{max}$
- If $U_j^{min} \le U_j^t \le U_j^{max}$ then set $U_j^t = U_j^t$

Step 17: Update dependent discharge matrix considering hydraulic coupling.
Step 18: Check for stopping criteria.

- If iter<iter_max then increase iteration count by 1 & go to step 6.

- Else go to step 19.

Step 19: Last G_best position of particles is optimal solution.

VI. Results and Analysis

MATLAB programming to determine the optimal generation schedule of test system using NEIW_PSO has been done. Where PSO parameters C1= 2, C2=2 no. of iterations = 120 are adopted. Hourly load demand is mentioned in Table no. (2). Program has been run on MATLAB 7.0.1 version on a Dual core 2GB RAM Hard disk 320GB.The results for the short term optimal generation scheduling of hydro-electric test system using NEIW_PSO method have been obtained for different population size 5, 10, 15, 20 and 25 as mentioned in Table no. (3). for each population size 10 trails of individual hours are done and amongst all 10 trials best suitable results are considered. From results it has been observed that population size 5 is giving best possible solution.

Table 2 : Hourly Load Demand (MW)

Hour	Demand	Hour	Demand	Hour	Demand
1	1350	9	1900	17	1850
2	1300	10	1800	18	1900
3	1350	11	2000	19	1750
4	1300	12	1800	20	1700
5	1350	13	2000	21	1600
6	1400	14	2000	22	1500
7	1500	15	1900	23	1550
8	1600	16	1900	24	1900

Table 3 : Best value of objective function at different Population size

Population Size	Best objective function
5	1.45E-16
10	4.49E-14
15	3.37E-16
20	5.34E-16
25	3.08E-16

Optimum generation schedule of all five hydro power plants and its corresponding hourly discharge trajectories and reservoir storage trajectories are given in Fig. (3)- (5) respectively .

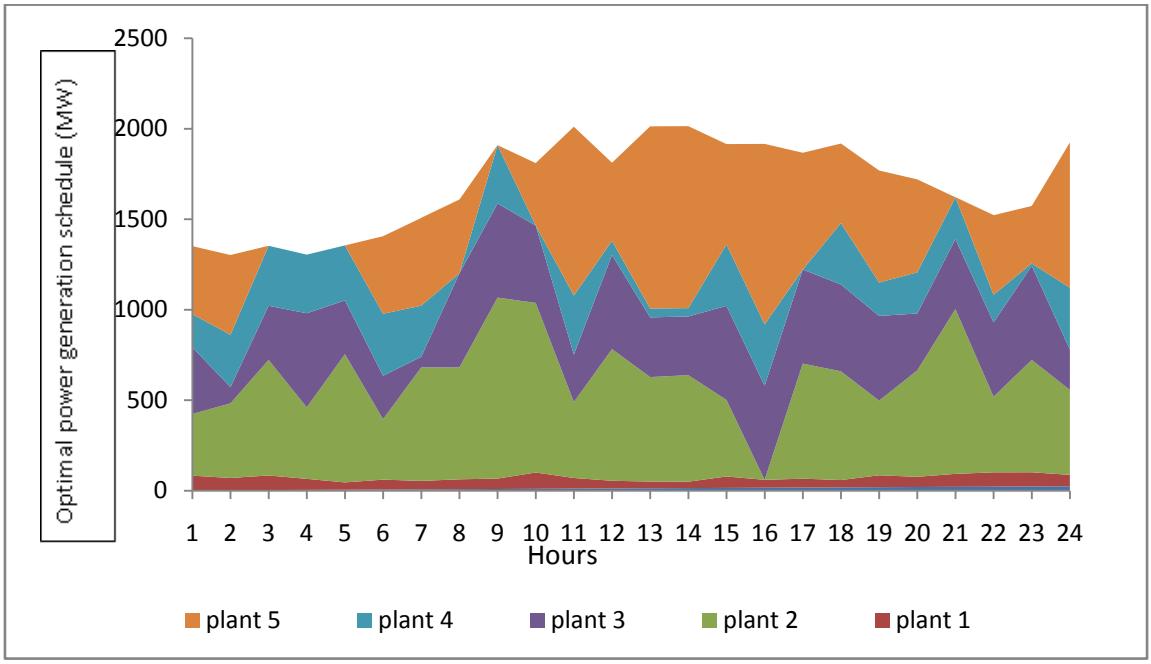

Fig. 3 : Optimal power generation schedule of hydro power plants of test system

Optimal power generation schedule of hydro power plants shows that the capacity factor of plant 5 is maximum i.e. 53.38% followed by plant 4(47.43%), plant 2 (44.14%), plant 1 (34.28%) and plant3 *(26.75%).*

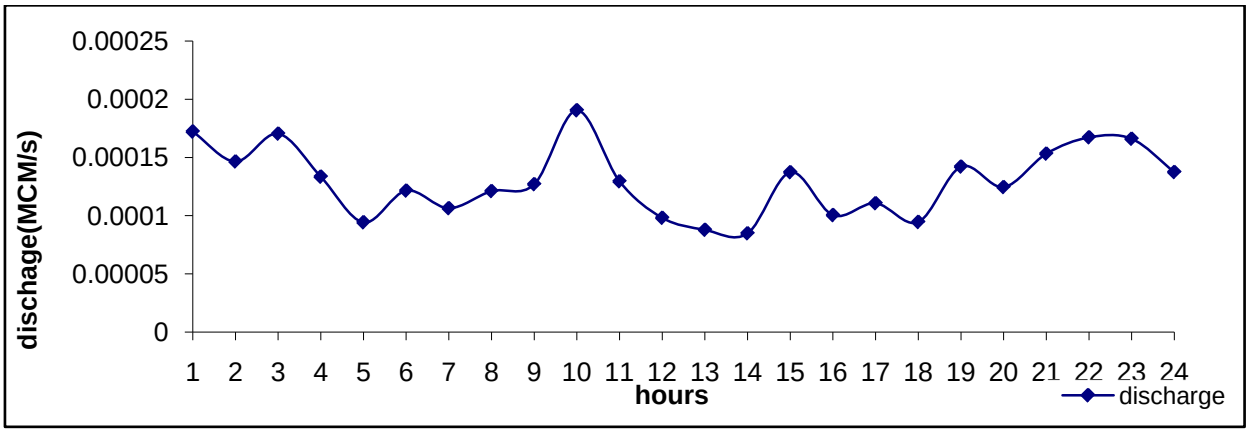

(a) Plant 1

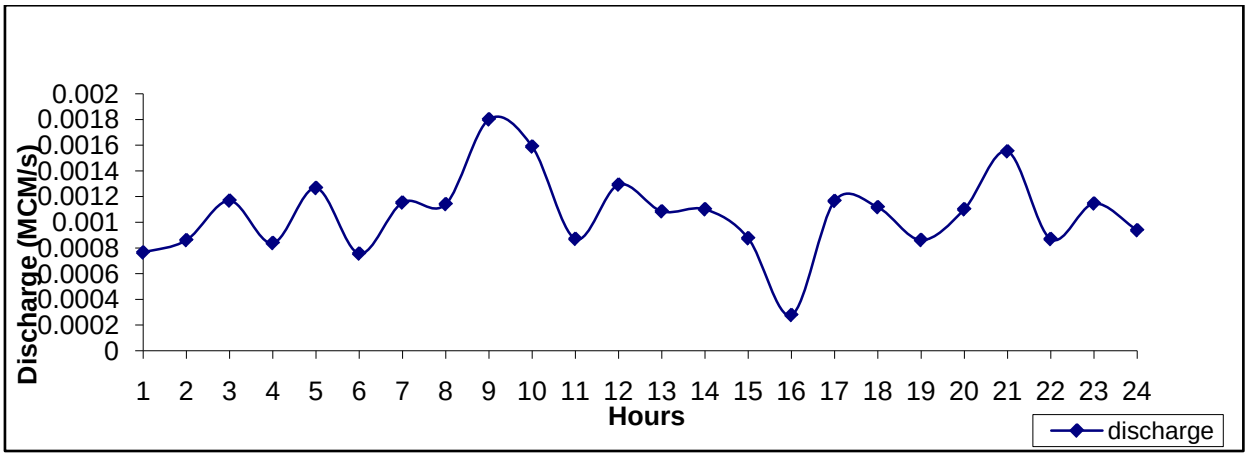

(b) Plant 2

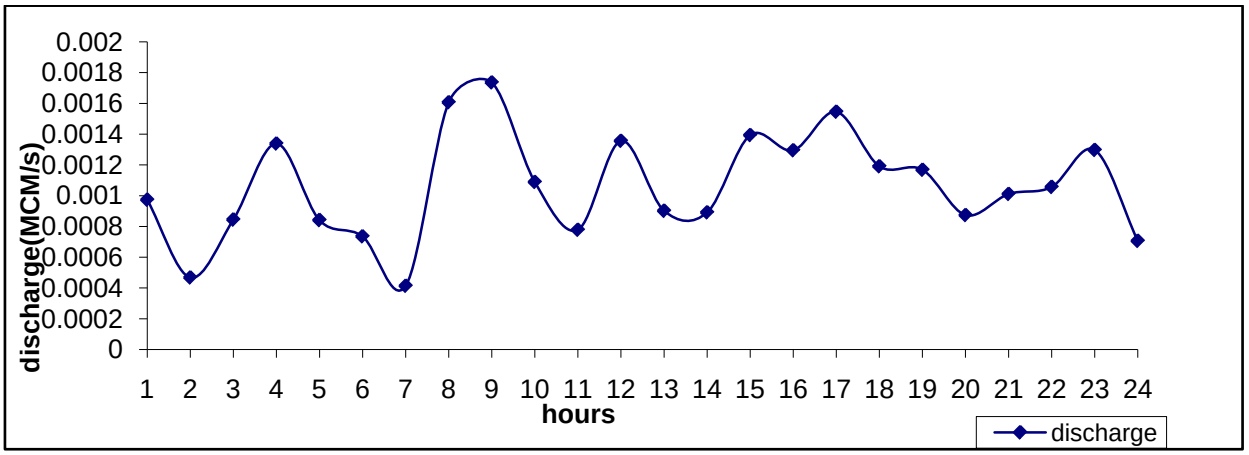

© Plant 3

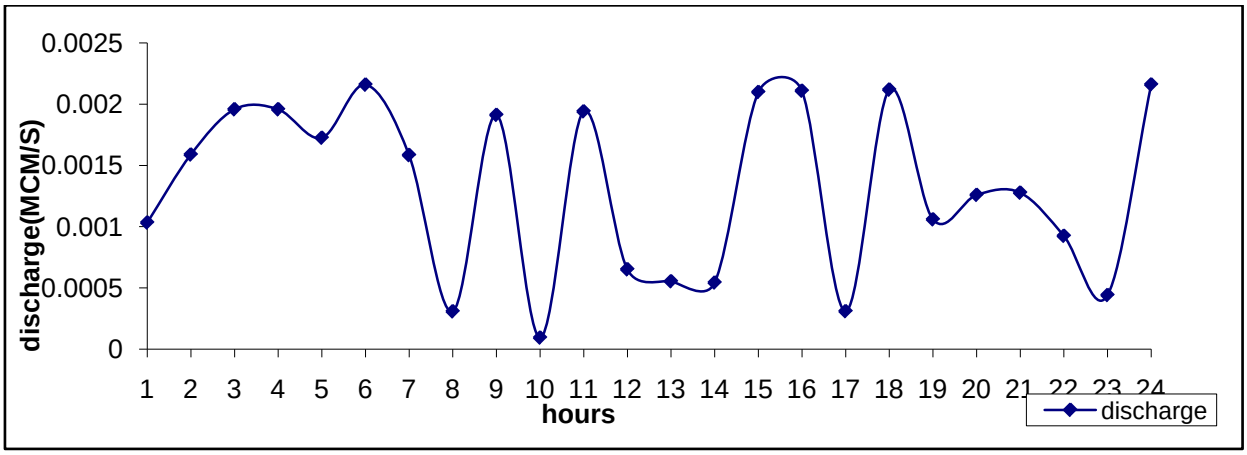

(d) Plant 4

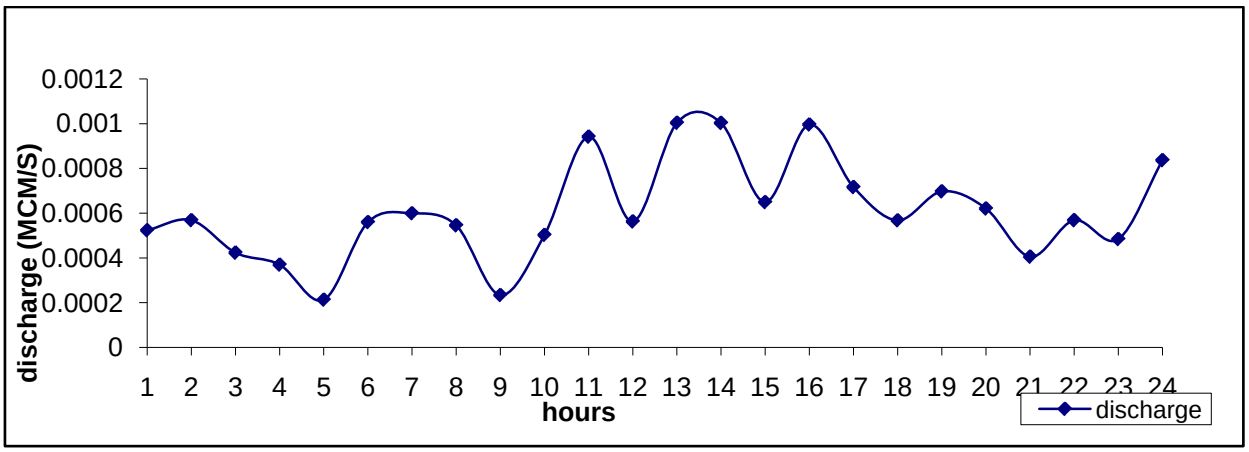

(e) Plant 5

Fig. 4 : (a)-(e) Discharge Trajectories of hydro power plants of test system

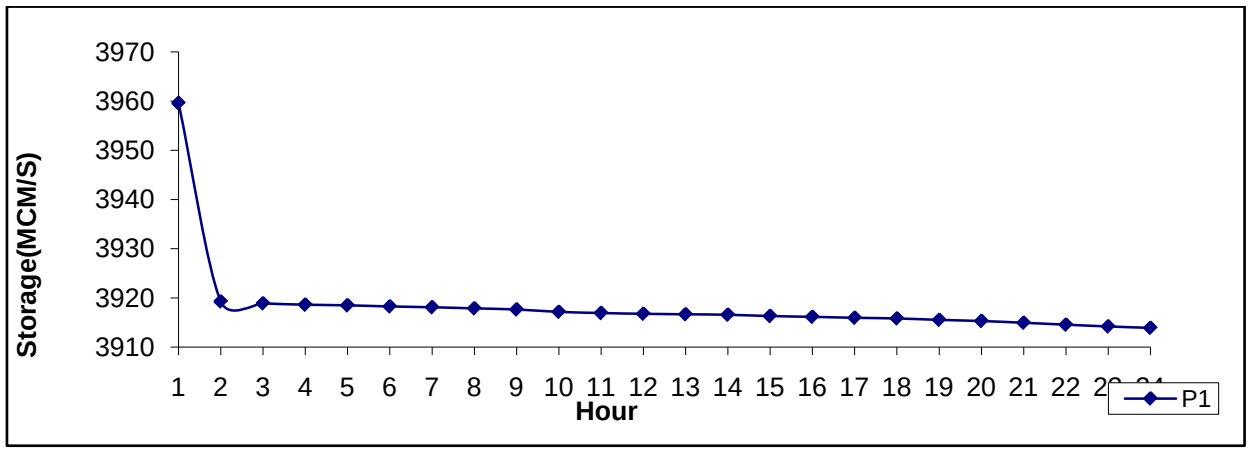

(a) Plant 1

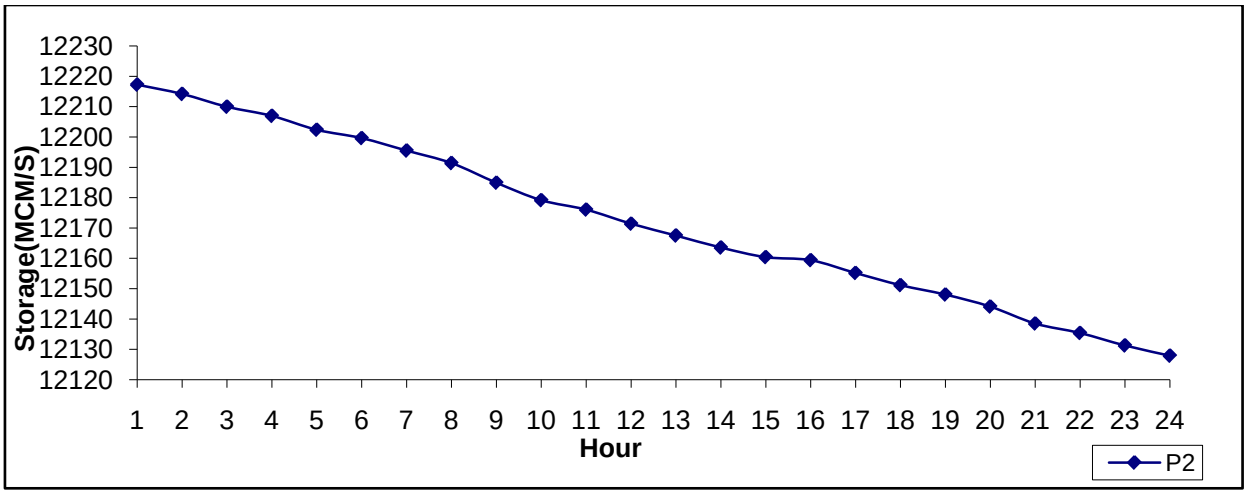

(b) Plant 2

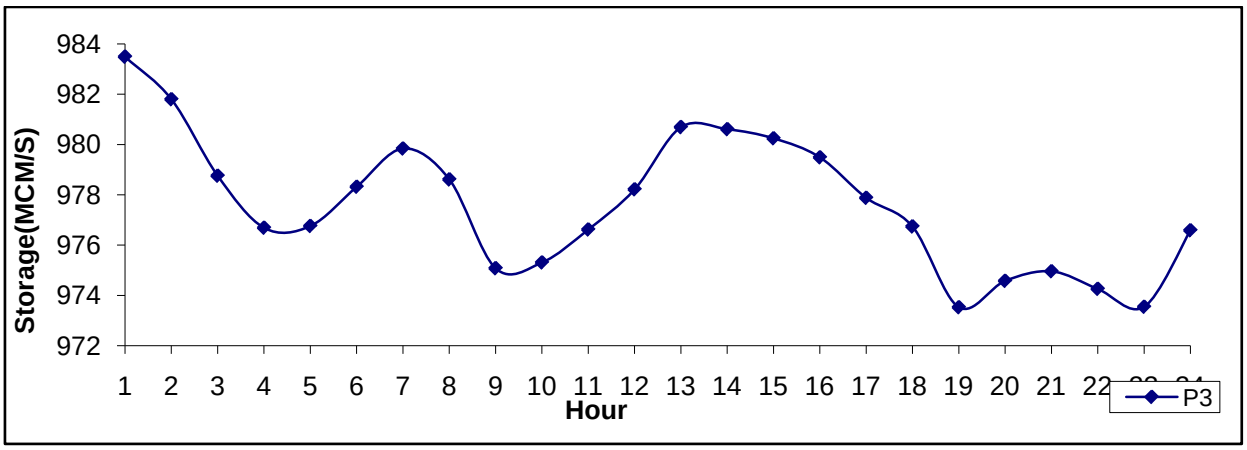

© Plant 3

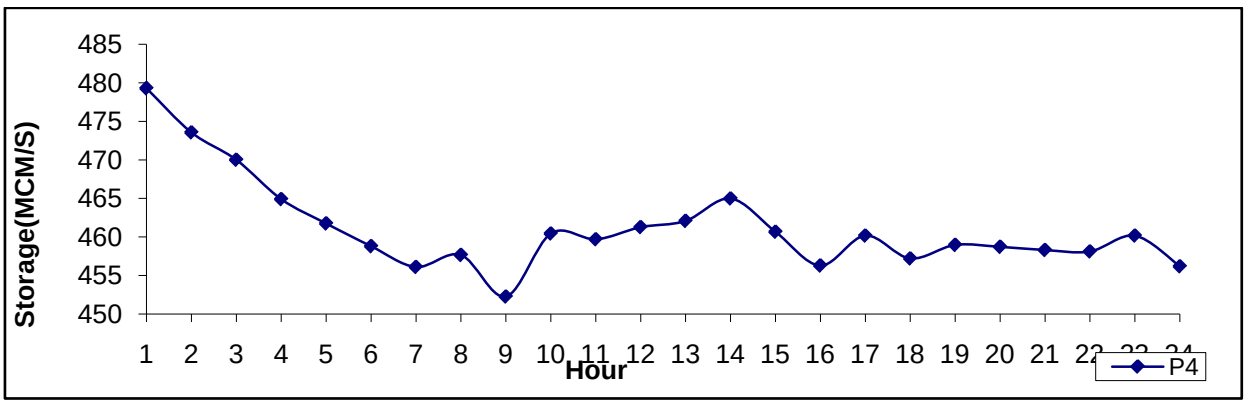

(d) Plant 4

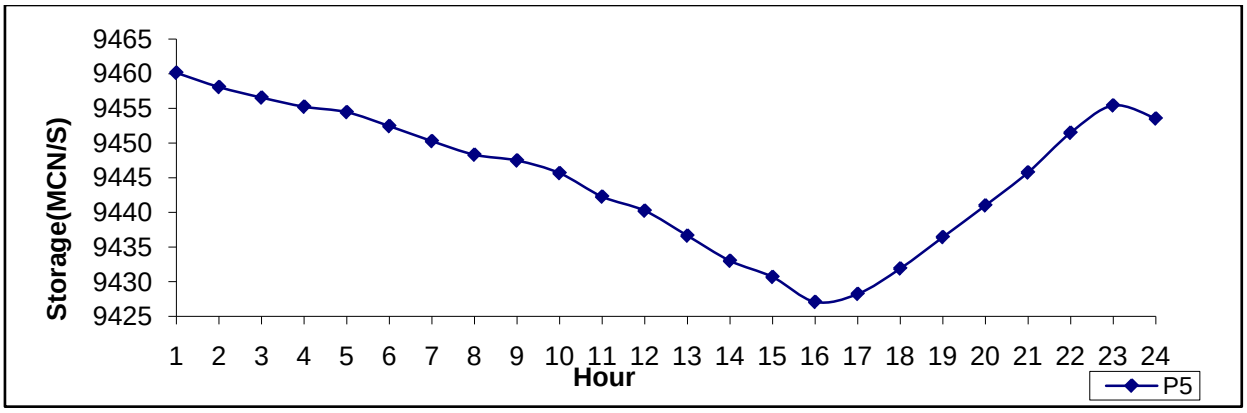

(e) Plant 5

Fig.5 : Reservoir storage trajectories of hydro power plants of test system

VII. Conclusion

In optimal generation scheduling problem of hydro electric system, complexity introduced by the cascaded pattern. This problem becomes more complex when there is hydraulic coupling between hydro plants of cascade system. Modern heuristic optimization techniques especially PSO gained popularly to solve such problem due to its simplicity. The performance of PSO is governed by its parameters like inertia weight, acceleration coefficients and personal and global experience of the particles. Here in present work NEIW_PSO has been adopted to determine the optimal generation schedule of hydro power plants of the test system for the time horizon of 24hrs. The results are obtained for different population sizes i.e. 5,10,15,20 and 25. It has been observed that population size 5 is giving best suitable value of objective function (1.45E-16). Apart from this results also show that capacity factor of plant 5 of the test system is maximum for effective utilization of water resources.

Acknowledgment

The authers gretfully acknowledge the support of Dr.S.C. Kapoor Director NIIST bhopal to provide facility for completion of this work.

Appendix

P^t_L Total load demand at time t
P^t_j Electrical power generted from J^{th} unit of plant at time t
X^t_j Reservoir storage of the J^{th} plant at time t
X_j^{min},X_j^{max} Minimum and maximum storage in $_j^{th}$ reservoir
Y^t_j Natural inflow in the J^{th} plant at time t
U^t_j Discharge through J^{th} plant at time t
U_j^{min},U_j^{max} Minimum & maximum discharge through turbine of J^{th} plant
S^t_j Spill from the J^{th} plant at time t
N Number of hydro power plant
δ Time delay for water flows from upstream plant to downstrem plant
V_i^k Velocity of particle I at iteration k
ω Inerta weight factor
C_1 ,C_2 Acceleration coeficient
R_1,R_2 Uniformly distributed random number between 0 to 1
X_i^k Position of particle I at k iteration
P_best(i) Best position of particle I until iteration k
G_best Best position of the group until iteration k
K Constriction factor
ω_{max} Final Inertia Weight
ω_{min} Iinal Inertia Weight
iter Current iteration number
it_max Maximum iteration number
k Iteration index
t Time
up Index of immediate upstream power plant

References Références Referencias

1. Sjelvgren D,Dillon T.S. Seasonal planning of hydro-thermal system using the network flow concept .In: Proceeding seventh power system computation conference (PSCC-7).Lausanne,Switzerland,July, 1981,pp.1191-9.
2. Sjelvgren D,Martin RW,Dillon TS.Stochastic optimization and modeling of large hydro-thermal system for long term regulation.Int J Electrical power energy system 1980,2(1):2-20.
3. Sinha N,Chakrabarti R,Chattopadhyay PK. Evolutionary programming techniques for economic load dispatch.IEEE Trans. Evol.Comput 2003;7 (February):83-94.
4. Basu M.A Simulated annealing based goal attainment method for economic emission load dispatchof fixed hydrothermal power system.Int Electrical power energy system 2005:27(2):147-53.

5. Huang Shyh Jier. Enhancement of hydroelectric generation scheduling using ant colony system based optimization approaches.IEEE Trans Energy Conver 2001;16(3):296-301.
6. Lin WM,Cheng FS. Tsay MT.An improved tabu search for economic dispatch with multiple minima.IEEE Trans Power system 2002:17:108-12.
7. Mandal KK,Basu M,Chakraborty N. Particle Swarm Optimization techniques based short term hydro thermal scheduling Appl. Soft Comput 2008;8(4):1392-9.
8. Amita Mahor, Saroj Rangnekar, "Short term scheduling of cascaded hydroelectric system using novel self adaptive inertia weight Particle Swarm Optimization", International Journal of Electrical Power & Energy system, Volume 34, pp. 1-9,Issue 1st January 2012.
9. James Kannedy, Russell Eberhart, "particle swarm optimization", Proc. IEEE Intelligence Conference Neural Network (ICNN-95), vol. IV, Perth, Australia, pp. 1942-1948, 1995.
10. Yuhui Shi,Russell C. Eberhart, "Empirical study of particle swarm optimization",IEEE, pp. 1945-1950, 1993.
11. Amita Mahor, Saroj Rangnekar, "Short term generation scheduling of cascaded hydroelectric system using time varying acceleration coefficients Particle Swarm Optimization", International Journal of Energy & Environment Volume 1, pp. 769-782,Issue 5, 2010.
12. Guimin Chen,Xinbo Huang,Jianyuan Jia and Zhengfeng Min " Natural exponential inertia weight strategy in particle swarm optimization" 6th World Congress on intelligent Control and automation, June 21-23,2006,Dalian,China.

Global Journal of researches in engineering
Electrical and electronics engineering
Volume 12 Issue 1 Version 1.0 January 2012
Type: Double Blind Peer Reviewed International Research Journal
Publisher: Global Journals Inc. (USA)
Online ISSN: 2249-4596 & Print ISSN: 0975-5861

Location Privacy in Mobile Ad Hoc Network Measuring V2X Location Based Communication Systems with Accumulated Information

By Yatin Chauhan, Prof Jaikaran Singh, Prof Mukesh Tiwari, Dr Anubhuti Khare

Department of Electronics and Communication University

Abstract - Wireless Mobile Ad Hoc Networks are particularly vulnerable due to their fundamental characteristics such as an open medium, dynamic topology, distributed cooperation, Vehicle - to - vehicle / vehicle - to - infrastructure (V2X) communication systems are envisioned to greatly improve road safety, traffic efficiency, and driver convenience. However, many V2X applications rely on continuous and detailed location information, which raises location privacy concerns. A multitude of privacy protection mechanisms have been proposed in recent years. However, few efforts have been made to develop privacy metrics, which can provide a rigorous way to assess the privacy risk, evaluate the effectiveness of a given mechanism, and exploit the full possibilities of protection methods in V2X systems. Therefore, in this paper we present a trip-based location privacy metric for measuring user location privacy in V2X systems. The most distinguishable aspect of the metric is to take into account the accumulated information, which is the privacy-related information acquired by an adversary for an extended period of time, e.g., days or weeks.

Keywords : *Vehicle-to-vehicle/vehicle-to infrastructure (V2X) communication Ad Hoc Networks systems.*

GJRE-F Classification: *FOR Code: 090604*

Strictly as per the compliance and regulations of:

Location Privacy in Mobile Ad Hoc Network Measuring V2X Location Based Communication Systems with Accumulated Information

Yatin Chauhan [α], Prof Jaikaran Singh [σ], Prof Mukesh Tiwari [ρ], Dr Anubhuti Khare [ω]

Abstract - Wireless Mobile Ad Hoc Networks are particularly vulnerable due to their fundamental characteristics such as an open medium, dynamic topology, distributed cooperation, Vehicle - to - vehicle / vehicle - to - infrastructure (V2X) communication systems are envisioned to greatly improve road safety, traffic efficiency, and driver convenience. However, many V2X applications rely on continuous and detailed location information, which raises location privacy concerns. A multitude of privacy protection mechanisms have been proposed in recent years. However, few efforts have been made to develop privacy metrics, which can provide a rigorous way to assess the privacy risk, evaluate the effectiveness of a given mechanism, and exploit the full possibilities of protection methods in V2X systems. Therefore, in this paper we present a trip-based location privacy metric for measuring user location privacy in V2X systems. The most distinguishable aspect of the metric is to take into account the accumulated information, which is the privacy-related information acquired by an adversary for an extended period of time, e.g., days or weeks. We develop methods to model and process the accumulated information, and reflect the impact on the privacy level in the metric. We further prove the viability and correctness of the metric by various case studies. Our simulations find out that under certain conditions, accumulated information can significantly decrease the level of user location privacy. The metric and our findings in this paper give some valuable insights into location privacy, which can contribute to the development of effective privacy-protection mechanisms for the users of V2X systems. and constrained capability. Location information of nodes can be critical in wireless ad hoc networks, especially in those deployed for military purposes. In this paper, we present study of various method of receiver location privacy in mobile adhoc network.

Keywords : Vehicle-to-vehicle/vehicle-to infrastructure (V2X) communication Ad Hoc Networks systems.

I. Introduction

The emerging vehicle-to-vehicle/vehicle-to infrastructure (V2X) communication systems enable a new way of cooperation among vehicles, traffic operators, and service providers. Based on Dedicated Short Range Communications (DSRC) technology, vehicles can communicate among each others and with the entities in the back-end system via Roadside Units (RSU). It is envisioned that V2X communication systems can significantly improve road safety, traffic efficiency, and driver convenience. Example V2X applications include collision warning, floating car data, and location-based services. If deployed, such systems will be one of the biggest realizations of Mobile Ad Hoc Networks (MANET).However, many V2X applications rely on continuous Recent wireless research indicates that wireless Mobile Ad Hoc Networks (MANET) present a larger security problem than conventional wired and wireless networks [1,2]. In the traditional Internet, routers within the central parts of the network are owned by a few well-known operators and are therefore assumed to be somewhat trustworthy. This and detailed location information of the vehicles. Vehicles are personal devices. Locations of a vehicle reveals the movements and activities of its driver and passengers. Sending and disseminating location information of the users of V2X systems has the potential to infringe the users' location privacy. The location privacy issue inV2X communication systems has been identified and amultitude of privacy-protection mechanisms have been proposed in recent years, e.g., in [1]-[4].To evaluate the effectiveness of these mechanisms, a metric for measuring the level of user location privacy is crucial and indispensable. For example, we need a metric which can tell us that the user privacy level has been increased by 20% after applying one of the protection mechanisms. However, so far the main focus on the topic is to devise privacy-protection mechanisms, very few metrics exist for measuring user location privacy in V2X systems in a rigorous way. Hence, the usefulness of privacy-protection mechanisms cannot be strictly evaluated and compared and the trustworthiness of V2X systems cannot be assessed. Furthermore, the range of possible protection methods cannot be fully exploited. In our previous work [5], we introduced a trip-based location privacy metric to measure the level of location privacy of individual users in V2X systems. Based on the observation that the uncertainty of a potential adversary and the user privacy level are indeed two sides of the same coin, the metric measures the level of location privacy as the link ability of location information to the individuals who generate it. The uncertainty in the information is quantified into entropy. Our previous work assumes that the information available to the adversary

Author [α σ ρ] : Department of Electronics and Communication, Sri Satya Sai Institute of Science and Technology,Sehore M.P. India.
E-mails : yatin.dd@gmail.com, jksingh81@yahoo.co.in
Author [ω] : Department of Electronics and Communication University Institute of Technology,RGPV Bhopal M.P. India.

is limited to a short period of time. To stay realistic, it is reasonable to assume that an adversary will do its best to decrease the uncertainty of the obtained information. Therefore, the adversary is likely to take the maximum available information into account. In particular, the adversary will try to utilize the accumulated information, which is privacy-related information acquired by capturing communications from running V2X systems for an extended period of time, e.g., days or weeks. Hence, the assumption of a limited time period is over-simplified from the real world.

To reflect the true underlying privacy value in V2X communication systems, the metric must take into account the impact of accumulated information on privacy level. Intuitively, the more information an adversary has, the more it can draw conclusions with fewer uncertainties. However, the impact of accumulated information on location privacy has not been investigated up to now. In this paper, we address this issue by extending the current location privacy metric to take into account accumulated information. As a result, the metric can more accurately reflect users' privacy value in V2X communication systems. Specifically, in this paper we develop a method to model the accumulated information, design approaches to process, propagate, and utilize the accumulated information, and reflect the effect in the metric, prove the viability and correctness of the metric by means of various case studies. In the following, Section II gives the background information on the basics of the trip-based location privacy metric. Section III describes the method to model the accumulated information. Section IV introduces two approaches to process the accumulated information and reflects it in the metric. Section V evaluates the metric by case studies. Section VI discusses the related work, followed by the conclusion in Section VII

II. Metric Fundamentals

This section gives the necessary background information on the tripbased location privacy metric introduced in [5].In V2X communication systems, each time a vehicle sends a message, it gives out its location information to the system. Although there are different levels of granularities, the location information in V2X systems can be categorized into three types, i.e., single locations, tracks, and trips. Location information only becomes privacy relevant if it can be linked to identifiable individuals. Since for privacy concerns vehicles are very likely to use pseudonyms in communications [6], [7], information on single locations and tracks are less privacy-sensitive than the information on trips, which can be used to infer an individual's identity and activities. The first step to measure privacy is to capture the information on trips and individuals in an arbitrary defined area and time period. Hence the metric virtually takes a "snapshot" of the dynamic V2X systems. he information captured in the snapshot is then modelled in a weighted tripartite graph, shown in Fig.1. The graph contains three distinct sets of vertices,i.e., I , 0 , and D, which represent Individuals, Origins and Destinations of the trips. An adversary's knowledge on the link ability of an individual to a set of trips is expressed in probability distributions. The probabilities are used as the weights on the directed edges. For example, Pjk is a weight on an edge (Vj ,Vk) between the vertices Vj and Vk .

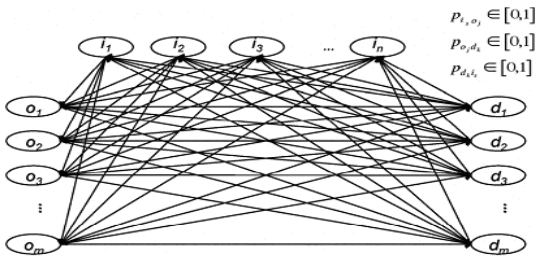

information modelled in weighted tripartite graph

For an individual to make a trip (e.g., 01 -----. d1) , he or she must start from one of the origins, e.g., i 1 from 01 . If the trip from 01 ends at one of the destinations, it must be possible to link i 1 to d1 as well. Due to the uncertainty in the information, there can be many of such possible linkings among the vertices. A closed walk or a cycle starting from a vertex *is* and passing vertices *{oj ,dd* in the graph has the semantics of is 's probability *Pjk* to make a trip with origin *OJ* and destination *dk.* By collecting all cycles connected to a particular individual in the graph, we can extract the probability distribution of the link ability of that individual to a set of trips. The probability distribution can be graphically expressed as a hub-and-spoke structure, shown in Fig. 2. The last spoke with probability*pC* in the clock-wise order denotes the probability of an individual not making any trips, i.e.,"staying at home". assumption no longer holds in an Ad Hoc network, since all nodes entering the network are expected to take part in routing. Also, because the links are usually wireless, any security that was gained because of the difficulty of tapping into the network is lost.

Furthermore, because the topology in such a network can be highly dynamic, traditional routing protocols can no longer be used. Thus, Ad Hoc network has much harder security requirements than the traditional network and the routing in Ad Hoc networks is an especially hard task to accomplish securely, robustly, and efficiently.

In general, the wireless MANET is particularly vulnerable due to its fundamental characteristics of open medium, dynamic topology, absence of central authorities, distributed cooperation, and constrained capability. The existing security solutions for wired networks cannot be applied directly in wireless MANETs.

Applications that make use of ad hoc routing have heterogeneous security requirements. *Authentication*, *message integrity*, and *nonrepudiation* to an ad hoc environment are part of a minimal security policy. Apart from these, there are several other security issues [1, 3] such as *black hole attacks, denial of service*, and *information disclosure*. A location disclosure attack can reveal something about the locations of nodes or the structure of the network. The information gained might reveal as to which other nodes are adjacent to the target, or the physical location of a node. In the end, the attacker knows which nodes are situated on the route to the target node. If the locations of some of the intermediary nodes are known, one can gain information about the location of the target as well. In many cases, the location information might be very crucial. In MANETs installed for tactical/military missions in a hostile and/or unknown territory, these types of attacks have to be prevented. In many cases, the communicating nodes need to be anonymous—no other node in the network should know who is communicating with whom. Initially, we present a solution that achieves complete anonymity and discuss trade-offs between complete anonymity and difficulty in identifying misbehaving nodes.

We then present enhancements to our protocol to prevent these attacks albeit at the cost of complete anonymity The problem we are going to address in this paper is receiver location privacy even while the routing protocol is already supporting identity anonymity. In such a scenario the eavesdropping adversary tries to track the route discovery messages to infer some information about the destination's venue or the route established between source and destination. To realize the importance of location privacy imagine a MANET in a battlefield where the nodes are living soldiers. If the adversary breaks the location privacy of the nodes in such a scenario the existence of the soldiers would be revealed and also their lives Might be in danger The rest of this paper is organized as follows. In section II some related works are reviewed. Section III gives an overview of the ANODR protocol. Section IV describes the adversary model. Section V concludes this paper

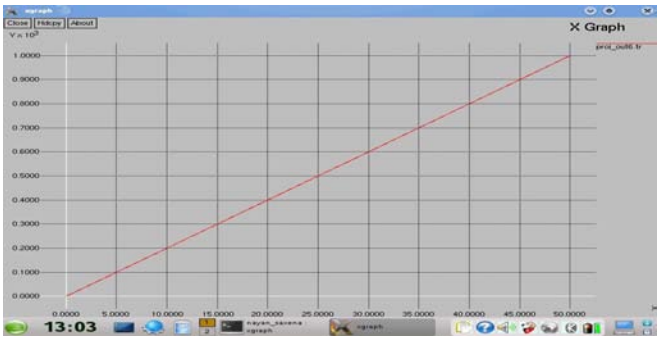

III. Related Work

Chaum's mixnet [8] and DC-net [9] were the origin of many future ideas to address private communication. Mixnet removes the correlation between sources and destinations. A mix node is a network member that performs encryption and padding on its received messages and sends them out in a random order so that it is impossible for outsiders to distinguish which output message belongs to which input message. DC-net [9] is based on binary superposed sending. In DC-net the anonymity set is composed of all potential senders. Each sender shares a secret key at least with one other user. If sender A is wishing to send a message, it should superpose the message with its exchanged secrets. Other users superpose in the same manner (if no message to send they superpose zero with shared keys). All messages are transmitted to the receiver. The sum of these messages is the message of A, because every secret is added twice and canceled. Therefore, the message is delivered without revealing the originator. Another solution proposed for wired networks is Crowds [10]. Crowds consists of a number of network users. Before a data request is sent to the server it is chained randomly through a number of crowds members, so that the server knows that it came from one of the members, but he has no idea about the original sender. The protocols proposed to provide anonymity

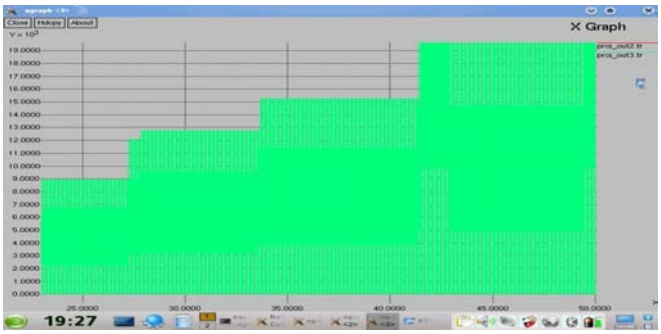

in wired networks assume having a fixed topology and usually having trusted third parties. Such solutions are not suitable for MANETs as well as any other mobile scenario in which the network topology might change all the time. Most of the routing-based anonymous protocols for MANETs try to address the identity anonymity issue, e.g. are static and data is always sent to a powerful sink. One of the first simple ideas to address the destination location privacy in ad hoc routing protocols was not to stop the route request packet flow at the destination node and continue with that for several extra hops to hide the receiver's venue. Also for route location privacy the authors of ARM [7] proposed not to forward the RREP message only on the discovered route which is the case in every other MANET routing protocols, but to form a cloud of routes around the real one. This is done by adding a TTL field to the packets which is used to forward them for a number of hops around the discovered path. The neighbors of the nodes en route who receive the RREP message should broadcast it after replacing some fields

by random numbers and their neighbors would do so till the TTL reaches zero. Therefore the discovered route is covered by some fake flows. Also the data packets will be broadcasted in a limited number of hops around the discovered route for the same purpose. This solution provides *route location privacy* to some level, i.e. makes the adversary uncertain about the real route's location inside the cloud, but can not hide the destination's location which might be of higher importance. We refer to this idea of ARM as *route cloud idea*. Some location privacy solutions for MANETS are proposed for geo-routing scenarios, e.g. [14] addresses destination location privacy for the category of MANETs in which geographic information of the nodes is available.

This protocol uses the location information of the destination node to generate an area including the destination to deliver the data packets to all of the nodes in that. The number of nodes inside the anonymity zone determines the privacy level provided by the protocol. On the other hand, measuring the network anonymity in general is another issue in private communication research area. [15] and [16] have proposed information theory based metrics to quantify privacy. The basic idea is that the privacy degree is maximized when all anonymity set members have the same probability to be the real object of interest.

IV. Overview of the Underlying Routing Protocol

We use the identity free routing protocol, ANODR [5], to evaluate the location privacy ideas of RDIS. We apply our ideas to ANODR as an underlying routing protocol to Provide it with destination location privacy. In fact, it could be possible to apply RDIS techniques to other identity anonymous MANET routing protocols in appropriate ways. ANODR is an ID-free anonymous routing protocol in which each hop on the route is associated with a random route pseudonym. The sender initiates a RREQ packet containing a sequence number, a global trapdoor and an onion. The sender initiates the onion by generating some random nonce as the onion core and encrypting it with its own secret key. The global trapdoor is some well known tag encrypted by the destination node's public key, so it can be opened only by the intended destination. If a node receives a RREQ, it will try to open the trapdoor with its private key. If it succeeds and sees the well known tag it will consider itself as the destination and initiates the RREP message. Otherwise, it adds a self aware layer to the one is a highly motivated passive avesdropper who has the ability to monitor the traffic all over the network, for example by employing several overhearing nodes in different points of the network to cover the whole area. Our goal against this adversary is to prevent it from finding the destination's venue and also the path between communicating pairs. The second attacker considered is an internal adversary, which is a compromised node in the network. The adversary can take control of the compromised node. The private routing protocol should make it impossible for him to break the location privacy of the destination even if it is located on the route. Internal Adversaries should be prevented from finding out if their neighbor nodes are source or destination even if they are on the same route. We suppose that the compromising capability of the adversary is not unlimited onion and encrypts the new onion with its secret key and also attaches a one time public key to the message and rebroadcasts it. The next nodes would do the same and would record the one time public key sent by the previous node which will be used in RREP phase. Eventually if the destination receives the RREQ message it will initiate the RREP message. The nodes on the route from the destination to the sender will directly forward this message to the sender. The RREP message includes the proof of trapdoor opening, *Proofdes*, generated by the destination, which the sender will use to verify if the RREP is initiated by the intended destination. Every node on the route generates a random route pseudonym, *Kseed*, encrypts it by the one time public key of the previous node and replaces that in the appropriate field of the received RREP message. The route seudonym will be used as the shared secret key between every two consecutive nodes en route in data forwarding phase. The onion and the proof of trapdoor opening are encrypted by the route pseudonym to hide them from outsiders. Every intermediate node opens the random route pseudonym with its one time public key and then uses it to extract the onion. Then it strips its own layer from the onion expecting to see what it has encrypted a while ago and modifies that with its route pseudonym and stored one time public key and forwards that to the previous node on the route. Eventually when the sender receives the RREP packet it will open the onion and check for the appropriate proof of successful trapdoor decryption. If the onion data matches the previously generated onion core and the proof of trapdoor decryption is shown, the route discovery is done.

The RREQ and RREP packet formats are as follows:

$$RREQ : < RREQ, seq\#, global\ trap, onion, PK - 1time >$$

$$RREP : < RREP, \{Kseed\}PK-1time, fKseed\ (Proofdes, onion) >$$

Each intermediate node records the correspondence between its own route pseudonym and its upstream node's route pseudonym in its routing table. When a data packet is received, the intermediate node looks up its routing table for the received route seudonym. If it is found, the node would replace the route pseudonym with the next hop's corresponding one and forward the packet. Otherwise, the packet will be discarded. A symmetric key would be piggybacked in

the first global trapdoor from the destination to the sender as the end to end encryption key for next contacts. To avoid public cryptosystem's expenses, this symmetric key will be used for the next RREQ messages from the same sender to the same destination

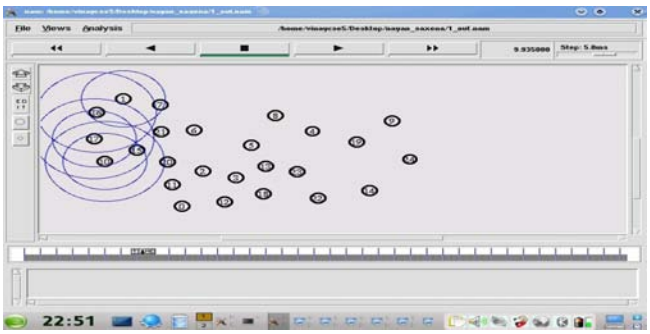

e.g. in case that the route is broken due to node mobility and a new route shall be reestablished [17].

V. Attacker Model

a) Message Type Unification Idea

In ad hoc routing protocols when the intermediate nodes receive the route reply packet, they typically use their keys/secrets stored in RREQ forwarding phase to realize that they are located on the route and they must forward the received reply message. A global eavesdropper can track the RREP message flow to find the discovered route between the source and the destination. Also he is able to discover the physical location of the communicating pair by observing the origins of RREQ/RREP messages. The main contribution of this work is to hide the destinations' location by making it impossible for the adversary to determine the origin of route reply packets. We use the same message type, *RDIS*, for RREQ and RREP packets. The nodes on the route use the keys to check if this is a RREP message intended to them. So when a RDIS-RREP message is forwarded, the nodes out of the route would behave exactly as they do about a RDISRREQ message till the TTL field reaches zero. As we will describe, after a random number of hops the RDIS-RREP packet is changed to a RREP packet as Figure 1 shows. This is because forwarding the reply packet in RDIS-RREP format toward the source causes a high overhead due to two reasons. First, the RDIS-RREP packet will be broadcasted by every node receiving that till $TTL = 0$, and second the size of a RDIS-RREP packet is larger than a normal RREP packet.

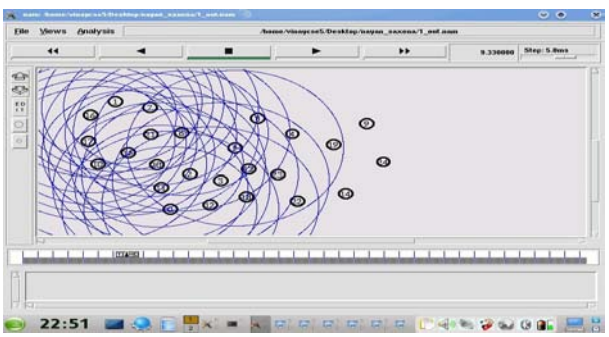

b) Applying RDIS to ANODR

In this section we are going to describe how the ideas of RDIS can be applied to ANODR to provide destination location privacy as well as route privacy. To apply RDIS to ANODR we need to change the appearance of the route request and the route reply messages to the unified one so that the RDIS-RREP flow seems to be part of the RDIS-RREQ flow to any outsider without losing the routing functionalities. For this purpose several properties should be considered. One is the size of RDIS-RREP and RDIS-RREQ packets which should be the same to prevent the outsider to distinguish them. Another one is that the appearance difference from the RDISRREQ packet the destination node receives and the RDISRREP packet it initiates should be similar to the difference between a received RDISRREQ packet received at any other node and the RDIS-RREQ packet broadcasted consequently by it. Therefore the initiation of the RDISRREP message would look like a part of the RDIS-RREQ flow. Also every field of one of these two message types should change with the same pattern as the other one. For example, the sequence number which is a fixed field in RDIS-RREQ should be preserved the same in the corresponding RDIS-RREP flow. As a matter of course we change the content of the message type field in both of them to the same packet type, *RDIS*. When a node receives a *RDIS* packet with a new *seq#*, it will generate a random number between 0 and 1. If the number is less than a fixed parameter *Pf* the node will proceed with the packet, otherwise it will do nothing and therefore discard the packet.If the node decides to proceed with the received packet it will record the *seq#* in its routing table and will proceed with the message to follow the ordinary ANODR behavior (described in section III). When the destination node receives the RDISRREQ message it generates the corresponding RDIS-RREP packet. It decreases the received TTL by one. The RDIS-RREP packet includes a sequence number field filled with the same *seq#* of the corresponding RDISRREQ (in regular ANODR there is no sequence number or TTL in reply packets). The global trapdoor is preserved in RDIS-RREP. We change $Kseed\}PK-1time$ to $\{REPLY,Kseed\}PK-1time$ in the RDISRREP packet. In order to match the size of the RDIS-RREP packets we need to add an additional field in the RDIS-RREQ packets filled with random data. So all in all a RDIS-RREQ packet will look like < *RDIS, TTL, seq#, global trap, onion, PK− 1time, random field* > and a RDIS-RREP packet will look like < *RDIS,TTL, seq#, global trap, REPLY,Kseed}PK−1time, fKseed* (*Proofdes, onion*) > The adversary may distinguish between the RDIS-RREQ and RDIS-RREP messages because he knows that the onion length in RREQ messages increases as the message nears the destination and the onion length in RREP messages decreases as the message gets further from the destination. Therefore the onion length should be fixed. In an improved version of ANODR the length of

the onion is fixed at 128 bit [18].Every node applies its symmetric key encryption on the 128 bit long onion. In RDIS, we use this mechanism to prevent the adversary from using the varying length of the onion to analyze the message type or the distance from the destination. When a node receives a *RDIS* message while it has forwarded another *RDIS* message with the same *seq#* before, it will try to open $\{REPLY,Kseed\}PK-1time$ using its one time public key generated during the RREQ phase. If after such a decryption the node can see the REPLY tag it realizes that this packet is a RDIS-RREP intended to it. Then it will generate a random number between 0 and 1. If this number is greater than a fixed parameter *Pr* it will decrease TTL by one and replace the *Kseed* and the onion with its own (see section III). Otherwise, it will change the RDIS-RREP message to a normal RREP message as shown below, but the TTL field will be preserved to be used for the route cloud idea. So one of the nodes en route randomly will change the RDIS-RREP packet to a normal RREP as follows, which except having the TTL field is the ordinary reply packet format in ANODR: $< RREP, TTL, \{Kseed\}PK-1time, fKseed (Proofdes, onion) >$ Let us assume *Trep* is the maximum time that a source node waits to receive the corresponding RREP after initiating the RREQ. We consider the recorded one time public keys at the nodes as fresh keys during *Trep* seconds after being generated. When a node receives a packet like the above RREP packet and it has a fresh one time public key it will use it to find out if the packet is intended to it (by opening the onion as in ordinary ANODR). If so, the node will modify the reply packet as described in III and will also decrease TTL by a random number among 1,2,3 and 4. Therefore this packet will be forwarded on the discovered route normally till it reaches the destination. When a node that is not located on the discovered route receives such a packet and it realizes that the packet is not intended to it, it will generate a random number among 1,2,3 and 4 and will decrease the TTL by that. It will also replace the next two fields with random bits without changing the packet size and broadcasts the packet. Therefore a cloud of routes will be formed around the route and the discovered route will be hidden among them. This will provide the protocol with route location privacy.

c) Ring route idea in RDIS

As mentioned before, in RDIS instead of a route between the source and destination we form a ring route such that the two communication end nodes are located on that. For this purpose the destination node should respond not only to the first received RREQ message but to the first two of them. Therefore two routes will be formed between the source and the destination. As mentioned above, in RDIS every received RREQ packets are proceeded by every node by some probability. One consequence of this property is that the first discovered route is not necessarily the shortest one and also the first two discovered routes might be quite far from each other (because the intermediate nodes are chosen quite randomly and the two paths are not necessarily the shortest ones). When the source node realizes that two routes are discovered it starts sending data packets to the receiver through the first one. We use the established routes bidirectionally. It is possible because every two neighboring nodes on a route are sharing a link pseudonym pair which are used to forward the data packets over the route. When the destination receives any data packet it forwards it to the first node on the other route and the data packet will be forwarded (in the reverse direction) through that route to reach the source node. Then the source node will discard it. Therefore it is impossible for any eavesdropping adversary to distinguish the destination among the nodes on the ring by tracing the data packets.

VI. Conclusion and Future Work

In this paper we present a trip-based location privacy metric for measuring location privacy of the users of V2X communication systems. To reflect the true underlying privacy values, the metric includes accumulated information and reflects the impact in the privacy measurement. We model the accumulated information and develop approaches to process, propagate, and utilize the accumulated information in the metric. We evaluate the viability and correctness of the metric by various case studies and extensive simulations. Our simulations show that under certain conditions, accumulated information can significantly decrease users' location privacy. is a valuable tool to evaluate and develop privacy- V2X systems. In future work, we will further evaluate our metric with more scenarios and realistic V2X applications. The evaluation will also include existing privacy-protection mechanisms proposed to V2X systems. The current metric only measures privacy of individual users. The possible interrelations among individuals and their impacts on the level of location privacy will be investigated to determine location privacy in a global view. The metric is extensible, which means when it is necessary, we can add other identified attacks on location privacyto the metric in the future.

References References Referencias

1. G. Resta, P. Santi, and J. Simon, “Analysis of multi-hop emergency message propagation in vehicular ad hoc networks,” in *MobiHoc ’07*. New York, NY, USA: ACM, 2007, pp. 140–149.
2. H. W. Y.C. Hu, “A framework for location privacy in wireless networks,in *ACM SIGCOMM Asia Workshop 2005*.
3. Q. He, D. Wu, and P. Khosla, “Quest for personal control over mobile location privacy,” *IEEE Communications Magazine*, vol. 42, 2004.
4. P. Kamat, Y. Zhang, W. Trappe, and C. Ozturk,

"Enhancing sourcelocation privacy in sensor network routing," in *ICDCS '05*, 2005.

5. J. Kong and X. Hong, "Anodr: anonymous on demand routing with untraceable routes for mobile ad-hoc networks," in *MobiHoc '03:Proceedings of the 4th ACM international symposium on Mobile ad hoc networking & computing*, New York, NY, USA, 2003, pp. 291–302.
6. J. Kong, X. Hong, and M. Gerla, "An identity-free and ondemand routing scheme against anonymity threats in mobile ad hoc networks," *IEEE Transactions on Mobile Computing*, vol. 6, no. 8, 2007.
7. S. Seys and B. Preneel, "Arm: Anonymous routing protocol for mobile ad hoc networks," pp. 133–137, 2006.
8. *L. Chaum, "Untraceable electronic mail, return addresses, and digital pseudonyms," Commun. ACM, vol. 24, no. 2, pp. 84–90, 1981.*
9. *Chaum, "The dining cryptographers problem: Unconditional sender and recipient untraceability," Journal of Cryptology, vol. 1, 1988.*
10. M. K. Reiter and A. D. Rubin, "Crowds: anonymity for Web transactions,"*ACM Transactions on Information and System Security*, vol. 1, no. 1, pp. 66–92, 1998.
11. Y. Zhang, W. Liu, and W. Lou, "Anonymous communications in mobile ad hoc networks," in *INFOCOM 2005*, pp. 1940–1951 vol. 3.
12. Hong, J. Kong, and M. Gerla, "Mobility changes anonymity: new passive threats in mobile ad hoc networks: Research articles," *Wirel. Commun. Mob. Comput.*, vol. 6, no. 3, pp. 281–293, 2006.
13. K. Mehta, D. Liu, and M. Wright, "Location privacy in sensor networks against a global avesdropper." in *ICNP*. IEEE, 2007, pp. 314–323.
14. Wu, J. Liu, X. Hong, and E. Bertino, "Anonymous geoforwarding in manets through location cloaking," *IEEE Trans. Parallel Distrib. Syst.*, vol. 19, no. 10, pp. 1297–1309, 2008.
15. C. D´ıaz, S. Seys, J. Claessens, and B. Preneel, "Towards measuring anonymity," in *Privacy Enhancing Technologies*, 2002, pp. 54–68.
16. A. Serjantov and G. Danezis, "Towards an information theoretic metric for anonymity." Springer- Verlag, 2002, pp. 41–53.
17. S. K. Makki, P. Reiher, K. Makki, N. Pissinou, and S. Makki, *Mobile and Wireless Network Security and Privacy*. Springer, 2007.
18. J. Kong, "Anonymous and untraceable communications in mobile wireless networks," Ph.D. dissertation, 2004, chair-Gerla, Mario.
19. S. network Technologies (SNT) Qualnet, *http://www.qualnet.com*.

This page is intentionally left blank

Global Journal of researches in engineering
Electrical and electronics engineering
Volume 12 Issue 1 Version 1.0 January 2012
Type: Double Blind Peer Reviewed International Research Journal
Publisher: Global Journals Inc. (USA)
Online ISSN: 2249-4596 & Print ISSN: 0975-5861

Real Time Implementation of Analysis of Ecg Characteristic Points Using Discrete Wavelets

By Manimegalai.P, Bharathi.P, Dr.K.Thanushkodi
Karunya University, Coimbatore, Tamil Nadu, INDIA

Abstract - Automatic extraction of time plane features is important for cardiac disease diagnosis. ECG signals commonly change their statistical property over time and are highly non- stationary signals. For the analysis of ECG signals wavelet transform is a powerful tool. This paper presents a discrete wavelet transform based system for detection and extraction of P wave, QRS complex, and ST segment. The features like amplitude, frequency, energy are extracted from the Electrocardiogram (ECG) to classify them into normal and arrhythmic. The extracted features are given as input to neural network to classify them into normal and arrhythmic. The algorithm was implemented in MATLAB and the same was implemented in real time using Lab VIEW by acquiring the signal from subjects using BioKit(3-lead ECG).The above wavelet technique provides less computational time and better accuracy for classification, analysis and characterization of normal and abnormal patterns of ECG.

Keywords : P, Qrs, St Segment, Discrete Wavelets, Cardiological Analysis, Artificial Neural Networks, Matlab, Lab View.

GJRE-F Classification: FOR Code: 090609

Real Time Implementation of Analysis of Ecg Characteristic Points Using Discrete Wavelets

Manimegalai.P[α], Bharathi.P[σ], Dr.K.Thanushkodi[ρ]

Abstract - Automatic extraction of time plane features is important for cardiac disease diagnosis. ECG signals commonly change their statistical property over time and are highly non- stationary signals. For the analysis of ECG signals wavelet transform is a powerful tool. This paper presents a discrete wavelet transform based system for detection and extraction of P wave, QRS complex, and ST segment. The features like amplitude, frequency, energy are extracted from the Electrocardiogram (ECG) to classify them into normal and arrhythmic. The extracted features are given as input to neural network to classify them into normal and arrhythmic. The algorithm was implemented in MATLAB and the same was implemented in real time using Lab VIEW by acquiring the signal from subjects using BioKit(3-lead ECG).The above wavelet technique provides less computational time and better accuracy for classification, analysis and characterization of normal and abnormal patterns of ECG.

Keywords : P, Qrs, St Segment, Discrete Wavelets, Cardiological Analysis, Artificial Neural Networks, Matlab, Lab View.

I. Introduction

The ECG is a graphic record of the direction and magnitude of the electrical activity that is generated by depolarization and repolarization of the atria and ventricles.[1] One cardiac cycle in an ECG signal consists of the P-QRS-T waves. To find a heart disease, physicians inspect ECG for the existence of abnormal patterns like irregular beat, inter- atrial block, ST level change, morphologic change, and so on. However, bio-signals being non-stationary signals, the reflection may occur at random in the time-scale (that is, the disease symptoms may not show up all the time, but would manifest at certain irregular intervals during the day). From the practical point of view, for the effective diagnostics, the study of ECG parameters have to be carried out over several hours. The volume of the data being enormous, the study is tedious and time consuming and the possibility of the analyst missing the vital information is high. Hence, computer based analysis and classification of diseases can be very helpful in diagnosis.

A large number of techniques exist in the literature for the automatic detection and classification of ECG beats, P wave features and myocardial ischemia through the identification of ST deviations and P -wave variations in the ECG. These include the use of Time Domain Approaches, Artificial Neural Networks, Principal Component Analysis, Fuzzy and Neuro-Fuzzy Systems etc.

While the use of wavelets for analysis and classification of biomedical signals, including some components of the ECG, are well documented [6, 7]. Wavelets offer an important information-rich parameterization method for data reduction of the ECG time-series [8]. Recently, of the number of techniques proposed to detect these features, our procedure using discrete wavelets proved to be one among the best.

II. Electrocardiogram

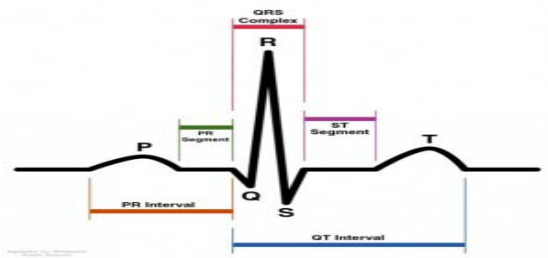

Fig 1 : ECG waveform

An electrocardiogram (ECG) is a graphical record produced by an electrocardiograph, which records the electrical activity of the heart over time. The signal is constructed by measuring electrical potentials between various points of the body using a galvanometer. Understanding the various waves and normal vectors of depolarization and repolarization is very important to obtain useful diagnostic information. ECG signals have a wide array of applications throughout the medical field in determining whether the heart is functioning properly or suffering from any abnormalities. Fig.1 shows an example of a normal ECG trace, which consists of a P wave, a QRS complex and a T wave. The P wave is the electrical signature of the current that causes atrial contraction; the QRS complex corresponds to the current that causes contraction of the left and right ventricles. The T-wave results from the current generated during rapid repolarization of the heart.

a) P-wave features

This is a recording of atrial depolarisation. Most

Author α : Assistant Professor, EIE Department, Karunya University, Coimbatore, Tamil Nadu, INDIA.
E-mail : manimegalai.vairavan@gmail.com
Author σ : PG Scholar, EIE Department, Karunya University, Coimbatore, Tamil Nadu, INDIA. E-mail : bharathibmie@gmail.com
Author ρ : The Director, Akshaya College of Engineering and Technology, Coimbatore, Tamil Nadu, INDIA.

of the time this starts in the sinoatrial (SA) node and the predominant direction of the impulse across the atria is inferiorly and from right to left. This generates a positive deflection in the leads that look at the heart from below. A typical P wave is is 0.06 to 0.10 sec (60 to 100 ms) in duration and is 0.2 mv to 0.3 mv in amplitude. As five of the six chest leads are mostly on the left side of the body and in approximately the same vertical plane there will generally not be much difference in the P-wave in these leads with small positive deflections seen in each. Lead V1 looks across the atria and sees the atrial depolarisation pass across its view. Thus the P-wave typically has a biphasic waveform in this particular lead. Occasionally, if there is damage to the SA node, the initiation of the electrical activity can arise from other parts of the atria. If this is lower down in the atria the impulse has to move in the opposite direction to normal. In these circumstances P-wave deflections are in the opposite direction. The P-wave can be thought to have two components. The first half of the P-wave is made mainly by the right atrium. The second half comes from the left atrium. The best two leads to examine the P-wave are leads II and V1 as they look at the atria in opposite directions. These two leads are typically used as rhythm strips as they emphasis the P-wave. (Lead II looks along the axis of the atria, and V1 looks across the atria.) Disease processes that cause strain on the right atrium cause a typical enlargement of the first half of the P-wave. This gives a taller, peaked P-wave. Lung disease could lead to right atrial strain and thus this tall P-wave is known as P pulmonale. Enlargement of the left atrium causes exaggeration of second part of the P-wave and this leads to the typical bifid "m" shape in lead II, and larger negative deflection in second part of the P-wave in lead V1. This is called P mitrale.

b) QRS Complex

The QRS complex is a structure on the ECG that corresponds to the depolarization of the ventricles. Because the ventricles contain more muscle mass than the atria, the QRS complex is larger than the P wave. In addition, because the His/Purkinje system coordinates the depolarization of the ventricles, the QRS complex tends to look "spiked" rather than rounded due to the increase in conduction velocity. A normal QRS complex is 0.06 to 0.10 sec (60 to 100 ms) in duration. Not every QRS complex contains a Q wave, an R wave, and an S wave. By convention, any combination of these waves can be referred to as QRS complex.

i. *Tachycardia*

Tachycardia typically refers to a heart rate that exceeds the normal range for a resting heart rate. Ventricular tachycardia is a potentially life-threatening cardiac arrhythmia that originates in the ventricles. It is usually a regular, wide complex tachycardia with a rate between 120 and 250 beats per minute. a. Some tachycardias are relatively harmless and need no treatment, but others can be life- threatening [22]. Ventricular tachycardia is a common, and often lethal, complication of a myocardial infarction (heart attack).

ii. *Bradycardia*

A slow rhythm, (less than 60 beats/min), is labeled Bradycardia. This may be caused by a slowed signal from the sinus node (termed sinus Bradycardia), a pause in the normal activity of the sinus node (termed sinus arrest), or by blocking of the electrical impulse on its way from the atria to the ventricles (termed AV block or heart block). Bradycardia may also be present in the normally functioning heart of athletes or other well conditioned persons. Sinus bradycardia is an unusually slow heartbeat where the normal pacemaker is still in control. This commonly occurs in athletes or during a state of deep relaxation. However, the slowing of the heart rate can also be abnormal. [23]

iii. *Bundle branch block*

A bundle branch block refers to a defect of the heart's electrical conduction system. Prompted by the clinical impression that patients with right bundle branch block have a better prognosis than do those with cardiographic evidence of a left bundle lesion. [24]. When a bundle branch or fascicle becomes injured (due to underlying heart disease, myocardial infarction, or cardiac surgery), it may cease to conduct electrical impulses appropriately. This results in altered pathways for ventricular depolarization. Since the electrical impulse can no longer use the preferred pathway across the bundle branch, it may move instead through muscle fibers in a way that both slows the electrical movement and changes the directional propagation of the impulses. As a result, there is a loss of ventricular synchrony, ventricular depolarization is prolonged, and there may be a corresponding drop in cardiac output.

iv. *Ventricular fibrillation*

Ventricular fibrillation occurs in the ventricles (lower chambers) of the heart; it is always a medical emergency. If left untreated, ventricular fibrillation can lead to death within minutes. When a heart goes into V-fib, effective pumping of the blood stops. V-fib is considered a form of cardiac arrest, and an individual suffering from it will not survive unless cardiopulmonary resuscitation (CPR) and defibrillation are provided immediately. Ventricular Fibrillation (VF) and Ventricular Tachycardia (VT) are life-threatening cardiac arrhythmias generally observed in adults with coronary artery disease[21].

c) ST-SEGMENT

The ST segment represents the time between the ventricular depolarisation and the repolarisation. The ST segment begins at the end of the QRS complex (called J point) and ends at the beginning of the T wave. Normally, the ST segment measures 0.12 second or less. The precise end of depolarisation (S) is difficult to determine as some of the ventricular cells are beginning to repolarise. Abnormalities of the ST segment may

consist of either abnormal straightening, depression, or elevation. ST segment changes can be caused by serious impairments such as hypertension or coronary artery disease.

i. *Myocardial Ischemia*

Heart disease is the one of the leading causes of death all over the world with Myocardial Ischemia and Infarction (collectively called Coronary Heart Disease or CHD) being the most common among these cardiac disorders. Myocardial Ischemia and Infarction stem from the insufficient supply of blood to the heart muscle (myocardium) due to blockages in the coronary artery, which is responsible for providing blood to the heart. The development of plaque within the coronary artery that blocks more than 7000 of the lumen of the vessel can cause symptoms of Myocardial Ischemia, such as decreased exercise tolerance and exertional angina to appear. At times this may be the first instance where the subject begins to experience effects of the suboptimal operation of the heart due to decreased blood supply. As large areas of the heart muscle become ischemic, its relaxation and contraction patterns are affected which causes variations in the ST-level and T-wave in the Electrocardiogram (ECG) due to the development of an injury current [10] between the ischemic and non-ischemic regions of the heart. If the blood supply to the heart muscle is restored, Myocardial Ischemia can be reversed thus making the early and correct diagnosis of Myocardial Ischemia an imperative task. Myocardial Infarction, however, is not reversible and represents the death of heart muscle due to prolonged lack of blood supply to the heart.

III. Wavelet Transform

Wavelets are a powerful tool for the representation and analysis of such physiologic waveforms because a wavelet has finite duration (compact support) as contrasted with Fourier methods based on sinusoids of infinite duration. It is possible to analyse any signal by using an alternative approach called the multi resolution analysis (MRA). MRA, as implied by its name, analyses the signal at different frequencies with different resolutions. Every spectral component is not resolved equally as was the case in the STFT. MRA is designed to give good time resolution and poor frequency resolution at high frequencies and good frequency resolution and poor time resolution at low frequencies. The Wavelet analysis does this by using a windowing technique with variable-sized regions. Discrete wavelet transform (DWT) is obtained simply by passing a discrete signal through a filter bank.

Wavelet theory can be understood and developed only by using such digital filters[4]. This is the meeting point between wavelets and sub band coding and the origin of two different nomenclatures for the same concepts. In fact, wavelet transform and sub band coding are so closely connected that both terms are often used interchangeably. Filter banks are structures that allow a signal to be decomposed into sub signals through digital filters, typically at lower sampling figure 2 shows a two-band filter bank.

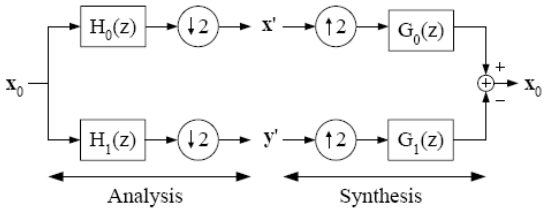

Fig 2 : One-level two band perfect reconstruction filter bank.

The DWT analyses the signal at different resolution (hence, multiresolution) through the decomposition of the signal into several successive frequency bands. The DWT utilizes two set of functions ø(t) and Ψ(t), each associated with the low pass and the high pass filters respectively [11].These functions have a property that they can be obtained as the weighted sum of the scaled (Dilated) and shifted version of the scaling function itself:

$$\phi(t) = \sum_n h[n]\phi(2t - n) \quad (1)$$

$$\psi(t) = \sum_n g[n]\phi(2t - n) \quad (2)$$

Here, h[n] and g[n] are the half band low pass filter and high pass filter respectively.

IV. Methodology

The block diagram shown below are the steps to detect and extract the P, QRS, ST segment .The individual steps are described separately in the following topics.

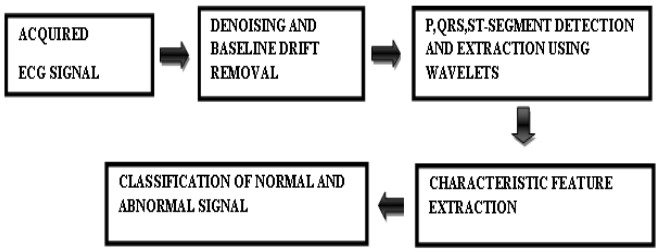

Fig 3 : Block Diagram of ECG characteristic points extraction

a) Denoising And Baseline Drift Removal

The ECG signal is acquired using Biokit physiograph and abnormal data are collected from www.physionet.org. Pre-processing of ECG signals helps us to remove unwanted components in ECG comprises of Power line interference, Electrode pop or

contact noise, Patient–electrode motion artifacts, Electromyographic (EMG) noise, Baseline wandering.

Among these noises, the power line interference and the baseline wandering are most significant and can strongly affect ECG signal analysis. The power line interference is a narrow-band noise centered at 60 Hz (or 50 Hz) with a bandwidth of less than 1 Hz. Usually the ECG signal acquisition hardware can remove the power line interference. However the baseline wandering and other wideband noises are not easy to be suppressed by hardware equipments. Instead, the software scheme is more powerful and feasible for offline ECG signal processing. Digital filtering methods as well as wavelet based methods are used to remove baseline wandering and the other wideband noise.

Pre-processing is done by three different methodologies. To facilitate P wave extraction the baseline drift is removed using a 4th order low-pass Butterworth filter with a 3 dB cut-off at 0.05 Hz. To aid QRS complex extraction, the baseline wandering and the above noises are removed by taking two approximation level coefficients such as A4 and A10 of Daubechies wavelet. Because of increasing the levels of decomposition the baseline wander gets corrected automatically. Moving Average Algorithm is used to remove the baseline drift and discrete wavelets are used to remove the noises for ST segment detection.

b) P Wave Extraction

P-wave extraction or isolation can be performed by various methods like Emperical Mode Decomposition (EMD), Fast Fourier Transform, Dyadic Transform, Application of time window or a moving average filter etc. Here P wave extraction, was performed by using Daubechies wavelets.

c) QRS Complex Extraction

i. *R peak detection*

Peaks of the R waves in signals from the MLII lead have the largest amplitudes among other leads. In order to detect the peaks, specific details of the signal were selected. Details 2^3 – 2^5 were kept and all the details were removed. This procedure removes low frequencies and high frequencies. The attained signal samples were then squared. High amplitude transitions of the signal were then more noticeable, even if R peaks are deformed. Then a practically lower limit is applied on the signal to remove unrelated noisy peaks. Since no subsequent beats will occur in less than 0.25 second, pseudo-beats are also removed. Detection of R peaks is very important because they define the cardiac beats. Heart rate is the important parameter that is detected for analyzing the abnormality in the heart. Heart rate is calculated based on R-R interval.

ii. *QRS complex extraction*

For QRS complex extraction the denoised ECG signal is decomposed into 6 levels by using DWT and the approximation (A4 and A6) coefficients are reconstructed separately. By subtracting A6 from the A4, QRS complex is extracted.

d) St-Segment Detection By Fft Approach

An FFT computes the DFT and produces exactly the same result as evaluating the DFT definition directly; the only difference is that an FFT is much faster. The DFT is defined by the formula. [12][13]

$$X_k = \sum_{n=0}^{N-1} x_n e^{-\frac{2\pi i}{N} kn} \qquad k = 0, \ldots, N-1 \qquad (1)$$

And the FFT is given by-

$$X(k) = \sum_{j=1}^{N} x(j)\omega_N^{(j-1)(k-1)} \qquad (2)$$

Inverse discrete Fourier transform (IDFT) is given by

$$x_n = \frac{1}{N} \sum_{k=0}^{N-1} X_k e^{\frac{2\pi i}{N} kn} \qquad n = 0, \ldots, N-1. \qquad (3)$$

Where as the IFFT can be formulated as-

$$x(j) = (1/N) \sum_{k=1}^{N} X(k)\omega_N^{-(j-1)(k-1)} \qquad (4)$$

Fast Fourier transform (FFT) is speed-up technique for calculating discrete Fourier transform where DFT, which in turn is discrete version of continuous Fourier transform, which indeed is origin for all its versions. So, historically continuous form of the transform was discovered, then discrete form was created for sampled signals and then algorithm for fast calculation of discrete version was invented.

ALGORITHM

1) As one can see the ECG is uneven. Thus our first step is to straighten it. The idea is to apply direct fast Fourier transform (FFT), remove low frequencies
2) Restore ECG with the help of inverse FFT (IFFT).
3) Our third step is to find local maxima. To do that we use windowed filter that “sees” only maximum in his window and ignores all other values. On this step we use window of default size.
4) Now we should remove small values and preserve significant ones. Here we are using a threshold filter.
5) In this case the result is good but in general case we cannot be sure we have all the peaks. So the next step is to adjust filter window size and repeat filtering. (All peaks of the signal detected)
6) Find all the peaks (R-peaks) values.
7) Create two temporary matrixes according to length of the input sequences.

8) Move the two matrixes (naming i.e. current and next) from the peak value towards down and compare the current and next matrixes value. It should decreases from top to bottom.
9) When these two values became equal or started increasing; at that point we will get the S or J point.
10) The same process can be repeated for T onset point detection or considering the sampling rate of the signal we can get T onset by adding sample value from S/J point (here we can get T-onset by adding 150 samples).

This technique is called as falling edge method and a small demerit of this method is that here we have to consider S and j point as same. As our main motto is to find out Ischemia, so this method can be useful because in most of the cases; as the S and J point is same in Ischemic condition. This method can also be implemented for other ECG signals like (ST Segment starting from J point) and we can analyses the problems with accuracy. [14]

i. *Wavelet Compression*

Instead of submitting the ST segments directly to the classification phase, they were pre-processed to reduce the number of classifier parameters. Pre-processing was performed by using biorthogonal wavelets, bior1.1 and bior2.2, with decomposition levels from 1 to 3.

In many filtering applications we need filters with symmetrical coefficients to achieve linear phase. None of the orthogonal wavelet systems except Haar are having symmetrical coefficients. But Haar is too adequate for many practical applications. Biorthogonal wavelet systems can be designed to have this property. This is our motivation for designing such wavelet system. But the price is that non-zero coefficients in analysis filters and synthesis filters are not same. In orthogonal wavelet system, Ø(t) is orthogonal to Ψ(t) and its translates. In biorthogonal system our requirement is that Ø(t) be orthogonal to Ψ'(t) and its translates.

e) Characteristic Feature Extraction And Classification

To classify the abnormalities of the P wave, QRS complex, ST segment some features are extracted. Some of the features like amplitude, frequency, energy, Heart rate are extracted. These are given to the neural network classifier for the classification. The abnormalities like atrial block, Tachycardia and Bradycardia, Bundle block, ventricular fibrillation, ischemia can be detected.

V. Results

The algorithm for P wave extraction, R peak detection, QRS complex extraction, ST segment detection of ECG signal is implemented using MATLAB and LabVIEW. The wavelet analysis helps to find all the intervals in the ECG signal, which helps in detecting various cardiac abnormalities.

a) Matlab Simulation Results

i. *Baseline Drift Removal And Noise Cancellation*

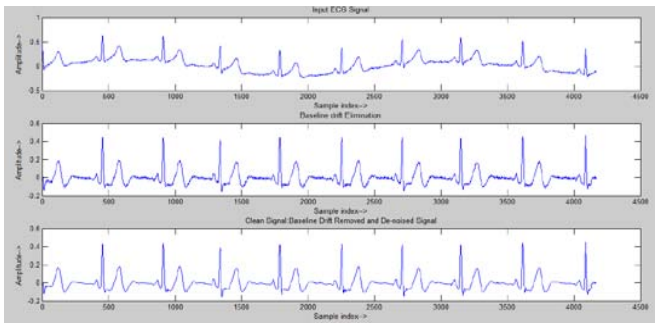

Fig 4 : Performing Baseline Drift removal and Noise cancellation.

ii. *P Wave Extraction*

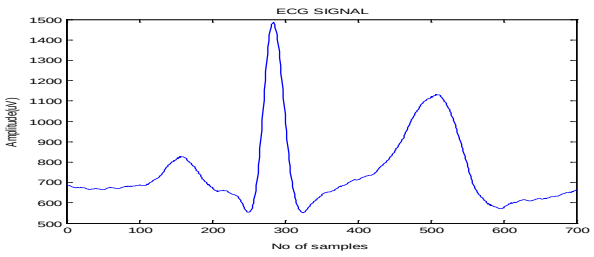

Fig 5 : A single ECG signal

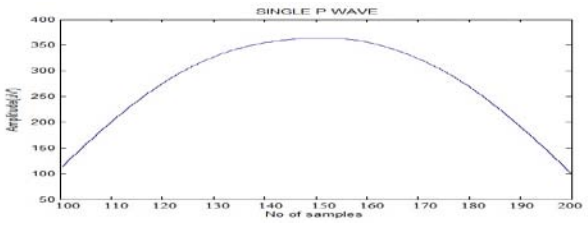

Fig 6 : Isolated P wave

iii. *Qrs Complex Extraction*

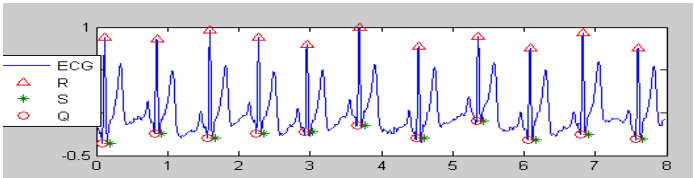

Fig 7 : QRS detected signal

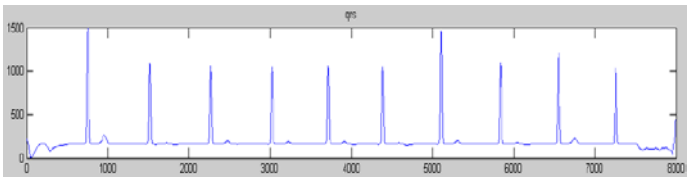

Fig 8 : Extracted QRS complex

iv. *St-Segment Detection*

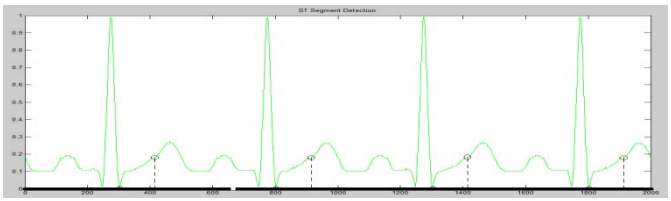

Fig 9 : ST Segment Detection of Standard or Normal ECG Signal

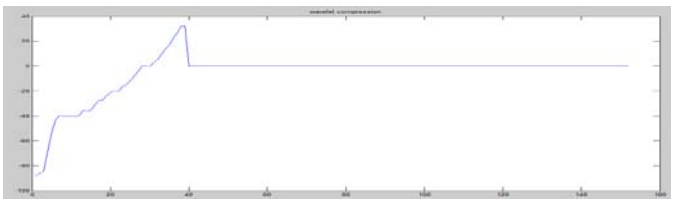

Fig10 : Level-2 Wavelet Decomposed ST-Segment of Normal ECG signal.

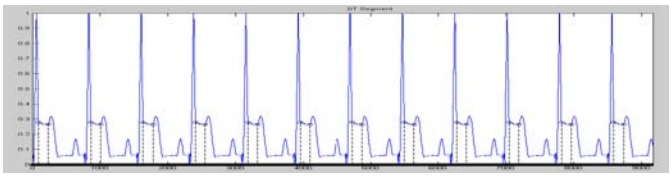

Fig 11 : ST- Elevated Segment Detection (J-point & T-onset point)

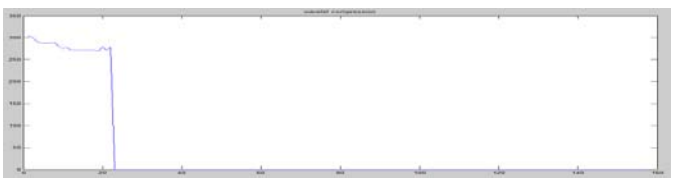

Fig 12 : Level-3 Wavelet Decomposed ST-Elevated Segment.

b) Labview Simulation Results

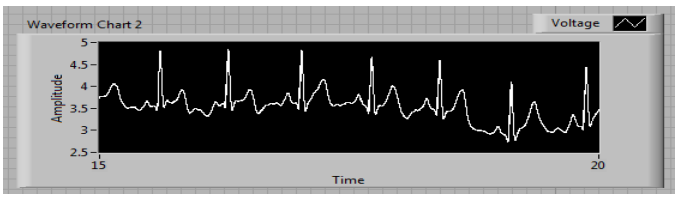

Fig 13 : ECG signal acquired from Biokit using DAQ

Fig 14 : ECG signal after baseline correction and noise removal

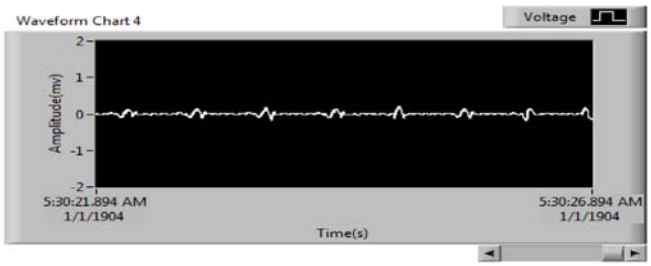

Fig 15 : ECG signal with P waves

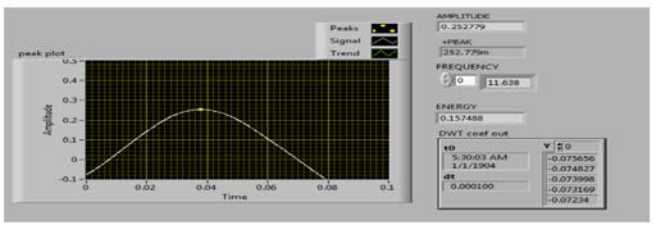

Fig 16 : Isolated P wave and its characteristics

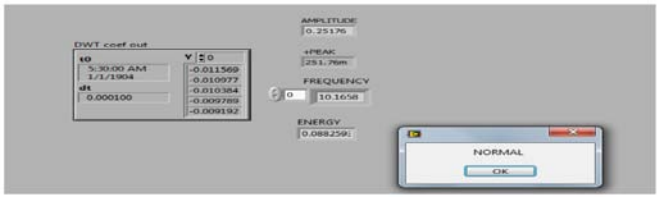

Fig17 : Classification of the signal as normal using neural netwoks

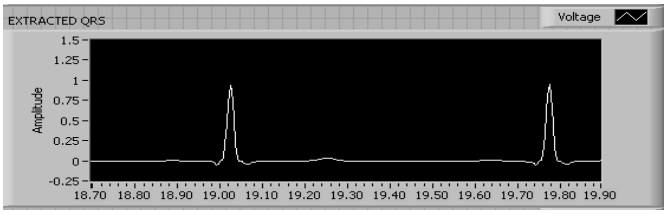

Fig 18 : Extracted QRS complex

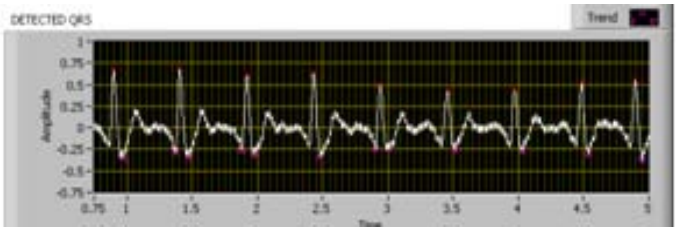

Fig 19 : QRS complex detection in Tachycardia signal

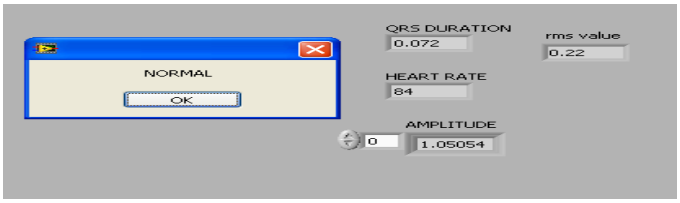

Fig 20 : BPN classification- Normal signal

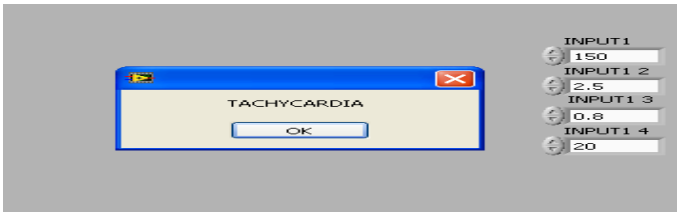

Fig 21 : BPN classification -Tachycardia signal

VI. Conclusion and Future Enhancement

In this paper, we have proposed an algorithm based on discrete wavelet transform for the extraction of P wave, QRS complex, ST segment. T wave extraction and analysis is currently under our research.The above wavelet technique provides less computational time and better accuracy for classification, analysis and characterization of normal and abnormal patterns of ECG. The automatic feature extraction and classification was implemented using MATLAB and Lab VIEW. So this feature extraction method can be used as a primary measurement tool for automatic and on line disease classification. But some of the ECG waveform may show very erratic nature due to electrode contact noise or some complicated cardiac abnormalities. The algorithm is not tested with them because of lack of availability of that special kind of database.

References References Referencias

1. Brendan P. Phibbs, Advanced Ecg : Boards and beyond, Saunders Elsevier, 2006.
2. C.S.Burrus, R.A.Gopinath, H.Guo,(1997) Introduction to Wavelets and Wavelet Transforms", a Primer, Prentice Hall Inc. 46.
3. Z. Dokur, T. Ölmez, E. Yazgan, "Comparison Of Discrete Wavelet and Fourier Transforms for Ecg Beat Classification",Electronics Letters 35 (18) (1999) 1502–1503.
4. P.S. Addison, "Wavelet Transforms and the Ecg": a review, Physiological Measurement 26 (2005) R155–R19.
5. K. Vajarian, R. Splinter, "Biomedical signal and Image processing", CRC Press, Boca Raton, FL, 2006 (chapters 6, 9.)
6. *Saritha, V. Sukanya, Y. Narasimha Murthy, "Ecg Signal Analysis Using Wavelet Transforms" Bulg. J.hys. 35 (2008) 68–77.*
7. S. Z. Mahmoodabadi, A. Ahmadian, M. D. Abolhasani Ecg Feature Extraction using Daubechies Wavelets, Proceedings of the fifth IASTED International conference, Visulalization, imaging and image processing September 7-9,2005,Benidorm,Spain.
8. K. Sternickel, "Automatic Pattern Recognition in Ecg Time Series", Computer Methods and Programs in Biomedicine 68, pp109–115, (2002).
9. Ariyarajah, K. Mercado, S. Apiyasawat, P.Puri, D.H. Spodick, "Correlation of Left Atrial Size with P-Wave Duration In Interatrial Block", Chest 28 (4) (2005) 2615–261.
10. Gettes, L.S., and Cascio, W.E., "Effect of Acute Ischemia on Cardiac Electrophysiology" in The Heart and cardiovascular System, HA Fozzard et al (Edts), Raven Press, vol.2, pp. 2021-2054, 1991.
11. Mohammad Ali Tinati and BehzadMozaffary, "A Wavelet Packets approach to Electrocardiograph Baseline Drift Cancellation", Communication Department, Faculty of Electrical and Computer Engineering, University of Tabriz, Tabriz 51666-16471, Iran.
12. Duhamel, P. and M. Vetterli, "Fast Fourier Transforms: A Tutorial Review and a State of the Art," Signal Processing, Vol. 19, April 1990, pp. 259-299.
13. Frigo, M. and S. G. Johnson, "FFTW: An Adaptive Software Architecture for the FFT,"Proceedings of the International Conference on Acoustics, Speech, and Signal Processing, Vol. 3, 1998, pp. 1381-1384.
14. Hangzhou,,"Heart Rate Variability Analysis of Ischemic and Heart Rate Related ST-Segment Deviation Episodes based on Time-Frequency

Method", Proceedings of NFSI & ICFBI 2007, China, October 12-14, 2007.
15. S.Sumathi1, Dr.M.Y. Sanavullah2, "Comparative Study of QRS Complex Detection in Ecg based on Discrete Wavelet Transform",1 V.M.K.V. Engineering College, Salem, International Journal of Recent Trends in Engineering, Vol 2, No. 5, November 2009
16. L. Pasti[a], B. Walczak[1, a], D. L. Massart[a, *] and P. Reschiglian[b], "Optimization of Signal Denoising in Discrete Wavelet Transform", Science direct, June 1999.
17. A.E. Cetin, A.H. Tewfik, Y. Yardimci, "Coding of Ecg Signals by Wavelet Transform Extrema", IEEE, 0-7803-2127-8/94, pp 544-547, Aug, 1994.
18. P. de Chazal', B. G. Celler' and R. B. Reilly, "Using Wavelet Coefficient for the Classification of the Electrocardiogram", Proceedings of the 22"d Annual EMBS International Conference, July 23-28, 2000 Chicago IL.
19. Mehmet Engin, "Ecg Beat Classification using Neuro-Fuzzy Network, Pattern Recognition Letters, 25, 2004,pp. 1715–172.
20. P.S. Addison, J.N. Watson, G.R. Clegg, M. Holzer, G. Sterz, C.E.Robertson, "Evaluating Arrhythmias in ECG Signals using Wavelet Transforms", IEEE Engineering in Medicine and Biology,pp 104-109, Sept/Oct, 2000.
21. Emran M Abu Anas, Soo Y Lee, Md K Hasan,"Sequential algorithm for life threatening cardiac pathologies detection based on mean signal strength and EMD functions", Anas et al. BioMedical Engineering OnLine 2010.
22. L. Holly, MD," Rapid Heart Beat or Tachycardia James", Your Life Your Health The Examiner January 22, 2009.
23. "Bradycardia(Slow Heart Rhythm)", Arrhythmia Alliance, www.heartrhythmcharity.org.uk, 2010.
24. George A. Perera, Samuel A. Levine, and Herman Erlanger, "Prognosis of Right Bundle Branch Block: A Study of 104 Cases", From the Medical Clinic of the Peter Bent Brigham Hospital, U.S.A. Received December 29, 1941.

This page is intentionally left blank

Global Journal of researches in engineering
Electrical and electronics engineering
Volume 12 Issue 1 Version 1.0 January 2012
Type: Double Blind Peer Reviewed International Research Journal
Publisher: Global Journals Inc. (USA)
Online ISSN: 2249-4596 & Print ISSN: 0975-5861

High speed low power out put Buffer amplifier for large -size LCD applications

By Niraj Kumar, Prof Mukesh Tiwari, Prof Jaikaran Singh
Sri Satya Sai Institute of Science and Technology

Abstract - The present paper Performance improvement in high speed low power out put Buffer amplifier for large –LCD applications The proposed buffer achieves high-speed driving performance while drawing a low quiescent current during static operation. The circuit offers enhanced slewing capabilities with limited power consumption by exploiting a slew detector which monitors the output voltage of the input differential amplifier and outputs an additional current signal providing slew-rate enhancement at the output stage. Post-layout simulations show that the proposed buffer can drive a 1000pF column line load with 8.5-V/**µ**s slew-rate and 0.6-**µ**s settling time, while drawing only 8-**µ**A static current from a 1.2 - V power supply

Keywords : *LCD driver, source driver, buffer amplifier.*

GJRE-F Classification: *FOR Code: 090605*

HIGH SPEED LOW POWER OUT PUT BUFFER AMPLIFIER FOR LARGE -SIZE LCD APPLICATIONS

Strictly as per the compliance and regulations of:

High speed low power out put Buffer amplifier for large -size LCD applications

Niraj Kumar [α], Prof Mukesh Tiwari [σ], Prof Jaikaran Singh [ρ]

Abstract - The present paper Performance improvement in high speed low power out put Buffer amplifier for large –LCD applications The proposed buffer achieves high-speed driving performance while drawing a low quiescent current during static operation. The circuit offers enhanced slewing capabilities with limited power consumption by exploiting a slew detector which monitors the output voltage of the input differential amplifier and outputs an additional current signal providing slew-rate enhancement at the output stage. Post-layout simulations show that the proposed buffer can drive a 1000pF column line load with 8.5-V/μs slew-rate and 0.6-μs settling time, while drawing only 8-μA static current from a 1.2 -V power supply.

Index Terms : *LCD driver, source driver, buffer amplifier,*

I. Introduction

As the display resolution increases, the load capacitance of buffer amplifier increases, whereas the required settling time decreases. Beside that, large number of buffer amplifiers built into a single chip creates power dissipation problem. Consequently, a high driving capability buffer amplifier with low static power consumption is indispensable [1]. In order that the TFT-LCD displays beyond 512 gray levels each color, each gray level is required to be less than 6.4 mV for a 1.2.V full scale. Therefore, the output buffer must have an offset voltage less than ±3.2 mV [2].There are many works on LCD drivers [1-4]. As reported in [1], [3-5], the static power consumption of a folded-cascode amplifier is larger than that of a telescope-cascode one for more current summing circuits and tail current. Also the maximum efficiency of a folded-cascode amplifier is less than 50 percent [6], and thus has poor driving capability. The offset voltages of the folded-cascode operational amplifiers described in [1], [4], are 10 mV and 12.2 mV, respectively. These reported offset voltages are too high that will create incorrect activation for gray level above 512. As mentioned in [1], [7], a buffer with complementary differential pair is able to deliver larger current and thus have better driving capability. In order to achieve higher driving capability with low static power and low offset voltage, we design a newly developed telescope-cascode based buffer amplifier with complementary differential input stage for low power and high resolution applications. Low offset voltage and high driving capability are attained further by a designed pair of auxiliarydrivingtransistors

Author [α σ ρ]: Department of Electronics and Communication, Sri Satya Sai Institute of Science and Technology, Sehore M.P. India.
E-mails : nknirajkumar4@gmail.com, jksingh81@yahoo.co.in, mukeshtiwari_79@yahoo.co.in

II. Circuit and Operation

The designed buffer amplifier with two complementary differential input amplifiers is shown in Fig.1. The circuit was formed by a common-source push-pull stage, The open-loop amplifier transfer function, , can be derived by interrupting the feedback loop in Assuming and yields, in the most general case, the following expression:

$$A_V(s) = A_0 \frac{\left(1+\frac{s}{\omega_Z}\right)}{\left(1+\frac{s}{\omega_{P1}}\right)\left(1+\frac{s}{\omega_{P2}}\right)\left(1+\frac{s}{\omega_{P3}}\right)}$$

where A0 is the DC open-loop gain expressed by

$$A_0 = g_{m1}R_{o1}g_{m2}R_{o2}$$

while, ω_{P1}, ω_{P2} and ω_{P3} are the frequencies of the three amplifier real poles, which are, respectively, given by

$$\omega_{P1} = \frac{1}{(R_{o2}+R_C)C_L} \approx \frac{1}{R_{o2}C_L}$$
$$\omega_{P2} = \frac{1}{R_{o1}C_{o1}}$$
$$\omega_{P3} = \frac{1}{(R_{o2}||R_C)C_{o3}} \approx \frac{1}{R_C C_{o3}}$$

And ω_Z is the frequency of the left-half plane zero introduced by the compensation resistor R_C, which is given by

$$\omega_Z = \frac{1}{R_C C_L}.$$

simulations are also performed to estimate the amplifier offset voltage for different common-mode input voltages. A mean value of 1.2 mV and a maximum value of 5.6 mVare found, with a standard deviation lower than 800 nV.To further demonstrate the effectiveness of the

present out put buffer, and provide a performance comparison other previously adopted solutions, a numeric figure of merit is here introduced for the first time, relying on the main performance parameters of an LCD output buffer. Its basic definition is

$$FOM = \frac{C_L}{T_S \cdot I_{DD}}$$

Mn and Mp, which offers good swing characteristics. In order to increase the driving capability, a pair of auxiliary driving transistors, MAp and MAn, are introduced and controlled by two comparators, nCMP and pCMP. The added comparators are merged with the original differential amplifiers to further reduce the power dissipation. Fig. 1 shows the detailed circuit of the buffer amplifier. In that, transistors and form the complementary telescope-cascode differentialstages. The inputs of these stages are connected in parallel. Each of them drives one half of the common-source push-pull stage, In the figure, forms the biasing current source, while and are two sets of comparators and is the auxiliary driving transistor. amplifiers without and with auxiliary driving transistors, loading with a 1000pF capacitor. It can be observed in the figure that the charging capability is greatly improved for the latter one. For the settling times being defined as the time required for the output signal reaching within 0.2% of the final voltage, the simulated settling times shown in Fig. for the rising edges of curves A and B, represented for the cases without and with auxiliary driving transistors, are 3.1μs and 0.4 μs, Defining R8A(B) and R9A(B) as the channel resistances of the output transistor and the auxiliary driving transistor respectively, the output response of the rising edge can be expressed where VI and VF are the initial and final values of the output voltage, respectively, and

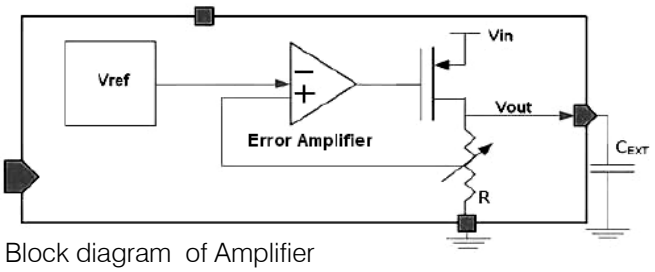

Block diagram of Amplifier

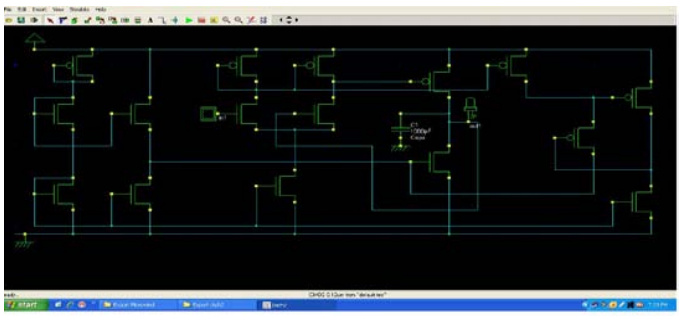

Circuit Diagram of (Fig.) Buffer Amplifier

where CL is the load capacitance of the buffer amplifier. The positive slew-rate can then be expressed as Transistors and of the input differential pair are active when Vin reaches the center of the supply voltage. Their biasing currents and VB. We choose longer length for transistor to reduce the channel length modulation and to the systematic offset. For the input differential amplifier, the W/L of is chosen the same value as that of but the aspect ratio of is designed smaller than that of while transistors and are designed to have the same sizes. The currents of and can be expressed as From the above equations, it can be observed that the slew From the above equations, it can

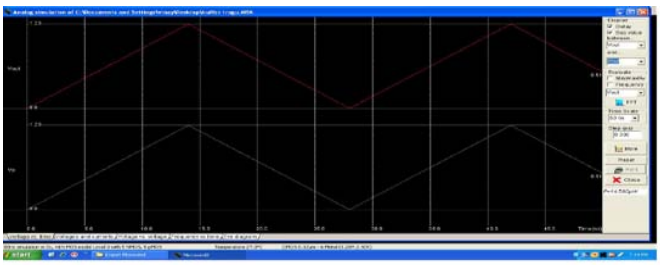

be observed that the slew rate can be increased by reducing τp, i.e., reducing the channel resistances of the output stage, R8B and R9B, if load capacitance is constant. In a similar way, we can increase the negative slew-rate by reducing the

Output Triangular Wave Buffer Amplifier Buffer

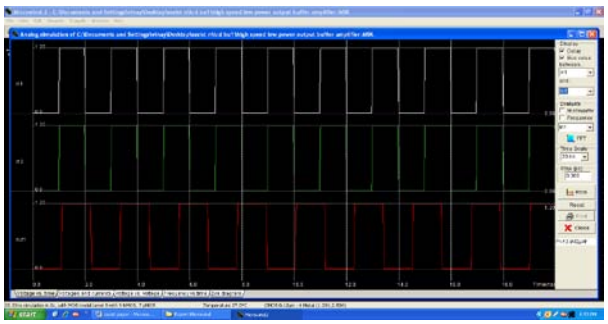

Output Square Wave Buffer Amplifier

channel resistances of R8A and R9A Fig. 2 shows the simulated slew rates versus load capacitances (500 pF-5 nF) with 3 V output voltage. Simulated result shows a possible slew rate higher than 18 V/µs for load capacitance less than 1000pF. The simulated offset voltages versus input circuit diagram of (fig2) the proposed buffer amplifier.

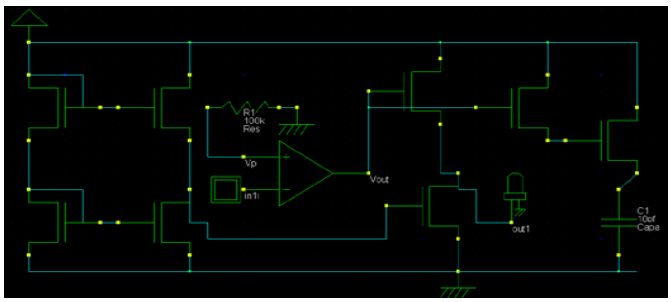

Circuit Diagram of (Fig.) Buffer Amplifier.

III. Experimental Results

The proposed output buffer amplifier was fabricated using the TSMC 0.6μm CMOS process. Several measurements have been done. The measured static current of the output buffer is 1 μA from a 1.2 V supply voltage. The maximum offset voltage is 2.5 mV, and the slew rate is higher than 18 V/μs for1000pF load capacitance. Fig. shows the measured result of the proposed buffer amplifier under a 50 KHz step input waveform with a 1.2 V amplitude and 1000pF load capacitance. shows the measured and simulated settling times for various load capacitances with 1.2 V voltage swing. It is worth mentioned that the settling time is only 1.62 μs even the load capacitance is up to 1000 pF. The die photograph is shown in since the designed circuit is rather neat, the size of the buffer amplifier is only The performance of the proposed buffer amplifier is summarized and compared with the other reported circuits in Table I. It can be observed from the table that the proposed buffer amplifier has a superior performance than that of the other circuits on slew rate, settling time, offset voltage, and static current

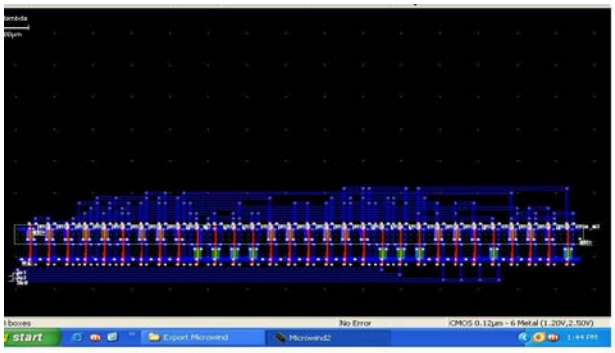

Fig : Die Photograph of the Designed Buffer Amplifier

IV. Conclusion

In this paper, we have designed and demonstrated a high driving capability CMOS buffer amplifier with low static power, and low offset voltage, which is suitable for the source drivers of high resolution LCD with gray levels above 512. The well designed telescope-cascode based buffer amplifier consumes only 1 μA static current and achieves 18 V/μs slew rate for 1000 pF load capacitance. Thus, the buffer amplifier is quite promising for high resolution flat-panel displays that require low static power, high driving capability and high accuracy Buffer amplifier for large -size LCD applications

References References Referencias

1. S.K. Kim, Y.-S. Son, and G.H. Cho, "Low-power high-slew-rate CMOS buffer amplifier for flat panel display drivers," Electron. Lett., vol. 42, no.4, 2006, pp. 214-215.
2. P.-C. Yu, and J.-C. Wu, "A class-B output buffer for flat-panel-display column driver," IEEE J. Solid-State Circuits, vol. 34, no. 1, 1999, pp.116–119.
3. C.-W. Lu, and K.-J. Hsu, "A high-speed low-power rail-to-rail column driver for AMLCD application," IEEE J. of Solid-State Circuits, vol. 39, no. 9, 2004, pp. 1313-1320.
4. C.-W. Lu, "High-speed driving scheme and compact high-speed low-power rail-to-rail class-B buffer amplifier for LCD applications," IEEE J. of Solid-State Circuits, vol. 39, no. 11, 2004, pp. 1938-1947.
5. Behzad Razavi, Design of Analog CMOS Integrated Circuits McGraw-Hill, NY, USA, 2001G.
6. Nicollini, F. Moretti, and M. Conti, "High-frequency fully differential filter using operational amplifiers without common-mode feedback," IEEE J. of Solid-State Circuits, vol. 24, no. 3, 1989,pp. 803-813.
7. J.M. Carrillo, R.G. Carvajal, A. Torralba, and J.F. Duque-Carrillo, "Rail-to-rail low-power high-slew-rate CMOS analogue buffer," Electron. Lett., vol. 40, no. 14, 2004, pp. 214-215.
8. R. L. Shuler and R. S. Askew, "Low offset rail-to-rail operational amplifier," United States Application 20060097791, 2006.

Global Journals Inc. (US) Guidelines Handbook 2012

www.GlobalJournals.org

FELLOW OF ASSOCIATION OF RESEARCH SOCIETY IN ENGINEERING (FARSE)

- 'FARSE' title will be awarded to the person after approval of Editor-in-Chief and Editorial Board. The title 'FARSE" can be added to name in the following manner. eg. Dr. John E. Hall, Ph.D., FARSE or William Walldroff Ph. D., M.S., FARSE
- Being FARSE is a respectful honor. It authenticates your research activities. After becoming FARSE, you can use 'FARSE' title as you use your degree in suffix of your name. This will definitely will enhance and add up your name. You can use it on your Career Counseling Materials/CV/Resume/Visiting Card/Name Plate etc.
- 60% Discount will be provided to FARSE members for publishing research papers in Global Journals Inc., if our Editorial Board and Peer Reviewers accept the paper. For the life time, if you are author/co-author of any paper bill sent to you will automatically be discounted one by 60%
- FARSE will be given a renowned, secure, free professional email address with 100 GB of space eg.johnhall@globaljournals.org. You will be facilitated with Webmail, Spam Assassin, Email Forwarders, Auto-Responders, Email Delivery Route tracing, etc.
- FARSE member is eligible to become paid peer reviewer at Global Journals Inc. to earn up to 15% of realized author charges taken from author of respective paper. After reviewing 5 or more papers you can request to transfer the amount to your bank account or to your PayPal account.
- Eg. If we had taken 420 USD from author, we can send 63 USD to your account.
- FARSE member can apply for free approval, grading and certification of some of their Educational and Institutional Degrees from Global Journals Inc. (US) and Open Association of Research, Society U.S.A.
- After you are FARSE. You can send us scanned copy of all of your documents. We will verify, grade and certify them within a month. It will be based on your academic records, quality of research papers published by you, and 50 more criteria. This is beneficial for your job interviews as recruiting organization need not just rely on you for authenticity and your unknown qualities, you would have authentic ranks of all of your documents. Our scale is unique worldwide.
- FARSE member can proceed to get benefits of free research podcasting in Global Research Radio with their research documents, slides and online movies.
- After your publication anywhere in the world, you can upload you research paper with your recorded voice or you can use our professional RJs to record your paper their voice. We can also stream your conference videos and display your slides online.
- FARSE will be eligible for free application of Standardization of their Researches by Open Scientific Standards. Standardization is next step and level after publishing in a journal. A team of research and professional will work with you to take your research to its next level, which is worldwide open standardization.

- FARSE is eligible to earn from their researches: While publishing his paper with Global Journals Inc. (US), FARSE can decide whether he/she would like to publish his/her research in closed manner. When readers will buy that individual research paper for reading, 80% of its earning by Global Journals Inc. (US) will be transferred to FARSE member's bank account after certain threshold balance. There is no time limit for collection. FARSE member can decide its price and we can help in decision.

MEMBER OF ASSOCIATION OF RESEARCH SOCIETY IN ENGINEERING (MARSE)

- 'MARSE' title will be awarded to the person after approval of Editor-in-Chief and Editorial Board. The title 'MARSE" can be added to name in the following manner. eg. Dr. John E. Hall, Ph.D., MARSE or William Walldroff Ph. D., M.S., MARSE
- Being MARSE is a respectful honor. It authenticates your research activities. After becoming MARSE, you can use 'MARSE' title as you use your degree in suffix of your name. This will definitely will enhance and add up your name. You can use it on your Career Counseling Materials/CV/Resume/Visiting Card/Name Plate etc.
- 40% Discount will be provided to MARSE members for publishing research papers in Global Journals Inc., if our Editorial Board and Peer Reviewers accept the paper. For the life time, if you are author/co-author of any paper bill sent to you will automatically be discounted one by 60%
- MARSE will be given a renowned, secure, free professional email address with 30 GB of space eg.johnhall@globaljournals.org. You will be facilitated with Webmail, SpamAssassin, Email Forwarders, Auto-Responders, Email Delivery Route tracing, etc.
- MARSE member is eligible to become paid peer reviewer at Global Journals Inc. to earn up to 10% of realized author charges taken from author of respective paper. After reviewing 5 or more papers you can request to transfer the amount to your bank account or to your PayPal account.
- MARSE member can apply for free approval, grading and certification of some of their Educational and Institutional Degrees from Global Journals Inc. (US) and Open Association of Research,Society U.S.A.
- MARSE is eligible to earn from their researches: While publishing his paper with Global Journals Inc. (US), MARSE can decide whether he/she would like to publish his/her research in closed manner. When readers will buy that individual research paper for reading, 40% of its earning by Global Journals Inc. (US) will be transferred to MARSE member's bank account after certain threshold balance. There is no time limit for collection. MARSE member can decide its price and we can help in decision.

AUXILIARY MEMBERSHIPS

ANNUAL MEMBER

- Annual Member will be authorized to receive e-Journal GJRE for one year (subscription for one year).
- The member will be allotted free 1 GB Web-space along with subDomain to contribute and participate in our activities.
- A professional email address will be allotted free 500 MB email space.

PAPER PUBLICATION

- The members can publish paper once. The paper will be sent to two-peer reviewer. The paper will be published after the acceptance of peer reviewers and Editorial Board.

Process of submission of Research Paper

The Area or field of specialization may or may not be of any category as mentioned in 'Scope of Journal' menu of the GlobalJournals.org website. There are 37 Research Journal categorized with Six parental Journals GJCST, GJMR, GJRE, GJMBR, GJSFR, GJHSS. For Authors should prefer the mentioned categories. There are three widely used systems UDC, DDC and LCC. The details are available as 'Knowledge Abstract' at Home page. The major advantage of this coding is that, the research work will be exposed to and shared with all over the world as we are being abstracted and indexed worldwide.

The paper should be in proper format. The format can be downloaded from first page of 'Author Guideline' Menu. The Author is expected to follow the general rules as mentioned in this menu. The paper should be written in MS-Word Format (*.DOC,*.DOCX).

The Author can submit the paper either online or offline. The authors should prefer online submission.Online Submission: There are three ways to submit your paper:

(A) (I) First, register yourself using top right corner of Home page then Login. If you are already registered, then login using your username and password.

(II) Choose corresponding Journal.

(III) Click 'Submit Manuscript'. Fill required information and Upload the paper.

(B) If you are using Internet Explorer, then Direct Submission through Homepage is also available.

(C) If these two are not conveninet , and then email the paper directly to dean@globaljournals.org.

Offline Submission: Author can send the typed form of paper by Post. However, online submission should be preferred.

Preferred Author Guidelines

MANUSCRIPT STYLE INSTRUCTION (Must be strictly followed)

Page Size: 8.27" X 11'"

- Left Margin: 0.65
- Right Margin: 0.65
- Top Margin: 0.75
- Bottom Margin: 0.75
- Font type of all text should be Swis 721 Lt BT.
- Paper Title should be of Font Size 24 with one Column section.
- Author Name in Font Size of 11 with one column as of Title.
- Abstract Font size of 9 Bold, "Abstract" word in Italic Bold.
- Main Text: Font size 10 with justified two columns section
- Two Column with Equal Column with of 3.38 and Gaping of .2
- First Character must be three lines Drop capped.
- Paragraph before Spacing of 1 pt and After of 0 pt.
- Line Spacing of 1 pt
- Large Images must be in One Column
- Numbering of First Main Headings (Heading 1) must be in Roman Letters, Capital Letter, and Font Size of 10.
- Numbering of Second Main Headings (Heading 2) must be in Alphabets, Italic, and Font Size of 10.

You can use your own standard format also.
Author Guidelines:

1. General,

2. Ethical Guidelines,

3. Submission of Manuscripts,

4. Manuscript's Category,

5. Structure and Format of Manuscript,

6. After Acceptance.

1. GENERAL

Before submitting your research paper, one is advised to go through the details as mentioned in following heads. It will be beneficial, while peer reviewer justify your paper for publication.

Scope

The Global Journals Inc. (US) welcome the submission of original paper, review paper, survey article relevant to the all the streams of Philosophy and knowledge. The Global Journals Inc. (US) is parental platform for Global Journal of Computer Science and Technology, Researches in Engineering, Medical Research, Science Frontier Research, Human Social Science, Management, and Business organization. The choice of specific field can be done otherwise as following in Abstracting and Indexing Page on this Website. As the all Global

Journals Inc. (US) are being abstracted and indexed (in process) by most of the reputed organizations. Topics of only narrow interest will not be accepted unless they have wider potential or consequences.

2. ETHICAL GUIDELINES

Authors should follow the ethical guidelines as mentioned below for publication of research paper and research activities.

Papers are accepted on strict understanding that the material in whole or in part has not been, nor is being, considered for publication elsewhere. If the paper once accepted by Global Journals Inc. (US) and Editorial Board, will become the copyright of the Global Journals Inc. (US).

Authorship: The authors and coauthors should have active contribution to conception design, analysis and interpretation of findings. They should critically review the contents and drafting of the paper. All should approve the final version of the paper before submission

The Global Journals Inc. (US) follows the definition of authorship set up by the Global Academy of Research and Development. According to the Global Academy of R&D authorship, criteria must be based on:

1) Substantial contributions to conception and acquisition of data, analysis and interpretation of the findings.

2) Drafting the paper and revising it critically regarding important academic content.

3) Final approval of the version of the paper to be published.

All authors should have been credited according to their appropriate contribution in research activity and preparing paper. Contributors who do not match the criteria as authors may be mentioned under Acknowledgement.

Acknowledgements: Contributors to the research other than authors credited should be mentioned under acknowledgement. The specifications of the source of funding for the research if appropriate can be included. Suppliers of resources may be mentioned along with address.

Appeal of Decision: The Editorial Board's decision on publication of the paper is final and cannot be appealed elsewhere.

Permissions: It is the author's responsibility to have prior permission if all or parts of earlier published illustrations are used in this paper.

Please mention proper reference and appropriate acknowledgements wherever expected.

If all or parts of previously published illustrations are used, permission must be taken from the copyright holder concerned. It is the author's responsibility to take these in writing.

Approval for reproduction/modification of any information (including figures and tables) published elsewhere must be obtained by the authors/copyright holders before submission of the manuscript. Contributors (Authors) are responsible for any copyright fee involved.

3. SUBMISSION OF MANUSCRIPTS

Manuscripts should be uploaded via this online submission page. The online submission is most efficient method for submission of papers, as it enables rapid distribution of manuscripts and consequently speeds up the review procedure. It also enables authors to know the status of their own manuscripts by emailing us. Complete instructions for submitting a paper is available below.

Manuscript submission is a systematic procedure and little preparation is required beyond having all parts of your manuscript in a given format and a computer with an Internet connection and a Web browser. Full help and instructions are provided on-screen. As an author, you will be prompted for login and manuscript details as Field of Paper and then to upload your manuscript file(s) according to the instructions.

To avoid postal delays, all transaction is preferred by e-mail. A finished manuscript submission is confirmed by e-mail immediately and your paper enters the editorial process with no postal delays. When a conclusion is made about the publication of your paper by our Editorial Board, revisions can be submitted online with the same procedure, with an occasion to view and respond to all comments.

Complete support for both authors and co-author is provided.

4. MANUSCRIPT'S CATEGORY

Based on potential and nature, the manuscript can be categorized under the following heads:

Original research paper: Such papers are reports of high-level significant original research work.

Review papers: These are concise, significant but helpful and decisive topics for young researchers.

Research articles: These are handled with small investigation and applications

Research letters: The letters are small and concise comments on previously published matters.

5.STRUCTURE AND FORMAT OF MANUSCRIPT

The recommended size of original research paper is less than seven thousand words, review papers fewer than seven thousands words also.Preparation of research paper or how to write research paper, are major hurdle, while writing manuscript. The research articles and research letters should be fewer than three thousand words, the structure original research paper; sometime review paper should be as follows:

Papers: These are reports of significant research (typically less than 7000 words equivalent, including tables, figures, references), and comprise:

(a)Title should be relevant and commensurate with the theme of the paper.

(b) A brief Summary, "Abstract" (less than 150 words) containing the major results and conclusions.

(c) Up to ten keywords, that precisely identifies the paper's subject, purpose, and focus.

(d) An Introduction, giving necessary background excluding subheadings; objectives must be clearly declared.

(e) Resources and techniques with sufficient complete experimental details (wherever possible by reference) to permit repetition; sources of information must be given and numerical methods must be specified by reference, unless non-standard.

(f) Results should be presented concisely, by well-designed tables and/or figures; the same data may not be used in both; suitable statistical data should be given. All data must be obtained with attention to numerical detail in the planning stage. As reproduced design has been recognized to be important to experiments for a considerable time, the Editor has decided that any paper that appears not to have adequate numerical treatments of the data will be returned un-refereed;

(g) Discussion should cover the implications and consequences, not just recapitulating the results; conclusions should be summarizing.

(h) Brief Acknowledgements.

(i) References in the proper form.

Authors should very cautiously consider the preparation of papers to ensure that they communicate efficiently. Papers are much more likely to be accepted, if they are cautiously designed and laid out, contain few or no errors, are summarizing, and be conventional to the approach and instructions. They will in addition, be published with much less delays than those that require much technical and editorial correction.

The Editorial Board reserves the right to make literary corrections and to make suggestions to improve briefness.

It is vital, that authors take care in submitting a manuscript that is written in simple language and adheres to published guidelines.

Format

Language: The language of publication is UK English. Authors, for whom English is a second language, must have their manuscript efficiently edited by an English-speaking person before submission to make sure that, the English is of high excellence. It is preferable, that manuscripts should be professionally edited.

Standard Usage, Abbreviations, and Units: Spelling and hyphenation should be conventional to The Concise Oxford English Dictionary. Statistics and measurements should at all times be given in figures, e.g. 16 min, except for when the number begins a sentence. When the number does not refer to a unit of measurement it should be spelt in full unless, it is 160 or greater.

Abbreviations supposed to be used carefully. The abbreviated name or expression is supposed to be cited in full at first usage, followed by the conventional abbreviation in parentheses.

Metric SI units are supposed to generally be used excluding where they conflict with current practice or are confusing. For illustration, 1.4 l rather than 1.4 × 10-3 m3, or 4 mm somewhat than 4 × 10-3 m. Chemical formula and solutions must identify the form used, e.g. anhydrous or hydrated, and the concentration must be in clearly defined units. Common species names should be followed by underlines at the first mention. For following use the generic name should be constricted to a single letter, if it is clear.

Structure

All manuscripts submitted to Global Journals Inc. (US), ought to include:

Title: The title page must carry an instructive title that reflects the content, a running title (less than 45 characters together with spaces), names of the authors and co-authors, and the place(s) wherever the work was carried out. The full postal address in addition with the e-mail address of related author must be given. Up to eleven keywords or very brief phrases have to be given to help data retrieval, mining and indexing.

Abstract, used in Original Papers and Reviews:

Optimizing Abstract for Search Engines

Many researchers searching for information online will use search engines such as Google, Yahoo or similar. By optimizing your paper for search engines, you will amplify the chance of someone finding it. This in turn will make it more likely to be viewed and/or cited in a further work. Global Journals Inc. (US) have compiled these guidelines to facilitate you to maximize the web-friendliness of the most public part of your paper.

Key Words

A major linchpin in research work for the writing research paper is the keyword search, which one will employ to find both library and Internet resources.

One must be persistent and creative in using keywords. An effective keyword search requires a strategy and planning a list of possible keywords and phrases to try.

Search engines for most searches, use Boolean searching, which is somewhat different from Internet searches. The Boolean search uses "operators," words (and, or, not, and near) that enable you to expand or narrow your affords. Tips for research paper while preparing research paper are very helpful guideline of research paper.

Choice of key words is first tool of tips to write research paper. Research paper writing is an art.A few tips for deciding as strategically as possible about keyword search:

- One should start brainstorming lists of possible keywords before even begin searching. Think about the most important concepts related to research work. Ask, "What words would a source have to include to be truly valuable in research paper?" Then consider synonyms for the important words.
- It may take the discovery of only one relevant paper to let steer in the right keyword direction because in most databases, the keywords under which a research paper is abstracted are listed with the paper.
- One should avoid outdated words.

Keywords are the key that opens a door to research work sources. Keyword searching is an art in which researcher's skills are bound to improve with experience and time.

Numerical Methods: Numerical methods used should be clear and, where appropriate, supported by references.

Acknowledgements: Please make these as concise as possible.

References

References follow the Harvard scheme of referencing. References in the text should cite the authors' names followed by the time of their publication, unless there are three or more authors when simply the first author's name is quoted followed by et al. unpublished work has to only be cited where necessary, and only in the text. Copies of references in press in other journals have to be supplied with submitted typescripts. It is necessary that all citations and references be carefully checked before submission, as mistakes or omissions will cause delays.

References to information on the World Wide Web can be given, but only if the information is available without charge to readers on an official site. Wikipedia and Similar websites are not allowed where anyone can change the information. Authors will be asked to make available electronic copies of the cited information for inclusion on the Global Journals Inc. (US) homepage at the judgment of the Editorial Board.

The Editorial Board and Global Journals Inc. (US) recommend that, citation of online-published papers and other material should be done via a DOI (digital object identifier). If an author cites anything, which does not have a DOI, they run the risk of the cited material not being noticeable.

The Editorial Board and Global Journals Inc. (US) recommend the use of a tool such as Reference Manager for reference management and formatting.

Tables, Figures and Figure Legends

Tables: Tables should be few in number, cautiously designed, uncrowned, and include only essential data. Each must have an Arabic number, e.g. Table 4, a self-explanatory caption and be on a separate sheet. Vertical lines should not be used.

Figures: Figures are supposed to be submitted as separate files. Always take in a citation in the text for each figure using Arabic numbers, e.g. Fig. 4. Artwork must be submitted online in electronic form by e-mailing them.

Preparation of Electronic Figures for Publication

Even though low quality images are sufficient for review purposes, print publication requires high quality images to prevent the final product being blurred or fuzzy. Submit (or e-mail) EPS (line art) or TIFF (halftone/photographs) files only. MS PowerPoint and Word Graphics are unsuitable for printed pictures. Do not use pixel-oriented software. Scans (TIFF only) should have a resolution of at least 350 dpi (halftone) or 700 to 1100 dpi (line drawings) in relation to the imitation size. Please give the data for figures in black and white or submit a Color Work Agreement Form. EPS files must be saved with fonts embedded (and with a TIFF preview, if possible).

For scanned images, the scanning resolution (at final image size) ought to be as follows to ensure good reproduction: line art: >650 dpi; halftones (including gel photographs) : >350 dpi; figures containing both halftone and line images: >650 dpi.

Color Charges: It is the rule of the Global Journals Inc. (US) for authors to pay the full cost for the reproduction of their color artwork. Hence, please note that, if there is color artwork in your manuscript when it is accepted for publication, we would require you to complete and return a color work agreement form before your paper can be published.

Figure Legends: Self-explanatory legends of all figures should be incorporated separately under the heading 'Legends to Figures'. In the full-text online edition of the journal, figure legends may possibly be truncated in abbreviated links to the full screen version. Therefore, the first 100 characters of any legend should notify the reader, about the key aspects of the figure.

6. AFTER ACCEPTANCE

Upon approval of a paper for publication, the manuscript will be forwarded to the dean, who is responsible for the publication of the Global Journals Inc. (US).

6.1 Proof Corrections

The corresponding author will receive an e-mail alert containing a link to a website or will be attached. A working e-mail address must therefore be provided for the related author.

Acrobat Reader will be required in order to read this file. This software can be downloaded

(Free of charge) from the following website:

www.adobe.com/products/acrobat/readstep2.html. This will facilitate the file to be opened, read on screen, and printed out in order for any corrections to be added. Further instructions will be sent with the proof.

Proofs must be returned to the dean at dean@globaljournals.org within three days of receipt.

As changes to proofs are costly, we inquire that you only correct typesetting errors. All illustrations are retained by the publisher. Please note that the authors are responsible for all statements made in their work, including changes made by the copy editor.

6.2 Early View of Global Journals Inc. (US) (Publication Prior to Print)

The Global Journals Inc. (US) are enclosed by our publishing's Early View service. Early View articles are complete full-text articles sent in advance of their publication. Early View articles are absolute and final. They have been completely reviewed, revised and edited for publication, and the authors' final corrections have been incorporated. Because they are in final form, no changes can be made after sending them. The nature of Early View articles means that they do not yet have volume, issue or page numbers, so Early View articles cannot be cited in the conventional way.

6.3 Author Services

Online production tracking is available for your article through Author Services. Author Services enables authors to track their article - once it has been accepted - through the production process to publication online and in print. Authors can check the status of their articles online and choose to receive automated e-mails at key stages of production. The authors will receive an e-mail with a unique link that enables them to register and have their article automatically added to the system. Please ensure that a complete e-mail address is provided when submitting the manuscript.

6.4 Author Material Archive Policy

Please note that if not specifically requested, publisher will dispose off hardcopy & electronic information submitted, after the two months of publication. If you require the return of any information submitted, please inform the Editorial Board or dean as soon as possible.

6.5 Offprint and Extra Copies

A PDF offprint of the online-published article will be provided free of charge to the related author, and may be distributed according to the Publisher's terms and conditions. Additional paper offprint may be ordered by emailing us at: editor@globaljournals.org .

the search? Will I be able to find all information in this field area? If the answer of these types of questions will be "Yes" then you can choose that topic. In most of the cases, you may have to conduct the surveys and have to visit several places because this field is related to Computer Science and Information Technology. Also, you may have to do a lot of work to find all rise and falls regarding the various data of that subject. Sometimes, detailed information plays a vital role, instead of short information.

2. Evaluators are human: First thing to remember that evaluators are also human being. They are not only meant for rejecting a paper. They are here to evaluate your paper. So, present your Best.

3. Think Like Evaluators: If you are in a confusion or getting demotivated that your paper will be accepted by evaluators or not, then think and try to evaluate your paper like an Evaluator. Try to understand that what an evaluator wants in your research paper and automatically you will have your answer.

4. Make blueprints of paper: The outline is the plan or framework that will help you to arrange your thoughts. It will make your paper logical. But remember that all points of your outline must be related to the topic you have chosen.

5. Ask your Guides: If you are having any difficulty in your research, then do not hesitate to share your difficulty to your guide (if you have any). They will surely help you out and resolve your doubts. If you can't clarify what exactly you require for your work then ask the supervisor to help you with the alternative. He might also provide you the list of essential readings.

6. Use of computer is recommended: As you are doing research in the field of Computer Science, then this point is quite obvious.

7. Use right software: Always use good quality software packages. If you are not capable to judge good software then you can lose quality of your paper unknowingly. There are various software programs available to help you, which you can get through Internet.

8. Use the Internet for help: An excellent start for your paper can be by using the Google. It is an excellent search engine, where you can have your doubts resolved. You may also read some answers for the frequent question how to write my research paper or find model research paper. From the internet library you can download books. If you have all required books make important reading selecting and analyzing the specified information. Then put together research paper sketch out.

9. Use and get big pictures: Always use encyclopedias, Wikipedia to get pictures so that you can go into the depth.

10. Bookmarks are useful: When you read any book or magazine, you generally use bookmarks, right! It is a good habit, which helps to not to lose your continuity. You should always use bookmarks while searching on Internet also, which will make your search easier.

11. Revise what you wrote: When you write anything, always read it, summarize it and then finalize it.

12. Make all efforts: Make all efforts to mention what you are going to write in your paper. That means always have a good start. Try to mention everything in introduction, that what is the need of a particular research paper. Polish your work by good skill of writing and always give an evaluator, what he wants.

13. Have backups: When you are going to do any important thing like making research paper, you should always have backup copies of it either in your computer or in paper. This will help you to not to lose any of your important.

14. Produce good diagrams of your own: Always try to include good charts or diagrams in your paper to improve quality. Using several and unnecessary diagrams will degrade the quality of your paper by creating "hotchpotch." So always, try to make and include those diagrams, which are made by your own to improve readability and understandability of your paper.

15. Use of direct quotes: When you do research relevant to literature, history or current affairs then use of quotes become essential but if study is relevant to science then use of quotes is not preferable.

16. Use proper verb tense: Use proper verb tenses in your paper. Use past tense, to present those events that happened. Use present tense to indicate events that are going on. Use future tense to indicate future happening events. Use of improper and wrong tenses will confuse the evaluator. Avoid the sentences that are incomplete.

17. Never use online paper: If you are getting any paper on Internet, then never use it as your research paper because it might be possible that evaluator has already seen it or maybe it is outdated version.

18. **Pick a good study spot:** To do your research studies always try to pick a spot, which is quiet. Every spot is not for studies. Spot that suits you choose it and proceed further.

19. Know what you know: Always try to know, what you know by making objectives. Else, you will be confused and cannot achieve your target.

20. Use good quality grammar: Always use a good quality grammar and use words that will throw positive impact on evaluator. Use of good quality grammar does not mean to use tough words, that for each word the evaluator has to go through dictionary. Do not start sentence with a conjunction. Do not fragment sentences. Eliminate one-word sentences. Ignore passive voice. Do not ever use a big word when a diminutive one would suffice. Verbs have to be in agreement with their subjects. Prepositions are not expressions to finish sentences with. It is incorrect to ever divide an infinitive. Avoid clichés like the disease. Also, always shun irritating alliteration. Use language that is simple and straight forward. put together a neat summary.

21. Arrangement of information: Each section of the main body should start with an opening sentence and there should be a changeover at the end of the section. Give only valid and powerful arguments to your topic. You may also maintain your arguments with records.

22. Never start in last minute: Always start at right time and give enough time to research work. Leaving everything to the last minute will degrade your paper and spoil your work.

23. Multitasking in research is not good: Doing several things at the same time proves bad habit in case of research activity. Research is an area, where everything has a particular time slot. Divide your research work in parts and do particular part in particular time slot.

24. Never copy others' work: Never copy others' work and give it your name because if evaluator has seen it anywhere you will be in trouble.

25. Take proper rest and food: No matter how many hours you spend for your research activity, if you are not taking care of your health then all your efforts will be in vain. For a quality research, study is must, and this can be done by taking proper rest and food.

26. Go for seminars: Attend seminars if the topic is relevant to your research area. Utilize all your resources.

27. Refresh your mind after intervals: Try to give rest to your mind by listening to soft music or by sleeping in intervals. This will also improve your memory.

28. Make colleagues: Always try to make colleagues. No matter how sharper or intelligent you are, if you make colleagues you can have several ideas, which will be helpful for your research.

29. **Think technically:** Always think technically. If anything happens, then search its reasons, its benefits, and demerits.

30. Think and then print: When you will go to print your paper, notice that tables are not be split, headings are not detached from their descriptions, and page sequence is maintained.

31. Adding unnecessary information: Do not add unnecessary information, like, I have used MS Excel to draw graph. Do not add irrelevant and inappropriate material. These all will create superfluous. Foreign terminology and phrases are not apropos. One should NEVER take a broad view. Analogy in script is like feathers on a snake. Not at all use a large word when a very small one would be

sufficient. Use words properly, regardless of how others use them. Remove quotations. Puns are for kids, not grunt readers. Amplification is a billion times of inferior quality than sarcasm.

32. Never oversimplify everything: To add material in your research paper, never go for oversimplification. This will definitely irritate the evaluator. Be more or less specific. Also too, by no means, ever use rhythmic redundancies. Contractions aren't essential and shouldn't be there used. Comparisons are as terrible as clichés. Give up ampersands and abbreviations, and so on. Remove commas, that are, not necessary. Parenthetical words however should be together with this in commas. Understatement is all the time the complete best way to put onward earth-shaking thoughts. Give a detailed literary review.

33. Report concluded results: Use concluded results. From raw data, filter the results and then conclude your studies based on measurements and observations taken. Significant figures and appropriate number of decimal places should be used. Parenthetical remarks are prohibitive. Proofread carefully at final stage. In the end give outline to your arguments. Spot out perspectives of further study of this subject. Justify your conclusion by at the bottom of them with sufficient justifications and examples.

34. After conclusion: Once you have concluded your research, the next most important step is to present your findings. Presentation is extremely important as it is the definite medium though which your research is going to be in print to the rest of the crowd. Care should be taken to categorize your thoughts well and present them in a logical and neat manner. A good quality research paper format is essential because it serves to highlight your research paper and bring to light all necessary aspects in your research.

Informal Guidelines of Research Paper Writing

Key points to remember:

- Submit all work in its final form.
- Write your paper in the form, which is presented in the guidelines using the template.
- Please note the criterion for grading the final paper by peer-reviewers.

Final Points:

A purpose of organizing a research paper is to let people to interpret your effort selectively. The journal requires the following sections, submitted in the order listed, each section to start on a new page.

The introduction will be compiled from reference matter and will reflect the design processes or outline of basis that direct you to make study. As you will carry out the process of study, the method and process section will be constructed as like that. The result segment will show related statistics in nearly sequential order and will direct the reviewers next to the similar intellectual paths throughout the data that you took to carry out your study. The discussion section will provide understanding of the data and projections as to the implication of the results. The use of good quality references all through the paper will give the effort trustworthiness by representing an alertness of prior workings.

Writing a research paper is not an easy job no matter how trouble-free the actual research or concept. Practice, excellent preparation, and controlled record keeping are the only means to make straightforward the progression.

General style:

Specific editorial column necessities for compliance of a manuscript will always take over from directions in these general guidelines.

To make a paper clear

· Adhere to recommended page limits

Mistakes to evade

- Insertion a title at the foot of a page with the subsequent text on the next page

- Separating a table/chart or figure - impound each figure/table to a single page
- Submitting a manuscript with pages out of sequence

In every sections of your document

· Use standard writing style including articles ("a", "the," etc.)

· Keep on paying attention on the research topic of the paper

· Use paragraphs to split each significant point (excluding for the abstract)

· Align the primary line of each section

· Present your points in sound order

· Use present tense to report well accepted

· Use past tense to describe specific results

· Shun familiar wording, don't address the reviewer directly, and don't use slang, slang language, or superlatives

· Shun use of extra pictures - include only those figures essential to presenting results

Title Page:

Choose a revealing title. It should be short. It should not have non-standard acronyms or abbreviations. It should not exceed two printed lines. It should include the name(s) and address (es) of all authors.

Abstract:

The summary should be two hundred words or less. It should briefly and clearly explain the key findings reported in the manuscript--must have precise statistics. It should not have abnormal acronyms or abbreviations. It should be logical in itself. Shun citing references at this point.

An abstract is a brief distinct paragraph summary of finished work or work in development. In a minute or less a reviewer can be taught the foundation behind the study, common approach to the problem, relevant results, and significant conclusions or new questions.

Write your summary when your paper is completed because how can you write the summary of anything which is not yet written? Wealth of terminology is very essential in abstract. Yet, use comprehensive sentences and do not let go readability for briefness. You can maintain it succinct by phrasing sentences so that they provide more than lone rationale. The author can at this moment go straight to

shortening the outcome. Sum up the study, with the subsequent elements in any summary. Try to maintain the initial two items to no more than one ruling each.

- Reason of the study - theory, overall issue, purpose
- Fundamental goal
- To the point depiction of the research
- Consequences, including definite statistics - if the consequences are quantitative in nature, account quantitative data; results of any numerical analysis should be reported
- Significant conclusions or questions that track from the research(es)

Approach:

- Single section, and succinct
- As a outline of job done, it is always written in past tense
- A conceptual should situate on its own, and not submit to any other part of the paper such as a form or table
- Center on shortening results - bound background information to a verdict or two, if completely necessary
- What you account in an conceptual must be regular with what you reported in the manuscript
- Exact spelling, clearness of sentences and phrases, and appropriate reporting of quantities (proper units, important statistics) are just as significant in an abstract as they are anywhere else

Introduction:

The **Introduction** should "introduce" the manuscript. The reviewer should be presented with sufficient background information to be capable to comprehend and calculate the purpose of your study without having to submit to other works. The basis for the study should be offered. Give most important references but shun difficult to make a comprehensive appraisal of the topic. In the introduction, describe the problem visibly. If the problem is not acknowledged in a logical, reasonable way, the reviewer will have no attention in your result. Speak in common terms about techniques used to explain the problem, if needed, but do not present any particulars about the protocols here. Following approach can create a valuable beginning:

- Explain the value (significance) of the study
- Shield the model - why did you employ this particular system or method? What is its compensation? You strength remark on its appropriateness from a abstract point of vision as well as point out sensible reasons for using it.
- Present a justification. Status your particular theory (es) or aim(s), and describe the logic that led you to choose them.
- Very for a short time explain the tentative propose and how it skilled the declared objectives.

Approach:

- Use past tense except for when referring to recognized facts. After all, the manuscript will be submitted after the entire job is done.
- Sort out your thoughts; manufacture one key point with every section. If you make the four points listed above, you will need a least of four paragraphs.
- Present surroundings information only as desirable in order hold up a situation. The reviewer does not desire to read the whole thing you know about a topic.
- Shape the theory/purpose specifically - do not take a broad view.
- As always, give awareness to spelling, simplicity and correctness of sentences and phrases.

Procedures (Methods and Materials):

This part is supposed to be the easiest to carve if you have good skills. A sound written Procedures segment allows a capable scientist to replacement your results. Present precise information about your supplies. The suppliers and clarity of reagents can be helpful bits of information. Present methods in sequential order but linked methodologies can be grouped as a segment. Be concise when relating the protocols. Attempt for the least amount of information that would permit another capable scientist to spare your outcome but be cautious that vital information is integrated. The use of subheadings is suggested and ought to be synchronized with the results section. When a technique is used that has been well described in another object, mention the specific item describing a way but draw the basic

principle while stating the situation. The purpose is to text all particular resources and broad procedures, so that another person may use some or all of the methods in one more study or referee the scientific value of your work. It is not to be a step by step report of the whole thing you did, nor is a methods section a set of orders.

Materials:

- Explain materials individually only if the study is so complex that it saves liberty this way.
- Embrace particular materials, and any tools or provisions that are not frequently found in laboratories.
- Do not take in frequently found.
- If use of a definite type of tools.
- Materials may be reported in a part section or else they may be recognized along with your measures.

Methods:

- Report the method (not particulars of each process that engaged the same methodology)
- Describe the method entirely
- To be succinct, present methods under headings dedicated to specific dealings or groups of measures
- Simplify - details how procedures were completed not how they were exclusively performed on a particular day.
- If well known procedures were used, account the procedure by name, possibly with reference, and that's all.

Approach:

- It is embarrassed or not possible to use vigorous voice when documenting methods with no using first person, which would focus the reviewer's interest on the researcher rather than the job. As a result when script up the methods most authors use third person passive voice.
- Use standard style in this and in every other part of the paper - avoid familiar lists, and use full sentences.

What to keep away from

- Resources and methods are not a set of information.
- Skip all descriptive information and surroundings - save it for the argument.
- Leave out information that is immaterial to a third party.

Results:

The principle of a results segment is to present and demonstrate your conclusion. Create this part a entirely objective details of the outcome, and save all understanding for the discussion.

The page length of this segment is set by the sum and types of data to be reported. Carry on to be to the point, by means of statistics and tables, if suitable, to present consequences most efficiently.You must obviously differentiate material that would usually be incorporated in a study editorial from any unprocessed data or additional appendix matter that would not be available. In fact, such matter should not be submitted at all except requested by the instructor.

Content

- Sum up your conclusion in text and demonstrate them, if suitable, with figures and tables.
- In manuscript, explain each of your consequences, point the reader to remarks that are most appropriate.
- Present a background, such as by describing the question that was addressed by creation an exacting study.
- Explain results of control experiments and comprise remarks that are not accessible in a prescribed figure or table, if appropriate.
- Examine your data, then prepare the analyzed (transformed) data in the form of a figure (graph), table, or in manuscript form.

What to stay away from

- Do not discuss or infer your outcome, report surroundings information, or try to explain anything.
- Not at all, take in raw data or intermediate calculations in a research manuscript.

- Do not present the similar data more than once.
- Manuscript should complement any figures or tables, not duplicate the identical information.
- Never confuse figures with tables - there is a difference.

Approach

- As forever, use past tense when you submit to your results, and put the whole thing in a reasonable order.
- Put figures and tables, appropriately numbered, in order at the end of the report
- If you desire, you may place your figures and tables properly within the text of your results part.

Figures and tables

- If you put figures and tables at the end of the details, make certain that they are visibly distinguished from any attach appendix materials, such as raw facts
- Despite of position, each figure must be numbered one after the other and complete with subtitle
- In spite of position, each table must be titled, numbered one after the other and complete with heading
- All figure and table must be adequately complete that it could situate on its own, divide from text

Discussion:

The Discussion is expected the trickiest segment to write and describe. A lot of papers submitted for journal are discarded based on problems with the Discussion. There is no head of state for how long a argument should be. Position your understanding of the outcome visibly to lead the reviewer through your conclusions, and then finish the paper with a summing up of the implication of the study. The purpose here is to offer an understanding of your results and hold up for all of your conclusions, using facts from your research and generally accepted information, if suitable. The implication of result should be visibly described. Infer your data in the conversation in suitable depth. This means that when you clarify an observable fact you must explain mechanisms that may account for the observation. If your results vary from your prospect, make clear why that may have happened. If your results agree, then explain the theory that the proof supported. It is never suitable to just state that the data approved with prospect, and let it drop at that.

- Make a decision if each premise is supported, discarded, or if you cannot make a conclusion with assurance. Do not just dismiss a study or part of a study as "uncertain."
- Research papers are not acknowledged if the work is imperfect. Draw what conclusions you can based upon the results that you have, and take care of the study as a finished work
- You may propose future guidelines, such as how the experiment might be personalized to accomplish a new idea.
- Give details all of your remarks as much as possible, focus on mechanisms.
- Make a decision if the tentative design sufficiently addressed the theory, and whether or not it was correctly restricted.
- Try to present substitute explanations if sensible alternatives be present.
- One research will not counter an overall question, so maintain the large picture in mind, where do you go next? The best studies unlock new avenues of study. What questions remain?
- Recommendations for detailed papers will offer supplementary suggestions.

Approach:

- When you refer to information, differentiate data generated by your own studies from available information
- Submit to work done by specific persons (including you) in past tense.
- Submit to generally acknowledged facts and main beliefs in present tense.

Administration Rules Listed Before Submitting Your Research Paper to Global Journals Inc. (US)

Please carefully note down following rules and regulation before submitting your Research Paper to Global Journals Inc. (US):

Segment Draft and Final Research Paper: You have to strictly follow the template of research paper. If it is not done your paper may get rejected.

- The **major constraint** is that you must independently make all content, tables, graphs, and facts that are offered in the paper. You must write each part of the paper wholly on your own. The Peer-reviewers need to identify your own perceptive of the concepts in your own terms. NEVER extract straight from any foundation, and never rephrase someone else's analysis.

- Do not give permission to anyone else to "PROOFREAD" your manuscript.

- Methods to avoid Plagiarism is applied by us on every paper, if found guilty, you will be blacklisted by all of our collaborated research groups, your institution will be informed for this and strict legal actions will be taken immediately.)
- To guard yourself and others from possible illegal use please do not permit anyone right to use to your paper and files.

Criterion for Grading a Research Paper (Compilation) by Global Journals Inc. (US)

Please note that following table is only a Grading of "Paper Compilation" and not on "Performed/Stated Research" whose grading solely depends on Individual Assigned Peer Reviewer and Editorial Board Member. These can be available only on request and after decision of Paper. This report will be the property of Global Journals Inc. (US).

Topics	Grades		
	A-B	**C-D**	**E-F**
Abstract	Clear and concise with appropriate content, Correct format. 200 words or below	Unclear summary and no specific data, Incorrect form Above 200 words	No specific data with ambiguous information Above 250 words
Introduction	Containing all background details with clear goal and appropriate details, flow specification, no grammar and spelling mistake, well organized sentence and paragraph, reference cited	Unclear and confusing data, appropriate format, grammar and spelling errors with unorganized matter	Out of place depth and content, hazy format
Methods and Procedures	Clear and to the point with well arranged paragraph, precision and accuracy of facts and figures, well organized subheads	Difficult to comprehend with embarrassed text, too much explanation but completed	Incorrect and unorganized structure with hazy meaning
Result	Well organized, Clear and specific, Correct units with precision, correct data, well structuring of paragraph, no grammar and spelling mistake	Complete and embarrassed text, difficult to comprehend	Irregular format with wrong facts and figures
Discussion	Well organized, meaningful specification, sound conclusion, logical and concise explanation, highly structured paragraph reference cited	Wordy, unclear conclusion, spurious	Conclusion is not cited, unorganized, difficult to comprehend
References	Complete and correct format, well organized	Beside the point, Incomplete	Wrong format and structuring

INDEX

F

G

H

I

K

L

M

N

O

P

R

S

T

U

V

Global Journal of Researches in Engineering

Visit us on the Web at www.GlobalJournals.org | www.EngineeringResearch.org
or email us at helpdesk@globaljournals.org

ISSN 9755861